Temperate forest response to multiple ecosystem change drivers in the eastern United States: implications for forest carbon and water balance

Jacob D. Malcomb

Marietta, OH

Bachelor of Science
St. Lawrence University, 2010

A Dissertation presented to the Graduate Faculty of the University of Virginia in Candidacy for the Degree of Doctor of Philosophy

Department of Environmental Sciences

University of Virginia
May 2022

Committee:
Dr. Todd Scanlon (Advisor)
Department of Environmental Sciences

Dr. Howie Epstein (Advisor)
Department of Environmental Sciences

Dr. Xi Yang
Department of Environmental Sciences

Dr. Julianne Quinn (Dean's Representative)
Department of Engineering Systems and Environment

Acknowledgements

To my advisors, Drs. Todd Scanlon and Howie Epstein – it has been nearly six years since my four-day "interview" for this PhD position in West Virginia. I'm immensely grateful for the guidance, support, and mentorship you've given me ever since. Thank you for giving me an opportunity then, and I look forward to continuing to collaborate with you in the future.

To my committee members, Drs. Xi Yang and Julianne Quinn – thank you for your generous contributions of time and constructive feedback. Xi, I'm glad I signed up for the first class you taught at UVA. You've expanded my knowledge about plant physiology and remote sensing, and the scope of the questions I'm equipped to ask.

To Drs. Dan Druckenbrod and Matthew Vadeboncoeur – thank you for your time and patience in teaching me dendrochronological methods, as well as your thoughtful manuscript feedback. I've enjoyed my time in the field and the lab with you. To my other collaborators and co-authors: Dr. Lixin Wang, Matthew Lanning, Dr. Mary Beth Adams, Dr. Ivan Fernandez, Dr. Heidi Asbjornsen, and Linnea Saby – thank you for your invaluable contributions to this research. Drs. Amanda Armstrong, Larry Band, Dave Carr, Max Castorani, Manuel Lerdeau, Ami Riscassi, Atticus Stovall, and Elliott White provided useful insights, help with statistics and code, and interesting conversations that contributed to this work. It has been a pleasure sharing my time at UVA with you. I'd also like to thank Drs. Erika Barthelmess and Matthew Carotenuto for being such supportive friends and mentors over the years.

To Laura Barry, Dr. Alice Besterman, Dr. Cal Buelo, Dat Ha, Elise Heffernan, Kelsey Huelsman, Mitchell Kelleher, Kelcy Kent, Allie Parisian, Dr. Stephanie Roe, Dr. Charles Scaife, and Spencer Tassone, and others – I can't thank you enough for your friendship and support over the past five years.

To my parents – this PhD probably began unconsciously while I was stomping around a mountain stream in West Virginia. Thank you for taking me out in the woods and encouraging me to pursue my interests. To my brother, Nathan – thank you for sharing your love of the forest. I look forward to our hikes and conversations in years to come.

To Lyndsay – your love and support throughout this journey has meant everything. I'll never be able to thank you enough for keeping me organized, motivated, and feeling loved. To Miles – I hope this work contributes, in some small way, to making Earth a better planet for you to live on. I can't wait for many more adventures in the woods with you.

Funding for the research in Chapters 3, 4, and 5 was provided by NSF Hydrologic Sciences Award #1562019, a UVA Department of Environmental Sciences Moore Award (2017), and a UVA Department of Environmental Sciences Jefferson Conservation Award (2021). Work in Chapter 2 was supported by a UVA School of Data Science Presidential Fellowship in Data Science in the 2019-2020 academic year.

This work benefitted enormously from access to long-term hydrologic, biogeochemical, and forest inventory datasets funded, developed, and maintained by several agencies, including the National Science Foundation, US Forest Service, US Geological Survey, and National Park Service, and would not have been possible without access to field sites provided by Shenandoah National Park, the US Forest Service, the US Geological Survey, and the University of Maine.

Table of Contents

List of Tables

List of Figures

Chapter 1. Introduction to the Dissertation

1.1 Background and Motivation

Temperate mixed hardwood forests cover more than half of the land area in the eastern United States (Drummond & Loveland, 2010), and provide ecosystem services of both regional and global importance. In the conterminous US, eastern forests[1] account for approximately two-thirds of the terrestrial carbon sink (Lu et al., 2015), sequestering carbon in woody biomass and soils for time scales ranging from decades to millennia. Forests are also key mediators of the hydrologic cycle – by taking up soil water through their roots and transpiring it to the atmosphere via their stomata, trees directly influence atmospheric water vapor concentrations and the quantity of water available for streamflow. Forest health and water quality are intrinsically linked in the eastern United States, where more than 60% of the water supply originates in forested areas (Brown et al., 2008). Thus, improving our understanding of environmental processes that govern forest carbon and water balance can improve our ability to maintain, enhance, and predict the vital ecosystem services that forests provide.

In the past century, eastern US forests have undergone major structural, compositional, and biogeochemical changes as a result of anthropogenic drivers, including shifting land use patterns, declines in nitrogen (N) and sulfur (S) deposition, elevated atmospheric CO_2 concentrations, changing temperature and precipitation regimes, and disturbances caused by introduced forest pests. Understanding the net effects of these changes on forest growth and water use efficiency (WUE) – broadly defined as the ratio of photosynthetic carbon assimilation

[1] In this section "eastern forests" refers to mixed hardwood and evergreen forests located in AL, AR, CT, DE, FL, GA, KY, LA, MA, MD, ME, NC, NH, NJ, NY, PA, RI, SC, TN, VA, and WV, USA.

per unit of water transpired – has been a major research focus, with evidence indicating enhanced tree growth (McMahon et al. 2010; Fang et al., 2014; Boisenvue and Running, 2006) and WUE (Keenan et al., 2013; Frank et al., 2015; Guerrieri et al., 2019; Mathias and Thomas, 2021) in temperate forests over recent decades. Increases in tree productivity and WUE are often attributed to a CO_2 fertilization effect, in which elevated CO_2 enhances photosynthesis while reducing water lost via transpiration (Haverd et al., 2020). CO_2-driven enhancement of vegetation productivity provides an important negative feedback on atmospheric CO_2 growth, thus slowing climate change (Bonan, 2008; Walker et al., 2020). Forest productivity and WUE sometimes increase concurrently (Guerrieri et al., 2019), but even when they do not, enhanced WUE may indirectly slow the rate of atmospheric CO_2 growth by improving tree drought tolerance (enabling maintenance of carbon uptake in conditions where it would otherwise decline) and reducing climate-induced tree mortality (Heilman et al., 2021; Kannenberg et al., 2021). These CO_2-driven effects can have major implications for forest productivity, forest climate sensitivity, and water yields from forested catchments.

However, enhanced carbon gain under increasing CO_2 may only occur when other environmental factors, such as climate (Novick et al., 2016) and nutrients (Norby et al., 2010) are not limiting. Further, forecasting forest carbon and water dynamics is complicated by the fact that climate and nutrients may have additive, offsetting or interactive effects on tree growth and WUE (Anderson-Texeira et al., 2013; Levesque et al. 2017; Marchand et al. 2020), and these effects may themselves be mediated at local and individual scales by factors such as topography (Hawthorne & Miniat, 2018), tree size (Brienen et al., 2017; Anderson-Texeira et al., 2021), and forest stand age (Foster et al., 2016). As a result, despite the fact that temperate broadleaf forests are among the most well-studied ecosystem types on Earth (Martin, 2012), their response to

multiple concurrent drivers of change remains uncertain. Identifying dominant controls on forest productivity and water use is essential for reducing uncertainty in estimates of terrestrial carbon uptake and associated vegetation-climate feedbacks (Domke et al., 2018; Le Quéré et al., 2018).

While much of the recent research examining controls on forest productivity and WUE has focused on the effects of climate and CO_2, changes in atmospheric deposition may be overlooked as key drivers of recent tree growth and WUE trends. Atmospheric deposition of sulfur dioxide (SO_2), nitrogen oxides (NO_x), and reduced nitrogen (gaseous NH_3 and aerosol and wet-deposited NH_4^+) – herein referred to as acid deposition – have been major biogeochemical drivers in temperate forested regions of North America, Europe, and East Asia over the last century (Driscoll et al., 2001; Oulehe et al., 2011; Duan et al., 2016). Acid deposition influences tree physiology via both direct and indirect mechanisms. Foliar exposure to acid deposition may result in leaching of foliar nutrients and impairment of stomatal function (DeHayes et al., 1999; Borer et al., 2005). In forests with poorly-buffered soils, chronic acid deposition may result in soil acidification, mobilization of phytotoxic aluminum (Delhaize & Ryan, 1995; Kochian, 1995), and leaching of essential nutrient cations such as calcium (Ca^{2+}), magnesium (Mg^{2+}), and potassium (K^+) (de Vries et al., 2003; Likens et al., 1996). While depletion of soil base cations is associated with declines in forest health and productivity (Demchik & Sharpe, 2000; Long et al., 2009; Sullivan et al., 2013; Battles et al., 2014), N deposition itself often enhances temperate forest productivity (Magnani et al., 2007), depending on the amount and duration of exposure (Thomas et al., 2009, Horn et al., 2018). Disentangling the role of N deposition as an acidifying or fertilizing agent remains an ongoing research challenge.

In the United States, emissions of SO_2 and NO_x have declined 94% and 69%, respectively, between 1970 and 2020 as a result of the implementation of the Clean Air Act

(CAA) of 1963 and its subsequent amendments in 1970, 1977, and 1990 (Figure 1.1). While this legislation has been unequivocally successful at improving air quality (Aldy et al. 2022) – and by extension reduced adverse impacts of direct tree exposure to acid deposition – the legacy of acid deposition on forest soils is projected to be long-lasting. Recent reports suggest that soil base cations are beginning to recover in the northeastern United States, although recovery rates are spatially heterogenous and often slow (Sullivan et al., 2018; Hazlett et al., 2020). Recovery of forest soils may be particularly slow in the mid-Atlantic and southeastern US (Rice et al., 2014; Eng & Scanlon, 2021), where soils have high sulfate (SO_4^-) adsorption capacity, and stream exports of Ca^{2+} and Mg^{2+} continue to exceed weathering rates (Fernandez et al., 2010) at some sites. Biogeochemical models implemented in Great Smoky Mountains National Park watersheds predict continued declines in soil base saturation beyond the year 2150, even under low deposition scenarios (Fakhraei et al., 2016).

This lag between reductions in deposition and recovery of soil base cations suggests that the legacy of deposition on forest soils will be an important control on forest productivity in the next century. CO_2-driven increases in forest productivity, which can increase tree demand for nutrients, may even exacerbate tree nutrient deficiencies (Groffman et al., 2018; Jonard et al., 2015; McLauchlan et al., 2017). In the Northeastern United States, reductions in deposition may have thus far had a greater positive impact on the growth and physiology of species like red spruce (*Picea rubens*), which appear to be particularly sensitive to foliar exposure to acid deposition (DeHayes et al., 1999), as opposed to species like sugar maple (*Acer saccharum*), which may be relatively more sensitive to soil base cation availability (Juice et al., 2006; Long et al., 2011; Bishop et al., 2015). While much of the research on acid deposition impacts on tree physiology in eastern North America has focused on these two species, less is known about how

changes in deposition and related changes in soil nutrients have impacted the growth and physiology of other co-occurring tree species, or how interactive effects of deposition, climate, and CO_2 influence temperate forest water balance.

1.2 Dissertation Objectives and Structure

The objectives of this dissertation research are to examine how atmospheric deposition and climate individually and interactively influence the (1) climate sensitivity, (2) productivity, and (3) WUE of temperate forests of the eastern United States. This work uses a combination of tree ring, catchment hydrology, and remote sensing data from a network of sites ranging from Virginia to Maine. This dissertation is presented in four studies and formatted for peer-reviewed journals. In-text citation and references sections are in the format of the journal *JGR Biogeosciences.*

In **Chapter 2**, titled "Landscape controls on tree climate sensitivity in a montane broadleaf deciduous forest," I utilize remote sensing data to examine when and where temperate broadleaf forests are most sensitive to water stress by examining effects of topography, soil properties, and canopy height on forest climate sensitivity in Shenandoah National Park.

In **Chapter 3**, titled "Assessing temperate forest growth and climate sensitivity in response to a long-term whole-watershed acidification experiment" (published in *JGR Biogeosciences*, 2020), I examine whether experimental N and S additions to a forested watershed alter tree growth and sensitivity to climate in a paired watershed experiment at the Fernow Experimental Forest in West Virginia.

Chapter 4, titled "Soil nutrient manipulation effects on tree growth and intrinsic water use efficiency in midlatitude temperate forests," examines how tree growth and intrinsic water

use efficiency (iWUE) responded to soil nutrient manipulations in three paired watershed experiments in the northeastern United States: Hubbard Brook Experimental Forest, where soil calcium (Ca) was restored to preindustrial levels, and the Bear Brook Watersheds and Fernow Experimental Forest, where soils were acidified via experimental N and S additions for 25+ years.

In **Chapter 5**, titled "Tree functional traits and atmospheric pollution mediate temperate forest response to increasing CO_2" (prepared for submission to *Environmental Research Letters*) I assess trends in, and drivers of, tree iWUE derived from tree ring data in 13 evergreen and broadleaf deciduous species along climate and atmospheric deposition gradients in the eastern United States.

In **Chapter 6,** I summarize the findings of each chapter, discuss implications of the results, and future work to build upon the findings of these studies. Combined, the work presented herein could inform forest management practices related to forest carbon uptake and water yields, and models used to forecast terrestrial carbon, water, and nutrient dynamics, particularly in regions impacted by acid deposition.

Chapter 1 References

Aldy, J. E., Auffhammer, M., Cropper, M., Fraas, A., & Morgenstern, R. (2022). Looking Back at 50 Years of the Clean Air Act. *Journal of Economic Literature*, *60*(1), 179–232. https://doi.org/10.1257/jel.20201626

Anderson-Teixeira, K. J., Miller, A. D., Mohan, J. E., Hudiburg, T. W., Duval, B. D., & DeLucia, E. H. (2013). Altered dynamics of forest recovery under a changing climate. *Global Change Biology*, *19*(7), 2001–2021. https://doi.org/10.1111/gcb.12194

Anderson-Teixeira, K. J., Herrmann, V., Rollinson, C. R., Gonzalez, B., Gonzalez-Akre, E. B., Pederson, N., et al. (2022). Joint effects of climate, tree size, and year on annual tree growth

derived from tree-ring records of ten globally distributed forests. *Global Change Biology*, *28*(1), 245–266. https://doi.org/10.1111/gcb.15934

Battles, J. J., Fahey, T. J., Driscoll, C. T., Blum, J. D., & Johnson, C. E. (2014). Restoring Soil Calcium Reverses Forest Decline. *Environmental Science & Technology Letters*, *1*(1), 15–19. https://doi.org/10.1021/ez400033d

Bishop, D. A., Beier, C. M., Pederson, N., Lawrence, G. B., Stella, J. C., & Sullivan, T. J. (2015). Regional growth decline of sugar maple (Acer saccharum) and its potential causes. *Ecosphere*, *6*(10), art179. https://doi.org/10.1890/ES15-00260.1

Boisenvue, C., & Running, S. W. (2006). Impacts of climate change on natural forest productivity – evidence since the middle of the 20th century. *Global Change Biology*, *12*(5), 862–882. https://doi.org/10.1111/j.1365-2486.2006.01134.x

Bonan Gordon B. (2008). Forests and Climate Change: Forcings, Feedbacks, and the Climate Benefits of Forests. *Science*, *320*(5882), 1444–1449. https://doi.org/10.1126/science.1155121

Borer, C. H., Schaberg, P. G., & DeHayes, D. H. (2005). Acidic mist reduces foliar membrane-associated calcium and impairs stomatal responsiveness in red spruce. *Tree Physiology*, *25*(6), 673–680. https://doi.org/10.1093/treephys/25.6.673

Brienen, R. J. W., Gloor, E., Clerici, S., Newton, R., Arppe, L., Boom, A., et al. (2017). Tree height strongly affects estimates of water-use efficiency responses to climate and CO2 using isotopes. *Nature Communications*, *8*(1), 288. https://doi.org/10.1038/s41467-017-00225-z

Brown, T. C., Hobbins, M. T., & Ramirez, J. A. (2008). Spatial Distribution of Water Supply in the Coterminous United States [1]. *JAWRA Journal of the American Water Resources Association*, *44*(6), 1474–1487. https://doi.org/10.1111/j.1752-1688.2008.00252.x

DeHayes, D. H., Schaberg, P. G., Hawley, G. J., & Strimbeck, G. R. (1999). Acid Rain Impacts on Calcium Nutrition and Forest Health: Alteration of membrane-associated calcium leads to membrane destabilization and foliar injury in red spruce. *BioScience*, *49*(10), 789–800. https://doi.org/10.2307/1313570

Delhaize, E., & Ryan, P. R. (1995). Aluminum Toxicity and Tolerance in Plants. *Plant Physiology*, *107*(2), 315. https://doi.org/10.1104/pp.107.2.315

Demchik, M. C., & Sharpe, W. E. (2000). The effect of soil nutrition, soil acidity and drought on northern red oak (Quercus rubra L.) growth and nutrition on Pennsylvania sites with high and low red oak mortality. *Forest Ecology and Management*, *136*(1), 199–207. https://doi.org/10.1016/S0378-1127(99)00307-2

Domke, G., Williams, C. A., Birdsey, R., Coulston, J., Finzi, A., Gough, C., et al. (2018). Chapter 9: Forests. In Second State of the Carbon Cycle Report (SOCCR2): A Sustained Assessment Report [Cavallaro, N., G. Shrestha, R. Birdsey, M. A. Mayes, R. G. Najjar, S. C. Reed, P. -Romero-Lankao, and Z. Zhu (eds.)]. U.S. Global Change Research Program. Retrieved from https://doi.org/10.7930/SOCCR2.2018.Ch9.

Driscoll, C. T., Lawrence, G. B., Bulger, A. J., Butler, T. J., Cronan, C. S., Eagar, C., et al. (2001). Acidic Deposition in the Northeastern United States: Sources and Inputs, Ecosystem Effects, and

Management Strategies. *BioScience*, *51*(3), 180. https://doi.org/10.1641/0006-3568(2001)051[0180:ADITNU]2.0.CO;2

Drummond, M. A., & Loveland, T. R. (2010). Land-use Pressure and a Transition to Forest-cover Loss in the Eastern United States. *BioScience*, *60*(4), 286–298. https://doi.org/10.1525/bio.2010.60.4.7

Duan, L., Yu, Q., Zhang, Q., Wang, Z., Pan, Y., Larssen, T., et al. (2016). Acid deposition in Asia: Emissions, deposition, and ecosystem effects. *Acid Rain and Its Environmental Effects: Recent Scientific Advances*, *146*, 55–69. https://doi.org/10.1016/j.atmosenv.2016.07.018

Eng, L. E., & Scanlon, T. M. (2021). Comparison of northeastern and southeastern U.S. watershed response to the declines in atmospheric sulfur deposition. *Atmospheric Environment*, *253*, 118365. https://doi.org/10.1016/j.atmosenv.2021.118365

Fakhraei, H., Driscoll, C. T., Renfro, J. R., Kulp, M. A., Blett, T. F., Brewer, P. F., & Schwartz, J. S. (2016). Critical loads and exceedances for nitrogen and sulfur atmospheric deposition in Great Smoky Mountains National Park, United States. *Ecosphere*, *7*(10), e01466. https://doi.org/10.1002/ecs2.1466

Fang, J., Kato, T., Guo, Z., Yang, Y., Hu, H., Shen, H., et al. (2014). Evidence for environmentally enhanced forest growth. *Proceedings of the National Academy of Sciences*, *111*(26), 9527. https://doi.org/10.1073/pnas.1402333111

Fernandez, I. J., Adams, M. B., SanClements, M. D., & Norton, S. A. (2010). Comparing decadal responses of whole-watershed manipulations at the Bear Brook and Fernow experiments. *Environmental Monitoring and Assessment*, *171*(1), 149–161. https://doi.org/10.1007/s10661-010-1524-2

Foster, J. R., Finley, A. O., D'Amato, A. W., Bradford, J. B., & Banerjee, S. (2016). Predicting tree biomass growth in the temperate-boreal ecotone: Is tree size, age, competition, or climate response most important? *Global Change Biology*, *22*(6), 2138–2151. https://doi.org/10.1111/gcb.13208

Frank, D. C., Poulter, B., Saurer, M., Esper, J., Huntingford, C., Helle, G., et al. (2015). Water-use efficiency and transpiration across European forests during the Anthropocene. *Nature Climate Change*, *5*(6), 579–583. https://doi.org/10.1038/nclimate2614

Groffman, P. M., Driscoll, C. T., Durán, J., Campbell, J. L., Christenson, L. M., Fahey, T. J., et al. (2018). Nitrogen oligotrophication in northern hardwood forests. *Biogeochemistry*, *141*(3), 523–539. https://doi.org/10.1007/s10533-018-0445-y

Guerrieri, R., Belmecheri, S., Ollinger, S. V., Asbjornsen, H., Jennings, K., Xiao, J., et al. (2019). Disentangling the role of photosynthesis and stomatal conductance on rising forest water-use efficiency. *Proceedings of the National Academy of Sciences*, *116*(34), 16909. https://doi.org/10.1073/pnas.1905912116

Hawthorne, S., & Miniat, C. F. (2018). Topography may mitigate drought effects on vegetation along a hillslope gradient. *Ecohydrology*, *11*(1), e1825. https://doi.org/10.1002/eco.1825

Hazlett, P., Emilson, C., Lawrence, G., Fernandez, I., Ouimet, R., & Bailey, S. (2020). Reversal of Forest Soil Acidification in the Northeastern United States and Eastern Canada: Site and Soil

Factors Contributing to Recovery. *Soil Systems*, *4*(3). https://doi.org/10.3390/soilsystems4030054

Heilman, K. A., Trouet, V. M., Belmecheri, S., Pederson, N., Berke, M. A., & McLachlan, J. S. (2021). Increased water use efficiency leads to decreased precipitation sensitivity of tree growth, but is offset by high temperatures. *Oecologia*. https://doi.org/10.1007/s00442-021-04892-0

Horn, K. J., Thomas, R. Q., Clark, C. M., Pardo, L. H., Fenn, M. E., Lawrence, G. B., et al. (2018). Growth and survival relationships of 71 tree species with nitrogen and sulfur deposition across the conterminous U.S. *PLOS ONE*, *13*(10), e0205296. https://doi.org/10.1371/journal.pone.0205296

Jonard, M., Fürst, A., Verstraeten, A., Thimonier, A., Timmermann, V., Potočić, N., et al. (2015). Tree mineral nutrition is deteriorating in Europe. *Global Change Biology*, *21*(1), 418–430. https://doi.org/10.1111/gcb.12657

Juice, S. M., Fahey, T. J., Siccama, T. G., Driscoll, C. T., Denny, E. G., Eagar, C., et al. (2006). RESPONSE OF SUGAR MAPLE TO CALCIUM ADDITION TO NORTHERN HARDWOOD FOREST. *Ecology*, *87*(5), 1267–1280. https://doi.org/10.1890/0012-9658(2006)87[1267:ROSMTC]2.0.CO;2

Kannenberg Steven A., Driscoll Avery W., Szejner Paul, Anderegg William R. L., & Ehleringer James R. (2021). Rapid increases in shrubland and forest intrinsic water-use efficiency during an ongoing megadrought. *Proceedings of the National Academy of Sciences*, *118*(52), e2118052118. https://doi.org/10.1073/pnas.2118052118

Keenan, T. F., Hollinger, D. Y., Bohrer, G., Dragoni, D., Munger, J. W., Schmid, H. P., & Richardson, A. D. (2013). Increase in forest water-use efficiency as atmospheric carbon dioxide concentrations rise. *Nature*, *499*(7458), 324–327. https://doi.org/10.1038/nature12291

Kochian, L. V. (1995). Cellular Mechanisms of Aluminum Toxicity and Resistance in Plants. *Annual Review of Plant Physiology and Plant Molecular Biology*, *46*(1), 237–260. https://doi.org/10.1146/annurev.pp.46.060195.001321

Le Quéré, C., Andrew, R. M., Friedlingstein, P., Sitch, S., Hauck, J., Pongratz, J., et al. (2018). Global Carbon Budget 2018. *Earth Syst. Sci. Data*, *10*(4), 2141–2194. https://doi.org/10.5194/essd-10-2141-2018

Levesque, M., Andreu-Hayles, L., & Pederson, N. (2017). Water availability drives gas exchange and growth of trees in northeastern US, not elevated CO2 and reduced acid deposition. *Scientific Reports*, *7*(1), 46158. https://doi.org/10.1038/srep46158

Likens, G. E., Driscoll, C. T., & Buso, D. C. (1996). Long-Term Effects of Acid Rain: Response and Recovery of a Forest Ecosystem. *Science*, *272*(5259), 244. https://doi.org/10.1126/science.272.5259.244

Long, R. P., Horsley, S. B., Hallett, R. A., & Bailey, S. W. (2009). Sugar maple growth in relation to nutrition and stress in the northeastern United States. *Ecological Applications*, *19*(6), 1454–1466. https://doi.org/10.1890/08-1535.1

Lu, X., Kicklighter, D. W., Melillo, J. M., Reilly, J. M., & Xu, L. (2015). Land carbon sequestration within the conterminous United States: Regional- and state-level analyses. *Journal of Geophysical Research: Biogeosciences*, *120*(2), 379–398. https://doi.org/10.1002/2014JG002818

Magnani, F., Mencuccini, M., Borghetti, M., Berbigier, P., Berninger, F., Delzon, S., et al. (2007). The human footprint in the carbon cycle of temperate and boreal forests. *Nature*, *447*(7146), 849–851. https://doi.org/10.1038/nature05847

Marchand, W., Girardin, M. P., Hartmann, H., Depardieu, C., Isabel, N., Gauthier, S., et al. (2020). Strong overestimation of water-use efficiency responses to rising CO2 in tree-ring studies. *Global Change Biology*, *26*(8), 4538–4558. https://doi.org/10.1111/gcb.15166

Martin, L. J., Blossey, B., & Ellis, E. (2012). Mapping where ecologists work: biases in the global distribution of terrestrial ecological observations. *Frontiers in Ecology and the Environment*, *10*(4), 195–201. https://doi.org/10.1890/110154

Mathias, J. M., & Thomas, R. B. (2021). Global tree intrinsic water use efficiency is enhanced by increased atmospheric CO_2 and modulated by climate and plant functional types. *Proceedings of the National Academy of Sciences*, *118*(7), e2014286118. https://doi.org/10.1073/pnas.2014286118

McLauchlan, K. K., Gerhart, L. M., Battles, J. J., Craine, J. M., Elmore, A. J., Higuera, P. E., et al. (2017). Centennial-scale reductions in nitrogen availability in temperate forests of the United States. *Scientific Reports*, *7*(1), 7856. https://doi.org/10.1038/s41598-017-08170-z

McMahon, S. M., Parker, G. G., & Miller, D. R. (2010). Evidence for a recent increase in forest growth. *Proceedings of the National Academy of Sciences*, 200912376. https://doi.org/10.1073/pnas.0912376107

Norby, R. J., Warren, J. M., Iversen, C. M., Medlyn, B. E., & McMurtrie, R. E. (2010). CO_2 enhancement of forest productivity constrained by limited nitrogen availability. *Proceedings of the National Academy of Sciences*, *107*(45), 19368. https://doi.org/10.1073/pnas.1006463107

Novick, K. A., Ficklin, D. L., Stoy, P. C., Williams, C. A., Bohrer, G., Oishi, A. C., et al. (2016). The increasing importance of atmospheric demand for ecosystem water and carbon fluxes. *Nature Climate Change*, *6*(11), 1023–1027. https://doi.org/10.1038/nclimate3114

Oulehle, F., Evans, C. D., Hofmeister, J., Krejci, R., Tahovska, K., Persson, T., et al. (2011). Major changes in forest carbon and nitrogen cycling caused by declining sulphur deposition. *Global Change Biology*, *17*(10), 3115–3129. https://doi.org/10.1111/j.1365-2486.2011.02468.x

Rice, K. C., Scanlon, T. M., Lynch, J. A., & Cosby, B. J. (2014). Decreased Atmospheric Sulfur Deposition across the Southeastern U.S.: When Will Watersheds Release Stored Sulfate? *Environmental Science & Technology*, *48*(17), 10071–10078. https://doi.org/10.1021/es501579s

Sullivan, T. J., Lawrence, G. B., Bailey, S. W., McDonnell, T. C., Beier, C. M., Weathers, K. C., et al. (2013). Effects of Acidic Deposition and Soil Acidification on Sugar Maple Trees in the Adirondack Mountains, New York. *Environmental Science & Technology*, *47*(22), 12687–12694. https://doi.org/10.1021/es401864w

Sullivan, Timothy J., Driscoll, C. T., Beier, C. M., Burtraw, D., Fernandez, I. J., Galloway, J. N., et al. (2018). Air pollution success stories in the United States: The value of long-term observations. *Environmental Science & Policy*, *84*, 69–73. https://doi.org/10.1016/j.envsci.2018.02.016

Thomas, Q. R., Canham, C. D., Weathers, K. C., & Goodale, C. L. (2010). Increased tree carbon storage in response to nitrogen deposition in the US. *Nature Geoscience*, *3*(1), 13–17. https://doi.org/10.1038/ngeo721

de Vries, W., Reinds, G. J., & Vel, E. (2003). Intensive monitoring of forest ecosystems in Europe: 2: Atmospheric deposition and its impacts on soil solution chemistry. *Forest Ecology and Management*, *174*(1), 97–115. https://doi.org/10.1016/S0378-1127(02)00030-0

Walker, A. P., De Kauwe, M. G., Bastos, A., Belmecheri, S., Georgiou, K., Keeling, R. F., et al. (2021). Integrating the evidence for a terrestrial carbon sink caused by increasing atmospheric CO2. *New Phytologist*, *229*(5), 2413–2445. https://doi.org/10.1111/nph.16866

Chapter 2. Landscape controls on tree climate sensitivity in a montane broadleaf deciduous forest

Abstract

Moisture stress driven by climate change is projected to reduce temperate forest carbon uptake and storage, but when and where forests are most vulnerable to drought stress remains unclear, particularly in complex terrain. In this study we examined topographic, edaphic, species, and canopy height effects on forest climate sensitivity in Shenandoah National Park (Virginia, USA), where complex terrain generates environmental gradients that may buffer some forest communities from moisture stress. Climate sensitivity was defined as the standardized slope of the relationship between enhanced vegetation index (EVI) and precipitation or vapor pressure deficit (VPD). Precipitation and VPD in the early to mid-growing season had the strongest effects on mean growing season EVI. Overall, VPD was a stronger control on EVI than precipitation – we found positive relationships between EVI and precipitation in 64% of pixels, and negative relationships between EVI and VPD in 87% of pixels, and the mean sensitivity to VPD was roughly three times greater than the sensitivity to precipitation. Topography, soil properties, and canopy height explained relatively little variation in climate sensitivity across the landscape, but we observed modestly greater sensitivity in taller tress and trees growing on deeper soils, and lower climate sensitivity in areas with high topographic wetness index. EVI sensitivity to VPD was negative for all forest species communities examined. Our results suggest that VPD is a more important control on vegetation productivity than precipitation, and that projected increases in VPD will reduce productivity of montane forest trees, regardless species or position on the landscape.

2.1 Introduction

Temperate forests of the eastern United States are an important carbon sink, accounting for approximately two-thirds of terrestrial carbon uptake in the conterminous US (Lu et al., 2015). While removal of atmospheric CO_2 by forests is a critical negative feedback on climate change (Bonan et al., 2008; Pan et al., 2011), forest productivity is itself sensitive to changes in climate – evidence from tree ring (Helcoski et al., 2019; Anderson-Texeira et al., 2021), eddy-covariance (Baldocchi et al., 2018; Sulman et al., 2016), and remote sensing studies (Li & Xiao, 2020; Maurer et al., 2020; Yuan et al., 2019) indicate that temperate forest productivity tends to be positively related to growing season water availability and negatively associated with growing season temperature. Despite these relatively well-established growth-productivity relationships, how the strength of temperate forest carbon sinks – and associated vegetation-climate feedbacks – will respond to future changes in hydroclimate conditions remains a major source of uncertainty in Earth Systems Models (Arora et al., 2020; Le Quéré et al., 2018).

Much of this uncertainty stems from how forests will respond to increasing moisture stress (Kennedy et al., 2019; Swann et al., 2016). Temperate forest productivity in eastern North America tends to increase with growing season precipitation, even in humid forests that receive high rainfall (Brzostek et al., 2014; Elliott et al., 2015; Martin-Benito & Pederson, 2015; Helcoski et al., 2019). Models project more variable precipitation globally in the next century, including in the eastern United States (Pendergrass et al., 2017), which would likely reduce temperate forest productivity even if mean precipitation does not change (Medvigy et al., 2010; Ritter et al., 2020). Precipitation timing is also an important control on forest productivity – in eastern North America, effects of drought on tree growth are most severe when the drought occurs early in the growing season (D'Orangeville et al., 2018).

Mean annual temperature has risen in temperate montane regions of the eastern US in recent decades (Hwang et al., 2020) and is projected to increase throughout the next century (Robison & Scanlon, 2018). Tree response to increased temperature depends on seasonal timing, as well as humidity. In the eastern US, warmer spring temperatures have been shown to enhance growing season productivity (Richardson et al., 2009; Keenan et al., 2014). However, warmer temperatures also drive higher VPD, the difference between the saturation water vapor pressure (e_s) and actual vapor pressure (e_a). VPD is projected to increase during the growing season across the continental United States in the 21st century, driven primarily by a faster rate of temperature-driven increases in e_s as compared to e_a (Ficklin & Novick, 2017). Plants typically reduce stomatal conductance under increased VPD in order to minimize water loss (Grossiord et al., 2020), and as a result, VPD can limit gross primary production (GPP) even when soil moisture is plentiful (Novick et al., 2016; Sulman et al., 2016).

Predicting the impacts of climate change on forests is particularly complicated in mountainous terrain, where topography generates microclimates that can be decoupled from regional conditions (Elliott et al., 2015), and flux towers cannot reliably estimate land-atmosphere carbon exchange (Baldocchi, 2003). In the Appalachian Mountains of the eastern United States, environmental gradients have long been recognized as important determinants of forest structure, function, and composition (Whittaker, 1956). Environmental variables that influence forest productivity, including precipitation, temperature, solar radiation, and soil depth and texture vary along topographic gradients, typically resulting in mesic to xeric gradients from coves to ridges (Yeakley et al., 1998; Tromp-van Meerveld & McDonnell, 2006). This pattern is driven by topographic shading and lateral redistribution of soil water within catchments, which can provide water subsidies to downslope trees, both enhancing productivity and reducing

sensitivity to hydroclimate variability (Elliott et al., 2015, Dymond et al., 2015; Tai et al., 2021). Complex terrain may thus provide hydrologic refugia that buffers plants against drought stress (McLaughlin et al., 2017).

Tree height often varies along topographic gradients, and may also independently influence tree climate sensitivity. In complex terrain, tree canopy height and aboveground biomass are often greatest on concave hillslopes where trees have greater access to water (Swetnam et al., 2017; Hoylman et al., 2018), even in humid forests where trees are generally not considered to be moisture-limited (Detto et al., 2013; Hawthorne & Miniat, 2018). Taller trees have been found to be more sensitive to water stress and drought-induced mortality, owing to greater gravitational and xylem resistance on canopy conductance (McDowell et al., 2015; Stovall et al., 2019). Canopies of trees that are taller than their neighbors may experience microclimates with higher wind speeds and VPD, which could exacerbate water stress (Kunert et al., 2017; McGregor et al., 2021). On the other hand, large trees may have better access to water due to their more extensive root systems (Enquist et al., 2002), and tree intrinsic water use efficiency tends to increase with tree height (Breinen et al., 2017; Vadeboncoeur et al., 2020) – either of these mechanisms could reduce tree sensitivity to low soil water supply or increased atmospheric demand. While much of the research on tree height – climate sensitivity relationships has focused on boreal, semi-arid, and tropical forests (Bennett et al., 2015), relatively few studies have been conducted in eastern North America (but see McGregor et al., 2021), and even fewer have examined relationships between temperate deciduous tree height and climate sensitivity along topographic gradients.

In this study, we examined how the montane mixed deciduous forests of Shenandoah National Park (SNP) in Virginia, USA, respond to interannual variability in hydroclimate

conditions, and also how topography, soil properties, and tree height influence climate sensitivity across the landscape. Climate sensitivity was defined as the standardized slope of the relationship between Enhanced Vegetation Index (EVI), a widely-used proxy for vegetation productivity (Huang et al., 2019; Sims et al., 2006), and growing season climate variables (precipitation and VPD). Our objectives were to:

1) Identify the time range in which climate variables have the greatest impact on growing season (June-September) EVI;
2) Assess whether EVI is more sensitive to precipitation or VPD;
3) Examine the influence of topography, soil properties, species composition, and canopy height on forest climate sensitivity

We hypothesized that VPD would negatively impact growing season EVI, while precipitation would positively impact EVI. We also hypothesized that trees in downslope topographic positions, which receive more lateral subsurface water subsidies, would be less sensitive to interannual variation in climate. Finally, we hypothesized that tree height would vary along topographic gradients, and that tall trees would be more sensitive to interannual climate than short trees. This work has potential identify both when and where trees in humid temperate montane forests are most vulnerable to projected future increases in moisture stress.

2.2 Methods

2.1 Shenandoah National Park

Shenandoah National Park, in the Blue Ridge Mountains of northwestern Virginia, USA, covers 79,246 ha of mostly forested land. Elevation in the park ranges from ~150 to ~1200 m and the climate is classified as humid continental (Köppen zone Dfa) with mean annual temperatures ~12°C in the lowlands and ~9°C in high elevation areas. Precipitation is evenly

distributed throughout the year (Sullivan et al., 2003). SNP has three major geologic classes: felsic, mafic, and siliciclastic. Soils overlaying these bedrock types vary in their base saturation from base-poor (siliciclastic) to intermediate (felsic) to base-rich (mafic; Riscassi et al., 2018; Young et al., 2006; Figure 1). Forests are mostly secondary, owing to a mix of land uses including agriculture, logging, and human settlement prior to the establishment of the National Park in 1935 (Reich, 2001). Complex interactions of topography, lithology, microclimate, and disturbance history have shaped species composition in SNP (Young et al., 2006). Oaks (*Quercus montana, Quercus rubra*), tulip poplar (*Liriodendron tulipifera*), maples (*Acer rubrum, Acer saccharum*), birches (*Betula alleghaniensis, Betula lenta*), and black gum (*Nyssa sylvatica* Marshall) are the dominant tree species, with significant contributions of ash (*Fraxinus americana, F. pennsylvanica*), and hickory species (*Carya glabra*, *Carya cordiformis, Carya tomentosa, Carya ovalis*, *Carya ovata*) to forest composition (Cass et al, 2012). Conifers are less abundant, but are present in low quality sites on rocky outcrops (*Pinus rigida, Pinus pungens*), and in coves (*Pinus strobus, Tsuga canadensis*). Disturbances such as fires (Flatley et al., 2011) and invasive insects and pathogens (Anderson-Texeira et al., 2021) are important drivers of forest productivity, structure, and composition in SNP. Between 2000-2019, nearly one-third of park lands experienced fires of varying severity, and large areas of the park have experienced *Lymantria dispar* (spongy moth) defoliation events since 1950 (Asaro et al., 2015; Manderino et al., 2014; Figure S1).

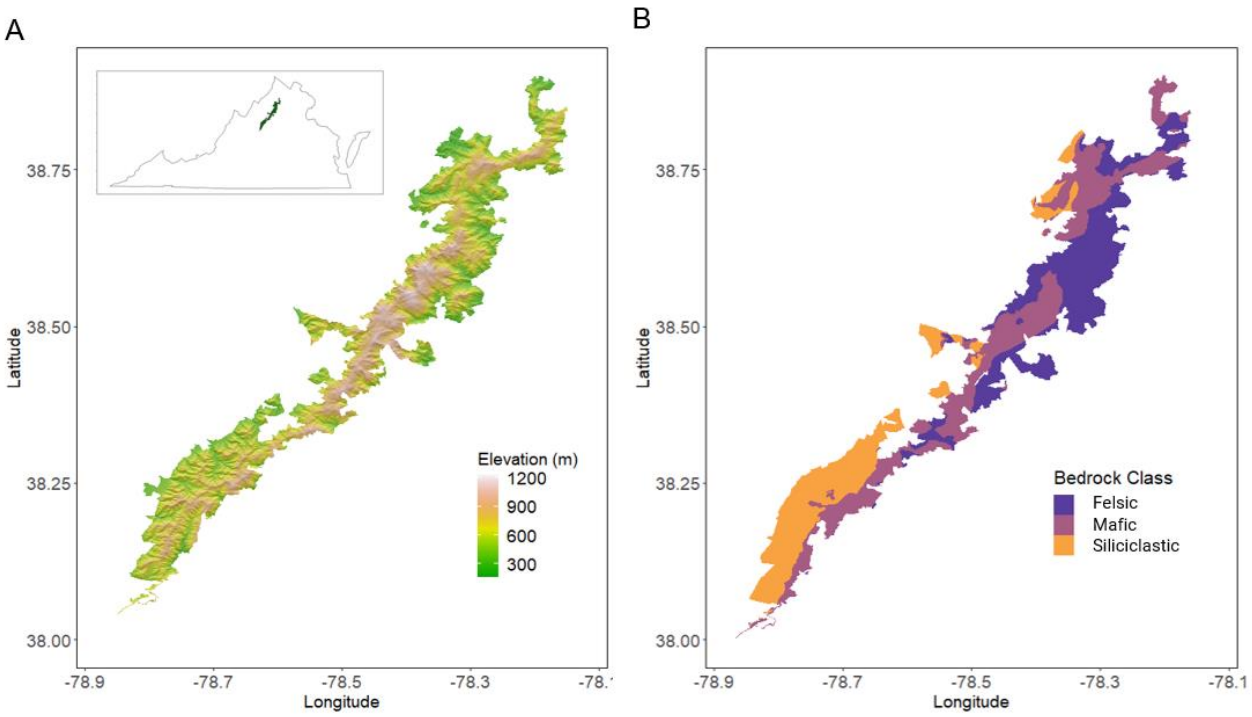

Figure 2.1 Elevation (A) and bedrock lithology (B) in Shenandoah National Park. The inset in panel A shows the location of Shenandoah in Virginia, USA.

2.2 Enhanced Vegetation Index (EVI) Calculation

EVI, an index of vegetation greenness, was selected as a surrogate for vegetation productivity (Rhaman et al., 2005; Sims et al., 2006). EVI was selected instead of the normalized difference vegetation index (NDVI), another commonly used proxy for vegetation productivity, because it may be less influenced by atmospheric aerosols than NDVI, and, because it includes blue band reflectance, may also be more sensitive to subtle variations in canopy greenness (Huete et al., 2002). EVI is calculated as:

$$EVI = G\frac{NIR - R}{NIR + C_1R - C_2B + L}$$

where G is the gain factor, NIR is near infrared band reflectance, R is red band reflectance, C_1 (6) and C_2 (7.5) are coefficients that correct for effects of aerosols on the red and blue bands, and L is the soil adjustment factor (Huang et al., 2019).

EVI was calculated using HISTARFM, a Landsat-MODIS fusion surface reflectance product that combines Landsat and MODIS surface reflectance data to generate gap-free, monthly surface reflectance data at 30 meter spatial resolution for the continental United States (Moreno-Martinez et al., 2020). High spatial resolution and gap-free data in monthly time steps make HISTARFM ideal for detecting changes in EVI in highly heterogeneous montane environments, and in environments where cloud cover may result in large gaps in Landsat data (although MODIS EVI data can also be susceptible to cloud interference – see Maeda et al., 2014). Currently, HISTARFM data are available on Google Earth Engine from 2009-2019.

2.3 Topography, Soils, and Bedrock Data

Elevation, slope, and aspect were derived from a 1/3 arc second (~10 meter) digital elevation model and resampled to HISTARFM resolution. Topographic wetness index (TWI), a steady-state soil moisture index, was calculated in SAGA GIS software using a multiple flow-routing algorithm (Sorensen et al, 2006; Kopecky et al., 2010). Solar radiation data for Julian Date 183 was calculated using the Area Solar Radiation tool in ArcMap version 10.8 and assumed to be indicative of total insolation received in each pixel throughout the year.

Soil percent clay, silt, and sand, depth to bedrock, and available water storage (0-150cm), were acquired from the gridded Soil Survey Geographic (gSSURGO) database (Soil Survey Staff, 2021). These variables were selected to represent soil texture and depth, both of which can

influence plant available water and thus may modulate vegetation climate sensitivity. Bedrock lithology data for SNP were acquired from the USGS Virginia Geological Map (USGS, 2005).

2.4 Vegetation and Forest Canopy Height Data

I used vegetation class data from a vegetation classification dataset that used Landsat and AVIRIS hyperspectral data to identify vegetation communities in SNP (Young et al., 2006). This survey identified 34 distinct vegetation communities within SNP, and spectral classification was verified with field plots, yielding an overall accuracy of 67%. Six vegetation communities covered 76% of the area of SNP, and pixels in these six types were subset in subsequent analyses (Table S2.1). Forest canopy height data was acquired from the GEDI (Global Ecosystem Dynamics Investigation) L2A product downloaded from Google Earth Engine. The GEDI instrument detects waveform LiDAR energy return from the ground surface to provide information about canopy height and vertical structure within a ~25 m footprint for each observation. GEDI collects data along eight parallel tracks separated by 60 m along track and 600 m across track. Here we define canopy height as relative height 95 (RH95), or 95% of the distance between the highest energy return and the ground return. Only pixels with a quality flag of 1, and data collected by one of the four GEDI "power beams," which are more sensitive in dense forests (Dubaya et al., 2020), were selected for further analysis. We also filtered pixels where canopy height was <5 and >50 m to ensure that we were not including non-forest pixels or pixels where data artifacts (*e.g.*, inaccurate surface elevation) resulted in unrealistically high estimates of canopy height.

2.5 Climate Sensitivity Analyses

We define forest climate sensitivity as the standardized slope of the relationship between EVI and a given climate variable. Forest climate sensitivity was calculated in Google Earth Engine using EVI derived from HISTARFM data and 4-kilometer gridded precipitation and VPD data from PRISM (PRISM Climate Group, 2004). EVI and climate variables were first standardized, and then the slopes of linear regression models assessing the relationship between EVI and each climate variable between 2009-2019 were calculated for each pixel. Several steps were taken to ensure that calculations were performed only on forested pixels, and to minimize effects of disturbances on EVI-climate sensitivity estimates. First, EVI was calculated for all pixels within SNP classified as deciduous, evergreen, or mixed forest according to the National Land Cover Database (NLCD). Pixels where documented fires or insect defoliation events have occurred since 2000 were masked in order to avoid potentially confounding effects of disturbance on EVI. We also filtered pixels in the upper 90th percentile of EVI temporal standard deviation across years, in order to minimize potential impacts of undocumented disturbances, such as ice storms, on climate sensitivity estimates. After applying these filters, approximately 750,000 pixels met criteria in SNP.

In order to determine the climate that is most influential on growing season EVI, we compared mean landscape-scale sensitivity to precipitation and VPD using EVI from June-September (the core growing season months) and all 15 combinations of climate windows with consecutive months between May and September (*i.e.*, May, May-June, May-July, May-August, etc.). Sensitivities were compared among different EVI-climate windows using analysis of variance (ANOVA), and pairwise comparisons were tested using Tukey's honest significant difference (HSD) tests.

2.6 Topographic, soil, species, and canopy height controls on climate sensitivity

For analyses of biophysical controls on forest climate sensitivity, we used a subset of data that was masked for disturbances, filtered to include the six vegetation classes that comprise 76% of SNP area, and included only the three most common bedrock types. Since we were specifically interested in examining links between tree height and climate sensitivity, we further subset the data to include only pixels where GEDI RH95 data were available (n=7094). To assess controls on climate sensitivity, we fit separate multiple regression models with EVI-precipitation and EVI-VPD sensitivity as dependent variables, respectively, and elevation, solar radiation, topographic wetness index, percent clay, and depth to bedrock as predictor effects. These variables were selected because of their potential effects on atmospheric demand for water (solar radiation), soil moisture (TWI and depth to bedrock), and soil texture (percent clay), which influences soil porosity and thus plant available water. We also fit a multiple regression model assessing how topography and soil variables influence tree height. Multicollinearity was assessed for each model, and in all cases, the variance inflation factor was <2. Normality of residuals and homogeneity of variance were verified using QQ plots and residuals vs. leverage plots.

For categorical variables (vegetation type and bedrock class), we compared EVI sensitivity to precipitation and VPD using ANOVA and Tukey's HSD tests. To more explicitly compare whether species communities differ in climate sensitivity depending on hydrotype (mesophytic or xerophytic; Elliott et al., 2017), we also separately compared a subset of data between two vegetation communities dominated by xerophytic species (Low Elevation Chestnut Oak and Montane Oak-Hickory), and two communities dominated by mesophytic species (Southern Appalachian Cove and Successional Tuliptree). This analysis was performed in order to gain a broader understanding of hydrotype effects on forest climate sensitivity, with the

acknowledgement that these communities may include species with a diverse range of hydraulic traits and drought tolerances.

2.3 Results

3.1 EVI sensitivity to precipitation and VPD

Across all pixels, we found significant differences in EVI sensitivity to climate depending on the temporal climate window examined. We found that June-September EVI was most positively sensitive to precipitation from May-July, and EVI was most negatively sensitive to VPD from May-August. Tukey's pairwise comparisons revealed that the effects of climate during those time windows were significantly greater than any other time period examined for each climate variable (Figure 2.2). Differences in the mean EVI sensitivity to VPD were very similar between May-July and May-August (mean ± 99% confidence interval =-0.3437 ± 0.009 and -0.3456 ± 0.01, respectively). This suggests high VPD conditions in August have a small, but significant influence on late growing season EVI. However, given the similarity in EVI sensitivity to VPD between these two time windows, subsequent analyses in this study used May-July VPD to align with the precipitation sensitivity analyses.

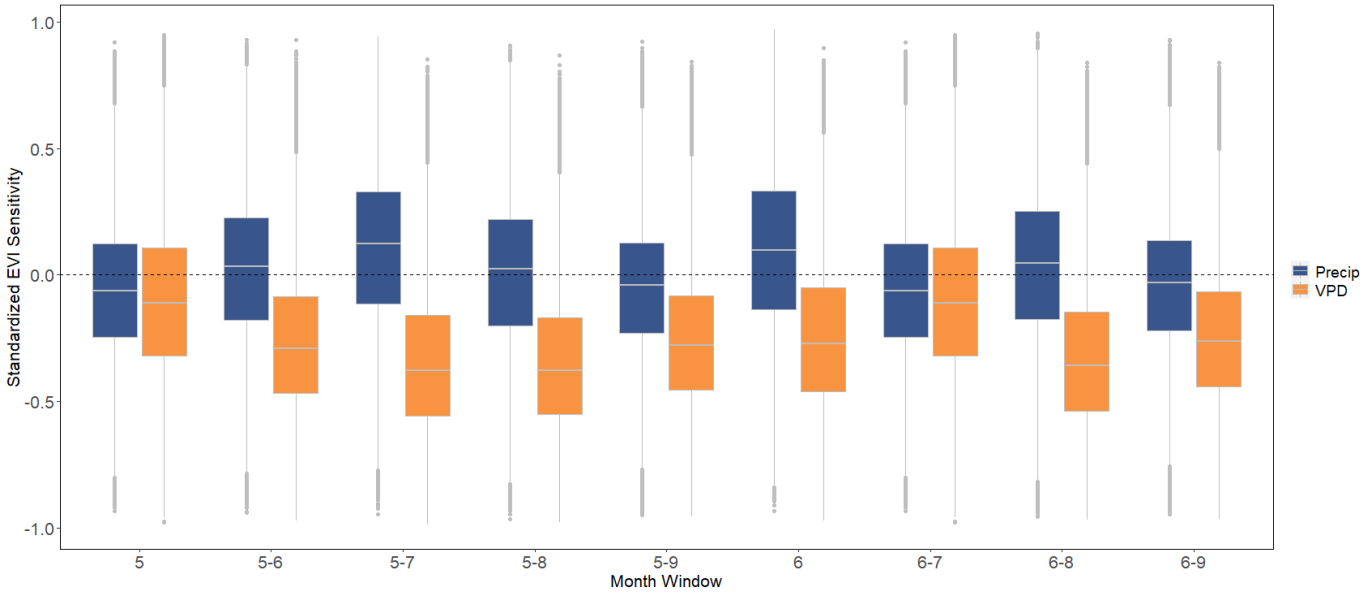

Figure 2.2 Standardized EVI sensitivity to precipitation and VPD assessed for different month ranges from 2009-2019. Numbers on x-axis represent month ranges examined. May-July climate (5-7) were ultimately selected for subsequent analyses because they had the highest average precipitation sensitivity and second-lowest average VPD sensitivity. 5=May, 5-6=May-June, 5-7=May-July, 5-8=May-August, 5-9=May-September, 6=June, 6-7=June-July, 6-8=June-August, and 6-9=June-September.

Mean EVI sensitivity to both precipitation and VPD was significantly different from zero across all pixels, indicating that both climate variables influence vegetation greenness. However, we observed positive relationships between EVI and precipitation in 64% of pixels, and negative relationships between EVI and VPD in 87% of pixels, and the mean absolute magnitude of negative responses to VPD (-0.3437 ± 0.009) was more than three times greater than the mean magnitude of positive responses to precipitation (0.09834 ± 0.001). While there was considerable variability in EVI responses to precipitation across the SNP landscape, EVI response to VPD was more homogeneous (Figure 2.3). Notably, there was a negative correlation between EVI sensitivity to VPD and EVI sensitivity to precipitation (Figure 2.4).

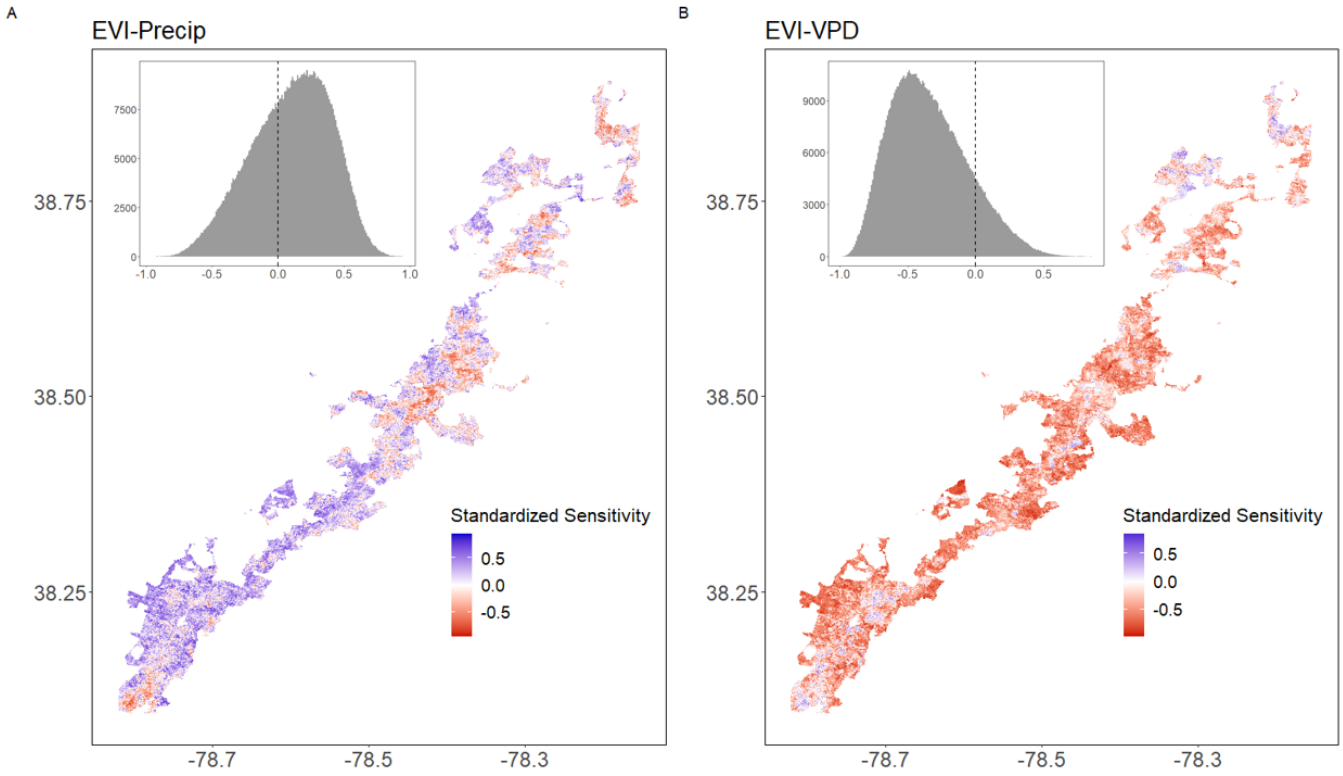

Figure 2.3 Standardized climate sensitivities of June-September EVI to May-July precipitation (A) and vapor pressure deficit (B) from 2009-2019. Pixels where fires or insect defoliation events have occurred are masked, as are pixels in the upper 90th percentile of EVI standard deviation. Histograms in the insets show distributions of standardized sensitivity data, with dashed lines at zero to aid visualization of positive and negative values.

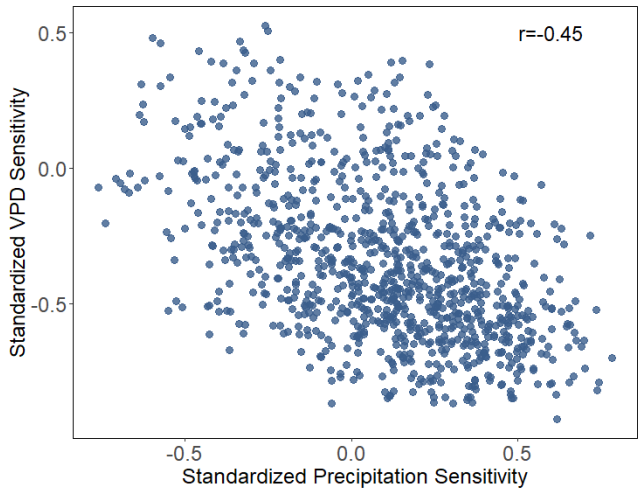

Figure 2.4 Correlation between 1000 randomly sampled standardized VPD and precipitation sensitivity observations. Pearson correlation coefficient (r) was calculated for the entire data set.

3.2 Effects of topography, soil properties, and canopy height on forest climate sensitivity

In general, multiple linear regression models including a suite of topographic, soil, and canopy height predictors poorly explained variance in forest climate sensitivity across the landscape, with R^2 values of 0.03 for both precipitation and VPD sensitivity models (Figure 2.5). Nonetheless, a variety factors had small but significant effects on precipitation and VPD sensitivity. EVI sensitivity to precipitation was negatively associated with elevation and TWI, but positively associated with tree height, percent clay, and depth to bedrock, but the effects of solar radiation were not significant (Figure 2.5, Tables S2.2 & S2.3). EVI sensitivity to VPD was negatively associated with TWI, solar radiation, tree height, and depth to bedrock (Figure 2.5, Tables S2.2 & S2.3). Notably, some of the factors (TWI, RH95, bedrock depth) had opposite effects on precipitation and VPD sensitivities. Categorizing aspect into eight bins of equal widths, we found a pattern showing that EVI sensitivity to VPD was highest (most negative) on south and southwest-facing slopes, and lowest (closer to zero) on north and east-facing slopes (Figure 2.6), indicating that negative effects of VPD on EVI are most severe on high-energy slopes. Overall, results provide only weak evidence that topographic, edaphic, or forest structural factors influence forest climate sensitivity.

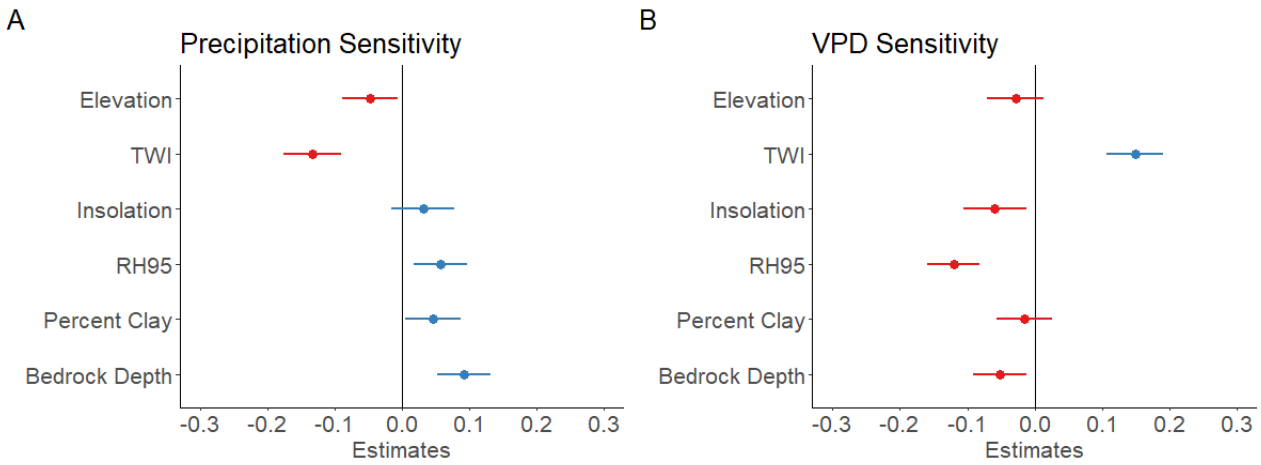

Figure 2.5 Standardized estimates from multiple regression models examining the effects of topography, soil properties, and canopy height on EVI sensitivity to precipitation (A) and VPD (B). Error bars represent 95% confidence intervals. Effects are significant when the confidence interval does not overlap zero. R^2=0.03 for the precipitation sensitivity model ($p<0.0001$), and R^2=0.03 for the VPD sensitivity model ($p<0.0001$).

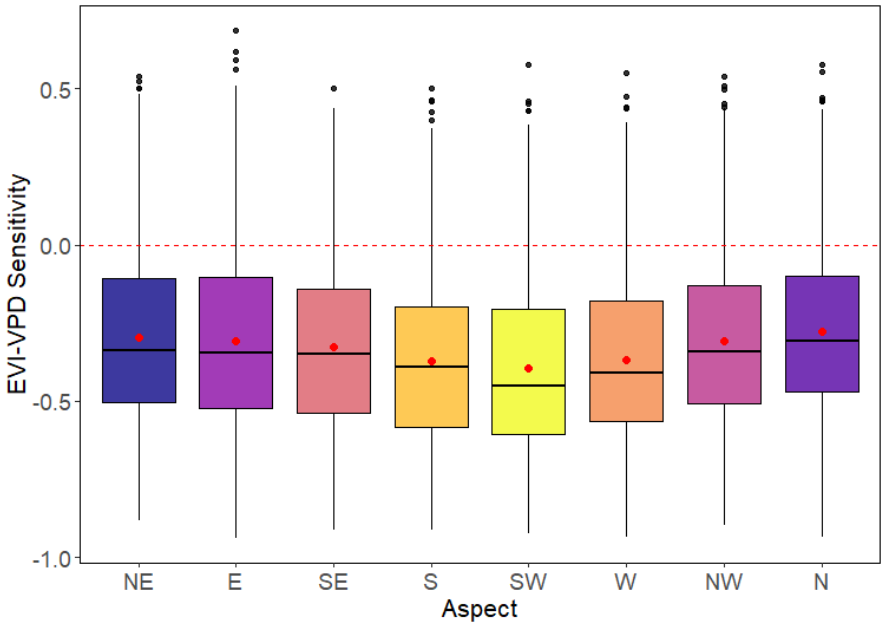

Figure 2.6 Standardized EVI sensitivity to May-July VPD across aspect classes. Dark lines in boxes represent median values, and red dots represent means. Lighter colors represent aspects that receive more solar radiation, not accounting for topographic shading. Aspects were binned into equal 45-degree categories.

3.3 Climate sensitivity across vegetation and bedrock classes

Across the six vegetation classes comprising 76% of the area of SNP, we observed mostly significant positive effects of precipitation on EVI, and negative effects of VPD on EVI. The only exception was Early Successional Forests, in which precipitation sensitivity was not significantly different from zero (Figure 2.7). Similar to our climate window analyses, negative effects of VPD on EVI were stronger than positive effects of precipitation on EVI across all vegetation classes. Comparison of EVI sensitivity to precipitation and VPD between two vegetation classes dominated by mesophytic species (Southern Appalachian Cove and Successional Tuliptree) and two vegetation classes dominated by more xerophytic species (Low Elevation Chestnut Oak and Montane Oak-Hickory) revealed that mesophytic communities were less sensitive to precipitation but more sensitive to VPD compared to xerophytic communities (Figure 2.8). However, sensitivity to precipitation and VPD differed from zero for both hydrotype communities.

We observed significant differences in EVI sensitivity to precipitation across the three major bedrock classes in SNP, but tree responses to VPD did not differ across bedrock types (Figure S2.2). Soils overlaying these bedrock types differ in their base cation availability, but nutrients did not appear to be the driver of differences in precipitation sensitivity – EVI sensitivity to precipitation was highest in forests growing on felsic bedrock, which have intermediate base availability, and did not differ between base-rich mafic and base-poor siliciclastic bedrock (Figure S2.2).

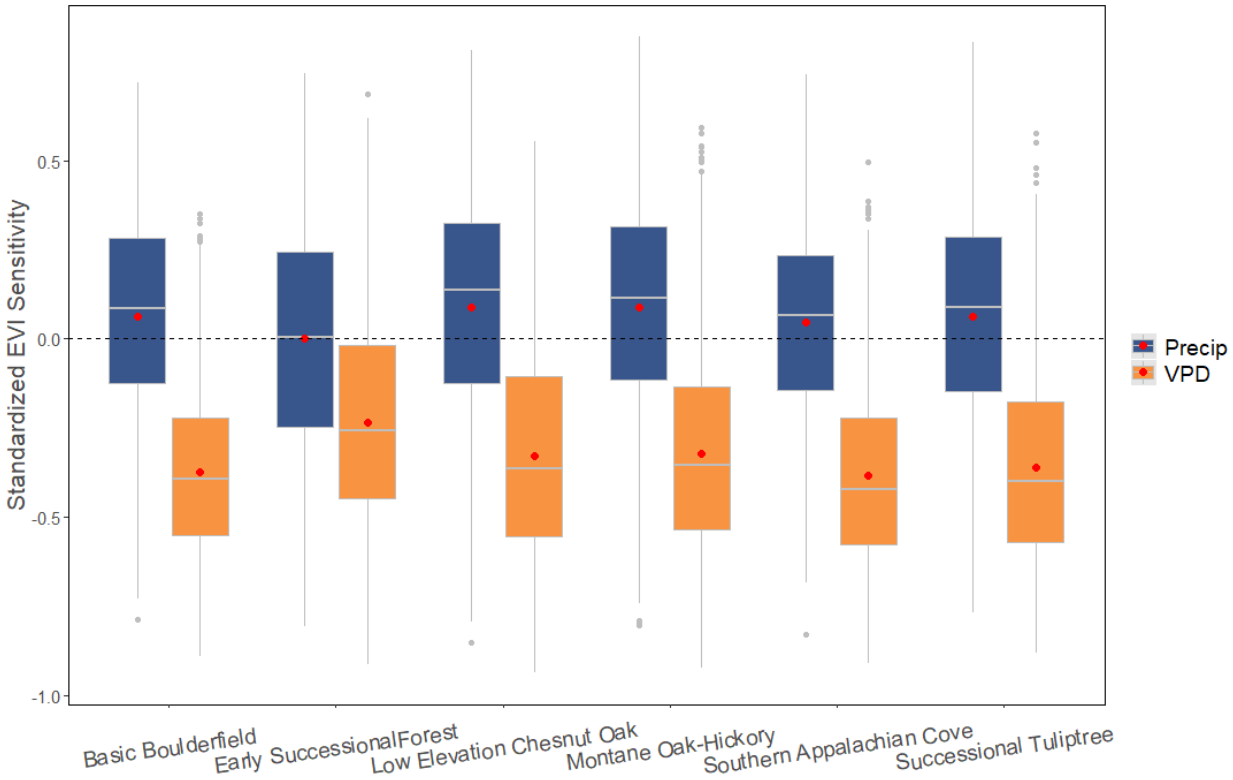

Figure 2.7 Standardized EVI climate sensitivity for the six most common vegetation classes in SNP. Grey horizontal lines represent median values and dots represent mean values. All means differed from zero except precipitation sensitivity of Early Successional forests. See Supplement Table 2.1 for more detailed descriptions of vegetation types, and Supplemental Table S2.5 and S2.6 for model output comparing climate sensitivity across vegetation classes.

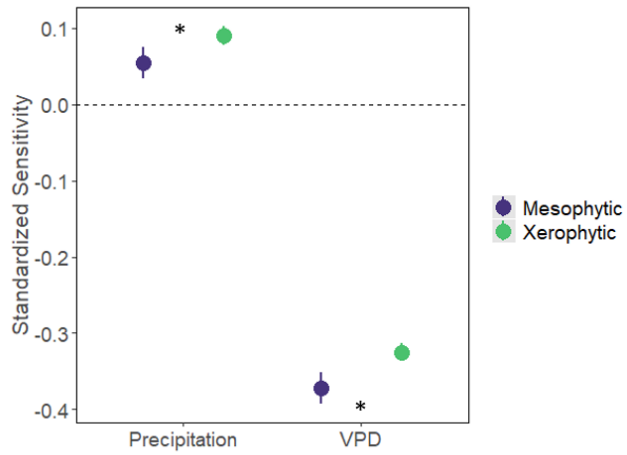

Figure 2.8 Comparison of EVI sensitivity to precipitation and VPD between two vegetation classes dominated by mesophytic species (Southern Appalachian Cove and Successional

Tuliptree) compared to two vegetation classes dominated by more xerophytic species (Low Elevation Chestnut Oak and Montane Oak-Hickory). Asterisks indicate $p<0.001$.

3.4 Landscape patterns in forest canopy height

Canopy height, estimated by RH95, varied across topographic gradients and forest species communities. Canopy height was greater on more light and energy-limited North and East-facing slopes, and shortest on Southwest-facing slopes, where there may be less competition for light (Figure 2.9). There were proportionally more trees in taller canopy classes (>30 m) growing on more energy-limited slopes as well (Figure 2.9). Canopy height differed across species communities, with the tallest trees growing in Successional Tuliptree and Southern Appalachian Cove communities, and the shortest canopies in Low Elevation Chestnut Oak and Basic Boulderfield Forest communities (Figure 2.9). A multiple regression model including topographic and edaphic variables explained substantially more variance in canopy height than for climate sensitivity ($R^2=0.16$, $p<0.0001$). We found significant negative associations between canopy height and elevation and solar radiation, and positive associations between canopy height and TWI, depth to bedrock, and percent clay (Figure 2.10). Combined, differences in canopy height across aspect classes, and the strong negative effect of solar radiation on canopy height, suggest that energy availability is an important control on canopy height at the landscape scale.

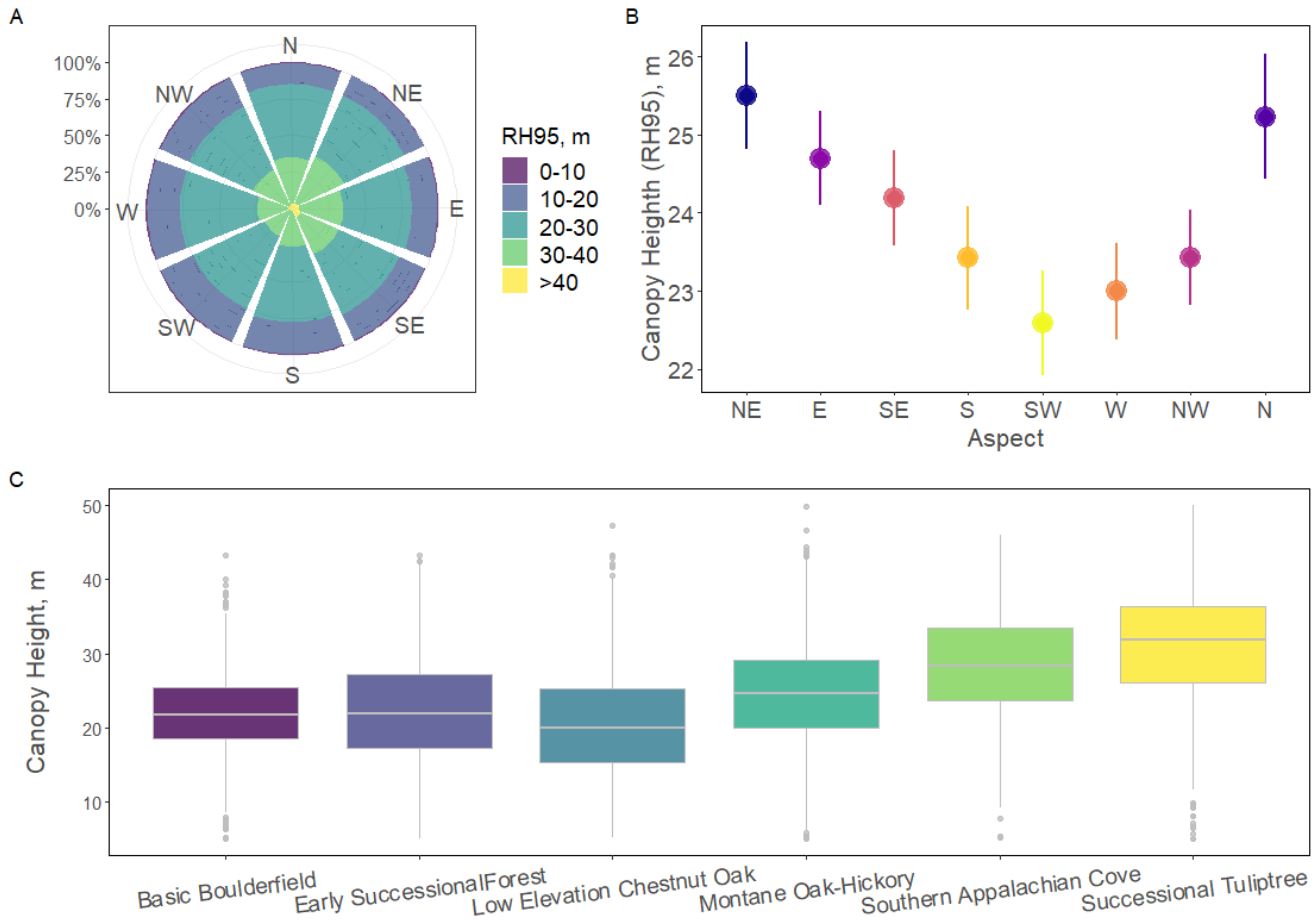

Figure 2.9 Proportions of canopy height classes by aspect (A), mean canopy heights ±99% confidence intervals by aspect class (B), and canopy height distributions across the six most common vegetation classes in SNP.

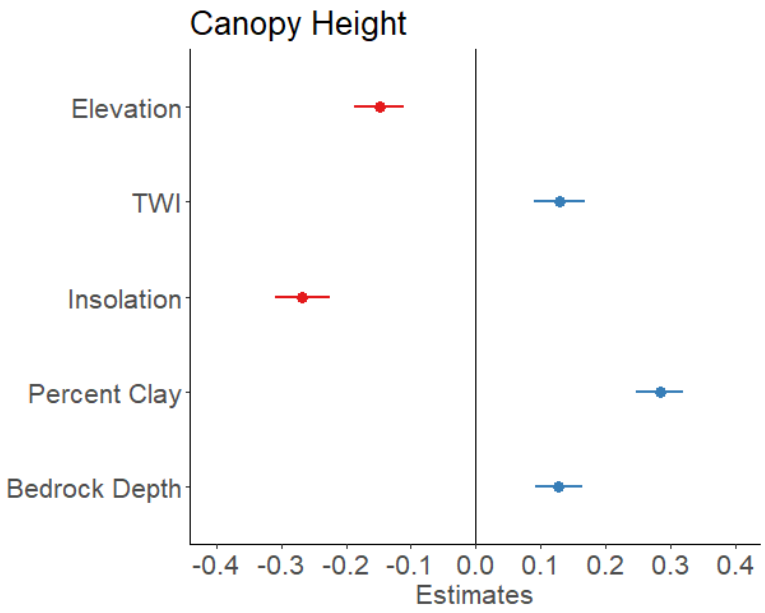

Figure 2.10 Standardized estimates from multiple regression model examining the effects of topography, and soil properties on canopy height (RH95). Error bars represent 95% confidence intervals. Effects are significant when the confidence interval does not overlap zero. R^2=0.16, p<0.0001.

2.4 Discussion

In montane environments, gradients in soil moisture, solar radiation, and soil properties are important determinants of forest structure, function, and composition (Hawthorne & Miniat 2018; Hwang et al., 2020; Reyes et al., 2018; Swetnam et al., 2017; Whittaker et al., 1956). In this study I evaluated the sensitivity of temperate montane forest trees to interannual variation in climate, and assessed topographic, edaphic, and forest structural controls on the spatial variability of climate sensitivity in the topographically complex landscape of Shenandoah National Park. EVI, a variable that reflects canopy leaf area and greenness, was used as a proxy for forest productivity. I found climate conditions in the early to mid-growing season have the greatest impact on EVI throughout the growing season, and that EVI is more sensitive to VPD than precipitation. Forest climate sensitivity differed across vegetation communities, and was

modulated by topography, soil properties, and canopy height. However, these variables poorly explained variance in climate sensitivity across the landscape. The ubiquity of negative EVI responses to VPD across the landscape suggests that environmental gradients may play a limited role in buffering forests from drought stress under projections of increasing aridity in the eastern US (Ficklin & Novick et al., 2017). Below, I discuss these findings and their implications in further detail.

4.1 Importance of VPD and seasonal timing

I found that EVI was most sensitive to precipitation between May and July, and most sensitive to VPD between May and September (Figure 2.2). The cumulative and lagged effects observed (*i.e.* early-mid growing season climate conditions affected EVI over the entire growing season) are a common way in which ecosystems respond to drought (Peng et al., 2019), and suggest that arid conditions that occur over multiple months have the strongest influence on EVI in SNP. Overall, the negative effect of VPD on EVI was more than three-times greater than the positive effect of precipitation, and it was also more widespread across the landscape (Figure 2; Figure 2.3). Advanced leaf senescence is a commonly reported effect of atmospheric aridity in temperate forests (Estiarte & Penuelas 2014; Xie et al., 2015), and this may explain why EVI – which reflects both canopy leaf area and greenness – was negatively associated with VPD in this study. VPD is projected to increase in the eastern US in the next century (Ficklin & Novick, 2017), and results of this study add to a growing body of evidence suggesting that increases in VPD will have wide-ranging impacts on terrestrial productivity (Grossiord et al., 2020; Novick et al., 2016; Yuan et al., 2019; Zhang et al., 2019).

While VPD was a more important control on EVI, we still found positive EVI responses to precipitation in the majority of pixels (Figures 2.2, 2.3). This contrasts with a recent analysis

of vegetation response to precipitation across the entire conterminous US that reported very low NDVI sensitivity to annual (as opposed to growing season) precipitation in humid temperate deciduous forests (Maurer et al., 2020). It is unlikely that precipitation that falls outside the growing season has large impacts on EVI at SNP, as snowpack is short-lived (Sullivan et al., 2003), and relatively shallow soils leave little room for water storage. I found that precipitation on the margins of the growing season had little effect on EVI – mean EVI sensitivity to May precipitation was near zero, as was sensitivity to precipitation in climate windows that included August and September (Figure 2.2). This suggests that June and July are critical months for EVI precipitation sensitivity in SNP. Our results are consistent with tree ring studies that suggest drought has the most severe impacts on tree growth when it coincides with the phenology of wood formation, which mostly occurs in the early-mid growing season (D'Orangeville et al., 2018; Kannenberg et al., 2019). While relatively few studies have examined links between remotely-sensed vegetation indices and tree radial growth, in some cases vegetation indices and tree growth are correlated (Correa-Diaz, 2019; Decuyper et al., 2020). EVI primarily reflects leaf area and the greenness of the canopy – thus EVI may be an indicator of photosynthetic capacity at the canopy scale, and subsequently, the potential of trees to allocate carbon towards woody growth. Future research that integrates remote sensing and tree ring data may provide a better mechanistic understanding of how trees allocate carbon during periods of water stress, and enable scaling of tree ring data to landscapes.

We also observed a significant negative correlation between the sensitivities of EVI to precipitation and VPD (Figure 2.4). This may be due to the fact that wetter growing seasons are also likely to be cooler and more humid, which would negatively influence VPD. Alternately, there may be tradeoffs between optimizing tree functional traits for drought avoidance versus

optimizing for wet conditions, and vice-versa. For example, trees with greater leaf mass per area tend to be more drought resistant, but have lower photosynthetic capacity and leaf-level conductance (Hallik et al., 2009; Nardini et al., 2014), which may constrain their ability to capitalize when moisture is abundant. I also found that mesophytic species communities, which tend to be taller and occupy wetter microsites, were less sensitive to precipitation and more sensitive to VPD than xerophytic tree communities (Figure 2.8). This suggests a trade-off between hydraulic traits for high water availability and stress avoidance in high VPD conditions (Liu et al., 2019). This potential mechanism is discussed in more detail below.

4.2 Landscape controls on forest climate sensitivity

Overall, topography, soils, and tree height explained only ~3% of variation in forest climate sensitivity, although several environmental variables were found to marginally affect forest climate response (Figure 2.5). Topographic wetness index was negatively associated with precipitation sensitivity and positively associated with VPD sensitivity, suggesting some degree of buffering from moisture stress in convergent downslope positions. Lower sensitivity to drought stress in downslope trees has also been observed in southern Appalachia (Hawthorne & Miniat, 2018; Tromp van Meerveld & McDonnel, 2006). VPD sensitivity was most negative on slopes receiving greater solar radiation (Figures 2.5, 2.6), indicating that trees on high-energy aspects are more sensitive to atmospheric demand for water. This is consistent with work suggesting that oaks exposed to greater solar radiation are more sensitive to drought that trees in closed canopies (Scharnweber et al., 2020), and may be related to the challenge of regulating leaf temperature when exposed to more direct solar radiation.

The weak relationships observed between climate sensitivity and topographic predictors may be the result of several factors, including, but not limited to, tree adaptation to local

conditions, lack of severe drought during our study period, or unaccounted-for disturbances. Trees are highly sensitive to climate in the recruitment and sapling stages (Canham & Murphy, 2016), and by the time they reach canopy status, they have likely experienced varying degrees of water stress throughout their lifetimes. To mitigate water stress (and also balance tradeoffs with other requirements, such as light and nutrient acquisition), trees adjust their physiology and hydraulic architecture to the local conditions in which they grow. As a result, intraspecific trait variation is common among tree populations, and is key to their ecological success along climate gradients (Reich et al., 2014; Seifert et al., 2015). For example, trees of the same species varied in their allocation to leaf and sapwood areas along a regional moisture gradient in Spain (Rosas et al., 2019). Similar patterns have been observed at hillslope scales – in southern Appalachia, trees in downslope topographic positions that receive water subsidies have greater sapwood area than trees in upslope topographic positions (Hawthorne & Miniat, 2018). In this study, it is possible that adaptation to local moisture conditions resulted in similar relative changes in EVI with interannual climate variability along hillslope-scale moisture gradients.

Further, while several severe droughts have occurred in the SNP region in the last century (McGregor et al., 2021), none occurred between 2009-2019. In humid temperate deciduous forests in Europe, only severe droughts and disturbance events induced significant changes in EVI (Decuyper et al., 2020). It is possible that topographic effects on climate sensitivity may become more pronounced under intense drought, as soil moisture along hillslope gradients may be more homogeneous during wet conditions, but highly heterogeneous in dry conditions (Western et al., 1999). Disturbances other than drought may have also influenced EVI and thus climate sensitivity in our study area. We attempted to mitigate confounding effects of disturbances in our analyses of climate sensitivity by masking pixels where documented fires and

insect outbreaks have occurred since 2000, and masking pixels that were in the upper 90th percentile of EVI standard deviation. However, I cannot discount the possibility that disturbances such as flooding, ice storms (Lafon, 2016), or insect defoliation events not caused by *Lymantria dispar* (Anderson-Texeira et al., 2020) affected our EVI time series.

Soil properties also modulated climate sensitivity, sometimes in unexpected ways. We anticipated that precipitation sensitivity would be lower in trees growing on deeper soils, which may have more room for water storage and thus provide a buffer from moisture limitation (Tromp van Meerveld & McDonnel, 2006). Instead, we found that precipitation sensitivity was greater, but VPD sensitivity was lower, on deeper soils (Figure 2.5). Notably, larger drought legacy effects on tree growth have been reported in trees growing on soils with greater depth to water table, which are often deeper (Kannenberg et al., 2018). Reliance on deeper water sources may be a liability for trees following severe drought, as soil water recharge takes longer with depth (Chitra-Tarak et al., 2017). We also found that EVI precipitation sensitivity was greater on soils with higher clay content. This effect may be related to the low water potential of soils with high clay content, which can inhibit tree ability to extract water from the soil (Jackson et al., 2000).

Soil nutrients may also be an important control on forest response to climate (Levesque et al., 2016; Malcomb et al., 2020), and thus we included bedrock type as a proxy for soil nutrient availability given known differences in soil base cations among the three major bedrock classes in SNP (Riscassi et al., 2018). Soil nutrient availability is influenced by the parent material of underlying bedrock, and may also vary along hillslope gradients, where weathering and erosion can result in greater nutrient availability in downslope positions (St. Clair & Lynch, 2005). At landscape scales, differences in soil nutrients related to underlying bedrock have been

found to be an important determinant of forest productivity in central Appalachia (Reed & Kaye, 2020). However, we did not find strong evidence for differences in climate sensitivity based on bedrock type – VPD sensitivity did not differ across the three major bedrock classes in SNP, and precipitation sensitivity did not differ between trees growing over base-rich mafic bedrock and base-poor siliciclastic bedrock (Figure S2.2). Similarly, tree height was greatest on soils overlaying felsic bedrock of intermediate nutrient availability, and lowest on siliciclastic bedrock (Figure S2.4). Thus, while we cannot discount that soil nutrient availability has some influence on tree height and climate sensitivity in SNP, other factors, such as water and light availability, likely play a larger role.

Recent studies in the southern portion of the Blue Ridge Mountains report conflicting results regarding the influence of topography on tree response to climate. Hawthorne and Miniat (2018) found that trees in lower slope positions maintained consistent transpiration rates across wet and dry years, while transpiration was severely reduced in dry years in trees in upslope positions. In contrast, at the same site, Hwang et al., (2020) reported that growth and NDVI in trees in downslope topographic positions are more sensitive to recent warming trends. A remote sensing-based study found that ET has increased more dramatically in higher elevation forests in the Blue Ridge Mountains, potentially reducing lateral subsurface flow to lower elevation trees, which are less drought tolerant (McQuillan et al., 2022). Accounting for changes in water subsidies and differences in species hydraulic traits between high and low elevation forest communities may reconcile the divergent impacts of moisture stress between higher and lower elevation forests reported in earlier studies (McQuillan et al., 2022). In this study, I found that TWI had a weak but significant effect on precipitation sensitivity, suggesting downslope water subsidies may modestly reduce sensitivity to moisture stress (Figure 2.5). Nonetheless, I found

that atmospheric demand for water, and not belowground supply, is a strong control on EVI regardless of topographic position.

4.3 Forest species composition and climate sensitivity

Over the last century, fire suppression and a shift towards wetter growing season conditions have contributed to increasing dominance of mesophytic species such as red maple and tulip poplar, at the expense of more xerophytic and fire-tolerant oak and hickory species in eastern US forests (McEwan et al., 2011; Nowacki & Abrams, 2008). Mesophytic species with diffuse-porous wood anatomy tend to be more prolific water users, and more sensitive to moisture stress compared to ring-porous deciduous trees and conifers (Meinzer et al., 2013). It has been suggested that "mesophication" of southeastern US forests makes them more vulnerable to drought (Hwang et al., 2020). While it was long believed that oak species in the eastern US are more drought tolerant than other co-occurring genera, a recent synthesis suggests that they may be equally susceptible to drought-related growth reductions and mortality (Novick et al., 2022). In this study, I found that species communities dominated by oaks (Montane Oak-Hickory and Low Elevation Chestnut Oak) were more sensitive to water availability than Southern Appalachian Cove communities, but as sensitive as Successional Tuliptree or Basic Boulderfield forests (Figure 2.7; Table S2.5). Overall, I found that mesophytic tree species communities were less sensitive to water availability but more sensitive to VPD than xerophytic communities dominated by oak species (Figure 2.8). However, given that mesophytic species communities tend to occur on wetter, more energy-limited sites, whether these effects were mediated by differences in species hydraulic traits or topography remains unclear.

Finally, I found that EVI of successional forests growing on abandoned fields or pastures (Young et al., 2009) were the least sensitive to both precipitation and VPD (Figure 2.7). This

may be a result of incomplete canopy closure in successional forests, resulting in a greater proportion of understory vegetation in the EVI signal, or generally low climate sensitivity among pioneer tree species in the eastern US (Fridley et al., 2012). This suggests that forest age and successional status may be important determinants of climate sensitivity, and that relatively young secondary forests that cover much of the eastern United States (Thompson et al., 2013) may have been less sensitive to droughts than mature forests in recent decades, but may become more sensitive as they age.

4.4 Forest canopy height – landscape patterns and effects on climate sensitivity

Forest canopy height data have become widely available due to recent advances in spaceborne LiDAR (Schneider et al., 2020), enabling examination of relationships between forest height and ecosystem function at landscape scales. Tree height can influence climate sensitivity via various mechanisms, including: gravitational constraints on conductance (McDowell et al., 2015), differences in microclimate conditions between the subcanopy and upper canopy (Kunert et al., 2017; McGregor et al., 2021), and increases in water use efficiency with tree height (Brienen et al., 2017, Vadeboncoeur, 2020). I hypothesized that forest climate sensitivity would increase with canopy height, due to the challenge of maintaining transpiration over longer distances, and higher temperatures and wind speeds experienced by emergent trees (Bennet et al., 2015; McGregor et al., 2021). I found support for these hypotheses, with the caveat that height explained only a small percentage of variation in climate sensitivity. EVI sensitivity to precipitation increased with canopy height, and sensitivity to VPD was more negative in taller canopies (Figure 2.5). Forest communities dominated by mesophytic species had the tallest canopies (Figure 2.9) – this, combined with the greater sensitivity of mesophytic species to VPD (Figure 2.8), suggests that the taller, higher biomass forests of SNP may also be

most vulnerable to moisture stress. This may have important implications for the impacts of drought on forest carbon balance in SNP. While this study showed small effects of canopy height on climate sensitivity, height itself is likely less important than height relative to surrounding trees, which our point-based GEDI data could not capture. To more thoroughly investigate whether canopy structure-driven differences in microclimate influence climate sensitivity, future work should use wall-to-wall forest height data and more advanced structural metrics such as rugosity (Atkins et al., 2018).

Topographic and edaphic variables explained more variation in tree height than they did climate sensitivity (R^2=0.16, p<0.0001; Figure 2.10). Across the landscape, canopy height was negatively associated with elevation and solar radiation, and positively associated with TWI, percent clay, and bedrock depth (Figure 2.10). While it may be harder for trees to extract water from soils with high percent clay, it is also possible that deeper soils with high clay content have greater shear strength and enable trees to root more deeply, enhancing stability from uprooting as they grow taller (Cushman et al., 2022). Topographic effects are likely driven by greater competition for light in sites receiving less solar radiation, and greater soil moisture (TWI) in downslope positions, which may enable trees to grow to greater heights (Detto et al., 2013). I also found a distinct pattern of shorter canopies and fewer tall (>30 m) trees on high-energy slopes (Figure 2.9). Similar patterns in forest biomass along topographic gradients have been reported in the more water-limited western United States (Holyman et al., 2018; Swetnam et al., 2017), but a study in Pennsylvania reported that forest carbon density was greatest on south-facing slopes in convergent terrain at a site that may be more energy-limited than SNP (Smith et al., 2017).

5. Conclusions

Understanding how forests respond to climate variability is essential to projecting the strength of the terrestrial carbon sink, but dominant controls on forest climate sensitivity at landscape scales remain uncertain. In this study I examined forest sensitivity to precipitation and VPD in a topographically complex temperate broadleaf forest, and how topography, soil properties, and forest canopy height influence climate sensitivity. Forests were sensitive to both precipitation and VPD, but the effects of VPD were roughly three times greater than those of precipitation. I found clear negative effects of early to mid-season VPD on growing season EVI across the landscape, which were greatest (most negative) on slopes receiving more solar radiation. Overall, I found only marginal evidence that climate effects were buffered by topographic or edaphic factors. The ubiquity of negative effects across the landscape suggests that projected future increases in VPD (Ficklin & Novick) will suppress forest productivity across SNP.

Acknowledgements

This work was supported by a Presidential Fellowship in Data Science through the School of Data Science at UVA during the 2019-2020 academic year. Research ideas, and early stages of data analyses, were generated in collaboration with Linnea Saby with input from Drs. Larry Band and Johnathan Goodall. Dr. Elliot White provided helpful assistance with Google Earth Engine. Dr. Xi Yang offered useful input during the early stages of this investigation. Dr. Ami Riscassi provided assistance accessing SNP bedrock, fire, and vegetation data.

Chapter 2 References

Anderson-Teixeira, K. J., Herrmann, V., Cass, W. B., Williams, A. B., Paull, S. J., Gonzalez-Akre, E. B., et al. (2021). Long-Term Impacts of Invasive Insects and Pathogens on Composition, Biomass, and Diversity of Forests in Virginia's Blue Ridge Mountains. *Ecosystems*, *24*(1), 89–105. https://doi.org/10.1007/s10021-020-00503-w

Anderson-Teixeira, K. J., Herrmann, V., Rollinson, C. R., Gonzalez, B., Gonzalez-Akre, E. B., Pederson, N., et al. (2022). Joint effects of climate, tree size, and year on annual tree growth derived from tree-ring records of ten globally distributed forests. *Global Change Biology*, *28*(1), 245–266. https://doi.org/10.1111/gcb.15934

Arora, V. K., Boer, G. J., Friedlingstein, P., Eby, M., Jones, C. D., Christian, J. R., et al. (2013). Carbon–Concentration and Carbon–Climate Feedbacks in CMIP5 Earth System Models. *Journal of Climate*, *26*(15), 5289–5314. https://doi.org/10.1175/JCLI-D-12-00494.1

Asaro, C., & Chamberlin, L. A. (2015). Outbreak History (1953-2014) of Spring Defoliators Impacting Oak-Dominated Forests in Virginia, with Emphasis on Gypsy Moth (Lymantria dispar L.) and Fall Cankerworm (Alsophila pometaria Harris). *American Entomologist*, *61*(3), 174–185. https://doi.org/10.1093/ae/tmv043

Atkins, J. W., Bohrer, G., Fahey, R. T., Hardiman, B. S., Morin, T. H., Stovall, A. E. L., et al. (2018). Quantifying vegetation and canopy structural complexity from terrestrial LiDAR data using the forestr r package. *Methods in Ecology and Evolution*, *9*(10), 2057–2066. https://doi.org/10.1111/2041-210X.13061

Baldocchi, D., Chu, H., & Reichstein, M. (2018). Inter-annual variability of net and gross ecosystem carbon fluxes: A review. *Agricultural and Forest Meteorology*, *249*, 520–533. https://doi.org/10.1016/j.agrformet.2017.05.015

Bennett, A. C., McDowell, N. G., Allen, C. D., & Anderson-Teixeira, K. J. (2015). Larger trees suffer most during drought in forests worldwide. *Nature Plants*, *1*(10), 15139. https://doi.org/10.1038/nplants.2015.139

Bonan, G. B. (2008). Forests and Climate Change: Forcings, Feedbacks, and the Climate Benefits of Forests. *Science*, *320*(5882), 1444. https://doi.org/10.1126/science.1155121

Brienen, R. J. W., Gloor, E., Clerici, S., Newton, R., Arppe, L., Boom, A., et al. (2017). Tree height strongly affects estimates of water-use efficiency responses to climate and CO2 using isotopes. *Nature Communications*, *8*(1), 288. https://doi.org/10.1038/s41467-017-00225-z

Brzostek, E. R., Dragoni, D., Schmid, H. P., Rahman, A. F., Sims, D., Wayson, C. A., et al. (2014). Chronic water stress reduces tree growth and the carbon sink of deciduous hardwood forests. *Global Change Biology*, *20*(8), 2531–2539. https://doi.org/10.1111/gcb.12528

Canham, C. D., & Murphy, L. (2016). The demography of tree species response to climate: seedling recruitment and survival. *Ecosphere*, *7*(8), e01424. https://doi.org/10.1002/ecs2.1424

Cass, W. B., Hochstedler, W. W., & Williams, A. B. (2012). Forest Vegetation Status in Shenandoah National Park: Long-term Ecological Monitoring Summary Report. NPS/MIDN/NRDS.

Chitra-Tarak, R., Ruiz, L., Dattaraja, H. S., Mohan Kumar, M. S., Riotte, J., Suresh, H. S., et al. (2018). The roots of the drought: Hydrology and water uptake strategies mediate forest-wide demographic response to precipitation. *Journal of Ecology*, *106*(4), 1495–1507. https://doi.org/10.1111/1365-2745.12925

Clark, J. S., Iverson, L., Woodall, C. W., Allen, C. D., Bell, D. M., Bragg, D. C., et al. (2016). The impacts of increasing drought on forest dynamics, structure, and biodiversity in the United States. *Global Change Biology*, *22*(7), 2329–2352. https://doi.org/10.1111/gcb.13160

Cushman, K. C., Detto, M., García, M., & Muller-Landau, H. C. (2022). Soils and topography control natural disturbance rates and thereby forest structure in a lowland tropical landscape. *Ecology Letters*, *n/a*(n/a). https://doi.org/10.1111/ele.13978

Decuyper, M., Chávez, R. O., Čufar, K., Estay, S. A., Clevers, J. G. P. W., Prislan, P., et al. (2020). Spatio-temporal assessment of beech growth in relation to climate extremes in Slovenia – An integrated approach using remote sensing and tree-ring data. *Agricultural and Forest Meteorology*, *287*, 107925. https://doi.org/10.1016/j.agrformet.2020.107925

Detto, M., Muller-Landau, H. C., Mascaro, J., & Asner, G. P. (2013). Hydrological Networks and Associated Topographic Variation as Templates for the Spatial Organization of Tropical Forest Vegetation. *PLoS ONE*, *8*(10), e76296. https://doi.org/10.1371/journal.pone.0076296

D'Orangeville, L., Maxwell, J., Kneeshaw, D., Pederson, N., Duchesne, L., Logan, T., et al. (2018). Drought timing and local climate determine the sensitivity of eastern temperate forests to drought. *Global Change Biology*, *24*(6), 2339–2351. https://doi.org/10.1111/gcb.14096

Drummond, M. A., & Loveland, T. R. (2010). Land-use Pressure and a Transition to Forest-cover Loss in the Eastern United States. *BioScience*, *60*(4), 286–298. https://doi.org/10.1525/bio.2010.60.4.7

Dubaya, R., Hofton, M., Blair, J., Tang, H., & Luthcke, S. (2022, April 11). GEDI L2A Elevation and Height Metrics Data Global Footprint Level V001 [Data set]. NASA EOSDIS Land Processes DAAC. Retrieved from https://doi.org/10.5067/GEDI/GEDI02_A.001

Dymond, S. F., D'Amato, A. W., Kolka, R. K., Bolstad, P. V., Sebestyen, S. D., & Bradford, J. B. (2016). Growth–climate relationships across topographic gradients in the northern Great Lakes. *Ecohydrology*, *9*(6), 918–929. https://doi.org/10.1002/eco.1700

Elliott, K. J., Caldwell, P. V., Brantley, S. T., Miniat, C. F., Vose, J. M., & Swank, W. T. (2017). Water yield following forest–grass–forest transitions. *Hydrol. Earth Syst. Sci.*, *21*(2), 981–997. https://doi.org/10.5194/hess-21-981-2017

Elliott, Katherine J., Miniat, C. F., Pederson, N., & Laseter, S. H. (2015). Forest tree growth response to hydroclimate variability in the southern Appalachians. *Global Change Biology*, *21*(12), 4627–4641. https://doi.org/10.1111/gcb.13045

Enquist Brian J. & Niklas Karl J. (2002). Global Allocation Rules for Patterns of Biomass Partitioning in Seed Plants. *Science*, *295*(5559), 1517–1520. https://doi.org/10.1126/science.1066360

Estiarte, M., & Peñuelas, J. (2015). Alteration of the phenology of leaf senescence and fall in winter deciduous species by climate change: effects on nutrient proficiency. *Global Change Biology*, *21*(3), 1005–1017. https://doi.org/10.1111/gcb.12804

Ficklin, D. L., & Novick, K. A. (2017). Historic and projected changes in vapor pressure deficit suggest a continental-scale drying of the United States atmosphere. *Journal of Geophysical Research: Atmospheres*, *122*(4), 2061–2079. https://doi.org/10.1002/2016JD025855

Flatley, W. T., Lafon, C. W., & Grissino-Mayer, H. D. (2011). Climatic and topographic controls on patterns of fire in the southern and central Appalachian Mountains, USA. *Landscape Ecology*, *26*(2), 195–209. https://doi.org/10.1007/s10980-010-9553-3

Fridley, J. D., & Wright, J. P. (2012). Drivers of secondary succession rates across temperate latitudes of the Eastern USA: climate, soils, and species pools. *Oecologia*, *168*(4), 1069–1077. https://doi.org/10.1007/s00442-011-2152-4

Grossiord, C., Buckley, T. N., Cernusak, L. A., Novick, K. A., Poulter, B., Siegwolf, R. T. W., et al. (2020). Plant responses to rising vapor pressure deficit. *New Phytologist*, *226*(6), 1550–1566. https://doi.org/10.1111/nph.16485

Hallik, L., Niinemets, Ü., & Wright, I. J. (2009). Are species shade and drought tolerance reflected in leaf-level structural and functional differentiation in Northern Hemisphere temperate woody flora? *New Phytologist*, *184*(1), 257–274. https://doi.org/10.1111/j.1469-8137.2009.02918.x

Hawthorne, S., & Miniat, C. F. (2018). Topography may mitigate drought effects on vegetation along a hillslope gradient. *Ecohydrology*, *11*(1), e1825. https://doi.org/10.1002/eco.1825

Helcoski, R., Tepley, A. J., Pederson, N., McGarvey, J. C., Meakem, V., Herrmann, V., et al. (2019). Growing season moisture drives inter-annual variation in woody productivity of a temperate deciduous forest. *New Phytologist*. https://doi.org/10.1111/nph.15906

Hoylman, Z. H., Jencso, K. G., Hu, J., Martin, J. T., Holden, Z. A., Seielstad, C. A., & Rowell, E. M. (2018). Hillslope Topography Mediates Spatial Patterns of Ecosystem Sensitivity to Climate. *Journal of Geophysical Research: Biogeosciences*, *123*(2), 353–371. https://doi.org/10.1002/2017JG004108

Huang, X., Xiao, J., & Ma, M. (2019). Evaluating the Performance of Satellite-Derived Vegetation Indices for Estimating Gross Primary Productivity Using FLUXNET Observations across the Globe. *Remote Sensing*, *11*(15). https://doi.org/10.3390/rs11151823

Huete, A., Didan, K., Miura, T., Rodriguez, E. P., Gao, X., & Ferreira, L. G. (2002). Overview of the radiometric and biophysical performance of the MODIS vegetation indices. *The Moderate Resolution Imaging Spectroradiometer (MODIS): A New Generation of Land Surface Monitoring*, *83*(1), 195–213. https://doi.org/10.1016/S0034-4257(02)00096-2

Hwang, T., Band, L. E., Miniat, C. F., Vose, J. M., Knoepp, J. D., Song, C., & Bolstad, P. V. (2020). Climate Change May Increase the Drought Stress of Mesophytic Trees Downslope With Ongoing Forest Mesophication Under a History of Fire Suppression. *Frontiers in Forests and Global Change*, *3*. Retrieved from https://www.frontiersin.org/article/10.3389/ffgc.2020.00017

Jackson, R. B., Sperry, J. S., & Dawson, T. E. (2000). Root water uptake and transport: using physiological processes in global predictions. *Trends in Plant Science*, *5*(11), 482–488. https://doi.org/10.1016/S1360-1385(00)01766-0

Justin Reich. (2001). Re-Creating the Wilderness: Shaping Narratives and Landscapes in Shenandoah National Park. *Environmental History*, *6*(1), 95–117. https://doi.org/10.2307/3985233

Kannenberg, S. A., Maxwell, J. T., Pederson, N., D'Orangeville, L., Ficklin, D. L., & Phillips, R. P. (2019). Drought legacies are dependent on water table depth, wood anatomy and drought timing across the eastern US. *Ecology Letters*, *22*(1), 119–127. https://doi.org/10.1111/ele.13173

Keenan, T. F., Gray, J., Friedl, M. A., Toomey, M., Bohrer, G., Hollinger, D. Y., et al. (2014). Net carbon uptake has increased through warming-induced changes in temperate forest phenology. *Nature Climate Change*, *4*(7), 598–604. https://doi.org/10.1038/nclimate2253

Kennedy, D., Swenson, S., Oleson, K. W., Lawrence, D. M., Fisher, R., Lola da Costa, A. C., & Gentine, P. (2019). Implementing Plant Hydraulics in the Community Land Model, Version 5. *Journal of Advances in Modeling Earth Systems*, *11*(2), 485–513. https://doi.org/10.1029/2018MS001500

Kopecký, M., & Čížková, Š. (2010). Using topographic wetness index in vegetation ecology: does the algorithm matter? *Applied Vegetation Science*, *13*(4), 450–459. https://doi.org/10.1111/j.1654-109X.2010.01083.x

Kunert, N., Aparecido, L. M. T., Wolff, S., Higuchi, N., Santos, J. dos, Araujo, A. C. de, & Trumbore, S. (2017). A revised hydrological model for the Central Amazon: The importance of emergent canopy trees in the forest water budget. *Agricultural and Forest Meteorology*, *239*, 47–57. https://doi.org/10.1016/j.agrformet.2017.03.002

Lafon, C. W. (2016). Ice Storms in Central Hardwood Forests: The Disturbance Regime, Spatial Patterns, and Vegetation Influences. In C. H. Greenberg & B. S. Collins (Eds.), *Natural Disturbances and Historic Range of Variation: Type, Frequency, Severity, and Post-disturbance Structure in Central Hardwood Forests USA* (pp. 147–166). Cham: Springer International Publishing. https://doi.org/10.1007/978-3-319-21527-3_7

Le Quéré, C., Andrew, R. M., Friedlingstein, P., Sitch, S., Hauck, J., Pongratz, J., et al. (2018). Global Carbon Budget 2018. *Earth Syst. Sci. Data*, *10*(4), 2141–2194. https://doi.org/10.5194/essd-10-2141-2018

Lévesque, M., Walthert, L., & Weber, P. (2016). Soil nutrients influence growth response of temperate tree species to drought. *Journal of Ecology*, *104*(2), 377–387. https://doi.org/10.1111/1365-2745.12519

Li, X., & Xiao, J. (2020). Global climatic controls on interannual variability of ecosystem productivity: Similarities and differences inferred from solar-induced chlorophyll fluorescence and enhanced vegetation index. *Agricultural and Forest Meteorology*, *288–289*, 108018. https://doi.org/10.1016/j.agrformet.2020.108018

Liu Hui, Gleason Sean M., Hao Guangyou, Hua Lei, He Pengcheng, Goldstein Guillermo, & Ye Qing. (n.d.). Hydraulic traits are coordinated with maximum plant height at the global scale. *Science Advances*, *5*(2), eaav1332. https://doi.org/10.1126/sciadv.aav1332

Lu, X., Kicklighter, D. W., Melillo, J. M., Reilly, J. M., & Xu, L. (2015). Land carbon sequestration within the conterminous United States: Regional- and state-level analyses. *Journal of Geophysical Research: Biogeosciences*, *120*(2), 379–398. https://doi.org/10.1002/2014JG002818

Maeda, E. E., Heiskanen, J., Aragão, L. E. O. C., & Rinne, J. (2014). Can MODIS EVI monitor ecosystem productivity in the Amazon rainforest? *Geophysical Research Letters*, *41*(20), 7176–7183. https://doi.org/10.1002/2014GL061535

Malcomb, J. D., Scanlon, T. M., Epstein, H. E., Druckenbrod, D. L., Vadeboncoeur, M. A., Lanning, M., et al. (2020). Assessing Temperate Forest Growth and Climate Sensitivity in Response to a Long-Term Whole-Watershed Acidification Experiment. *Journal of Geophysical Research: Biogeosciences*, *125*(7), e2019JG005560. https://doi.org/10.1029/2019JG005560

Manderino, R., Crist, T. O., & Haynes, K. J. (2014). Lepidoptera-specific insecticide used to suppress gypsy moth outbreaks may benefit non-target forest Lepidoptera. *Agricultural and Forest Entomology*, *16*(4), 359–368. https://doi.org/10.1111/afe.12066

Martin-Benito, D., & Pederson, N. (2015). Convergence in drought stress, but a divergence of climatic drivers across a latitudinal gradient in a temperate broadleaf forest. *Journal of Biogeography*, *42*(5), 925–937. https://doi.org/10.1111/jbi.12462

Maurer, G. E., Hallmark, A. J., Brown, R. F., Sala, O. E., & Collins, S. L. (2020). Sensitivity of primary production to precipitation across the United States. *Ecology Letters*, *23*(3), 527–536. https://doi.org/10.1111/ele.13455

McDowell, N. G., & Allen, C. D. (2015). Darcy's law predicts widespread forest mortality under climate warming. *Nature Climate Change*, *5*(7), 669–672. https://doi.org/10.1038/nclimate2641

McEwan, R. W., Dyer, J. M., & Pederson, N. (2011). Multiple interacting ecosystem drivers: toward an encompassing hypothesis of oak forest dynamics across eastern North America. *Ecography*, *34*(2), 244–256. https://doi.org/10.1111/j.1600-0587.2010.06390.x

McGregor, I. R., Helcoski, R., Kunert, N., Tepley, A. J., Gonzalez-Akre, E. B., Herrmann, V., et al. (2021). Tree height and leaf drought tolerance traits shape growth responses across droughts in a temperate broadleaf forest. *New Phytologist*, *231*(2), 601–616. https://doi.org/10.1111/nph.16996

McLaughlin, B. C., Ackerly, D. D., Klos, P. Z., Natali, J., Dawson, T. E., & Thompson, S. E. (2017). Hydrologic refugia, plants, and climate change. *Global Change Biology*, *23*(8), 2941–2961. https://doi.org/10.1111/gcb.13629

McQuillan, K. A., Tulbure, M. G., & Martin, K. L. (2022). Forest water use is increasingly decoupled from water availability even during severe drought. *Landscape Ecology*. https://doi.org/10.1007/s10980-022-01425-9

Medvigy David, Wofsy Steven C., Munger J. William, & Moorcroft Paul R. (2010). Responses of terrestrial ecosystems and carbon budgets to current and future environmental variability. *Proceedings of the National Academy of Sciences*, *107*(18), 8275–8280. https://doi.org/10.1073/pnas.0912032107

Meinzer, F. C., Woodruff, D. R., Eissenstat, D. M., Lin, H. S., Adams, T. S., & McCulloh, K. A. (2013). Above- and belowground controls on water use by trees of different wood types in an eastern US deciduous forest. *Tree Physiology*, *33*(4), 345–356. https://doi.org/10.1093/treephys/tpt012

Moreno-Martínez, Á., Izquierdo-Verdiguier, E., Maneta, M. P., Camps-Valls, G., Robinson, N., Muñoz-Marí, J., et al. (2020). Multispectral high resolution sensor fusion for smoothing and gap-filling in the cloud. *Remote Sensing of Environment*, *247*, 111901. https://doi.org/10.1016/j.rse.2020.111901

Mu, Q., Zhao, M., Heinsch, F. A., Liu, M., Tian, H., & Running, S. W. (2007). Evaluating water stress controls on primary production in biogeochemical and remote sensing based models. *Journal of Geophysical Research: Biogeosciences*, *112*(G1). https://doi.org/10.1029/2006JG000179

Novick, K., Jo, I., D'Orangeville, L., Benson, M., Au, T. F., Barnes, M., et al. (2022). The Drought Response of Eastern US Oaks in the Context of Their Declining Abundance. *BioScience*, *72*(4), 333–346. https://doi.org/10.1093/biosci/biab135

Novick, K. A., Ficklin, D. L., Stoy, P. C., Williams, C. A., Bohrer, G., Oishi, A. C., et al. (2016). The increasing importance of atmospheric demand for ecosystem water and carbon fluxes. *Nature Climate Change*, *6*(11), 1023–1027. https://doi.org/10.1038/nclimate3114

Pan Yude, Birdsey Richard A., Fang Jingyun, Houghton Richard, Kauppi Pekka E., Kurz Werner A., et al. (2011). A Large and Persistent Carbon Sink in the World's Forests. *Science*, *333*(6045), 988–993. https://doi.org/10.1126/science.1201609

Pendergrass, A. G., Knutti, R., Lehner, F., Deser, C., & Sanderson, B. M. (2017). Precipitation variability increases in a warmer climate. *Scientific Reports*, *7*(1), 17966. https://doi.org/10.1038/s41598-017-17966-y

Peng, J., Wu, C., Zhang, X., Wang, X., & Gonsamo, A. (2019). Satellite detection of cumulative and lagged effects of drought on autumn leaf senescence over the Northern Hemisphere. *Global Change Biology*, *25*(6), 2174–2188. https://doi.org/10.1111/gcb.14627

Reed, W. P., & Kaye, M. W. (2020). Bedrock type drives forest carbon storage and uptake across the mid-Atlantic Appalachian Ridge and Valley, U.S.A. *Forest Ecology and Management*, *460*, 117881. https://doi.org/10.1016/j.foreco.2020.117881

Reich Peter B., Rich Roy L., Lu Xingjie, Wang Ying-Ping, & Oleksyn Jacek. (2014). Biogeographic variation in evergreen conifer needle longevity and impacts on boreal forest carbon cycle projections. *Proceedings of the National Academy of Sciences*, *111*(38), 13703–13708. https://doi.org/10.1073/pnas.1216054110

Richardson, A. D., Hollinger, D. Y., Dail, D. B., Lee, J. T., Munger, J. W., & O'keefe, J. (2009). Influence of spring phenology on seasonal and annual carbon balance in two contrasting New England forests. *Tree Physiology*, *29*(3), 321–331. https://doi.org/10.1093/treephys/tpn040

Riscassi, A., Scanlon, T., & Galloway, J. (2019). Stream geochemical response to reductions in acid deposition in headwater streams: Chronic versus episodic acidification recovery. *Hydrological Processes*, *33*(4), 512–526. https://doi.org/10.1002/hyp.13349

Ritter, F., Berkelhammer, M., & Garcia-Eidell, C. (2020). Distinct response of gross primary productivity in five terrestrial biomes to precipitation variability. *Communications Earth & Environment*, *1*(1), 34. https://doi.org/10.1038/s43247-020-00034-1

Robison, A. L., & Scanlon, T. M. (2018). Climate Change to Offset Improvements in Watershed Acid-Base Status Provided by Clean Air Act and Amendments: A Model Application in Shenandoah National Park, Virginia. *Journal of Geophysical Research: Biogeosciences*, *123*(9), 2863–2877. https://doi.org/10.1029/2018JG004519

Rosas, T., Mencuccini, M., Barba, J., Cochard, H., Saura-Mas, S., & Martínez-Vilalta, J. (2019). Adjustments and coordination of hydraulic, leaf and stem traits along a water availability gradient. *New Phytologist*, *223*(2), 632–646. https://doi.org/10.1111/nph.15684

Scharnweber, T., Heinze, L., Cruz-García, R., van der Maaten-Theunissen, M., & Wilmking, M. (2019). Confessions of solitary oaks: We grow fast but we fear the drought. *Dendrochronologia*, *55*, 43–49. https://doi.org/10.1016/j.dendro.2019.04.001

Schneider, F. D., Ferraz, A., Hancock, S., Duncanson, L. I., Dubayah, R. O., Pavlick, R. P., & Schimel, D. S. (2020). Towards mapping the diversity of canopy structure from space with GEDI. *Environmental Research Letters*, *15*(11), 115006. https://doi.org/10.1088/1748-9326/ab9e99

Siefert, A., Violle, C., Chalmandrier, L., Albert, C. H., Taudiere, A., Fajardo, A., et al. (2015). A global meta-analysis of the relative extent of intraspecific trait variation in plant communities. *Ecology Letters*, *18*(12), 1406–1419. https://doi.org/10.1111/ele.12508

Sims, D. A., Rahman, A. F., Cordova, V. D., El-Masri, B. Z., Baldocchi, D. D., Flanagan, L. B., et al. (2006). On the use of MODIS EVI to assess gross primary productivity of North American ecosystems. *Journal of Geophysical Research: Biogeosciences*, *111*(G4). https://doi.org/10.1029/2006JG000162

Smith, L. A., Eissenstat, D. M., & Kaye, M. W. (2017). Variability in aboveground carbon driven by slope aspect and curvature in an eastern deciduous forest, USA. *Canadian Journal of Forest Research*, *47*(2), 149–158. https://doi.org/10.1139/cjfr-2016-0147

Soil Survey Staff. (n.d.). Gridded Soil Survey Geographic (gSSURGO) Database for Virginia. United States Department of Agriculture, Natural Resources Conservation Service. Retrieved from https://gdg.sc.egov.usda.gov/

Sørensen, R., Zinko, U., & Seibert, J. (2006). On the calculation of the topographic wetness index: evaluation of different methods based on field observations. *Hydrol. Earth Syst. Sci.*, *10*(1), 101–112. https://doi.org/10.5194/hess-10-101-2006

ST CLAIR, S. B., & LYNCH, J. P. (2005). Differences in the success of sugar maple and red maple seedlings on acid soils are influenced by nutrient dynamics and light environment. *Plant, Cell & Environment*, *28*(7), 874–885. https://doi.org/10.1111/j.1365-3040.2005.01337.x

Stovall, A. E. L., Shugart, H., & Yang, X. (2019). Tree height explains mortality risk during an intense drought. *Nature Communications*, *10*(1), 4385. https://doi.org/10.1038/s41467-019-12380-6

Sullivan, T. J., Cosby, B. J., Laurence, J. A., Dennis, R. L., Savig, K., Webb, J. R., & Kern, J. S. (2003). Assessment of air quality and related values in Shenandoah National Park. NPS/NERCHAL/NRTR-03/090.

Sulman, B. N., Roman, D. T., Yi, K., Wang, L., Phillips, R. P., & Novick, K. A. (2016). High atmospheric demand for water can limit forest carbon uptake and transpiration as severely as dry soil. *Geophysical Research Letters*, *43*(18), 9686–9695. https://doi.org/10.1002/2016GL069416

Swann A. L. S., Hoffman F.M., Koven C.D., & Randerson J.T. (2016). Plant responses to increasing CO2 reduce estimates of climate impacts on drought severity. *Proceedings of the National Academy of Sciences*, *113*(36), 10019–10024. https://doi.org/10.1073/pnas.1604581113

Swetnam, T. L., Brooks, P. D., Barnard, H. R., Harpold, A. A., & Gallo, E. L. (2017). Topographically driven differences in energy and water constrain climatic control on forest carbon sequestration. *Ecosphere*, *8*(4), e01797. https://doi.org/10.1002/ecs2.1797

Tai, X., Venturas, M. D., Mackay, D. S., Brooks, P. D., & Flanagan, L. B. (2021). Lateral subsurface flow modulates forest mortality risk to future climate and elevated CO2. *Environmental Research Letters*, *16*(8), 084015. https://doi.org/10.1088/1748-9326/ac1135

Thompson, J. R., Carpenter, D. N., Cogbill, C. V., & Foster, D. R. (2013). Four Centuries of Change in Northeastern United States Forests. *PLoS ONE*, *8*(9), e72540. https://doi.org/10.1371/journal.pone.0072540

Tromp-van Meerveld, H. J., & McDonnell, J. J. (2006). On the interrelations between topography, soil depth, soil moisture, transpiration rates and species distribution at the hillslope scale. *Experimental Hydrology: A Bright Future*, *29*(2), 293–310. https://doi.org/10.1016/j.advwatres.2005.02.016

United States Geologic Survey. (2005). Preliminary integrated geologic map databases for the United States: Delaware, Maryland, New York, Pennsylvania, and Virginia. Retrieved from: https://pubs.usgs.gov/of/2005/1325/

Vadeboncoeur, M. A., Jennings, K. A., Ouimette, A. P., & Asbjornsen, H. (2020). Correcting tree-ring δ13C time series for tree-size effects in eight temperate tree species. *Tree Physiology*, *40*(3), 333–349. https://doi.org/10.1093/treephys/tpz138

Western, A. W., Grayson, R. B., Blöschl, G., Willgoose, G. R., & McMahon, T. A. (1999). Observed spatial organization of soil moisture and its relation to terrain indices. *Water Resources Research*, *35*(3), 797–810. https://doi.org/10.1029/1998WR900065

Whittaker, R. H. (1956). Vegetation of the Great Smoky Mountains. *Ecological Monographs*, *26*(1), 1–80. https://doi.org/10.2307/1943577

Xie Yingying, Wang Xiaojing, & Silander John A. (2015). Deciduous forest responses to temperature, precipitation, and drought imply complex climate change impacts. *Proceedings of the National Academy of Sciences*, *112*(44), 13585–13590. https://doi.org/10.1073/pnas.1509991112

Yeakley, J. A., Swank, W. T., Swift, L. W., Hornberger, G. M., & Shugart, H. H. (1998). Soil moisture gradients and controls on a southern Appalachian hillslope from drought through recharge. *Hydrology and Earth System Sciences Discussions, European Geosciences Union*, *2*(1), 41–49.

Young, J., Fleming, G., Cass, W., & Leah, C. (2009). Vegetation of Shenandoah National Park in Relation to Environmental Gradients, Version 2.0 Technical Report. NPS/NER/NRTR.

Young, John, Fleming, G., Townsend, P., & Foster, J. (2006). Vegetation of Shenandoah National Park in Relation to Environmental Gradients.

Yuan Wenping, Zheng Yi, Piao Shilong, Ciais Philippe, Lombardozzi Danica, Wang Yingping, et al. (n.d.). Increased atmospheric vapor pressure deficit reduces global vegetation growth. *Science Advances*, *5*(8), eaax1396. https://doi.org/10.1126/sciadv.aax1396

Zhang, Q., Ficklin, D. L., Manzoni, S., Wang, L., Way, D., Phillips, R. P., & Novick, K. A. (2019). Response of ecosystem intrinsic water use efficiency and gross primary productivity to rising vapor pressure deficit. *Environmental Research Letters*, *14*(7), 074023. https://doi.org/10.1088/1748-9326/ab2603

Chapter 2 Supplement

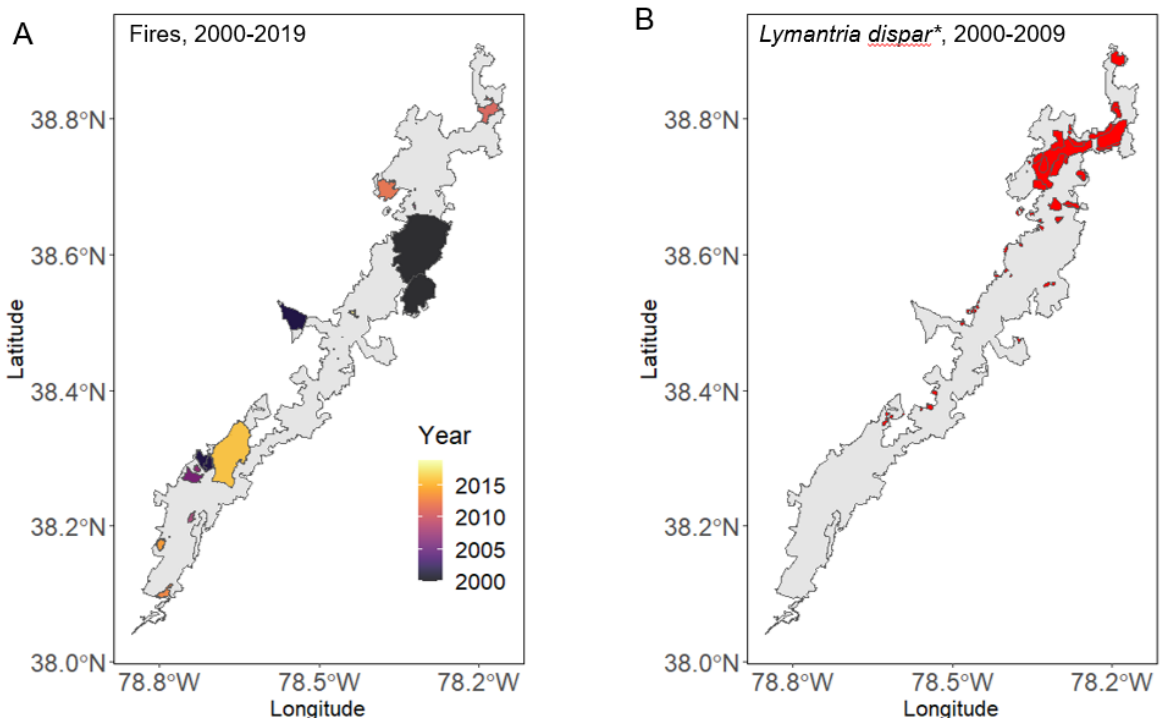

Figure S2.1. Fires (A) and *Lymantria dispar* defoliation areas (B) since 2000 in SNP. Pixels within these areas were excluded from climate sensitivity analyses. *Lymantria dispar are formerly known as gypsy moth.

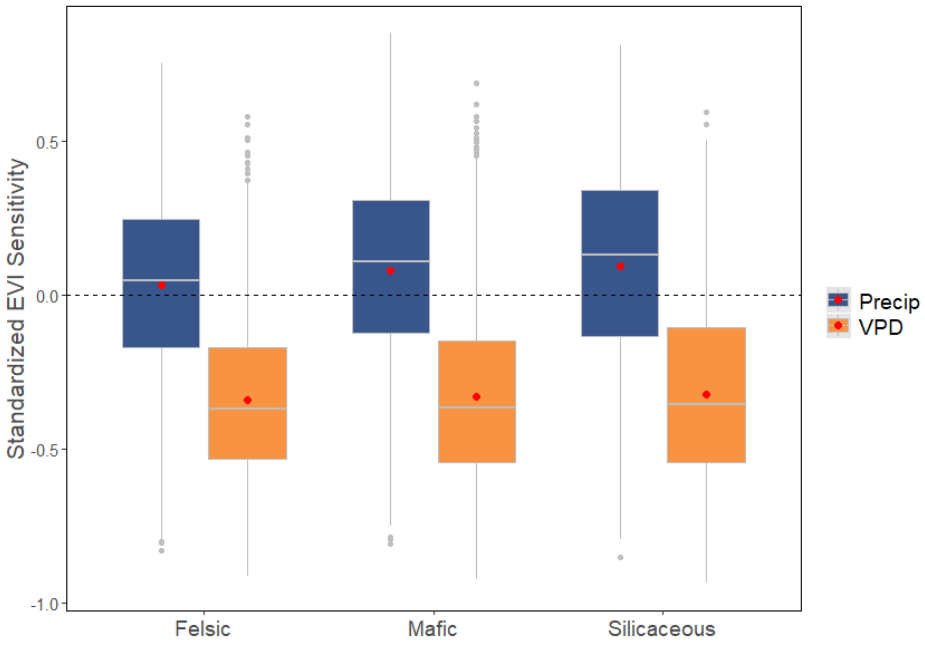

Figure S2.2. EVI sensitivity by bedrock type. Lines in boxes represent median values, while dots represent mean values.

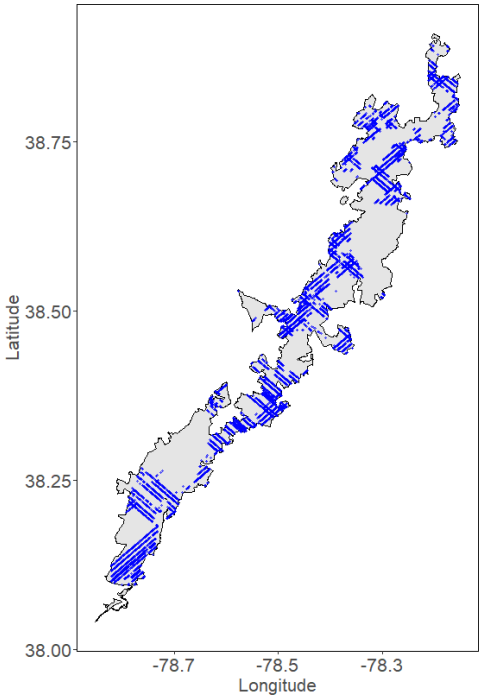

Figure S2.3. Locations of GEDI RH95 points in SNP after masking layer for disturbed pixels. Each blue dot is one observation.

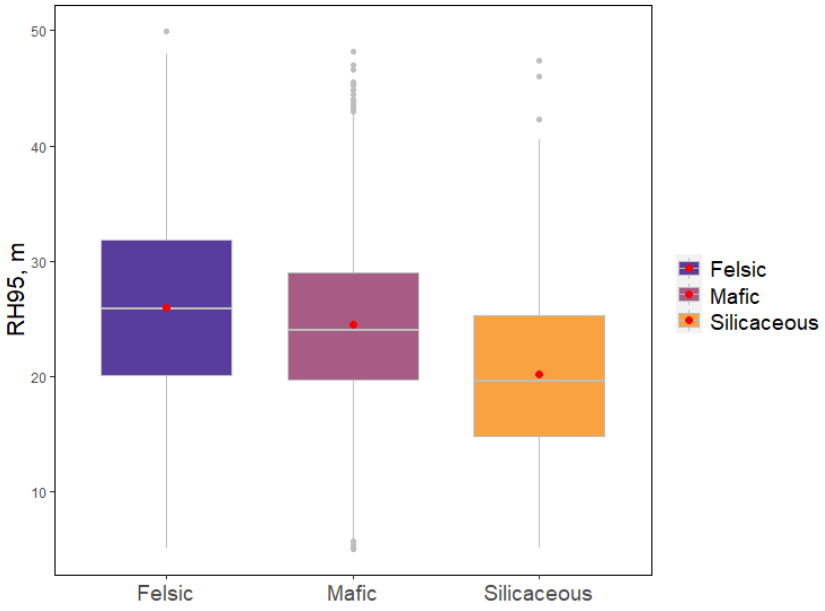

Figure S2.4. Canopy height by bedrock class.

Table S2.1. US National Vegetation Classification codes and descriptions.

Code	USNVC	Percent	Name
503	CEGL006299 / CEGL008523	22	Central Appalachian / Northern Piedmont Low-Elevation Chestnut Oak Forest
505	CEGL006057 / (CEGL008516 / CEGL008514	24	Central Appalachian Dry-Mesic Chestnut Oak – Northern Red Oak Forest / Montane Oak-Hickory / Basic Oak-Hickory
510	CEGL007710	6.2	Southern Appalachian Cove Forest (Typic Montane Type)
513	CEGL007220	6.7	Successional Tuliptree Forest (Circumneutral Type)
514	CEGL008528 / CEGL008516	11	Central Appalachian Basic Boulderfield Forest (Montane Basswood – White Ash Type)
515	CEGL006237	1.9	Central Appalachian Rich Cove Forest
521	CEGL006599 / CEGL002591 / CEGL006255	6.5	Prunus serotina Liriodendron Tulipifera / Pinus virginiana Ruderal forest / Northern Blue Ridge Montane Alluvial Forest

Notes: Percent is percent of SNP Area. For more information on these species communities, see Young et al., 2009.

Table S2.2. Output of multiple regression model assessing effects of topography, soil properties, and canopy height on precipitation sensitivity

Predictors	*Estimates*	*CI*	*p*
(Intercept)	0.06	-0.116 – 0.236	0.503
Elevation	0	-0.000 – -0.000	**0.026**

TWI	-0.058	-0.077 – -0.040	**<0.001**
Insolation	0	-0.000 – 0.000	0.194
RH95	0.002	0.001 – 0.004	**0.004**
Percent Clay	0.002	0.000 – 0.004	**0.027**
Bedrock Depth	0.001	0.000 – 0.001	**<0.001**
Observations	2874		
R^2 / R^2 adjusted	0.031 / 0.029		

Table S2.3. Output of multiple regression model assessing effects of topography, soil properties, and canopy height on VPD sensitivity

Predictors	*Estimates*	*CI*	*p*
(Intercept)	-0.107	-0.274 – 0.060	0.21
Elevation	0	-0.000 – 0.000	0.179
TWI	0.062	0.044 – 0.079	**<0.001**
Insolation	0	-0.000 – -0.000	**0.013**
RH95	-0.005	-0.006 – -0.003	**<0.001**
Percent Clay	-0.001	-0.003 – 0.001	0.485
Bedrock Depth	0	-0.001 – -0.000	**0.009**
Observations	2874		
R^2 / R^2 adjusted	0.029 / 0.027		

Table S2.4. Output of multiple regression model assessing effects of topography and soil properties on canopy height

Predictors	*Estimates*	*CI*	*p*
(Intercept)	42.319	38.553 – 46.086	**<0.001**
Elevation	-0.007	-0.009 – -0.005	**<0.001**
TWI	1.397	0.969 – 1.826	**<0.001**
Insolation	-0.005	-0.006 – -0.004	**<0.001**
Percent Clay	0.343	0.298 – 0.387	**<0.001**
Bedrock Depth	0.026	0.019 – 0.034	**<0.001**
Observations	2874		
R^2 / R^2 adjusted	0.161 / 0.160		

Table S2.5. Means and confidence intervals of precipitation sensitivity by vegetation class.

Vegetation Class	Mean	SE	df	lower.CL	upper.CL
Basic Boulderfield	0.062	0.009	7088	0.039	0.084
Early Succesional Forest	0.003	0.011	7088	-0.025	0.03
Low Elevation Chestnut Oak	0.09	0.007	7088	0.07	0.109
Montane Oak-Hickory	0.09	0.006	7088	0.07	0.107
Southern Appalachian Cove	0.046	0.012	7088	0.016	0.0763
Succesional Tuliptree	0.061	0.011	7088	0.032	0.091

Table S2.6. Means and confidence intervals of VPD sensitivity by vegetation class.

Vegetation Class	Mean	SE	df	lower.CL	upper.CL
Basic Boulderfield	-0.375	0.008	7088	-0.396	-0.354
Early Succesional Forest	-0.236	0.01	7088	-0.262	-0.21
Low Elevation Chestnut Oak	-0.328	0.007	7088	-0.346	-0.31
Montane Oak-Hickory	-0.323	0.006	7088	-0.338	-0.307
Southern Appalachian Cove	-0.385	0.011	7088	-0.413	-0.357
Succesional Tuliptree	-0.36	0.011	7088	-0.388	-0.332

Young, J., Fleming, G., Cass, W., Leah, C. (2009). Vegetation of Shenandoah National Park in Relation to Environmental Gradients, Version 2.0 Technical Report NPS/NER/NRTR—2009/142.

Chapter 3. Assessing temperate forest growth and climate sensitivity in response to a long-term whole-watershed acidification experiment

Published in *JGR Biogeosciences* (2020), doi:10.1029/2019JG005560

Abstract

Acid deposition is a major biogeochemical driver in forest ecosystems, but the impacts of long-term changes in deposition on forest productivity remain unclear. Using a combination of tree ring and forest inventory data, we examined tree growth and climate sensitivity in response to 26 years of whole-watershed ammonium sulfate ($(NH_4)_2SO_4$) additions at the Fernow Experimental Forest (West Virginia, USA). Linear mixed effects models revealed species-specific responses to both treatment and hydroclimate variables. When controlling for environmental covariates, growth of northern red oak (*Quercus rubra*), red maple (*Acer rubrum*), and tulip poplar (*Liriodendron tulipifera*) was greater (40, 52, and 42%, respectively) in the control watershed compared to the treated watershed, but there was no difference in black cherry (*Prunus serotina*). Stem growth was generally positively associated with growing season water availability and spring temperature, and negatively associated with vapor pressure deficit. Sensitivity of northern red oak, red maple, and tulip poplar growth to water availability was greater in the control watershed, suggesting that acidification treatment has altered tree response to climate. Results indicate that chronic acid deposition may reduce both forest growth and climate sensitivity, with potentially significant implications for forest carbon and water cycling in deposition-affected regions.

3.1 Introduction

Acid deposition has profoundly altered the biogeochemistry of eastern North American forests, impacting forest ecosystem health, productivity, and biodiversity (Driscoll et al., 2001; Lovett et al., 2009). In areas with poorly buffered soils, deposition of nitrogen (N), sulfur (S), and H^+ has increased soil acidity and driven declines in the availability of essential plant nutrients (Likens et al., 1996). Although implementation of the Clean Air Act and its amendments has led to substantial declines in deposition since the 1970s (Sullivan et al. 2018), there is often a time-lag between deposition reduction and soil recovery (Johnson et al. 2018). In the mid-Atlantic and southeastern United States, recovery of soil nutrients to preindustrial levels is projected to take decades to centuries (Fahkraei et al., 2016). Soil nutrients influence both above- and belowground tree growth (e.g., Fahey et al., 2016; Levesque et al., 2016; Vadeboncoeur, 2010), suggesting that acidification-mediated changes in forest soil nutrients have the potential to alter both forest carbon uptake and response to climate. However, in the absence of controlled experiments, impacts of acid deposition on forest carbon and water balance can be difficult to separate from other long-term changes (e.g. forest succession, responses to changing climate and increasing atmospheric CO_2). Forest ecosystem response to changes in acid deposition has key implications for the productivity of eastern US temperate forests, which account for approximately two-thirds of the conterminous US carbon sink (Lu et al., 2015).

Acid deposition influences tree health and productivity via both direct and indirect mechanisms. As soil pH declines, phytotoxic aluminum is mobilized in the soil solution (Delhaize & Ryan, 1995; Kochian, 1995), and essential plant nutrient cations such as calcium (Ca^{2+}), magnesium (Mg^{2+}), and potassium (K^+) are leached from the soil (de Vries et al. 2003; Likens et al. 1996). Soil base cation depletion, aluminum mobilization, and associated nutrient

imbalances have been linked to symptoms of decline and mortality in ecologically important hardwood species including sugar maple (*Acer saccharum;* Long et al., 2009; Sullivan et al., 2013) and northern red oak (*Quercus rubra;* Demchik & Sharpe, 2000), as well as reduced productivity of eastern US forests overall (Elias et al. 2009). Direct acid-induced leaching of foliar calcium and subsequent winter freezing injury appear to be the primary mechanisms by which acid deposition affects growth of red spruce (*Picea rubens*; Borer et al., 2005; DeHayes et al., 1999). Recently observed increases in the growth of red spruce in the northeastern US and central Appalachia have been attributed to reductions in acid deposition following implementation of the Clean Air Act and its amendments (Kosiba et al., 2018; Wason et al., 2017; Mathias & Thomas, 2018). However, such recovery has not been documented in the deciduous broadleaf species that dominate eastern US forests.

In addition to reductions in acid deposition, eastern US forests are experiencing concurrent changes in other drivers of tree growth. While N deposition contributes to soil acidification, particularly on base-poor soils, evidence suggests that deposition-driven alleviation of N limitation has enhanced temperate forest productivity overall (Magnani et al., 2007), though the effects are species-specific (Thomas et al., 2010; Horn et al., 2019). As N deposition declines, some temperate forests are experiencing adverse legacy effects of excess N deposition (i.e. soil acidification, base cation depletion) while simultaneously becoming increasingly N-limited (Gilliam et al., 2018a; Groffman et al., 2018). Further, future trajectories of temperate forest productivity are likely to be strongly influenced by changes in climate. Even in the relatively wet eastern US, tree-ring evidence suggests that growth of many dominant species is positively associated with growing season moisture availability, but negatively associated with vapor pressure deficit (VPD) and temperature (Helcoski et al., 2019; Jennings et al, 2016;

Levesque et al., 2017; Maxwell et al., 2019). Warmer spring temperatures have been linked to increased growing season forest productivity in the eastern US (Keenan et al., 2014; Richardson et al., 2009), but also increased N limitation (Elmore et al., 2016). Climate models project more variable precipitation (Luce et al., 2016) and greater atmospheric evaporative demand over forested regions of the eastern US in coming decades (Dewes et al., 2017; Ficklin & Novick, 2017), but controls on temperate deciduous forest sensitivity to climate remain poorly characterized, and it remains uncertain how changes in climate, acid deposition, and soil nutrient availability will individually or interactively affect forest productivity and climate response.

Long-term acidification experiments provide unique opportunities to assess the impacts of acid deposition on forest productivity and climate sensitivity against a backdrop of other global change drivers. At the Fernow Experimental Forest in West Virginia, additions of ammonium sulfate ($(NH_4)_2SO_4$) have been applied to a forested watershed three times annually since 1989. The treated watershed has exhibited characteristic signs of acidification and N saturation, including reduced soil pH, higher soil water Al concentrations, soil base cation depletion, and elevated stream water nitrate compared to adjacent reference watersheds (Adams et al., 2006; Fernandez et al., 2010). However, analyses of tree growth response to acidification treatments at Fernow have been mixed or inconclusive. For example, DeWalle et al. (2006) reported that growth of black cherry (*Prunus serotina*) and tulip poplar (*Liriodendron tulipifera*) increased in the treated watershed relative to the control in the first seven years, perhaps due to N fertilization or base cation mobilization, but growth rates declined thereafter. Jensen et al. (2014) reported species-specific differences in growth, with black cherry exhibiting significantly greater growth in the treated watershed until 2003, and tulip poplar growing consistently faster in the control watershed from 1989-2011. Notably, previous studies in these watersheds have not

attempted to assess interactions between acidification treatments and forest climate response, or disentangle stand successional dynamics from treatment effects.

Here, we combine dendrochronological techniques, long-term monitoring of catchment hydrology, and repeat forest inventory data to examine productivity and climate sensitivity of trees in a forested watershed that has received experimental acidification treatments since 1989, compared to those in an adjacent control watershed. Our objectives were to (1) assess long-term effects of experimental acidification treatments on the aboveground growth of four temperate deciduous tree species, and (2) examine effects of acidification on tree response to climate in a regenerating hardwood forest. We present results of linear mixed effects models (LMMs) designed to assess the contributions of treatment, climate, and individual drivers to the growth of each species, and examine treatment-climate interactions. We compare species-specific responses to treatment to those at the stand-scale, and discuss potential mechanisms by which acid deposition-driven changes in soil nutrients mediate tree growth and climate sensitivity.

3. Materials and Methods

3.2.1 Site Description

This research was conducted in Watershed 3 (WS3, treatment) and Watershed 7 (WS7, control) at the Fernow Experimental Forest in the Allegheny Highlands of West Virginia, USA (39.05 N, -79.67 W). Mean annual temperature at Fernow is 9.2° C, and average precipitation is 1458 mm/year, distributed approximately evenly between growing and dormant seasons. WS3 and WS7 are 34.4 ha and 24 ha, respectively, and elevation in both watersheds ranges from ~730 to 860 m (Adams et al., 2006). Streamflow has been continuously monitored from both watersheds since the late 1950s (Edwards & Wood, 2011). Soils are thin (<1m), acidic, loamy-

skeletal, mixed, active, mesic Typic Dystrochrepts overlying quartzose sandstone and shale (Adams et al. 2006, Fernandez et al. 2010). Between 1994 and 2015, surface soil pH dropped from 4.34 to 4.02 in the treated watershed, and 4.50 to 4.39 in the control watershed (Gilliam et al., 2016; Gilliam et al., 2018b). This suggests ongoing soil acidification in both watersheds, but at a faster rate in the treated watershed.

The forest on WS3 was clear cut in 1969-1970 before being allowed to regenerate naturally; WS7 was clear cut and maintained barren with herbicides between 1963-1969 and has regenerated naturally from 1969-present. Forests on both watersheds are mixed-mesophytic, dominated by black cherry (*Prunus serotina*), northern red oak (*Quercus rubra*), tulip poplar (*Liriodendron tulipifera*), red maple (*Acer rubrum*), and sweet birch (*Betula lenta*). Forest inventory data, including DBH and canopy position classification of all trees greater than 2.54 cm diameter within 25 0.1-ha plots in each watershed, were collected by the Forest Service in 1990 (1991 in WS7), 1996, 1999, 2003, 2009, and 2018.

Acidification treatments in the treatment watershed have consisted of three aerial applications (March, July, and November) of ammonium sulfate fertilizer annually since 1989, totaling an additional 40.6 kg S ha^{-1} and 35.4 kg N ha^{-1} per year (Adams et al., 2006). At the onset of the acidification experiment, this represented approximately double the bulk N and S throughfall inputs measured at Fernow. Experimental ammonium sulfate inputs to the treated watershed at Fernow have remained the same even as background deposition has declined in recent decades. For reference, in 2015 background total deposition of N and S at the National Atmospheric Deposition Program (NADP) monitoring station in Parsons, WV (4.4 km from the study watersheds) was 3.1 and 4.0 kg ha^{-1}, respectively (Figure S3.1; National Atmospheric Deposition Program, 2018).

3.2.2 Field Sampling

Our field sampling design was based on the goal of collecting increment cores from at least 15 black cherry (*Prunus serotina*), northern red oak (*Quercus rubra*), red maple (*Acer rubrum*), and tulip poplar (*Liriodendron tulipifera*) individuals in the treatment and control watersheds. Tree cores were collected in plots spaced ~50 meters apart along transects running from stream edge to ridge in order capture elevation and aspect gradients within each watershed (Figure 3.1). At each plot, beginning at magnetic north and moving clockwise for odd-numbered points and counter-clockwise for even-numbered points, we first searched within 10 meters for trees of the target species at least 15 cm in DBH, selecting the first satisfactory tree encountered for sampling. If no satisfactory trees were found within 10 meters, we repeated the procedure with a radius of 20 meters. Trees were rejected for sampling if they had defects in the bottom two meters that indicated a likelihood of center rot, or if they had a severe lean or a visible history of major crown damage (more than a third of the crown removed in a single event). Trees were also rejected if they were the subject of ongoing research (e.g. trees within permanent plots or with dendrometer bands). Two cores were collected from each tree using a 5.3 mm diameter increment borer. Cores were taken on opposite sides of the bole, perpendicular to the slope to avoid reaction wood. Because of our minimum diameter requirement, trees sampled tended to be canopy dominant or co-dominant (with the exception of shade-tolerant red maple), potentially biasing our results towards larger trees in these stands (Nehrbass-Ahles et al., 2014). As a result, tree growth results more closely reflect the "optimal" response of trees to treatment and climate (Jennings et al., 2016).

After scraping away the litter layer, two 15-cm soil samples were also collected within the 20 m plot radius. Soil cores were frozen until they could be processed for C and N analyses.

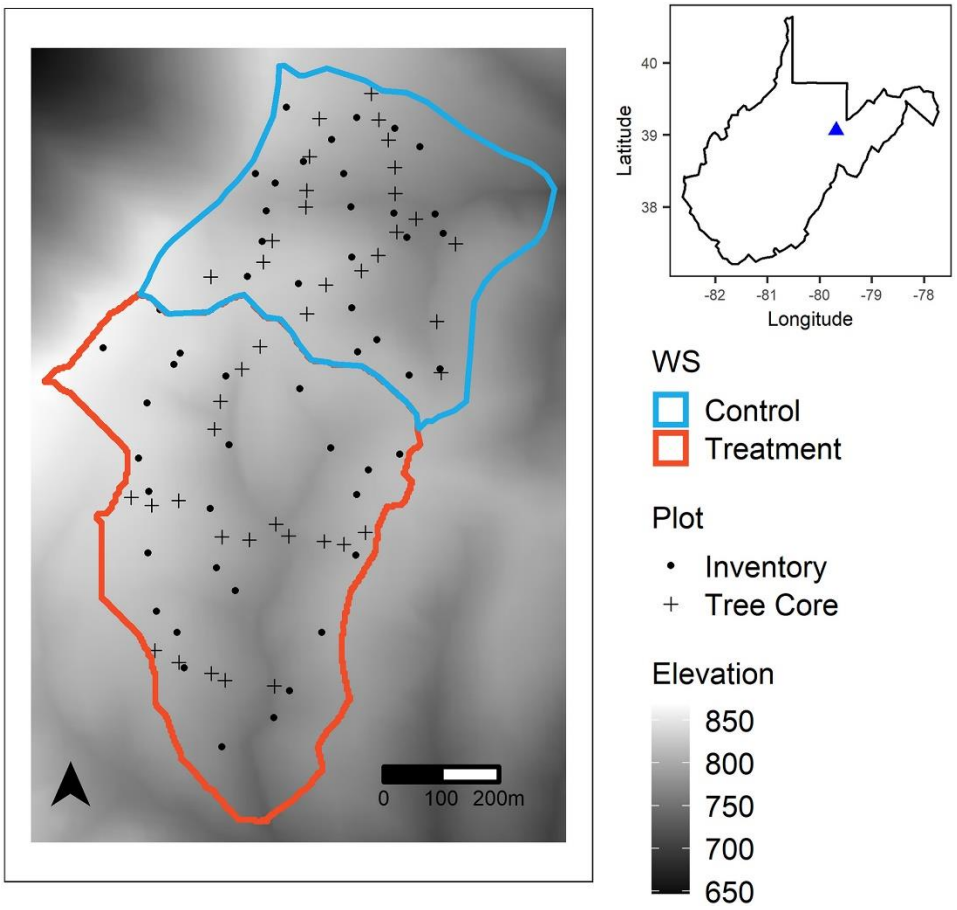

Figure 3.1 Locations of tree core and soil sampling plots and forest inventory plots. WS3 (treatment) has received aerial applications of ammonium sulfate since 1989.

3.2.3 Tree Core and Soil Sample Processing

Increment cores were air-dried, hand-sanded, skeleton-plotted, and visually cross dated using standard dendrochronological procedures (Speer, 2012). Tree rings were measured using a sliding scale micrometer (Velmex Measuring System, Velmex, Inc., Bloomfield, NY) and MeasureJ2X software (VoorTech Consulting, Holderness, NH). Cross dating was statistically validated using COFECHA (Holmes, 1983). For each tree, the core with the greater correlation with the master series for that species/watershed was selected for subsequent analyses. Raw ring

widths were converted to basal area increment (BAI) using the R package dplR (Bunn et al., 2018). BAI allows for a comparison of growth rates across trees of different sizes by accounting for the often-negative correlation between measured ring width and diameter, while preserving both high and low frequency variability in the tree growth (Martin-Benito et al., 2011). However, while BAI is a useful proxy for estimating annual stem growth increment, converting ring widths to BAI assumes uniform cross-sectional growth, even though tree stems are not perfectly circular.

Frozen soil samples were thawed and then sieved to 2 mm. Subsamples of oven-dried soil were ground and analyzed for total C and N concentrations using a Carlo Erba Elemental Analyzer (CE Instruments, Ltd., Wigam, UK). Soil ammonium and nitrate were extracted from 10 g subsamples of field-moist soil in 50 mL of 2.0 M KCl, which was shaken for one hour, allowed to settle, then filtered through Whatman Grade 1 filter paper. Filtered extracts were analyzed for NH_4^+-N and NO_3^--N using a QuickChem 8500 Series Flow Injection Analyzer (Lachat Instruments, Loveland, CO).

3.2.4 Climate, Deposition, and Streamflow Data

Precipitation data were collected from rain gauges within the treatment and control watersheds. Temperature data were collected at a meteorological station at the top of Fernow Watershed 4 (adjacent to the treated watershed). Daily maximum vapor pressure deficit (VPD_{max}) data were acquired from PRISM (PRISM Climate Group 2004) and converted to monthly averages. Nitrogen and S deposition data were collected at the National Atmospheric Deposition Program (NADP) monitoring station in Parsons, WV (National Atmospheric Deposition Program, 2018). Growing season evapotranspiration (ET) was calculated by differencing precipitation and stream discharge, assuming changes in catchment storage to be

negligible. Hydrograph separation was performed to partition streamflow into baseflow and quickflow components (Hewlett & Hibbert, 1967). Catchment wetting (W) was calculated by differencing precipitation and quickflow, and determined to be a better estimate of plant available water than precipitation alone. This approach was originally developed by Horton (1933), and was more recently reintroduced (Troch et al., 2009, Voepel et al., 2011). Total growing season (June-August) W, mean March and April temperatures, and mean growing season maximum daily VPD (VPD_{max}) were used as predictors of tree growth in statistical analyses.

3.2.5 Statistical Analyses

Total soil C, N, C:N ratios, NO_3^-, and NH_4^+ from the treatment and control catchments were compared using nonparametric Mann-Whitney U tests. Mann-Kendall tests were used to examine temporal trends in hydroclimate variables (temperature, precipitation, catchment wetting, and ET) during two time periods: 1957-2015, coinciding with the instrumental record for both watersheds at Fernow, and 1990-2015, coinciding with the ammonium sulfate treatment period. Trends in wet deposition of SO_4^{2-}, NO_3^-, and NH_4^+ were also examined between 1990-2015. Preliminary analyses using Kendall's rank correlation (τ) were performed to examine relationships between BAI of each species and climate and deposition variables, and correlations of potential environmental drivers with each other. These analyses indicated that atmospheric CO_2, SO_4^{2-} deposition, and NO_3^- deposition were highly collinear, and because they increased/decreased monotonically, were also strongly correlated with tree age. To avoid collinearity issues, CO_2 and background deposition variables were excluded as predictors in subsequent analyses, which focus on the effects of acidification treatment and hydroclimate variables that have a higher degree of interannual variability.

Linear mixed-effects models (LMMs) were used to determine environmental controls on tree growth while accounting for the hierarchical structure of our data (growth rings in trees, trees in plots, plots in watersheds), and also temporal autocorrelation in BAI chronologies (e.g., Martin-Benito et al., 2011, Levesque et al., 2016). BAI data were right-skewed, and were square root transformed to achieve normality for use as the response variable in LMMs. For each species, fixed effects in the LMMs included ammonium sulfate treatment, tree development (age and canopy class), hydroclimate variables (VPD_{max}, W, and mean March/April temperatures), local plot factors (solar radiation, topographic wetness index, soil nutrients), and also interactions between acidification and tree response to climate. A conceptual equation for the fixed structure of the 'beyond optimal' model (Zuur, 2009) is expressed as:

$$\sqrt{BAI} = \beta_0 + \beta_1(Treatment) \times \beta_2(Climate) + \beta_3(Development) + \beta_4(Local) + \varepsilon,$$

where β_0 represents the intercept, β_{1-4} represent regression parameters describing effects of treatment, hydroclimate variability, tree development, and local factors, and ε is the residual term. Tree ID was specified as a random effect in order to isolate growth differences attributable to fixed effects and those due to individual variability among trees. An AR(1,0) structure was used to account for residual autocorrelation. Models with random intercepts and random slopes and intercepts were compared using Akaike Information Criterion (AIC). The difference in AIC between random intercepts and random slopes and intercepts models was <4, and thus models were determined to be sufficiently similar to justify the use of more parsimonious random intercepts models. LMMs were fitted using the R version 3.4.4 (R Core Team 2018) and the package nlme (Pinheiro et al., 2018). Optimal models for each species were determined using a stepwise selection method, with F tests to assess significance of model terms (i.e., Zuur et al., 2009). Because we were specifically interested in the effects of acidification treatment, we

included treatment in each model, regardless of whether or not it improved model fit. Residual normality was verified using histograms and quantile-quantile plots.

Variance explained by fixed effects (marginal r^2) and total variance explained by fixed and random effects (conditional r^2) were computed using the MuMIn R package (Barton, 2018). Importance of individual predictors was determined from LMM output using partial regression coefficients for the relationships between BAI and standardized predictor variables. To test for evidence of a treatment effect, we calculated estimated marginal means (EMMs), which describe the effects of acidification treatment while controlling for fixed covariates, using the emmeans package in R (Lenth, 2017). Reported effect sizes for tree growth in treated and control watersheds are thus back-transformed, covariate-adjusted EMMs. For each species, *t* tests were used to compared EMMs between trees in WS3 and WS7, with significance of α=0.05.

3.3 Results

3.3.1 Deposition, Hydroclimate, and Soils

Annual background wet deposition of sulfate declined 83% between 1990-2015, while nitrate wet deposition declined 55%. There was no significant temporal trend in wet ammonium deposition (Figure S3.1; Table S3.1). Between 1957-2015, mean June-August temperature increased by an average of 0.02°C per year, mean April temperature also increased 0.02°C per year, and there was a significant positive trend in June-August ET in both watersheds (Table S3.1). However, there were no clear trends in growing season precipitation or VPD_{max} during this time period. Due to substantial interannual variability in temperature, precipitation, and VPD, there were no significant trends in any examined hydroclimate variables between 1990-2015. The soil C:N ratio was 10% greater in samples from the treated catchment (p=0.02; Figure 3.2a), but total soil N did not differ between watersheds (Figure 3.2b). NO_3^--N in the upper 15cm of soil

was 375% greater in the treated catchment compared to the control ($p<0.0001$; Figure 3.2c). NH_4^+-N did not differ between the treatment and control watersheds (Figure 3.2d).

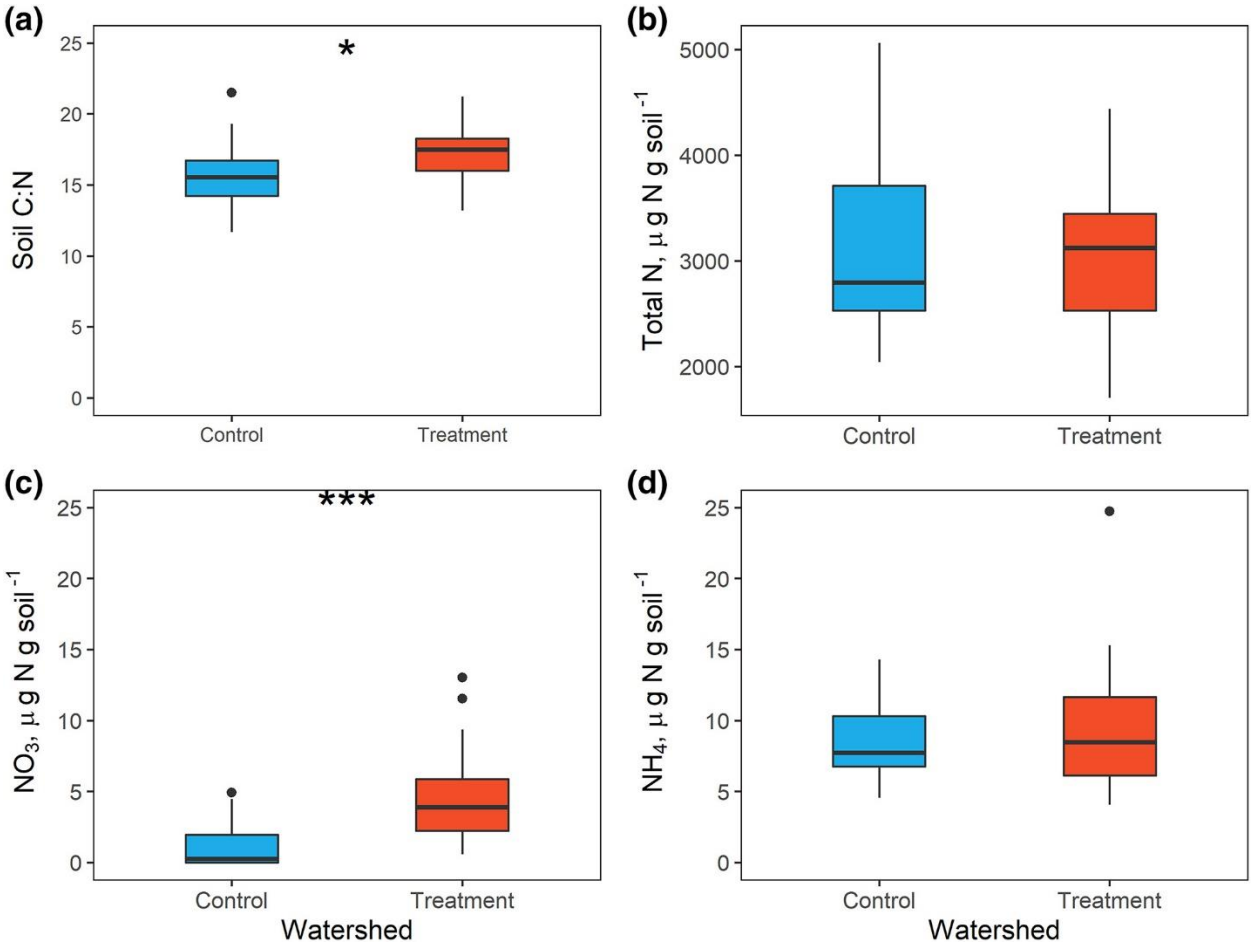

Figure 3.2 Comparisons of (a) soil C:N ratios, (b) total N, (c) NO_3-N, and (d) NH_4-N between treatment and control watersheds at Fernow. Boxes represent upper and lower quartiles of each distribution, inner lines represent median values, and dots represent values greater than 1.5 times the interquartile range. Mean values were compared using nonparametric Mann-Whitney U tests (*P < 0.05, ***P < 0.001).

3.3.2 Environmental Controls on BAI

Catchment wetting, a proxy for plant-available water, was the most important hydroclimate predictor of BAI in red maple, northern red oak, and tulip poplar across years. There was a significant interaction between catchment wetting and treatment in these three

species, with trees in the control watershed more sensitive to water availability than those in the treated watershed (Table 3.1, Figures S3.3-3.5). Black cherry, red maple, and tulip poplar responded negatively to VPD_{max} in both watersheds, and the effect did not differ with treatment. To a lesser extent, mean April and March temperatures contributed positively to BAI for all species examined except red maple (Table 3.1, Figures S3.2-3.5).

Canopy class was an important predictor of BAI for all species -- dominant and codominant trees had greater growth rates than sub-canopy trees (Table 3.1). Tree age was a significant predictor of BAI for northern red oak and tulip poplar, as annual stem growth of both of these species has generally increased over time (Figure 3.3; Table 3.1). Soil NO_3^- and NH_4^+ were generally not important predictors of tree growth across plots. However, there were notable differences in within-species responses to soil N content between the treatment and control watersheds. Soil NO_3^- was positively associated with red maple growth in the control watershed, but there was no relationship in the treated watershed. Soil NH_4^+ was negatively associated with black cherry growth in the control watershed, but there was no relationship in the treated watershed. While soil NO_3^- was not a significant predictor of northern red oak growth ($p>0.05$), its inclusion marginally improved model fit (Table 3.1).

As hypothesized, acidification treatments influenced tree growth in species-specific ways. Comparisons of EMMs revealed that acidification treatment reduced BAI by 40% in northern red oak ($p=0.047$), 52% in red maple ($p=0.002$), and 42% in tulip poplar ($p=0.004$), but there was no difference in black cherry growth (Figure 3.4).

Fixed effects in the LMMs explained between 20-53% of the total variance in BAI, as indicated by the marginal r^2 values, while fixed and random effects combined explained between 26-74% of variance, as indicated by the conditional r^2 values (Table 3.1). The considerable

increase in explained variance when random effects are included indicates a relatively high degree of among-tree variation in BAI in a given year for black cherry, northern red oak, and tulip poplar.

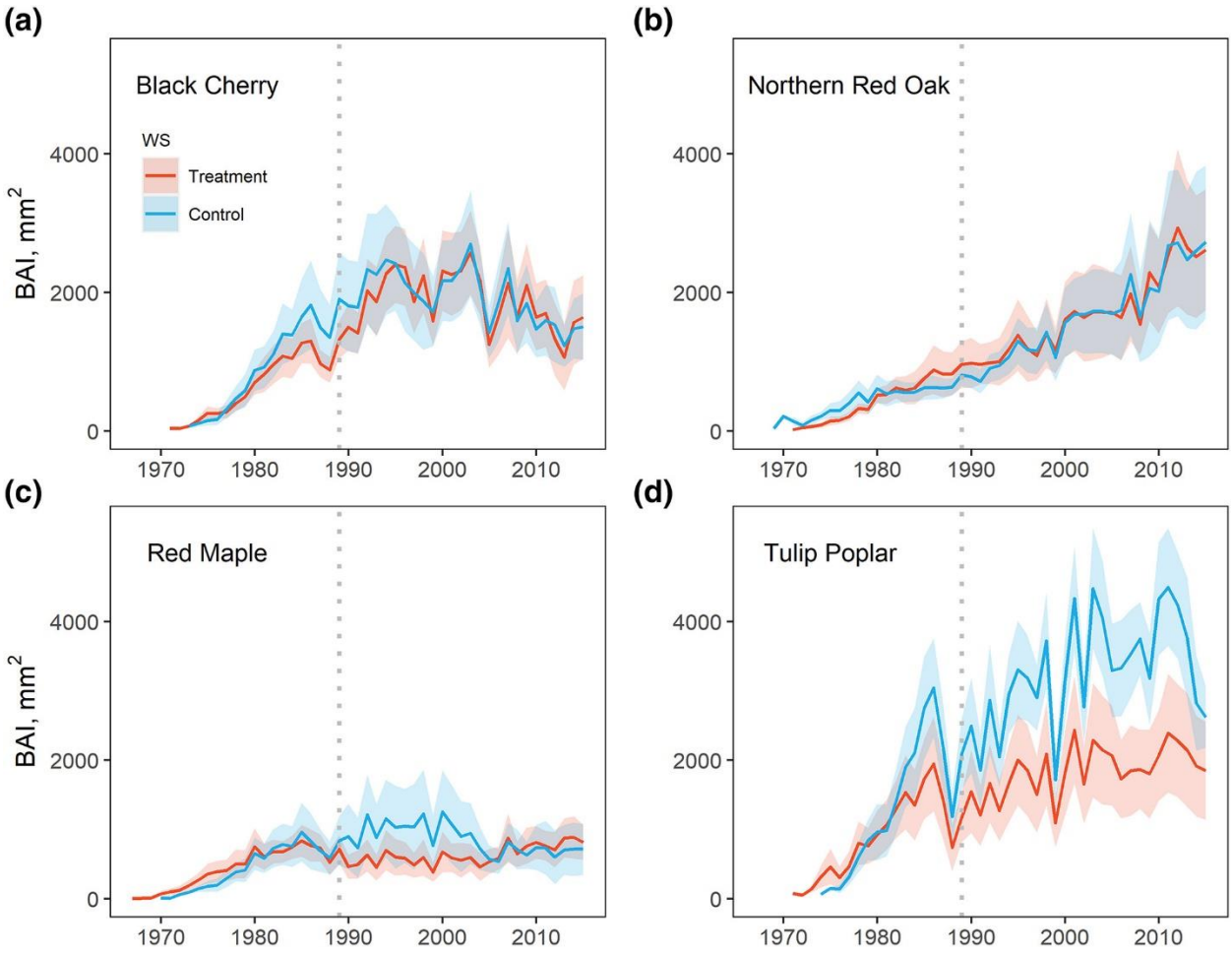

Figure 3.3 Mean basal area increment chronologies for each focal species: (a) black cherry, (b) northern red oak, (c) red maple, and (d) tulip oplar. Shaded regions represent 95% confidence intervals for each year, and vertical dotted lines mark the beginning of acidification treatments (1989).

Table 3.1 Results of LMMs Examining Effects of Acidification Treatment, Canopy Class, Soil Nutrients, and Hydroclimate on BAI of Focal Species.

Species	Marginal r^2	Conditional r^2	Fixed Effects	df	Estimate	P
Black Cherry	0.2	0.5	Treatment	29	0	0.97
			Treatment:Soil NH_4	29	6.2	**0.02**
			Soil NH_4	29	1.5	0.22
			Spring Temperature	873	20.2	<0.0001
			VPD	873	86.3	<0.0001
			Canopy Class	29	4.1	0.03
Northern Red Oak	0.47	0.63	Treatment	24	1.2	0.27
			Treatment:Wetting	721	17.1	**<0.0001**
			Wetting	721	57.2	<0.0001
			Spring Temperature	721	11.9	0.0006
			Soil NO_3	24	3.8	0.06
			Age	721	77.8	<0.0001
			Canopy Class	24	9.3	0.001
Red Maple	0.27	0.27	Treatment	26	8.1	**0.002**
			Treatment:Wetting	767	13.9	**0.0002**
			Treatment:Soil NO_3	26	6.7	**0.015**
			Wetting	767	131.2	<0.0001
			Soil NO_3	26	0.3	0.56
			VPD	767	39.1	<0.0001
			Canopy Class	26	13.8	0.001
Tulip Poplar	0.52	0.73	Treatment	29	10.5	**0.003**
			Treatment:Wetting	818	18.3	**<0.0001**
			Wetting	818	81.5	<0.0001
			VPD	818	43.7	<0.0001
			Spring Temperature	818	26.4	<0.0001
			Age	818	24.7	<0.0001
			Canopy Class	29	27.1	<0.0001

Notes: Bold text indicates P<0.05 for acidification treatment and its interactions. The response variable is square-root transformed BAI of each species. Treatment:Variable indicates an interaction between treatment and a given predictor variable.

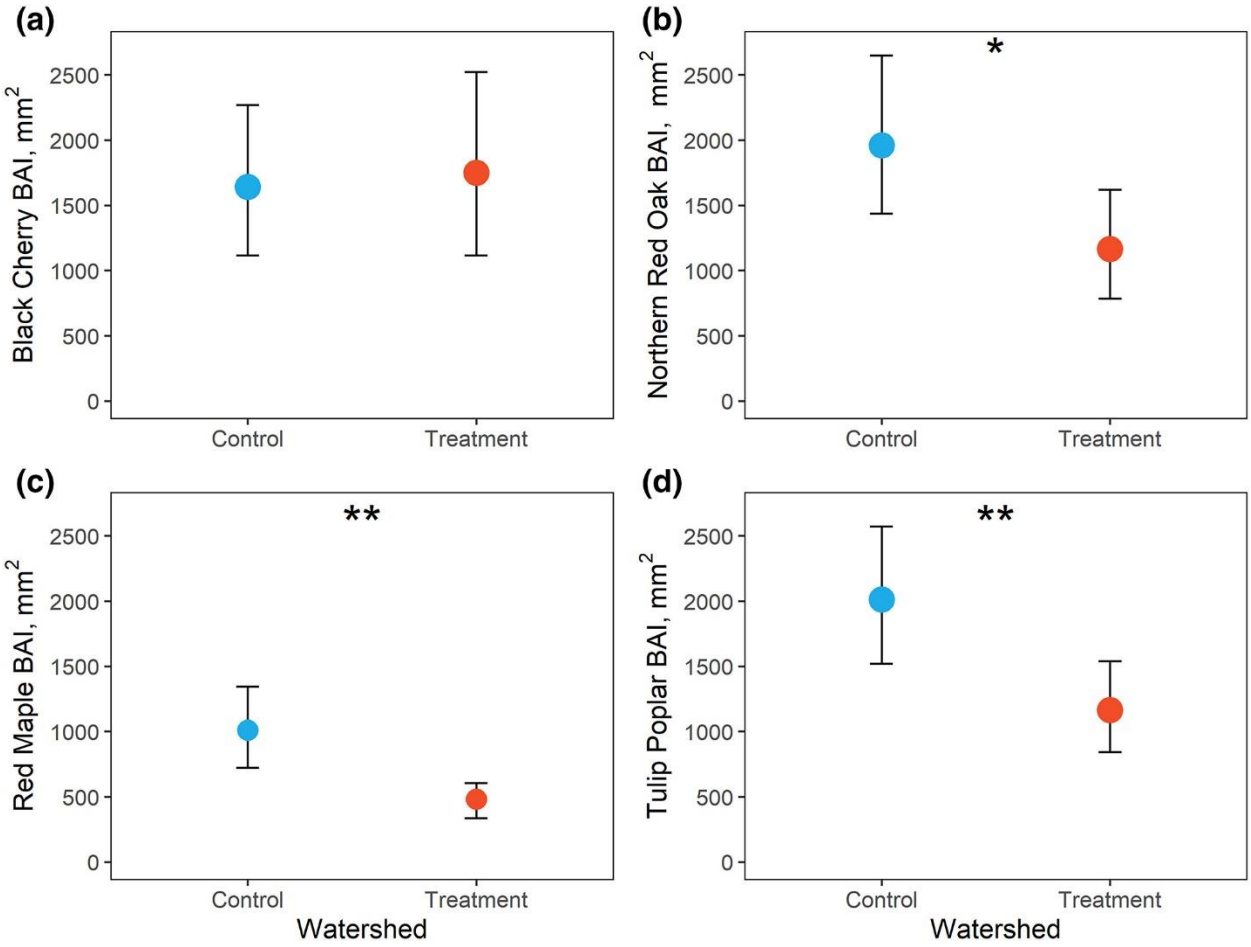

Figure 3.4 Estimated marginal means (BAI adjusted for fixed covariates) derived from LMMs for (a) black cherry, (b) northern red oak, (c) red maple, and (d) tulip poplar in the treatment and control watersheds during the treatment period (1989–2015). Error bars represent 95% confidence intervals (*P < 0.05, **P < 0.01).

3.3.4 Forest Inventory Data

Between 1990 and 2018 (the most recent forest inventory year), the basal area of the four focal species increased from 61 to 79% of total stand basal area in the treated watershed, and from 41 to 65% of total stand basal area in the control (Figure 3.5). Black cherry was the dominant species in the treated watershed, increasing from 38 to 52% of total stand basal area during the 1990-2018 study period. Black cherry increased from 15-22% of stand basal area in the control watershed over the entire study period. In the most recent inventory measurement period (2009-2018), the fraction of black cherry declined in the treated watershed (53.6% to

51.9%) and increased only slightly in the control watershed (21.6% to 22.2%). Tulip poplar was the dominant species in the control watershed, comprising 18-35% of basal area. Red maple held a relatively constant fraction of basal area throughout the study period in both watersheds, making up 12-14% of stand basal area in the treated watershed, and ~8% of stand basal area in the control watershed. Northern red oak was the least important species of the four in each watershed, accounting for <8% of basal area in the treated watershed, and ~1% of basal area in the control. Total stand basal area was greater in the control watershed throughout the duration of the study period (Figure 3.6). However, the basal area of the average tree in each watershed (regardless of species) was similar in each inventory year until 2018, when tree size in the control watershed was 16% greater (Figure 3.6).

Tree canopy class data collected during inventory sampling between 1996-2018 reveals that while both stands have thinned overall, the proportion of canopy dominant or co-dominant black cherry, northern red oak, and tulip poplar has increased on both watersheds (Figure S3.6). Red maple was most common as an understory species in both watersheds during the study period. While black cherry remains an important canopy tree in both watersheds, it nearly disappeared from the understory by 2018 (Figure S3.6), consistent with its role as a shade-intolerant, early successional species (USDA, 2019).

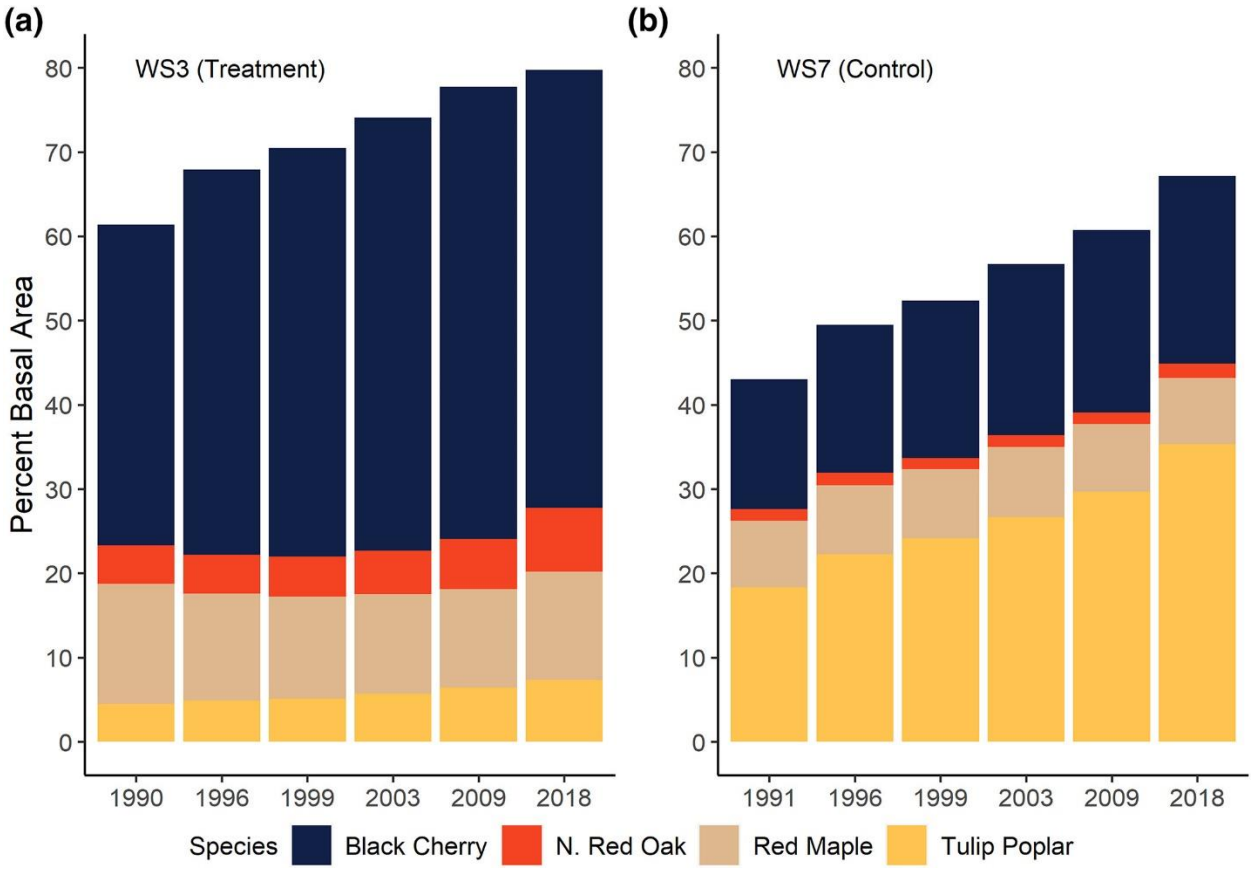

Figure 3.5 Percent of total stand basal area of the four focal species in each watershed between 1990 and 2018. The four species increased from 61–79% of total stand basal area in WS3 (a) and 41–65% of total stand basal area in WS7 (b) during the study period.

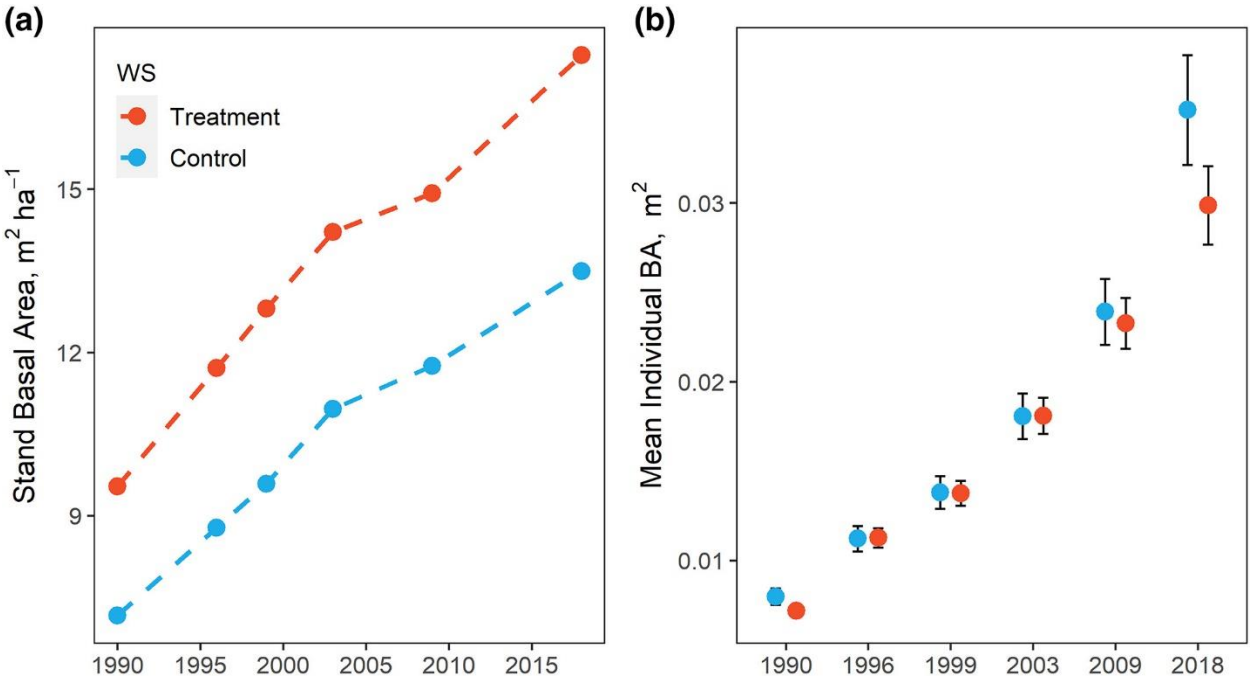

Figure 3.6 (a) Whole-watershed basal area, based on 25 0.1-ha inventory plots in each watershed. Dotted lines represent linear interpolations stand basal area between inventory years. (b) Mean basal area of the average tree in each watershed each inventory year. Error bars represent 95% confidence intervals. In each figure 1990 data for the control watershed are linearly extrapolated backward, since the first forest inventory data collection in this watershed occurred in 1991.

3.4 Discussion

3.4.1 Treatment effects on tree growth

Whole-watershed ammonium sulfate treatments reduced estimated marginal mean growth of northern red oak, red maple, and tulip poplar relative to an adjacent control watershed, but did not affect the growth of black cherry (Figure 3.4). The observed species-specific responses to treatment are generally consistent with previous tree ring studies at Fernow, which reported greater tulip poplar growth in the control catchment (Jensen et al., 2014), and comparable growth of black cherry after the first years of treatment (De Walle et al., 2006). Our findings are also consistent with studies showing that black cherry tends to be acid-tolerant (Long et al., 2009) and fast-growing, but shorter-lived than other co-occurring hardwood species (Auclair & Cottam,

1971). After rapid growth in the first two decades of stand development, black cherry growth has declined in both watersheds since ~2004 (Figure 3.3). We found 42% greater tulip poplar BAI in the control watershed compared to the treated watershed between 1990-2015. This contrasts with recent studies reporting that declines in atmospheric N and S deposition were not associated with tulip poplar growth (Levesque et al, 2017; Maxwell et al, 2019), but we note that experimental additions of ammonium sulfate at Fernow contribute substantially greater N and S loads than eastern US forests have received via background deposition.

Growth of red maple was 52% greater in the control watershed. Adverse effects of acid deposition and soil base depletion on sugar maple (*Acer saccharum*) have been examined extensively (e.g., Juice et al., 2006; Sullivan et al., 2013), but less is known about the sensitivity of red maple to deposition. Our results are consistent with evidence that S deposition is negatively associated with red maple growth (Horn et al., 2019), and the interactive effect between treatment and soil NO_3^- (positive BAI response in the control watershed, no relationship in the treated watershed; Figure S3.4), suggests that NO_3^- concentrations in the treated watershed have exceeded levels favorable to red maple growth.

While EMMs revealed significantly greater growth of northern red oak in the control catchment (Figure 3.4), the effect was weaker than that observed in red maple and tulip poplar. The modest negative effect of ammonium sulfate treatment on northern red oak BAI may be a result of negative effects of S-driven acidification (Demchik & Sharpe, 2000; Elias et al., 2009) outweighing positive effects of N fertilization (Thomas et al., 2010; Horn et al., 2019).

In recent national-scale study examining growth and survival of North American tree species in response to N and S deposition, Horn et al. (2019) found that N deposition was positively associated with growth of red maple, northern red oak, and tulip poplar, and reported a

threshold response for black cherry (increasing growth until >15 kg ha^{-1} N, but decreasing at higher levels). Given evidence that all four species examined in this study tend to respond positively to N deposition, the negative response to treatment in three of four species may reflect adverse acidifying effects of S, including Ca deficiency (Battles et al., 2014). Phosphorus (P) is often a co-limiting nutrient in temperate tree species subjected to elevated N (Goswami et al., 2018; Vadeboncoeur, 2010), and evidence of P limitation in understory plants has been reported in Fernow WS3 (Gress et al., 2010). Future work examining soil and plant stoichiometry in these watersheds may contribute to a better mechanistic understanding of treatment effects on above and belowground tree growth.

Although our tree ring evidence suggests negative tree growth responses to treatment, stand basal area (on a per hectare basis) was greater in the treated watershed throughout the entire study period (Figure 3.6). This may be attributable to the abundance of black cherry, which was insensitive to treatment, in the treated watershed (Figure 3.5). While black cherry remains a major component of the upper canopy in both watersheds, it has become less prevalent in the understory and will likely become less important in this forest as succession progresses, barring major gap-generating disturbances (Figure S3.6). While total stand basal area was greater in the treated watershed, the average tree in the control watershed was larger than that in the treated watershed in the 2018 inventory survey (Figure 3.6). However, the observed species-specific responses to treatment, and the differences in species composition between the two watersheds (both before and during the treatment period), make it difficult to assess forest response to treatment at the stand level. The increasing proportion of canopy dominant and codominant black cherry, tulip poplar, and northern red oak over time (Figure S3.6) suggests that stands in both watersheds are in the stem exclusion phase of stand development (Oliver &

Larson, 1996). Continued monitoring of forest structure, growth, and species composition will offer insights into the long-term impacts of chronic acidification on forest growth and successional trajectories in these watersheds.

3.4.2 Tree response to hydroclimate variability

Growing season catchment wetting was the strongest climatic predictor of BAI in all species except black cherry. Positive growth response to precipitation has been observed in broadleaf species throughout the eastern North American forest biome, even where growing season precipitation is generally considered to be abundant (Elliott et al., 2015; Helcoski et al., 2019; Levesque et al., 2017). Physiologically, this may reflect the importance of water availability in photosynthetic carbon assimilation (Lawlor & Conic 2002) and/or hydraulically-driven cell expansion during tree ring formation (Rathgeber et al., 2016; Zweifel et al., 2006). To a lesser extent, March and April temperatures were positively associated with BAI in all species except red maple. This is consisten with findings that extended growing season length driven by warm spring temperatures has been associated with greater growing season BAI (Elmore et al., 2016, Mathias & Thomas, 2018) and forest net primary production (Keenan et al., 2014; Ouimette et al., 2018) in temperate regions.

Growing season VPD has been found to be an important limitation on tree growth and carbon uptake in mesic forests (Jennings et al., 2016; Sulman et al., 2016). In this study, VPD was a negative control on BAI for all species except northern red oak. This likely reflects differences in xylem anatomy and hydraulic behavior between northern red oak and the other species examined. Ring-porous species such as northern red oak tend to exhibit anisohydric behavior, maintaining high rates of stomatal conductance (and thus carbon assimilation) when VPD is high, despite the risk of hydraulic failure (e.g., Yi et al., 2017). In contrast, diffuse-

porous tulip poplar and red maple exhibited negative growth response to VPD. These species tend to exhibit isohydric stomatal behavior, closely regulating stomatal conductance to maintain near-constant leaf water potential regardless of water status (Roman et al., 2015). Black cherry, which is semi-ring porous (Elliott et al., 2017), also responded negatively to growing season VPD. The observed negative response to VPD in the majority of species studied suggests that projected future increases in VPD (Ficklin & Novick, 2017) could result in reduced productivity mixed-mesophytic forests with species compositions similar to those at Fernow.

3.4.3 Treatment – Hydroclimate Interactions

Growth of northern red oak, red maple, and tulip poplar was more sensitive to water availability in the control watershed compared to the treated watershed (Table 3.1, Figures S3.3-3.5), suggesting that acidification treatment has altered tree physiological response to climate. While the proximate cause of reduced climate sensitivity is unknown, it may be related to reductions in tree root growth in the treated catchment. Gaines et al. (2016) determined that the majority of growing season water uptake for hardwood species in a Pennsylvania forest occurred at less than 60 cm depth, indicating that deciduous species in this region are reliant on relatively shallow soil water. Evidence from root surveys conducted in 1991 and 2013 at Fernow suggests that root density in the organic and upper mineral layers of the soil has declined relative to the control catchment during the experimental period (Adams, 2013; Peterjohn, 2013; Figure S3.7). Elevated soil Al^{3+}, which has been observed in WS3 at Fernow (Burnham et al., 2017), has been shown to reduce root growth (Delhaize & Ryan, 1995), impacting plant water and nutrient uptake (Kochian, 1995). In another study at Fernow, Carrara et al. (2018) observed 25% lower mineral soil (0-15 cm) root biomass in WS3, attributed to reduced belowground C allocation in response to elevated soil N. Whether driven by Al toxicity or changes in allocation, reduced root

growth could influence tree response to water availability. Acidification and/or nutrient effects on root growth warrant further examination, as rooting depth and distribution are important determinants of ecosystem productivity and drought response (Jackson et al., 1996), and they are important parameterizations in ecohydrologic models (Fan et al. 2017).

While foliar exposure to atmospheric pollution has been shown to affect tree stomatal function, and thus response to climate (Mansfield, 1998), we believe observed differences in tree growth and moisture sensitivity are primarily mediated via belowground effects. This is because ammonium sulfate is aerially applied in solid form three times annually, with two of the applications occurring outside the growing season (Adams et al., 2006). We found substantially higher NO_3^- in the treated watershed, consistent with findings from Burnham et al. (2017), although there was no difference in total N or NH_4^+ (Figure 3.2). Gilliam et al. (2018b) found that net nitrification rates did not differ between the control and treatment watersheds at Fernow, implying that reduced plant uptake of NO_3^- in the treated watershed, rather than elevated nitrification, is responsible for the observed difference in NO_3^- in the upper 15 cm of soil. Soil C:N ratios were higher in the treated watershed (Figure 3.2), a result consistent with slower decomposition rates reported in N addition and soil acidification experiments (Frey et al., 2014; Hobbie, 2008; Marinos & Bernhardt, 2018). While we considered the possibility that differences in soil organic material between watersheds could affect soil water retention, the treatment and control watersheds have exhibited similar hydrologic dynamics during the treatment period (Figure S3.8), suggesting that trees in the treatment and control watersheds have had similar access to available soil water.

Direct soil acidification effects may have also influenced tree climate response in the treated watershed. While we did not measure soil pH, soils in the treated watershed have

acidified to a greater extent than those in the control watershed during the study period (Gilliam et al., 2016; Gilliam et al., 2018b). Soil acidity has been found to diminish the capacity of red maple and white oak (*Quercus alba*) saplings to adjust coordination of hydraulic traits (xylem anatomy and leaf water relations) in response to N and P manipulations (Medeiros et al., 2018). Further, low soil pH has also been linked to reduced root hydraulic conductivity in paper birch (*Betula papyrifera*; Kamaluddin and Zwiazek, 2004). We cannot discount the possibility that, in addition to differences in root density, lower soil pH may play a role in the observed differences in tree climate sensitivity between the treated and control watersheds. Future studies examining interactions between soil pH, nutrients, and tree ecophysiology may improve our ability to predict tree response to climate in deposition-affected forests.

3.5 Conclusions

While the Clean Air Act and its amendments have resulted in substantial declines in N and S pollutant loads in Central Appalachia since 1989, acid deposition continues to be a globally important biogeochemical driver. Ammonium sulfate treatments to Fernow WS3 contribute 40.6 kg S ha^{-1} and 35.4 kg N ha^{-1} per year. Placing this in context, Yu et al. (2016) report that the average SO_4^{2-} and NO_3^- deposition over natural and agricultural systems in China between 2009-2014 was 116 kg S ha^{-1} and 33 kg N ha^{-1} per year, respectively. Thus, the Fernow Watershed Acidification Study has potential to offer insights into the impacts of acid deposition on temperate forest productivity at levels similar to or below globally realistic pollutant loads.

We found that ammonium sulfate addition reduced tree growth in the majority of hardwood species examined, and that this effect may be mediated by differences in tree sensitivity to water availability. Growing season water availability and spring temperatures were positively associated with tree growth, while VPD was generally a negative control on growth.

Together, results suggest that elevated acidic N and S deposition is a negative control on the productivity of canopy trees at Fernow, and acidification-mediated changes to soil chemistry may alter tree response to climate. This may have important implications for forest productivity, hydrology, and associated vegetation-climate feedbacks, in regions that are impacted by acid deposition. However, the extent to which acid deposition influences overall forest productivity likely depends on species-specific responses to deposition.

Acknowledgments

This study was co-authored by Todd M. Scanlon (University of Virginia), Howard E. Epstein (University of Virginia), Daniel L. Druckenbrod (Rider University), Matthew A. Vadeboncoeur (University of New Hampshire), Matthew Lanning (Indiana University-Purdue University Indianapolis), Mary Beth Adams (US Forest Service), and Lixin Wang (Indiana University-Purdue University). We thank Tim Forrest, Imani Guest, Yvonne Dinh, Carolyn Pugh, Nina Mauney, and Meg Miller for invaluable assistance in the field and the lab. Dr. Max Castorani assisted with implementation and interpretation of linear mixed effects models. Frederica Wood assisted with acquisition of Fernow streamflow and forest inventory data. This work was supported by NSF Hydrologic Sciences Award EAR-1562019. Tree ring, forest inventory, soil nutrient, hydroclimate, and atmospheric deposition data used to generate the results presented in this manuscript are available in an open-access UVA Dataverse repository (https://doi.org/10.18130/V3/FRZYXV).

Chapter 3 References

Adams, Mary Beth, DeWalle, D. R., & Hom, J. L. (2006). *The Fernow Watershed Acidification Study* (1st ed., Vol. 11). Springer Netherlands.

Adams, M.B., & Peterjohn, W. T. (2016). Fernow Experimental Forest Watershed Acidification Root Data, 1991. Department of Agriculture, US Forest Service North Central Research Station, Parsons, WV.

Auclair, A. N., & Cottam, G. (1971). Dynamics of Black Cherry (Prunus serotina Erhr.) in Southern Wisconsin Oak Forests. *Ecological Monographs*, *41*(2), 153–177. https://doi.org/10.2307/1942389

Barton, K. (2018). MuMIn: Multi-Model Inference. Retrieved from https://CRAN.R-project.org/package=MuMIn

Battles, J. J., Fahey, T. J., Driscoll, C. T., Blum, J. D., & Johnson, C. E. (2014). Restoring Soil Calcium Reverses Forest Decline. *Environmental Science & Technology Letters*, *1*(1), 15–19. https://doi.org/10.1021/ez400033d

Borer, C. H., Schaberg, P. G., & DeHayes, D. H. (2005). Acidic mist reduces foliar membrane-associated calcium and impairs stomatal responsiveness in red spruce. *Tree Physiology*, *25*(6), 673–680. https://doi.org/10.1093/treephys/25.6.673

Bunn, A. G., Korpela, M., Biondi, F., Campelo, F., Merian, P., Qeadan, F., et al. (2018). dplR: Dendrochronology Program Library in R. R package version 1.6.9. Retrieved from https://CRAN.R-project.org/package=dplR

Burnham, M. B., Cumming, J. R., Adams, M. B., & Peterjohn, W. T. (2017). Soluble soil aluminum alters the relative uptake of mineral nitrogen forms by six mature temperate broadleaf tree species: possible implications for watershed nitrate retention. *Oecologia*, *185*(3), 327–337. https://doi.org/10.1007/s00442-017-3955-8

Carrara, J. E., Walter, C. A., Hawkins, J. S., Peterjohn, W. T., Averill, C., & Brzostek, E. R. (2018). Interactions among plants, bacteria, and fungi reduce extracellular enzyme activities under long-term N fertilization. *Global Change Biology*, *24*(6), 2721–2734. https://doi.org/10.1111/gcb.14081

Chadwick Oliver, & Larson, B. (1996). *Forest Stand Dynamics, Update Edition*. Yale School of Forestry & Environmental Studies Other Publications. Retrieved from : https://elischolar.library.yale.edu/fes_pubs

DeHayes, D. H., Schaberg, P. G., Hawley, G. J., & Strimbeck, G. R. (1999). Acid Rain Impacts on Calcium Nutrition and Forest Health: Alteration of membrane-associated calcium leads to membrane destabilization and foliar injury in red spruce. *BioScience*, *49*(10), 789–800. https://doi.org/10.2307/1313570

Delhaize, E., & Ryan, P. R. (1995). Aluminum Toxicity and Tolerance in Plants. *Plant Physiology*, *107*(2), 315. https://doi.org/10.1104/pp.107.2.315

Demchik, M. C., & Sharpe, W. E. (2000). The effect of soil nutrition, soil acidity and drought on northern red oak (Quercus rubra L.) growth and nutrition on Pennsylvania sites with high and low red oak mortality. *Forest Ecology and Management*, *136*(1), 199–207. https://doi.org/10.1016/S0378-1127(99)00307-2

DeWalle, D. R., Kochenderfer, J. N., Adams, M. B., Miller, G. W., Gilliam, F. S., & Wood, F. (2006). Vegetation and Acidification, Chapter 5. In *The Fernow Watershed Acidification Study* (1st ed., pp. 137–188). Dordrecht: Springer Netherlands.

Dewes, C. F., Rangwala, I., Barsugli, J. J., Hobbins, M. T., & Kumar, S. (2017). Drought risk assessment under climate change is sensitive to methodological choices for the estimation of evaporative demand. *PLOS ONE*, *12*(3), e0174045. https://doi.org/10.1371/journal.pone.0174045

Driscoll, C. T., Lawrence, G. B., Bulger, A. J., Butler, T. J., Cronan, C. S., Eagar, C., et al. (2001). Acidic Deposition in the Northeastern United States: Sources and Inputs, Ecosystem Effects, and Management Strategies. *BioScience*, *51*(3), 180. https://doi.org/10.1641/0006-3568(2001)051[0180:ADITNU]2.0.CO;2

Edwards, P., & Wood, F. (n.d.). Fernow Experimental Forest daily streamflow. Newtown Square, PA: U.S. Department of Agriculture, Forest Service, Northern Research Station. Data publication updated 17 August 2017. Retrieved from https://doi.org/10.2737/RDS-2011-0015

Elias, P. E., Burger, J. A., & Adams, M. B. (2009). Acid deposition effects on forest composition and growth on the Monongahela National Forest, West Virginia. *Forest Ecology and Management*, *258*(10), 2175–2182. https://doi.org/10.1016/j.foreco.2009.05.004

Elliott, K. J., Miniat, C. F., Pederson, N., & Laseter, S. H. (2015). Forest tree growth response to hydroclimate variability in the southern Appalachians. *Global Change Biology*, *21*(12), 4627–4641. https://doi.org/10.1111/gcb.13045

Elliott, K. J., Caldwell, P. V., Brantley, S. T., Miniat, C. F., Vose, J. M., & Swank, W. T. (2017). Water yield following forest-grass-forest transitions. *Hydrology and Earth System Sciences*, *21*(2), 981–997. https://doi.org/10.5194/hess-21-981-2017

Elmore, A. J., Nelson, D. M., & Craine, J. M. (2016). Earlier springs are causing reduced nitrogen availability in North American eastern deciduous forests. *Nature Plants*, *2*(10). https://doi.org/10.1038/nplants.2016.133

Fahey, T. J., Heinz, A. K., Battles, J. J., Fisk, M. C., Driscoll, C. T., Blum, J. D., & Johnson, C. E. (2016). Fine root biomass declined in response to restoration of soil calcium in a northern hardwood forest. *Canadian Journal of Forest Research*, *46*(5), 738–744. https://doi.org/10.1139/cjfr-2015-0434

Fakhraei, H., Driscoll, C. T., Renfro, J. R., Kulp, M. A., Blett, T. F., Brewer, P. F., & Schwartz, J. S. (2016). Critical loads and exceedances for nitrogen and sulfur atmospheric deposition in Great Smoky Mountains National Park, United States. *Ecosphere*, *7*(10), e01466. https://doi.org/10.1002/ecs2.1466

Fan, Y., Miguez-Macho, G., Jobbágy, E. G., Jackson, R. B., & Otero-Casal, C. (2017). Hydrologic regulation of plant rooting depth. *Proceedings of the National Academy of Sciences*, *114*(40), 10572. https://doi.org/10.1073/pnas.1712381114

Fernandez, I. J., Adams, M. B., SanClements, M. D., & Norton, S. A. (2010). Comparing decadal responses of whole-watershed manipulations at the Bear Brook and Fernow experiments.

Environmental Monitoring and Assessment, *171*(1), 149–161. https://doi.org/10.1007/s10661-010-1524-2

Ficklin, D. L., & Novick, K. A. (2017). Historic and projected changes in vapor pressure deficit suggest a continental-scale drying of the United States atmosphere: Increasing U.S. Vapor Pressure Deficit. *Journal of Geophysical Research: Atmospheres*, *122*(4), 2061–2079. https://doi.org/10.1002/2016JD025855

Frey, S. D., Ollinger, S., Nadelhoffer, K., Bowden, R., Brzostek, E., Burton, A., et al. (2014). Chronic nitrogen additions suppress decomposition and sequester soil carbon in temperate forests. *Biogeochemistry*, *121*(2), 305–316. https://doi.org/10.1007/s10533-014-0004-0

Gaines, K. P., Stanley, J. W., Meinzer, F. C., McCulloh, K. A., Woodruff, D. R., Chen, W., et al. (2015). Reliance on shallow soil water in a mixed-hardwood forest in central Pennsylvania. *Tree Physiology*, *36*(4), 444–458. https://doi.org/10.1093/treephys/tpv113

Gilliam, F. S., Welch, N. T., Phillips, A. H., Billmyer, J. H., Peterjohn, W. T., Fowler, Z. K., et al. (2016). Twenty-five-year response of the herbaceous layer of a temperate hardwood forest to elevated nitrogen deposition. *Ecosphere*, *7*(4), e01250. https://doi.org/10.1002/ecs2.1250

Gilliam, F. S., Walter, C. A., Adams, M. B., & Peterjohn, W. T. (2018). Nitrogen (N) Dynamics in the Mineral Soil of a Central Appalachian Hardwood Forest During a Quarter Century of Whole-Watershed N Additions. *Ecosystems*, *21*(8), 1489–1504. https://doi.org/10.1007/s10021-018-0234-4

Gilliam, F. S., Burns, D. A., Driscoll, C. T., Frey, S. D., Lovett, G. M., & Watmough, S. A. (2019). Decreased atmospheric nitrogen deposition in eastern North America: Predicted responses of forest ecosystems. *Environmental Pollution*, *244*, 560–574. https://doi.org/10.1016/j.envpol.2018.09.135

Gress, S. E., Nichols, T. D., Northcraft, C. C., & Peterjohn, W. T. (2007). NUTRIENT LIMITATION IN SOILS EXHIBITING DIFFERING NITROGEN AVAILABILITIES: WHAT LIES BEYOND NITROGEN SATURATION? *Ecology*, *88*(1), 119–130. https://doi.org/10.1890/0012-9658(2007)88[119:NLISED]2.0.CO;2

Groffman, P. M., Driscoll, C. T., Durán, J., Campbell, J. L., Christenson, L. M., Fahey, T. J., et al. (2018). Nitrogen oligotrophication in northern hardwood forests. *Biogeochemistry*, *141*(3), 523–539. https://doi.org/10.1007/s10533-018-0445-y

Helcoski, R., Tepley, A. J., Pederson, N., McGarvey, J. C., Meakem, V., Herrmann, V., et al. (2019). Growing season moisture drives inter-annual variation in woody productivity of a temperate deciduous forest. *New Phytologist*. https://doi.org/10.1111/nph.15906

Hewlett, J. D., & Hibbert, A. R. (1967). Factors affecting the response of small watersheds to precipitation in humid areas. In *Forest Hydrology* (pp. 275–290). New York: Pergamon Press.

Hobbie, S. E. (2008). NITROGEN EFFECTS ON DECOMPOSITION: A FIVE-YEAR EXPERIMENT IN EIGHT TEMPERATE SITES. *Ecology*, *89*(9), 2633–2644. https://doi.org/10.1890/07-1119.1

Holmes, R. (1983). Cofecha: Computer Assisted Quality Control in Tree-Ring Dating and Measurement. *Tree-Ring Bulletin*, *44*, 69–75.

Horn, K. J., Thomas, R. Q., Clark, C. M., Pardo, L. H., Fenn, M. E., Lawrence, G. B., et al. (2018). Growth and survival relationships of 71 tree species with nitrogen and sulfur deposition across the conterminous U.S. *PLOS ONE*, *13*(10), e0205296. https://doi.org/10.1371/journal.pone.0205296

Horton, R. E. (1933). The Role of infiltration in the hydrologic cycle. *Eos, Transactions American Geophysical Union*, *14*(1), 446–460. https://doi.org/10.1029/TR014i001p00446

Jackson, R. B., Canadell, J., Ehleringer, J. R., Mooney, H. A., Sala, O. E., & Schulze, E. D. (1996). A global analysis of root distributions for terrestrial biomes. *Oecologia*, *108*(3), 389–411. https://doi.org/10.1007/BF00333714

Jennings, K. A., Guerrieri, R., Vadeboncoeur, M. A., & Asbjornsen, H. (2016). Response of *Quercus velutina* growth and water use efficiency to climate variability and nitrogen fertilization in a temperate deciduous forest in the northeastern USA. *Tree Physiology*, *36*(4), 428–443. https://doi.org/10.1093/treephys/tpw003

Jensen, N. K., Holzmueller, E. J., Edwards, P. J., Gundy, M. T.-V., DeWalle, D. R., & Williard, K. W. J. (2014). Tree Response to Experimental Watershed Acidification. *Water, Air, & Soil Pollution*, *225*(7), 2034. https://doi.org/10.1007/s11270-014-2034-6

Johnson, J., Graf Pannatier, E., Carnicelli, S., Cecchini, G., Clarke, N., Cools, N., et al. (2018). The response of soil solution chemistry in European forests to decreasing acid deposition. *Global Change Biology*, *24*(8), 3603–3619. https://doi.org/10.1111/gcb.14156

Juice, S. M., Fahey, T. J., Siccama, T. G., Driscoll, C. T., Denny, E. G., Eagar, C., et al. (2006). RESPONSE OF SUGAR MAPLE TO CALCIUM ADDITION TO NORTHERN HARDWOOD FOREST. *Ecology*, *87*(5), 1267–1280. https://doi.org/10.1890/0012-9658(2006)87[1267:ROSMTC]2.0.CO;2

Kamaluddin, M., & Zwiazek, J. J. (2004). Effects of root medium pH on water transport in paper birch (Betula papyrifera) seedlings in relation to root temperature and abscisic acid treatments. *Tree Physiology*, *24*(10), 1173–1180. https://doi.org/10.1093/treephys/24.10.1173

Keenan, T. F., Gray, J., Friedl, M. A., Toomey, M., Bohrer, G., Hollinger, D. Y., et al. (2014). Net carbon uptake has increased through warming-induced changes in temperate forest phenology. *Nature Climate Change*, *4*(7), 598–604. https://doi.org/10.1038/nclimate2253

Kochian, L. V. (1995). Cellular Mechanisms of Aluminum Toxicity and Resistance in Plants. *Annual Review of Plant Physiology and Plant Molecular Biology*, *46*(1), 237–260. https://doi.org/10.1146/annurev.pp.46.060195.001321

Kosiba, A. M., Schaberg, P. G., Rayback, S. A., & Hawley, G. J. (2018). The surprising recovery of red spruce growth shows links to decreased acid deposition and elevated temperature. *Science of The Total Environment*, *637–638*, 1480–1491. https://doi.org/10.1016/j.scitotenv.2018.05.010

Lawlor, D. W., & Cornic, G. (2002). Photosynthetic carbon assimilation and associated metabolism in relation to water deficits in higher plants. *Plant, Cell & Environment*, *25*(2), 275–294. https://doi.org/10.1046/j.0016-8025.2001.00814.x

Lenth, R., Singmann, H., Love, J., Buerkner, P., & Herve, M. (2017). emmeans: Estimated Marginal Means, aka Least-Squares Means. Retrieved from https://github.com/rvlenth/emmeans

Lévesque, M., Walthert, L., & Weber, P. (2016). Soil nutrients influence growth response of temperate tree species to drought. *Journal of Ecology*, *104*(2), 377–387. https://doi.org/10.1111/1365-2745.12519

Levesque, M., Andreu-Hayles, L., & Pederson, N. (2017). Water availability drives gas exchange and growth of trees in northeastern US, not elevated CO2 and reduced acid deposition. *Scientific Reports*, *7*(1). https://doi.org/10.1038/srep46158

Likens, G. E., Driscoll, C. T., & Buso, D. C. (1996). Long-Term Effects of Acid Rain: Response and Recovery of a Forest Ecosystem. *Science*, *272*(5259), 244. https://doi.org/10.1126/science.272.5259.244

Long, R. P., Horsley, S. B., Hallett, R. A., & Bailey, S. W. (2009). Sugar maple growth in relation to nutrition and stress in the northeastern United States. *Ecological Applications*, *19*(6), 1454–1466. https://doi.org/10.1890/08-1535.1

Lovett, G. M., Tear, T. H., Evers, D. C., Findlay, S. E. G., Cosby, B. J., Dunscomb, J. K., et al. (2009). Effects of Air Pollution on Ecosystems and Biological Diversity in the Eastern United States. *Annals of the New York Academy of Sciences*, *1162*(1), 99–135. https://doi.org/10.1111/j.1749-6632.2009.04153.x

Lu, X., Kicklighter, D. W., Melillo, J. M., Reilly, J. M., & Xu, L. (2015). Land carbon sequestration within the conterminous United States: Regional- and state-level analyses. *Journal of Geophysical Research: Biogeosciences*, *120*(2), 379–398. https://doi.org/10.1002/2014JG002818

Luce, C. H., Vose, J. M., Pederson, N., Campbell, J., Millar, C., Kormos, P., & Woods, R. (2016). Contributing factors for drought in United States forest ecosystems under projected future climates and their uncertainty. *Special Section: Drought and US Forests: Impacts and Potential Management Responses*, *380*, 299–308. https://doi.org/10.1016/j.foreco.2016.05.020

Magnani, F., Mencuccini, M., Borghetti, M., Berbigier, P., Berninger, F., Delzon, S., et al. (2007). The human footprint in the carbon cycle of temperate and boreal forests. *Nature*, *447*(7146), 849–851. https://doi.org/10.1038/nature05847

Mansfield, T. A. (1998). Stomata and plant water relations: does air pollution create problems? *Environmental Pollution*, *101*(1), 1–11. https://doi.org/10.1016/S0269-7491(98)00076-1

Marinos, R. E., & Bernhardt, E. S. (2018). Soil carbon losses due to higher pH offset vegetation gains due to calcium enrichment in an acid mitigation experiment. *Ecology*, *99*(10), 2363–2373. https://doi.org/10.1002/ecy.2478

Martin-Benito, D., Kint, V., del Río, M., Muys, B., & Cañellas, I. (2011). Growth responses of West-Mediterranean Pinus nigra to climate change are modulated by competition and productivity: Past trends and future perspectives. *Forest Ecology and Management*, *262*(6), 1030–1040. https://doi.org/10.1016/j.foreco.2011.05.038

Mathias, J. M., & Thomas, R. B. (2018). Disentangling the effects of acidic air pollution, atmospheric CO_2, and climate change on recent growth of red spruce trees in the Central Appalachian Mountains. *Global Change Biology*, *24*(9), 3938–3953. https://doi.org/10.1111/gcb.14273

Maxwell, J. T., Harley, G. L., Mandra, T. E., Yi, K., Kannenberg, S. A., Au, T. F., et al. (2019). Higher CO2 Concentrations and Lower Acidic Deposition Have Not Changed Drought Response

in Tree Growth But Do Influence iWUE in Hardwood Trees in the Midwestern United States. *Journal of Geophysical Research: Biogeosciences*, *124*(12), 3798–3813. https://doi.org/10.1029/2019JG005298

McDonnell, J. J. (2009). Hewlett, J.D. and Hibbert, A.R. 1967: Factors affecting the response of small watersheds to precipitation in humid areas. In Sopper, W.E. and Lull, H.W., editors, Forest hydrology, New York: Pergamon Press, 275—90. *Progress in Physical Geography: Earth and Environment*, *33*(2), 288–293. https://doi.org/10.1177/0309133309338118

Medeiros, J. S., Tomeo, N. J., Hewins, C. R., & Rosenthal, D. M. (2016). Fast-growing Acer rubrum differs from slow-growing Quercus alba in leaf, xylem and hydraulic trait coordination responses to simulated acid rain. *Tree Physiology*, *36*(8), 1032–1044. https://doi.org/10.1093/treephys/tpw045

National Atmospheric Deposition Program. (2018). NADP Program Office. Retrieved from http://nadp.slh.wisc.edu/

Nehrbass-Ahles, C., Babst, F., Klesse, S., Nötzli, M., Bouriaud, O., Neukom, R., et al. (2014). The influence of sampling design on tree-ring-based quantification of forest growth. *Global Change Biology*, *20*(9), 2867–2885. https://doi.org/10.1111/gcb.12599

Ouimette, A. P., Ollinger, S. V., Richardson, A. D., Hollinger, D. Y., Keenan, T. F., Lepine, L. C., & Vadeboncoeur, M. A. (2018). Carbon fluxes and interannual drivers in a temperate forest ecosystem assessed through comparison of top-down and bottom-up approaches. *Agricultural and Forest Meteorology*, *256–257*, 420–430. https://doi.org/10.1016/j.agrformet.2018.03.017

Peterjohn, W. T. (2013). Fernow Watershed Acidification Experiment Fine Root Mass Comparison. Retrieved from http://www.as.wvu.edu/fernow/data.html

Pinheiro, J., Bates, D., DebRoy, S., Sarkar, D., & R Core Team. (n.d.). nlme: Linear and Nonlinear Mixed Effects Models. Retrieved from https://CRAN.R-project.org/package=nlme

Pourmokhtarian, A., Driscoll, C. T., Campbell, J. L., Hayhoe, K., Stoner, A. M. K., Adams, M. B., et al. (2017). Modeled ecohydrological responses to climate change at seven small watersheds in the northeastern United States. *Global Change Biology*, *23*(2), 840–856. https://doi.org/10.1111/gcb.13444

PRISM, C. G. (2018). PRISM Climate Data. Oregon State University. Retrieved from http://prism.oregonstate.edu/

Quinn Thomas, R., Canham, C. D., Weathers, K. C., & Goodale, C. L. (2010). Increased tree carbon storage in response to nitrogen deposition in the US. *Nature Geoscience*, *3*(1), 13–17. https://doi.org/10.1038/ngeo721

R Core Team. (2018). *R: A language and environment for statistical computing.* Vienna, Austria: Foundation for Statistical Computing. Retrieved from https://www.R-project.org/

Richardson, A. D., Hollinger, D. Y., Dail, D. B., Lee, J. T., Munger, J. W., & O'keefe, J. (2009). Influence of spring phenology on seasonal and annual carbon balance in two contrasting New England forests. *Tree Physiology*, *29*(3), 321–331. https://doi.org/10.1093/treephys/tpn040

Roman, D. T., Novick, K. A., Brzostek, E. R., Dragoni, D., Rahman, F., & Phillips, R. P. (2015). The role of isohydric and anisohydric species in determining ecosystem-scale response to severe drought. *Oecologia*, *179*(3), 641–654. https://doi.org/10.1007/s00442-015-3380-9

Schlesinger, W. H., & Jasechko, S. (2014). Transpiration in the global water cycle. *Agricultural and Forest Meteorology*, *189–190*, 115–117. https://doi.org/10.1016/j.agrformet.2014.01.011

Speer, J. H. (2012). *Fundamentals of Tree Ring Research*. Tuscon, AZ: University of Arizona Press.

Sullivan, T. J., Lawrence, G. B., Bailey, S. W., McDonnell, T. C., Beier, C. M., Weathers, K. C., et al. (2013). Effects of Acidic Deposition and Soil Acidification on Sugar Maple Trees in the Adirondack Mountains, New York. *Environmental Science & Technology*, *47*(22), 12687–12694. https://doi.org/10.1021/es401864w

Sullivan, Timothy J., Driscoll, C. T., Beier, C. M., Burtraw, D., Fernandez, I., Galloway, J. N., et al. (2018). Air pollution success stories in the United States: The value of long-term observations. *Environmental Science & Policy*, *84*, 69–73. https://doi.org/10.1016/j.envsci.2018.02.016

Sulman, B. N., Roman, D. T., Yi, K., Wang, L., Phillips, R. P., & Novick, K. A. (2016). High atmospheric demand for water can limit forest carbon uptake and transpiration as severely as dry soil: VPD CONTROL OF GPP AND TRANSPIRATION. *Geophysical Research Letters*, *43*(18), 9686–9695. https://doi.org/10.1002/2016GL069416

Troch, P. A., Martinez, G. F., Pauwels, V. R. N., Durcik, M., Sivapalan, M., Harman, C., et al. (2009). Climate and vegetation water use efficiency at catchment scales. *Hydrological Processes*, *23*(16), 2409–2414. https://doi.org/10.1002/hyp.7358

USDA, N. (2019). The PLANTS Database, Black Cherry. Retrieved October 28, 2019, from https://plants.usda.gov/plantguide/pdf/pg_prse2.pdf

Vadeboncoeur, M. A. (2010). Meta-analysis of fertilization experiments indicates multiple limiting nutrients in northeastern deciduous forests. *Canadian Journal of Forest Research*, *40*(9), 1766–1780. https://doi.org/10.1139/X10-127

Vadeboncoeur, M. A., Green, M. B., Asbjornsen, H., Campbell, J. L., Adams, M. B., Boyer, E. W., et al. (2018). Systematic variation in evapotranspiration trends and drivers across the Northeastern United States. *Hydrological Processes*, *32*(23), 3547–3560. https://doi.org/10.1002/hyp.13278

Voepel, H., Ruddell, B., Schumer, R., Troch, P. A., Brooks, P. D., Neal, A., et al. (2011). Quantifying the role of climate and landscape characteristics on hydrologic partitioning and vegetation response. *Water Resources Research*, *47*(10). https://doi.org/10.1029/2010WR009944

de Vries, W., Reinds, G. J., & Vel, E. (2003). Intensive monitoring of forest ecosystems in Europe: 2: Atmospheric deposition and its impacts on soil solution chemistry. *Forest Ecology and Management*, *174*(1), 97–115. https://doi.org/10.1016/S0378-1127(02)00030-0

Wason, J. W., Dovciak, M., Beier, C. M., & Battles, J. J. (2017). Tree growth is more sensitive than species distributions to recent changes in climate and acidic deposition in the northeastern United States. *Journal of Applied Ecology*, *54*(6), 1648–1657. https://doi.org/10.1111/1365-2664.12899

Watmough, S. A., Aherne, J., Alewell, C., Arp, P., Bailey, S., Clair, T., et al. (2005). Sulphate, Nitrogen and Base Cation Budgets at 21 Forested Catchments in Canada, the United States and

Europe. *Environmental Monitoring and Assessment*, *109*(1–3), 1–36. https://doi.org/10.1007/s10661-005-4336-z

Yi, K., Dragoni, D., Phillips, R. P., Roman, D. T., & Novick, K. A. (2017). Dynamics of stem water uptake among isohydric and anisohydric species experiencing a severe drought. *Tree Physiology*, *37*(10), 1379–1392. https://doi.org/10.1093/treephys/tpw126

Yi, K., Maxwell, J. T., Wenzel, M. K., Roman, D. T., Sauer, P. E., Phillips, R. P., & Novick, K. A. (2019). Linking variation in intrinsic water-use efficiency to isohydricity: a comparison at multiple spatiotemporal scales. *New Phytologist*, *221*(1), 195–208. https://doi.org/10.1111/nph.15384

Yu, H., He, N., Wang, Q., Zhu, J., Xu, L., Zhu, Z., & Yu, G. (2016). Wet acid deposition in Chinese natural and agricultural ecosystems: Evidence from national-scale monitoring: Acid Deposition in Chinese Rural Areas. *Journal of Geophysical Research: Atmospheres*, *121*(18), 10,995-11,005. https://doi.org/10.1002/2015JD024441

Zurr, A., Ieno, E. N., Walker, N., Saveliev, A. A., & Smith, G. M. (n.d.). *Mixed Effects Models and Extensions in Ecology with R* (1st ed.). New York: Springer-Verlag.

Chapter 3 Supplement

The Chapter 3 supplement includes results of analyses examining temporal trends in hydroclimate and deposition variables at Fernow (Figure S3.1, Table S3.1), and results of Kendall's correlation tests examining bivariate relationships between tree BAI chronologies and hydroclimate/deposition variables (Table S3.2). Table S3.3 shows the estimated variance explained by LMMs with and without the inclusion of canopy class as a predictor of tree growth. Figures S3.2-3.5 provide partial regression plots from linear mixed effects models (LMM) output to aid interpretation of LMM results. Figure S3.6 shows changes in tree canopy class for the four focal species in Fernow Watersheds 3 and 7 across periodic inventories conducted between 1990 and 2018. Figure S3.7 shows results of publicly-available root density data from surveys conducted in 1991 and 2013, and is intended to supplement the mention of root density in the Discussion section. Figure S3.8 plots time series of hydrologic data from Watersheds 3 and 7, and is intended to demonstrate the hydrologic similarity of the two watersheds.

Supplementary Figures

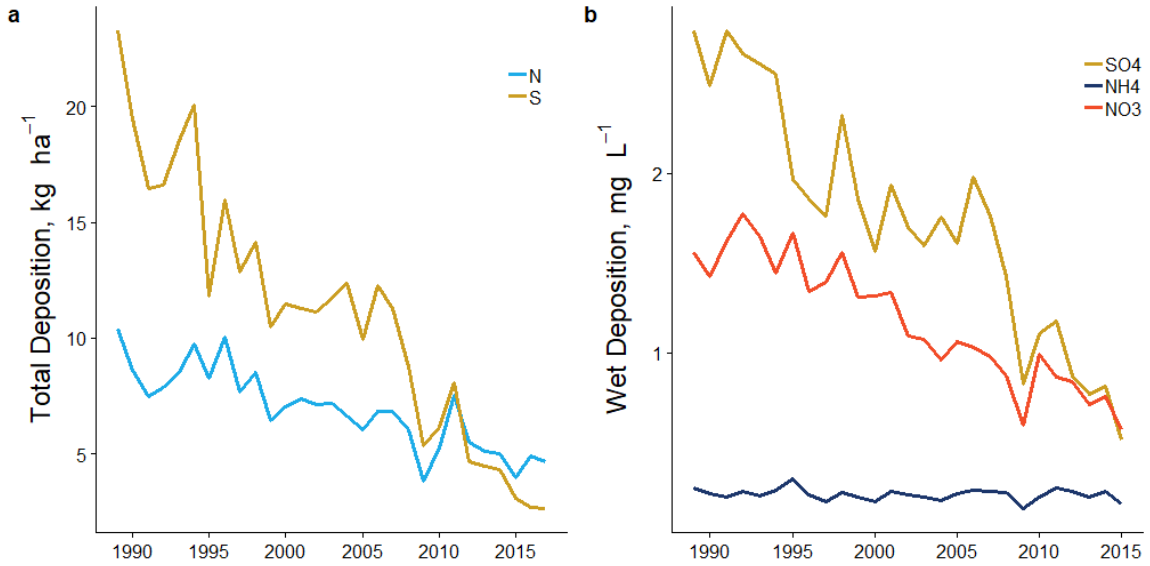

Figure S3.1. *(a)* Total N and S deposition (wet + dry) measured at the NADP WV18 site in Parsons, WV (~4.4 km from the study watersheds) between 1990-2015. *(b)* Annual wet deposition of sulfate (SO_4), nitrate (NO_3), and ammonium (NH_4) measured at the NADP WV18 site.

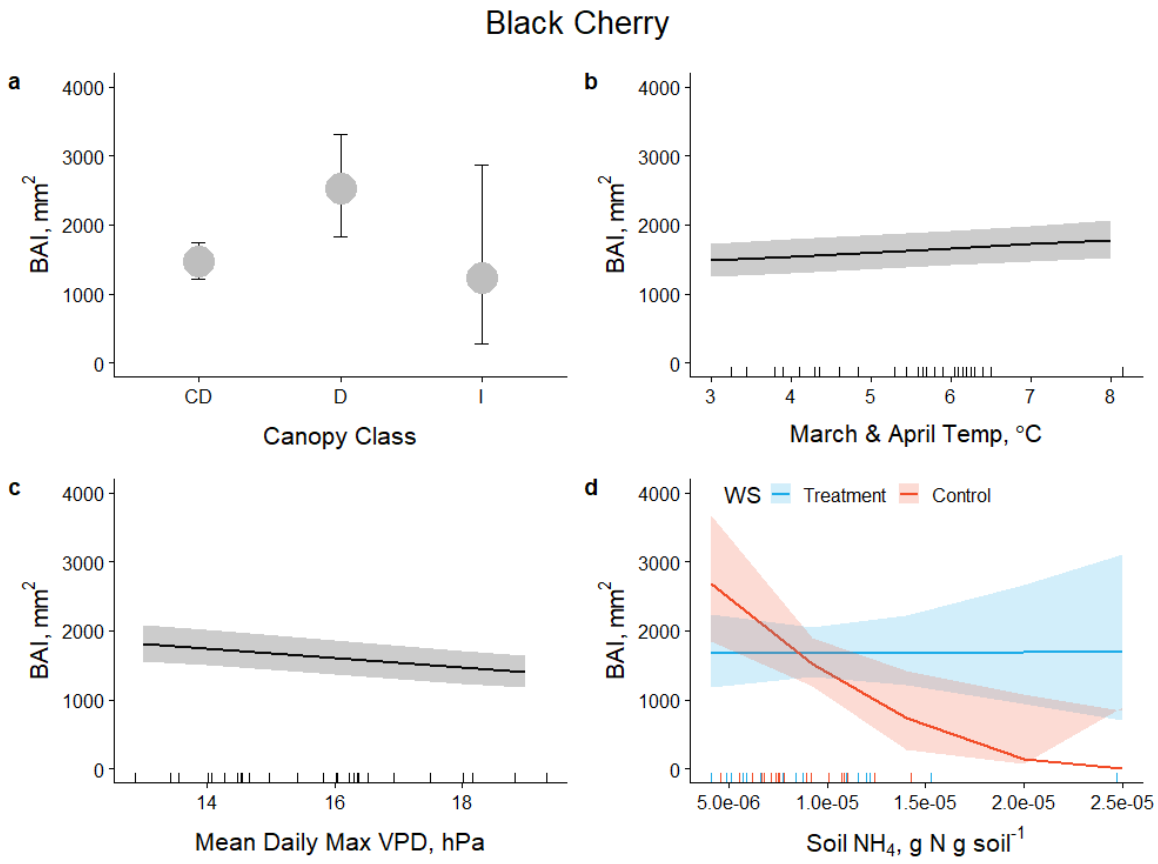

Figure S3.2. Partial regression plots showing the individual influence of LMM predictors on black cherry BAI. Error bars and confidence bands indicate 95% confidence intervals.

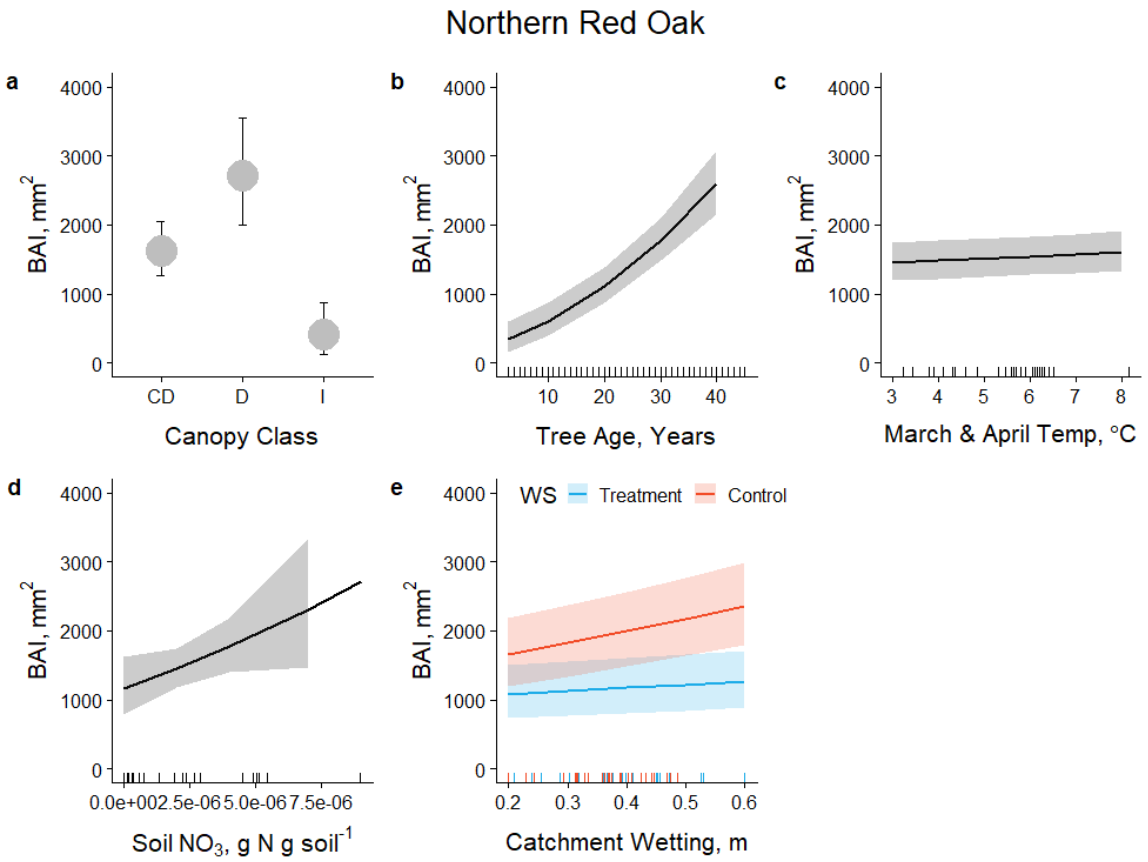

Figure S3.3. Partial regression plots showing the individual influence of LMM predictors on northern red oak BAI. Error bars and confidence bands indicate 95% confidence intervals.

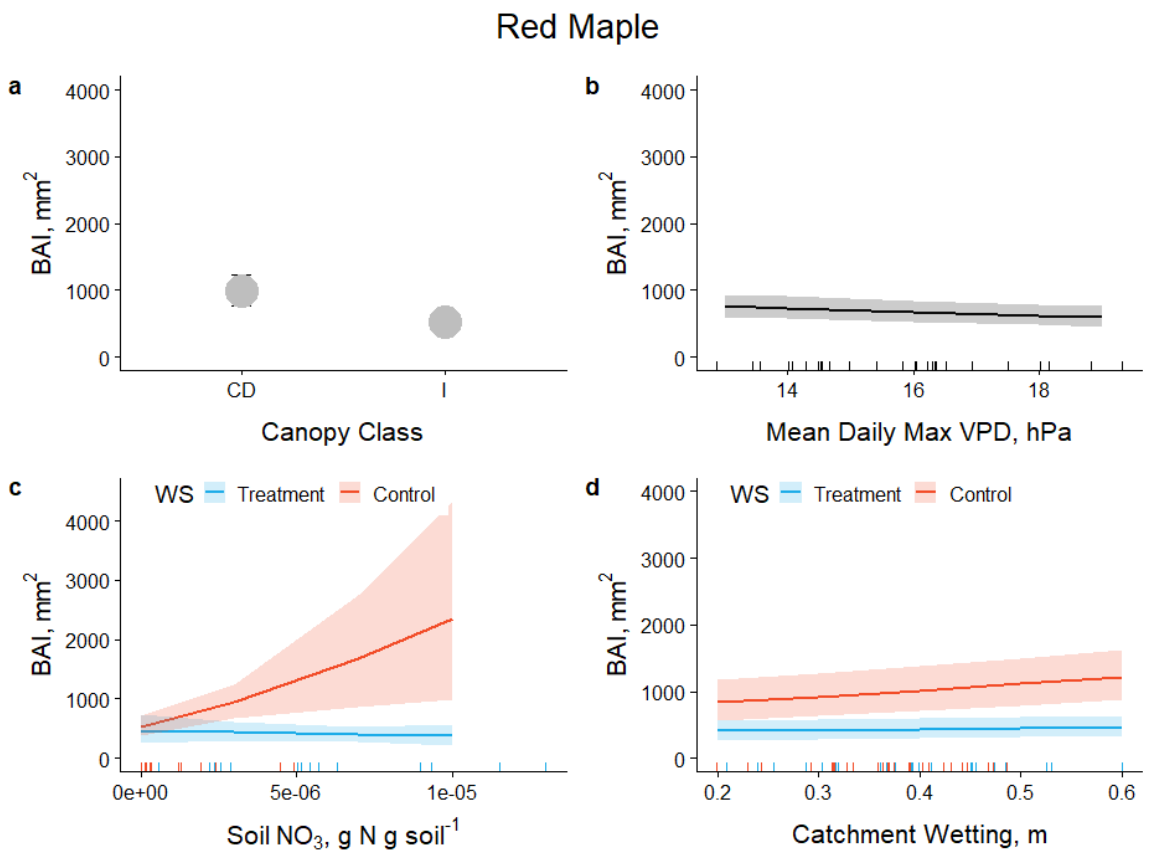

Figure S3.4. Partial regression plots showing the individual influence of LMM predictors on red maple. Error bars and confidence bands indicate 95% confidence intervals.

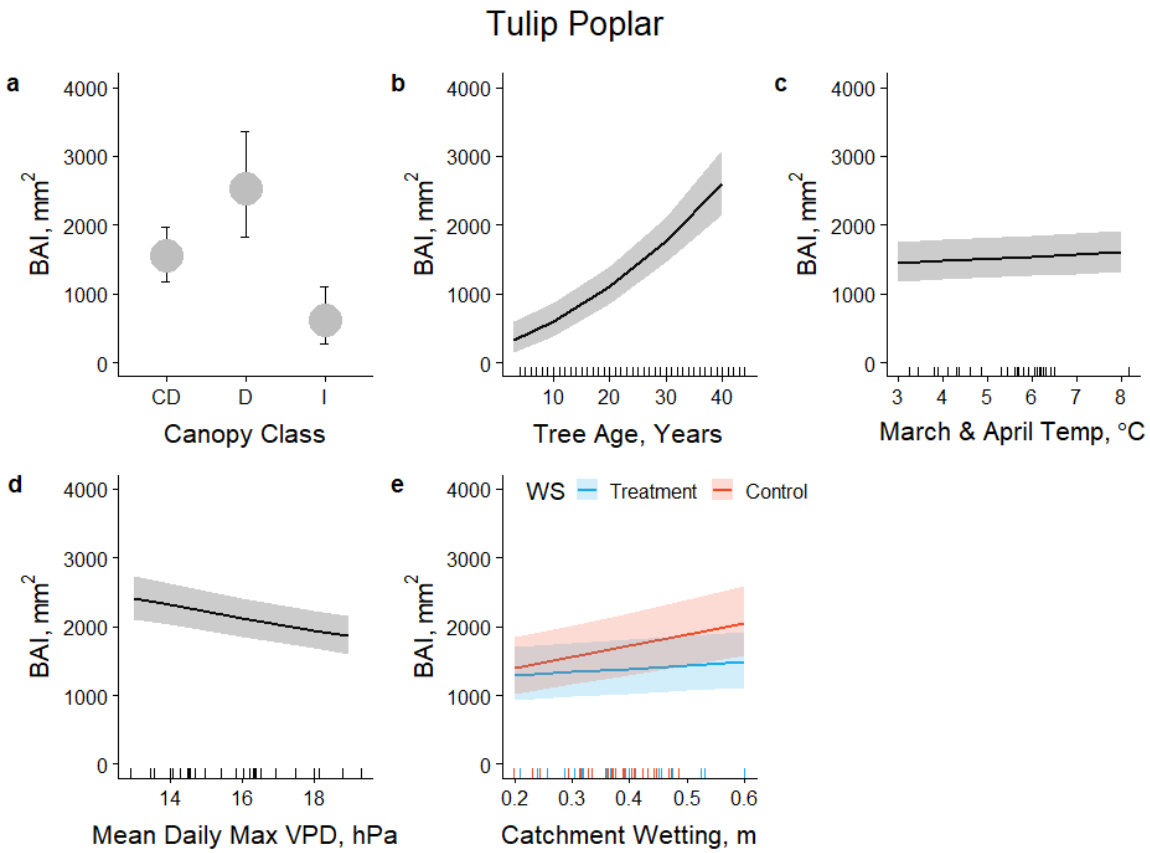

Figure S3.5. Partial regression plots showing the individual influence of LMM predictors on tulip poplar BAI. Error bars and confidence bands indicate 95% confidence intervals.

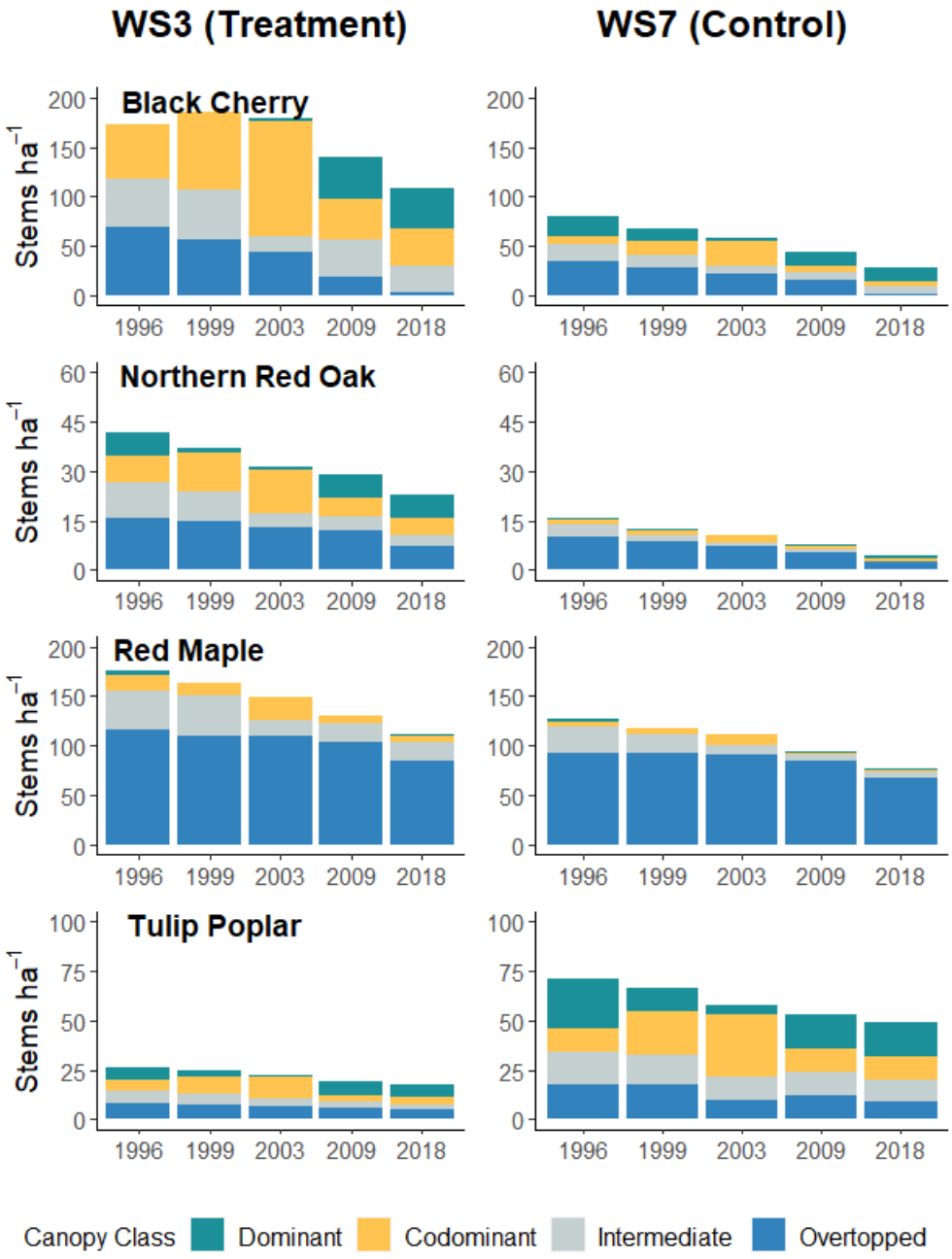

Figure S3.6. Changes in tree species canopy position through time, as recorded during forest inventory data collection conducted in 1996, 1999, 2003, 2009, and 2018. To aid readability, y-axes were not standardized across species.

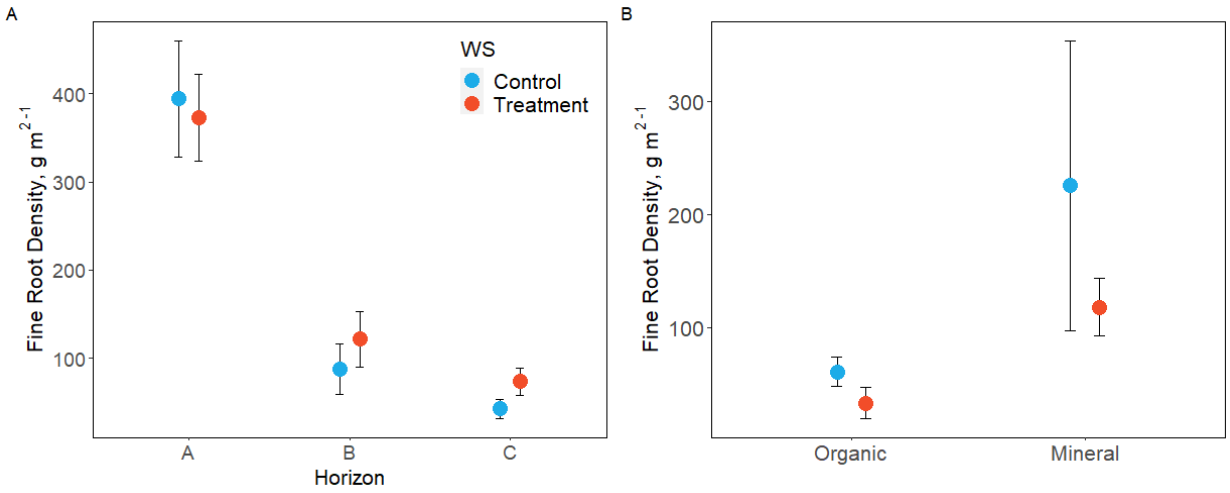

Figure S3.7. Results of fine root (<2 mm diameter) density surveys conducted in 1991 (A) and 2013 (B). While 1991 and 2013 data cannot be directly compared due to differences in methodology, (a) in 1991 there was no difference in fine root density in the a or b horizons, but significantly greater fine root density in the treated catchment in the c horizon. (b) Suggests greater fine root density in the organic and upper 15cm of mineral soil after 23 years of ammonium sulfate treatments. Samples from 17 plots in each watershed were collected in 1991, while samples from 7 plots in each watershed were collected in 2013. Error bars represent 95% confidence intervals and asterisks indicate significance (*P<0.05, **P<0.01). 1991 data was collected by Adams (2016), while 2013 data was collected by Peterjohn (2013).

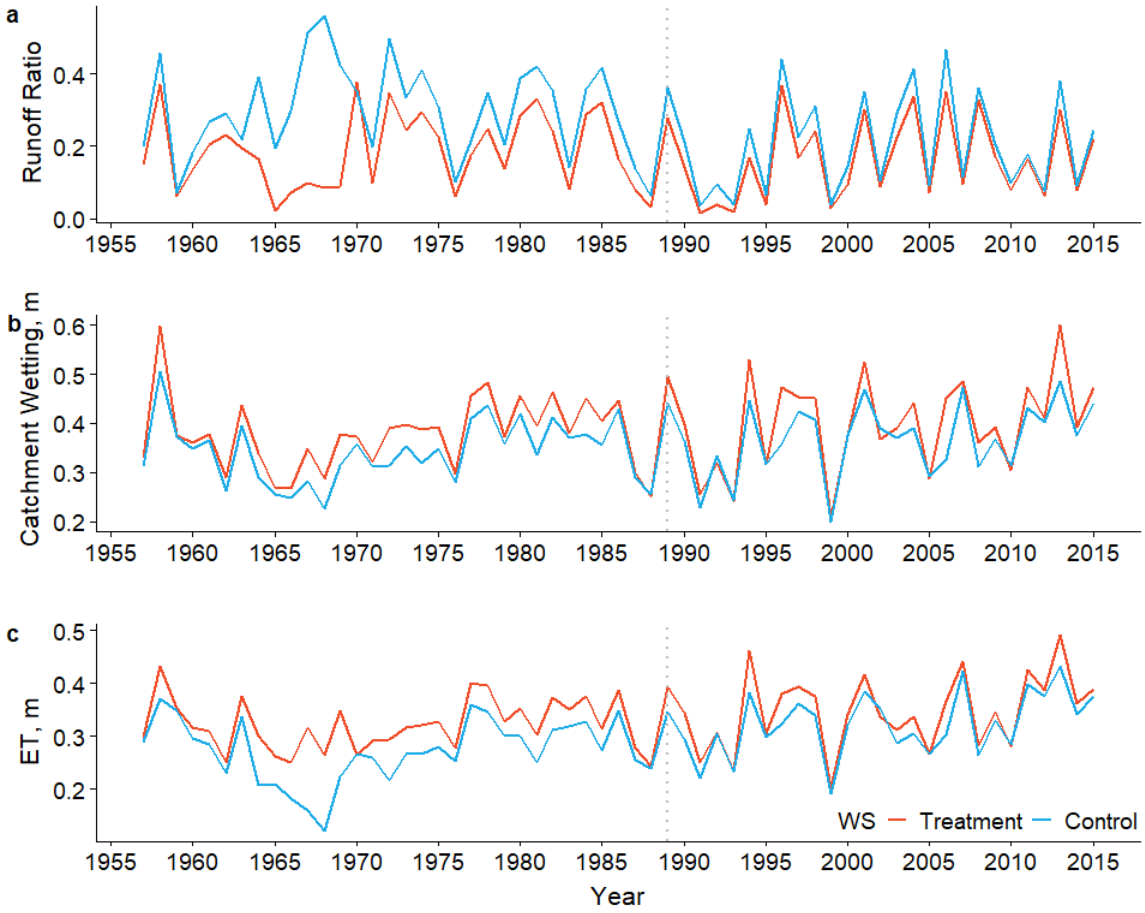

Figure S3.8. Time series of growing season (June-August) *(a)* runoff ratios, defined as the ratio of precipitation to stream discharge, *(b)* catchment wetting, defined as precipitation minus quickflow, and *(c)* evapotranspiration, precipitation minus stream discharge, over the streamflow record period in the treated and control watersheds at Fernow. Differences in catchment hydrology in the 1960s through early 1980s are attributable clear-cutting and subsequent forest regeneration. By 1989, when ammonium sulfate treatments began (dotted line) and throughout the treatment period, growing season hydrologic dynamics in the two watersheds were similar.

Supplementary Tables

Table S3.1. Sen's slope values for temporal trends in hydroclimate and deposition between 1957-2015 and 1990-2015. Deposition records are not available for the entire 1957-2015 period. Unless otherwise indicated, hydroclimate variables represent growing season (June-August) values. Where columns have single values, data is the same for both watersheds. (^{ms}P<0.1, *P<0.05, **P<0.01, ***P<0.001).

	1957-2015		1990-2015	
	WS3	WS7	WS3	WS7
Precipitation (m)	0.001^{ms}		0.005	
Wetting (m)	0.001*	0.001*	0.004	0.004^{ms}
ET (m)	0.001*	0.002***	0.003	0.003^{ms}
Temp (°C)	0.02***		0.020	
VPD (hPa)	0.000		0.006	
March Temp (°C)	0.008		-0.015	
April Temp (°C)	0.035**		0.050	
Annual Wet SO4 Deposition (mg/L)	--		-0.080***	
Annual Wet NO3 Deposition (mg/L)	--		-0.041***	
Annual Wet NH4 Deposition (mg/L)	--		0.000	
Total Annual S Deposition (kg/ha)	--		-0.603***	
Total Annual N Deposition (kg/ha)	--		-0.165***	

Table S3.2. Kendall's correlation coefficients (τ) of BAI and hydroclimate variables in each watershed. (^{ms}P<0.1, *P<0.05, **P<0.01, ***P<0.001). JJA is June-August, and MJJAS is May-September. Deposition variables are annual values.

	Black Cherry		Northern Red Oak		Red Maple		Tulip Poplar	
	WS3	WS7	WS3	WS7	WS3	WS7	WS3	WS7
JJA Precipitation				0.40*	0.38*		0.50**	0.52**
JJA Wetting			0.41*	0.54**	0.48*		0.53**	0.53**
JJA VPD	-0.44*	-0.34^{ms}				-0.36^{ms}		
MJJAS Precipitation							0.45*	0.53*
MJJAS Wetting				0.39^{ms}			0.49*	0.61*
MJJAS VPD	-0.46*	-0.38^{ms}				-0.37^{ms}		
Spring Temperature								0.38^{ms}
SO_2 Deposition		0.56**	-0.90***	-0.89***	-0.66***	0.52**	-0.50**	-0.41*
NO_3 Deposition	0.34^{ms}	0.55**		-0.87***	-0.62***	0.70***	-0.44*	-0.39*
NH_4 Deposition			-0.86***					
Atmospheric CO_2	0.39*	-0.62***	0.94***	0.96***	0.72***	-0.65***	0.53**	0.47*

Table S3.3. To examine the importance of canopy class in LMMs, canopy class was removed and models were re-run. For all species, removing canopy class only resulted in little/no change in the conditional r^2 (fixed plus random effects) value, but a large drop in the marginal r^2 (fixed effects) value. Since the random effects are structured to estimate otherwise unaccounted for variability in individual tree growth, we conclude that canopy class explains a substantial portion of this individual variability, and chose to leave it in the final models.

	With Canopy Class		Without Canopy Class	
Species	Marginal r^2	Conditional r^2	Marginal r^2	Conditional r^2
Black Cherry	0.20	0.50	0.10	0.50
N. Red Oak	0.47	0.63	0.22	0.64
Red Maple	0.27	0.27	0.14	0.29
Tulip Poplar	0.52	0.73	0.29	0.72

References

Adams, M.B., & Peterjohn, W. T. (2016). Fernow Experimental Forest Watershed Acidification Root Data, 1991. Department of Agriculture, US Forest Service North Central Research Station, Parsons, WV. Retrieved from http://www.as.wvu.edu/fernow/data.html

Peterjohn, W. T. (2013). Fernow Watershed Acidification Experiment Fine Root Mass Comparison. Retrieved from http://www.as.wvu.edu/fernow/data.html

Chapter 4. Soil nutrient manipulations effects on tree growth and intrinsic water use efficiency in midlatitude temperate forests

Abstract

Atmospheric deposition of nitrogen (N) and sulfur (S) has profoundly altered the biogeochemistry of midlatitude temperate forest ecosystems in recent decades. However, the impacts of deposition-linked changes in soil chemistry on forest carbon and water balance remain unclear, as they have occurred alongside changes in other environmental drivers, including climate and atmospheric CO_2. We examined how tree growth and intrinsic water use efficiency (iWUE) responded to soil nutrient manipulations in three paired watershed experiments in the northeastern United States: Hubbard Brook Experimental Forest, where soil calcium (Ca) was restored to preindustrial levels, and the Bear Brook Watersheds and Fernow Experimental Forest, where soils were acidified via experimental N and S additions for 25+ years. Ca addition resulted in enhanced growth in four of five species examined at Hubbard Brook, but iWUE was enhanced only in sugar maple (*Acer saccharum*). N and S additions resulted in generally positive tree growth responses at Bear Brook, but mostly negative growth responses at Fernow, where we also observed modest negative effects on iWUE. Analysis of temporal iWUE trends in reference trees revealed positive trends at Hubbard Brook and Bear Brook, but negative trends at Fernow, where historic background deposition loads have been substantially higher. Combined, our assessment of tree growth, iWUE, and catchment water balance ET suggest that nutrient manipulations have induced parallel changes in carbon uptake and transpiration in these watersheds, and that deposition-linked change in soil nutrient availability may modulate whether forest productivity and iWUE are enhanced by increases in atmospheric CO_2.

4.1 Introduction

Over the last century, mid-latitude temperate forests have been subjected to multiple climatic and biogeochemical changes, including increasing atmospheric CO_2, altered precipitation and temperature regimes (Hayhoe et al., 2007; Kjellstro et al., 2010; Qian and Zhou 2014), and elevated atmospheric nitrogen (N) and sulfur (S) deposition (Driscoll et al., 2001; Lajtha and Jones, 2013). Understanding the net effects of these changes on forest growth and water use efficiency (WUE) – broadly defined as the ratio of photosynthetic carbon assimilation per unit of water transpired – has been a major research focus, with evidence indicating enhanced tree growth (McMahon et al. 2010; Fang et al., 2014; Boisenvue and Running, 2006) and WUE (Keenan et al., 2013; Frank et al., 2015; Guerrieri et al., 2019; Mathias and Thomas, 2021) in temperate forests over recent decades. Increases in tree productivity and WUE are often attributed to a CO_2 fertilization effect, in which elevated atmospheric CO_2 (C_a) enhances photosynthesis while reducing water lost via transpiration (Haverd et al., 2020). However, enhanced carbon gain under increasing C_a may only occur when other environmental factors, such as climate (Novick et al., 2016) and nutrients (Norby et al., 2010) are not limiting. Thus, while global and continental-scale studies suggest that C_a is a dominant driver of increases in WUE (*e.g.* Guerrieri et al., 2019; Mathias and Thomas, 2021), other drivers may control carbon assimilation and WUE at local and regional scales.

Long-term trends in tree intrinsic water use efficiency (iWUE), the ratio of photosynthetic carbon assimilation (A) to stomatal conductance of water vapor (g_s), are commonly assessed using carbon isotope ($\delta^{13}C$) composition of tree rings (McCarroll and Loader, 2004). Recent studies suggest that tree iWUE response to C_a is modulated by water availability (Belmecheri et al., 2021; Levesque et al., 2017; Saurer et al., 2014), vapor pressure deficit (Zhang et al., 2019),

atmospheric N and S deposition (Mathias and Thomas, 2018; Maxwell et al., 2019; Rayback et al., 2020; Savard et al., 2020), ozone pollution (Holmes, 2014), and soil fertility (Marchand et al., 2020). Of these drivers, the influence of atmospheric N and S deposition on tree growth and iWUE remain the most poorly understood, in part due to the difficulty of distinguishing effects of direct plant exposure to NO_3^- and SO_4^{2-} anions (which drive leaching of base cations from foliage) from indirect, deposition-driven changes in soil acidity, N availability, and base cation supply. This mechanistic distinction is important – despite declines in N and S deposition since ~1980 in the United States following implementation of the Clean Air Act and its amendments (Sullivan et al., 2018), recovery of soil base cations is spatially heterogeneous and often slow (Bailey et al., 2021; Hazlett et al., 2020). This lag between reduced emissions and soil recovery has important implications for tree mineral nutrition and forest productivity (Battles et al., 2014; Jonard et al., 2015). In the Northeastern United States (NEUS), reductions in deposition may have thus far had a greater impact on the growth and physiology of species like red spruce (*Picea rubens*), which appear to be particularly sensitive to foliar exposure to acid deposition (DeHayes et al., 1999; Borer et al., 2005), as opposed to species like sugar maple (*Acer saccharum*), which may be relatively more sensitive to soil base cation availability (Juice et al., 2006; Long et al., 2011; Bishop et al., 2015).

Various direct and indirect mechanisms may explain how changes in iWUE – which can be driven by changes in A, g_s, or both (Scheidegger et al., 2000) – relate to changes in N and S deposition. Direct leaf exposure to S deposition has been shown to induce stomatal closure, resulting in a proportionally greater reduction in g_s than A, and thus increasing iWUE (Mathias and Thomas, 2018; Rinne et al., 2010; Savard, 2010). This direct effect has also been observed in response to leaf exposure to N deposition (Bukata and Kyser, 2007). On the other hand, elevated

N inputs to soils have been reported to increase iWUE by stimulating *A* (Jennings et al., 2016; Leonardi et al., 2012). Studies set in other biomes show that soil nutrient availability may also independently influence g_s. Lu et al. (2018) reported increased transpiration, and reduced intrinsic water use efficiency, in tropical forest trees following experimental N additions that acidified the soil. The authors suggested that trees acclimated to base cation limitation by upregulating transpiration to maintain mass flow of essential nutrients. While nutrient regulation of transpiration has also been observed in grasses (Cramer et al., 2008), it has rarely been evaluated in temperate forest species (but see Green et al., 2013 and Lanning et al., 2019 for catchment water balance-based analyses). Understanding whether deposition-linked changes in growth and iWUE are driven by direct or indirect mechanisms, and whether those mechanisms primarily influence *A* or g_s, is critical to predicting how forest carbon and water cycling will respond to future changes in atmospheric deposition and soil nutrient status.

Soil nutrient manipulation experiments provide opportunities to isolate the effects of deposition-driven changes in soil nutrients on tree growth and iWUE, independent of other potential controls on forest carbon and water balance. In this study, we examined tree growth and iWUE response to experimental whole-watershed nutrient manipulations at three sites in the NEUS: the Fernow Experimental Forest in West Virginia (FEF) and Bear Brook Watersheds in Maine (BBWM), which were acidified via N and S additions over 25+ years, and the Hubbard Brook Experimental Forest (HBEF), where a one-time calcium (Ca) amendment was applied in 1999. Previous studies at these sites have reported changes in both tree productivity and vegetation water use as a result of nutrient modifications. At HBEF, soil Ca amendment resulted in a transient (~3 year) increase in evapotranspiration (ET) in the treated catchment (Green et al. 2013), but a sustained increase in forest productivity (Battles et al., 2014) relative to a nearby

reference watershed. At FEF, increased ET was observed in the N and S-treated catchment (Lanning et al., 2019), an effect attributed to plant response to decreased soil Ca supply, and after an initial stimulation of tree growth attributed to N fertilization (DeWalle et al., 2006), treatments resulted in reduced growth of mature trees after 26 years (Malcomb et al., 2020). Evidence from tree sampling campaigns in 1999 (Elvir et al., 2003) and 2011 (Patel et al., 2019) at BBWM suggested that N and S additions enhanced growth of some species, but tree growth has not been evaluated at this site since experimental treatments ended in 2016. Further, tree iWUE chronologies have not been assessed at any of these three sites.

In this study, we employed an approach that combines tree ring-based estimates of growth, iWUE time series derived from tree ring carbon isotope ($\delta^{13}C$) chronologies, and catchment hydrological data to better understand how changes in soil nutrients influence the carbon and water balance of temperate mixed deciduous forests. Tree growth and catchment water balance data were analyzed to constrain our interpretation of whether changes in iWUE were driven by changes in A, g_s, or both. Within this framework we tested a set of hypotheses, informed by previous work at these sites and ecophysiological literature on tree response to changes in soil nutrients, related to how changes in soil acidity and base cations influence forest carbon and water balance (Figure 4.1). In the ammonium sulfate treated watersheds at BBWM and FEF, we hypothesized that after an initial stimulation of tree growth due to N fertilization (*i.e.* Elvir et al., 2003), both growth and iWUE would decline as base cations became depleted from the soil, and trees upregulated transpiration to sustain mass flow of nutrients, in keeping with Lu et al., (2018). At HBEF, we hypothesized that iWUE would not change in the initial years following Ca addition, as growth and transpiration would increase concurrently (*i.e.* Green et al, 2013; Battles et al., 2014), but that growth and iWUE would be greater in the Ca-treated

watershed over the entire study period as transpiration returned to pre-treatment levels and growth became relieved from Ca limitation. Together, these analyses may offer insights into how changes in soil nutrient availability influence coupled forest carbon and water relations, with implications for acid deposition-affected forests in temperate regions.

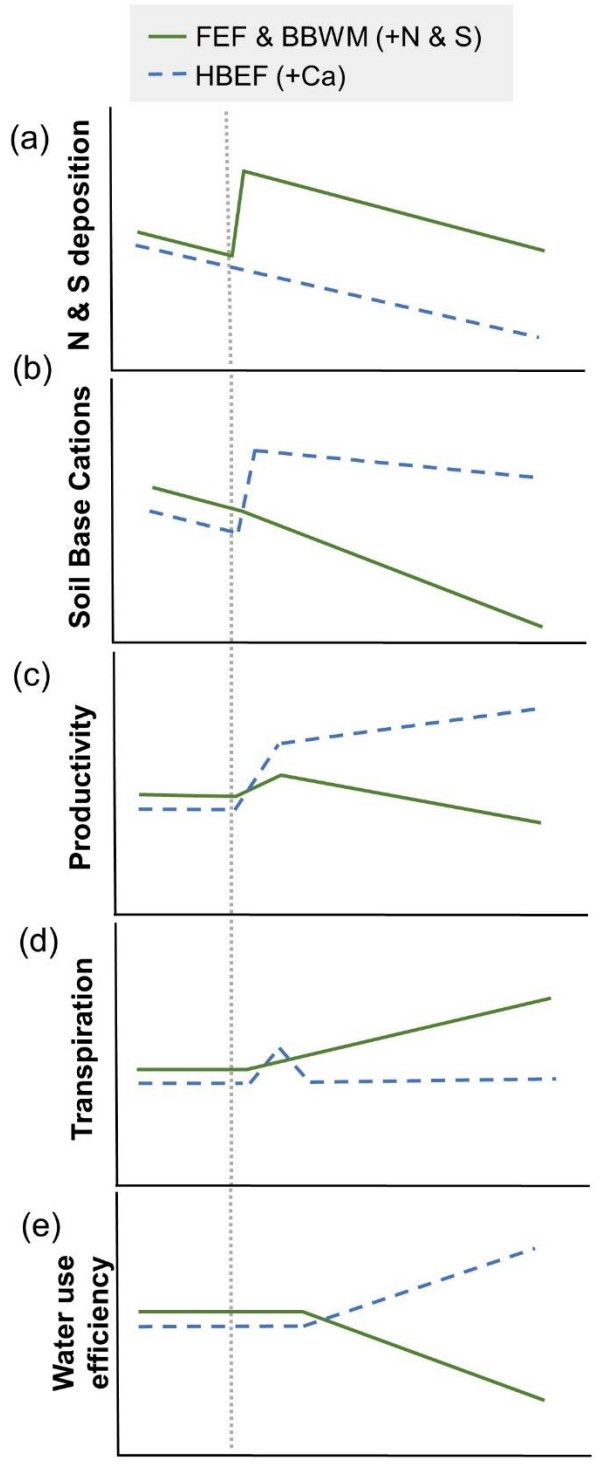

Figure 4.1 Proposed effects of experimental nutrient manipulations (a and b) on forest productivity (c), transpiration (d), and WUE (e) at Fernow and Bear Brook (green solid lines) and Hubbard Brook (blue dashed line). Vertical dotted grey lines represent treatment onset at each site. Lines represent hypothetical trajectories, not actual quantities, and do not account for

potential time lags between deposition and changes in soil nutrients. Productivity, transpiration, and WUE effects do not account for changes in background deposition, climate, or CO_2.

4.2 Methods

4.2.1 Study Sites

This study was conducted at three sites in NEUS where soil nutrients have been experimentally manipulated in whole watersheds (Figure 4.1, Table 4.1): Bear Brook Watersheds in Maine (BBWM), Fernow Experimental Forest in West Virginia (FEF), and Hubbard Brook Experimental Forest in New Hampshire (HBEF). All examined watersheds are small (<43 ha), gauged, completely forested watersheds with relatively long-term (28-65 year) hydrologic records. At HBEF, a one-time amendment of pelletized wollastonite ($CaSiO_3$; 293 kg Ca ha^{-1}) was applied to Watershed 1 (WS1) in October 1999 with the objective of restoring soil base saturation to pre-industrial conditions (Peters et al., 2004). At BBWM, West Bear Brook (BW) was treated with applications of ammonium sulfate [$(NH_4)_2SO_4$] every other month, at the rate of 28.8 kg S ha^{-1} $year^{-1}$ and 25.2 kg N ha^{-1} $year^{-1}$ beginning in November 1989 and continuing through 2016 (Norton et al., 2010; Patel et al., 2020). At FEF, Watershed 3 (WS3) has been treated with three aerial applications of ammonium sulfate (March, July, and November) annually since 1989, providing an additional 40.6 kg S ha^{-1} and 35.4 kg N ha^{-1} per year (Adams et al., 2006). Ammonium sulfate applications at Fernow and Bear Brook were intended to examine the effects of chronic atmospheric N and S deposition on forest ecosystems. At each site, we compared the experimental watershed to a nearby, untreated reference watershed (Figure 4.1, Table 4.1). The forest stands in HBEF and BBWM are second growth forests that were largely established in the early-mid 20^{th} century. At HBEF, the forest was cutover circa 1890 and

1910 and affected by a hurricane in 1938 (Peart et al., 1992). At FEF the stands are substantially younger, having regenerated naturally since clearcutting in the late 1960s.

Table 4.1 Locations and characteristics of study sites.

Site	Watershed	Lat., Lon.	Treatment	Treatment Date	Hydrologic Record	Elevation (m)	Area (ha)	WY Start	MAT (°C)	MAP (mm)	Discharge	ET (mm)
Hubbard Brook Experimental Forest	W1	43.952, -71.726	$CaSiO_3$	October 1999	1957-Present	488-747	11.8	June	5.6	1335	854	481
	W3	43.954, -71.722	Reference		1956-Present	527-732	42.4	June	5.6	1333	848	485
Bear Brook Watersheds Maine	West Bear	44.859, -68.105	$(NH_4)_2SO_4$	1989-2016	1988-2012	274-451	10.3	Oct	5.8	1160	968	167
	East Bear	44.859, -68.104	Reference		1988-2016	273-450	11	Oct	5.8	1160	936	200
Fernow Experimental Forest	WS3	39.054, -79.686	$(NH_4)_2SO_4$	1989-Present	1951-Present	736-870	34.3	May	8.8	1479	658	813
	WS7	39.064, -79.679	Reference		1956-Present	718-855	24.2	May	8.8	1401	844	565

Notes: WY=Water year, MAT=Mean annual temperature, MAP=Mean Annual Precipitation, ET=Water year evapotranspiration. Temperature and precipitation data were collected on-site at HBEF and FEF, while climate data from BBWM were acquired from PRISM.

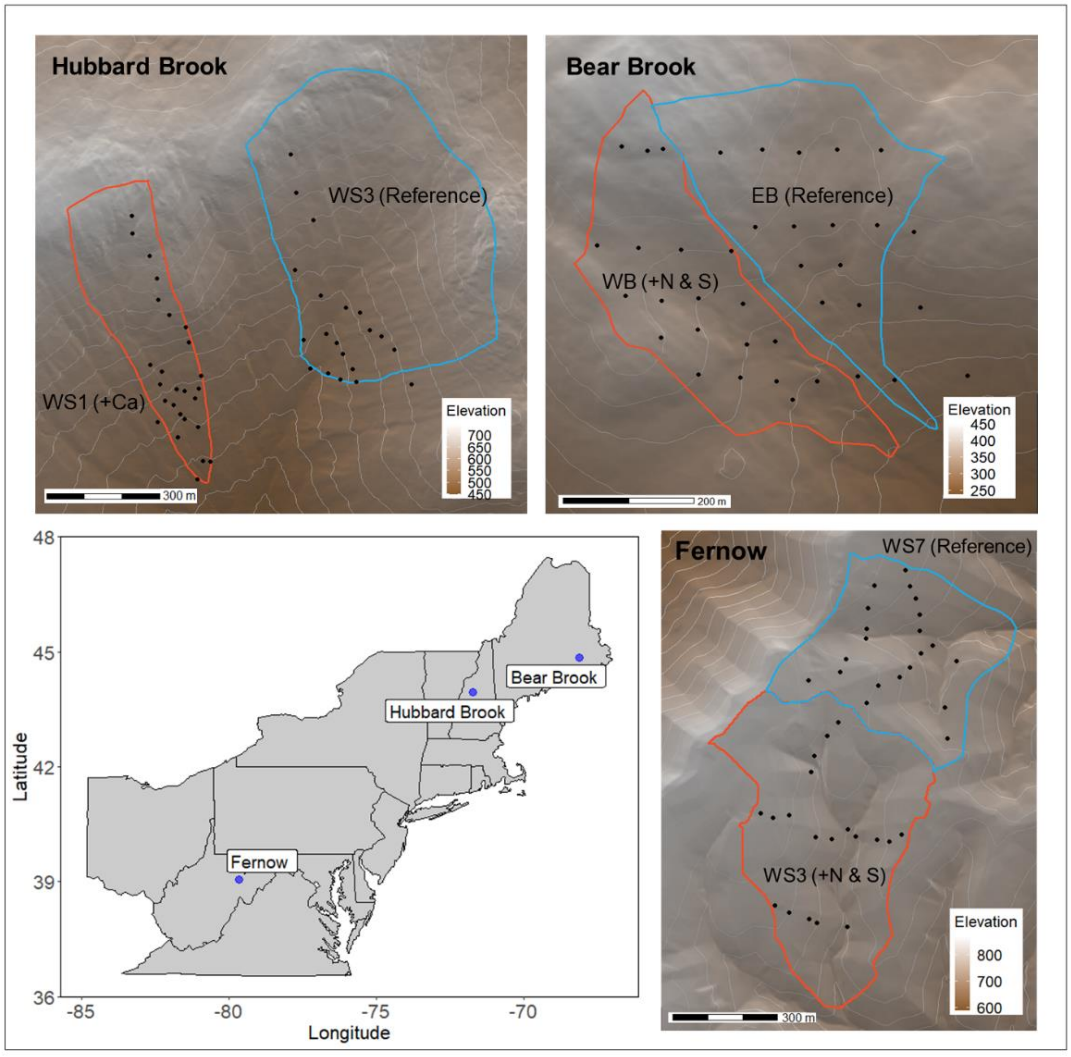

Figure 4.2 Overview of paired experimental watershed locations and tree coring plots at Hubbard Brook Experimental Forest, Bear Brook Watersheds, and Fernow Experimental Forest. Red outlines represent experimentally manipulated watersheds, while blue outlines represent reference watersheds at each site. Black dots represent tree coring plots. Note that GPS coordinates were not collected at all coring locations at Hubbard Brook.

4.2.2 Hydrometeorological Data

At HBEF and FEF, precipitation and temperature data were collected from rain gauges within the study watersheds. Precipitation and temperature data from BBWM were acquired from PRISM (Di Luzio et al., 2008). To assess impacts of nutrient manipulations on catchment

hydrology, catchment water balance evapotranspiration (ET) was calculated for each watershed. ET was calculated as the difference between water year precipitation and stream discharge, assuming negligible change in interannual water storage (Campbell et al., 2011). Water year was determined on a site-specific basis by calculating the annual interval with the highest correlation between precipitation and streamflow in the reference watershed at each site over the entire period of record, to reduce potential effects of interannual variation in storage (Vadeboncoeur et al., 2018). This resulted in water year starts of October 1st at BBWM, April 1st at FEF, and a June 1st at HBEF. Annual corrected ET deviation of watersheds from a long-term reference watershed was calculated by adopting the methods of Green et al. (2013). For these analyses, reference watersheds at BBWM, FEF, and HBEF were East Bear Brook, Fernow Watershed 4, and Hubbard Brook Watershed 3, respectively.

4.2.3 Field Sampling

Increment cores were collected from 14-18 individual trees that were at least 15 cm in diameter in the treatment and reference watersheds at each site. Two cores were collected to the pith of each tree, perpendicular to the hillslope at breast height, using 5.15 mm increment borers. Tree species sampled at each site are listed in Table 2. Trees at BBWM and FEF were sampled in July 2017 and August 2016, respectively. At BBWM, we established sampling plots along east-west transects of permanent stakes, selecting every other stake for sampling for a plot-center spacing of 60 m. At FEF, sampling plots were established 40-60 m apart along transects designed to capture variation in elevation and aspect across the watersheds. At FEF and BBWM, once a plot center was established, we selected the first suitable canopy tree within ~20 m of each focal species beginning at magnetic north and turning clockwise for odd-numbered plots and counter-

clockwise for even-numbered plots. Canopy position (dominant, co-dominant, or intermediate) was recorded for each tree.

Table 4.2 Tree species sampled at the three research sites. Yellow birch from HBEF were only included in growth analyses.

Site	Tree Species
Hubbard Brook Experimental Forest	Sugar maple (*Acer saccharum*) Yellow birch (*Betula alleghaniensis*) American beech (*Fagus grandifolia*) White ash (Fraxinus americana) Red spruce (*Picea rubens*)
Bear Brook Watersheds Maine	Sugar maple (*Acer saccharum*) Red maple *(Acer rubrum*) American beech (*Fagus grandifolia*) Red spruce (*Picea rubens*)
Fernow Experimental Forest	Red maple (*Acer rubrum*) Tulip poplar (*Liriodendron tulipifera*) Northern red oak (*Quercus rubra*) Black Cherry (*Prunus serotina*)

Tree cores from HBEF were collected during separate field campaigns in 2011, 2012, 2014, and 2017. In 2011 and 2012, American beech (*Fagus grandifolia*), sugar maple (*Acer saccharum*), yellow birch (*Betula alleghaniensis*), and red spruce (*Picea rubens*) were sampled from plots selected to span the elevations at which these trees are dominant, and the nearest suitable tree of each species to each sample point was selected. Supplemental sugar maple and red spruce cores were collected in 2014 along a single elevational transect in each watershed in order to increase the number of successfully cross-dated trees in the sample. In 2017, American beech and white ash (*Fraxinus americana*) were sampled in 2017 using a plot-based approach similar to that used at FEF and BBWM in WS3, and American beech were sampled along an elevation transect in WS1. At all sites, trees were rejected for sampling if they exhibited severe lean, or obvious signs

of bole or crown damage. A notable exception to this rule was American beech, which was afflicted with beech bark disease at both BBWM and HBEF.

4.2.4 Tree Core Processing

Increment cores were air-dried, hand-sanded, skeleton-plotted, and visually cross dated using standard dendrochronological procedures (Speer, 2012). Tree rings were measured using a sliding scale micrometer (Velmex Measuring System, Velmex, Inc., Bloomfield, NY) and MeasureJ2X software (VoorTech Consulting, Holderness, NH). Cross dating was statistically validated using COFECHA (Holmes, 1983). Growth analyses were conducted using the core from each tree that had the higher correlation with the master series for that species in that watershed. For growth analyses, raw ring widths were converted to basal area increment (BAI) using the bai.out function in the R package dplR (Bunn, 2018). BAI preserves high and low frequency variation in tree ring chronologies while accounting for the fact that ring widths often narrow as tree diameter increases.

4.2.5 Tree Ring $\delta^{13}C$ Chronologies

From each watershed, a subset of eight cores per species were selected for isotope analyses. To maintain a manageable number of isotope samples (but still sufficiently large enough to assess treatment effects and temporal trends), cores were sliced and analyzed in five-year segments beginning ten years prior to the first nutrient manipulation treatment at each site. Five-year whole-wood segments were hand-shredded using a razor blade. BBWM and HBEF samples were extracted for α-cellulose according to methods described by Leavitt and Danzer (1993), while α-cellulose was extracted from FEF samples using the Brendel method (Brendel et al., 2000). BBWM and HBEF samples were then analyzed for $\delta^{13}C$ on an Isoprime IRMS at the University

of New Hampshire (UNH) Instrumentation Center. Fernow samples were analyzed at Indiana University-Purdue University Indianapolis (IUPUI) on a Costech elemental analyzer coupled with Delta V IRMS. To ensure data consistence between the two facilities, reference cellulose was included in each analytic batch. After comparing $\delta^{13}C$ values for reference wood from which cellulose was extracted and analyzed at each lab, IUPUI $\delta^{13}C$ samples were adjusted by -0.9 ‰ to correct for bias caused by two different extraction methods between the two labs.

4.2.6 Intrinsic Water Use Efficiency

Plant intrinsic water use efficiency (iWUE) is defined as the ratio of photosynthetic carbon assimilation (A) to stomatal conductance to water vapor (g_s):

$$iWUE = \frac{A}{g_s} = \frac{C_a - C_i}{1.6}, \qquad \text{(Eq. 1)}$$

where C_a and C_i are the atmospheric and leaf intercellular CO_2 concentrations, respectively, and 1.6 is the diffusivity of water vapor relative to CO_2 according to Fick's Law. The carbon isotopic composition of plant tissues ($\delta^{13}C_p$) can be used to estimate C_i. During diffusion and photosynthesis, plants assimilate $^{12}CO_2$ more readily than $^{13}CO_2$, resulting in discrimination ($\Delta^{13}C$) against ^{13}C. $\Delta^{13}C$ can be calculated from $\delta^{13}C_p$ according to Farquhar and Richards (1984):

$$\Delta^{13}C = \frac{\delta^{13}C_a - \delta^{13}C_p}{1 + \delta^{13}C_p/1000} \text{ (Eq. 2)}$$

With known C_a, $\Delta^{13}C$ can then be used to solve for C_i using the equation (Farquhar, O'Leary, and Berry, 1982):

$$\Delta^{13}C = a + (b - a)\frac{C_i}{C_a} \text{ (Eq. 3)}$$

where *a* is diffusion fractionation (~4‰), *b* is carboxylation fractionation (~27‰). While this model does not account for fractionation during dark respiration or mesophyll conductance, it is considered sufficient for relative estimates of C_i and iWUE (Cernusak et al. 2013). For cellulose-based estimates of iWUE, a correction (*d*) is applied to account for post-photosynthetic fractionation processes that occur between photosynthate production and wood formation (Gessler et al., 2014). iWUE was calculated by combining Equations 1 and 3, with a correction for post-photosynthetic fractionation (*i.e.* Lavergne et al., 2019), yielding the equation:

$$iWUE = \frac{C_a}{1.6}\left(1 - \frac{\left(\frac{\delta^{13}C_a - (\delta^{13}C_p - d)}{1 + (\delta^{13}C_p - d)/\,1000}\right) - a}{(b - a)}\right) \text{ (Eq. 4)}$$

where *d* is the post-photosynthetic correction factor (2.1 ± 1.2 ‰). We used C_a and $\delta^{13}C_a$ time series from Belmecherri and Lavergne (2020). Temporal trends in iWUE for trees in reference watersheds were assessed using linear regression. Trends were calculated for each species, and all species pooled at each site.

4.2.7 Assessing Treatment Effects

Log response ratios (RRs), were used to assess effects of nutrient manipulations on BAI, iWUE, and catchment ET. RRs were defined as:

$$RR = \frac{\log(X_t)}{\log(X_r)} \text{ (Eq. 5)}$$

where X_t is the mean response in the treated watershed and X_r is the mean response in the reference watershed. To assess whether a change in a given response variable occurred due to treatment, we calculated the difference in RRs between the pre- and post-treatment periods

(ΔRR), using bootstrapped 95% confidence intervals on the mean difference calculation. This approach enables direct comparison of nutrient manipulation effects on response variables of different units and at different sites. At all sites, the pre-treatment period was defined as the ten years prior to the onset of nutrient manipulations. Because we hypothesized that some treatment effects would be transient and others would be cumulative, we examined the ΔRR of BAI and ET every five years during the treatment period at BBWM and FEF, and every five years since the one-time calcium addition at HBEF (*e.g.* 2000-2004, 2000-2009, etc.). We performed the same calculations on the iWUE data, beginning at 15 years since treatment onset to account for the lower sample size since isotopes were analyzed in 5-year segments. 95% confidence intervals were estimated on the ΔRR calculation using the R package *boot* with 1000 bootstrapped replicates. We considered a difference to be significant when the difference between the pre-treatment and post-treatment mean and its 95% confidence interval did not overlap zero.

4.3. Results

4.3.1 Basal Area Increment (BAI)

At HBEF, BAI of sugar maple, yellow birch, red spruce, and white ash were greater in the calcium-treated watershed 10-15 years after the one-time calcium addition compared to the reference watershed (Figure 4.3, Figure 4.5). The effect was strongest in sugar maple and yellow birch. There was a lagged response in white ash BAI, with no difference in the first five years after calcium addition, but significantly greater growth in treated trees beyond five years post-treatment (Figure 4.3). We observed a small but significant reduction in American beech BAI in the treated catchment relative to the control (Figure 4.5). At BBWM, BAI of American beech was enhanced in the ammonium sulfate treated watershed relative to the reference watershed throughout the entire 25-year post-treatment period (Figure 4.3, Figure 4.5). Transient 5-10 year

increases in BAI were observed in treated sugar maple, red maple, and red spruce following the onset of treatments, but there was no difference between watersheds when considering the entire post-treatment period. At FEF, we observed significant negative BAI responses in tulip poplar, red maple, and northern red oak in the ammonium sulfate-treated watershed throughout the 25-year post-treatment period. BAI of black cherry was significantly greater in the treated watershed throughout the entire treatment period.

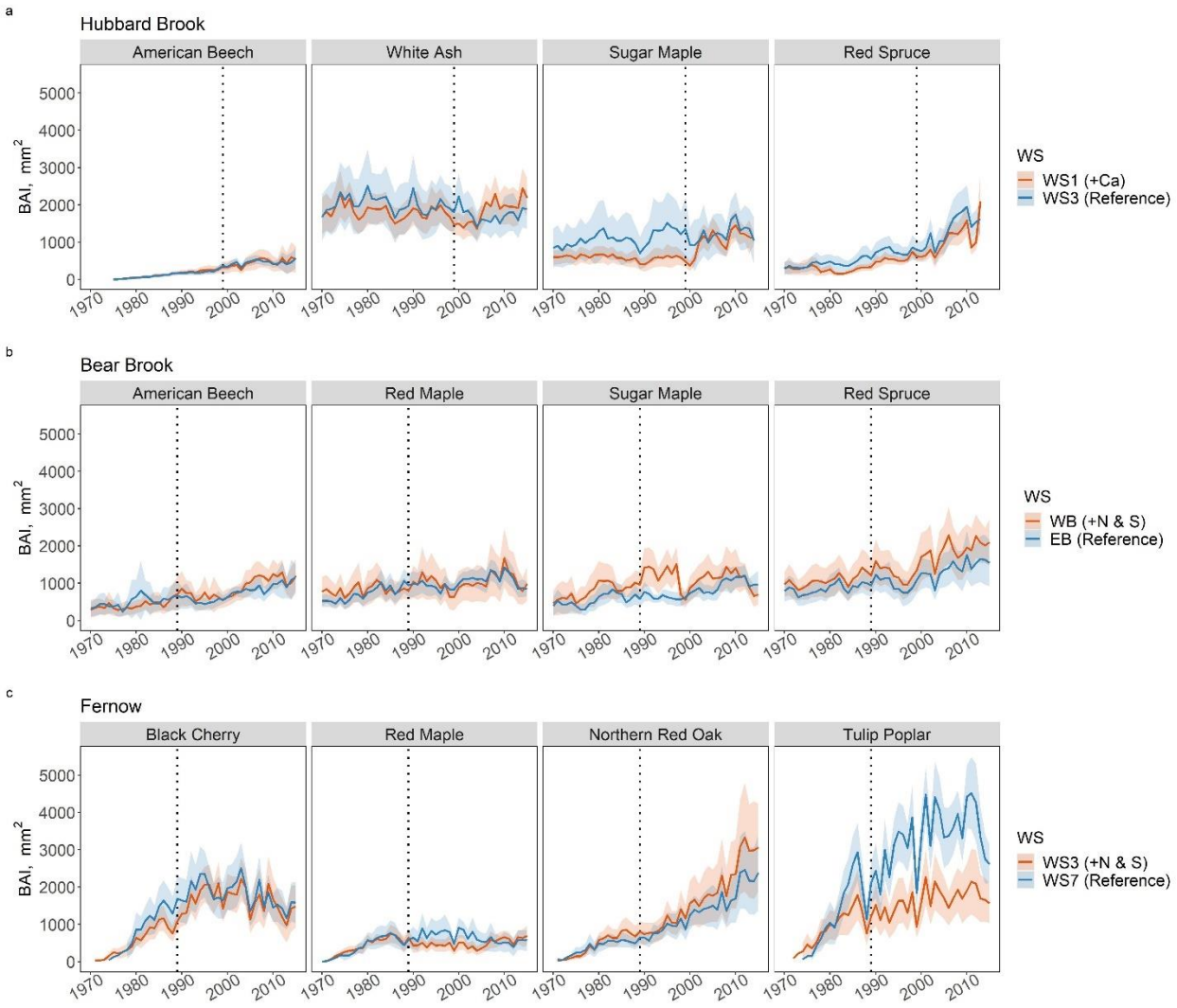

Figure 4.3 BAI time series for trees in the treated and reference watersheds at HBEF (a), BBWM (b), and FEF (c). Dotted vertical lines represent the onset of nutrient manipulations (or the one-time Ca addition in the case of HBEF). Lines and ribbons represent mean species BAI in

each watershed and 95% confidence intervals. Chronologies are plotted beginning in 1970 to focus on more recent temporal patterns, even though trees at HBEF and BBWM were substantially older.

4.3.2 Intrinsic Water Use Efficiency (iWUE)

Effects of nutrient manipulations on iWUE were generally less pronounced than effects on BAI. At HBEF, iWUE increased in calcium-treated sugar maple relative to reference trees, an effect that increased through time (Figure 4.4, Figure 4.6). We also observed small but significant reductions in iWUE of Ca-treated red spruce and white ash relative to control trees, but there was no effect on American beech. At BBWM, there was a weak negative effect of ammonium sulfate addition on American beech iWUE 15-25 years into the treatment period, but no other detectable differences in iWUE between trees in the treatment and reference watersheds in any of the other species at any time interval. At FEF, we observed significant negative effects of N and S treatment on black cherry iWUE after 15 years, negative effects on northern red oak iWUE 15-20 years into the treatment period, and negative effects on red maple iWUE 15-25 years into the treatment period.

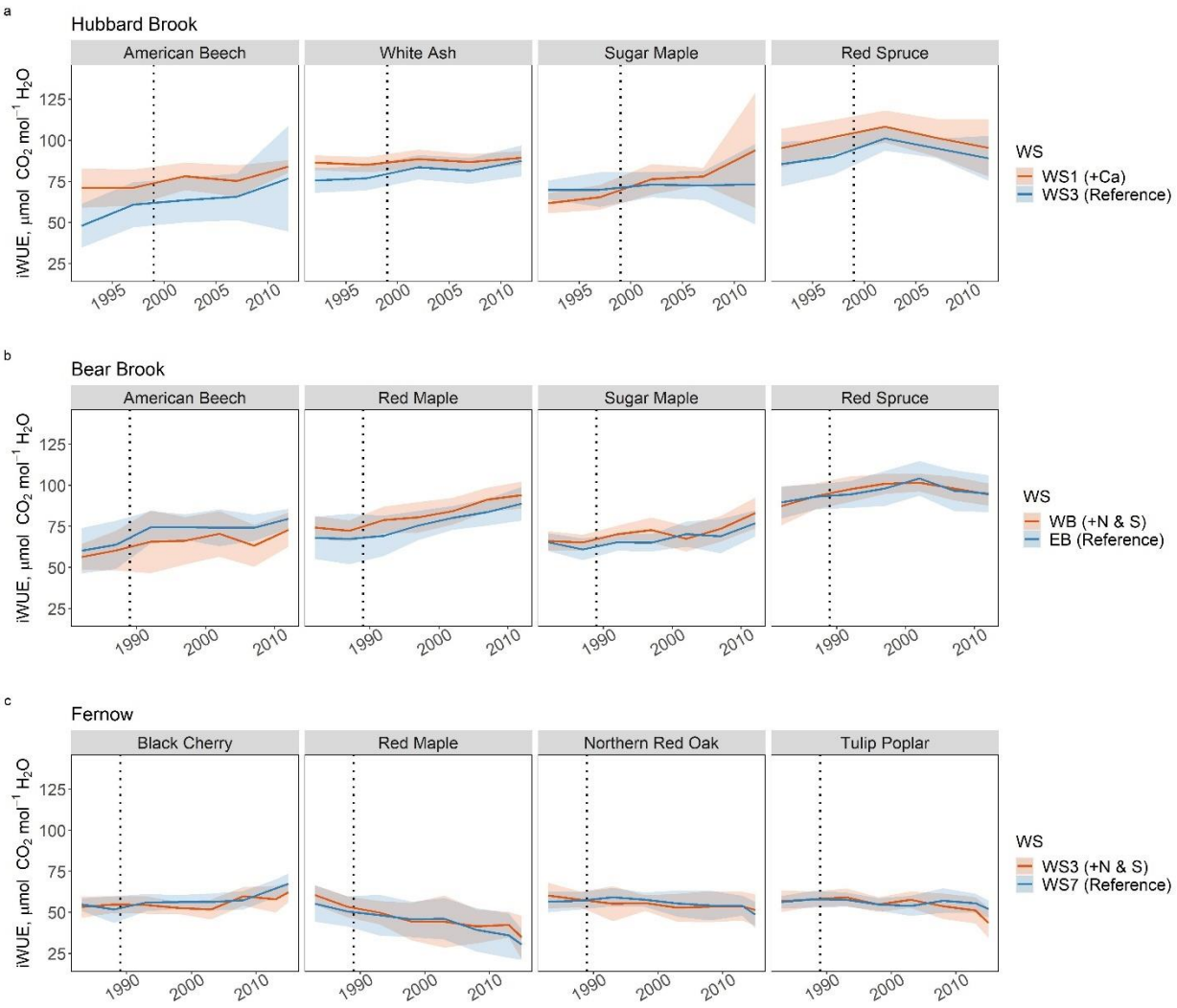

Figure 4.4 iWUE time series for trees in the treated and reference watersheds at HBEF (a), BBWM (b), and FEF (c). Dotted vertical lines represent the onset of nutrient manipulations (or the one-time Ca addition in the case of HBEF). Lines represent mean species iWUE in each watershed, while ribbons symbolize 95% confidence intervals.

While temporal dynamics of iWUE differed among species (Table 4.3), when pooled together, positive trends in iWUE (µmol CO_2 mol H_2O^{-1} $yr^{-}1$) were observed in reference trees at HBEF (slope=0.63, R^2=0.05, p=0.002) and BBWM (slope=0.49, R^2=0.08, p<0.0001; Figure 4.7). At both HBEF and BBWM, iWUE of red spruce peaked between 1999-2004 before declining in subsequent years. iWUE at FEF was characterized by a negative trend overall (slope=-0.14, R^2=0.02, p=0.02), but iWUE of black cherry at FEF increased over time. iWUE trends in red

maple differed dramatically between FEF and BBWM – decreasing throughout the study period at FEF (slope=-0.67, R^2=0.22, p<0.0001), but increasing at BBWM (slope=0.75, R^2=0.26, p<0.0001; Table 4.3).

Table 4.3 Temporal trends in iWUE for reference trees at each site.

Site	Species	Slope (μmol CO_2 mol H_2O^{-1} yr^{-1})	R^2	p
Hubbard Brook	Sugar Maple	0.20 ± 0.52	0	0.42
	American Beech	1.2 ± 0.84	0.18	0.006
	White Ash	0.56 ± 0.42	0.14	0.01
	Red Spruce	0.40 ± 0.63	0.02	0.2
	All Species	0.63 ± 0.40	0.05	0.02
Bear Brook	Red Maple	0.75 ± 0.34	0.26	<0.001
	Sugar Maple	0.39 ± 0.23	0.17	0.001
	American Beech	0.56 ± 0.33	0.15	0.001
	All Species	0.49 ± 0.21	0.08	<0.001
Fernow	Black Cherry	0.39 ± 0.15	0.27	<0.001
	Northern Red Oak	-0.21 ± 0.18	0.06	0.03
	Red Maple	-0.67 ± 0.27	0.22	<0.001
	Tulip Poplar	-0.10 ± 0.15	0.01	0.16
	All Species	-0.14 ± 0.12	0.02	0.02

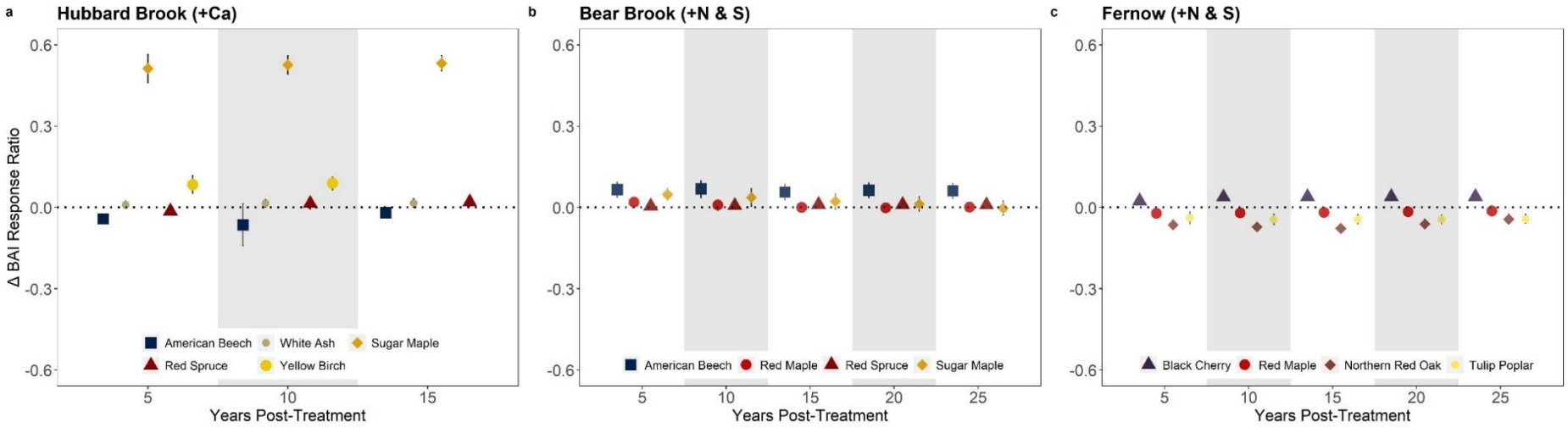

Figure 4.5 The difference in BAI response ratio between pre-and post-treatment periods at HBEF (a), BBWM (b), and FEF (c). Points represent the mean difference between the pre-and post-treatment response ratios, while the error bars represent 95% confidence intervals on the mean difference calculation. Positive values suggest BAI enhancement as a result of treatment, while negative values suggest a negative treatment effect, and treatment effects are considered significant when confidence intervals do not overlap zero. Temporal evolution of treatment effects are shown by performing this analysis at 5-year intervals from the onset of nutrient manipulations.

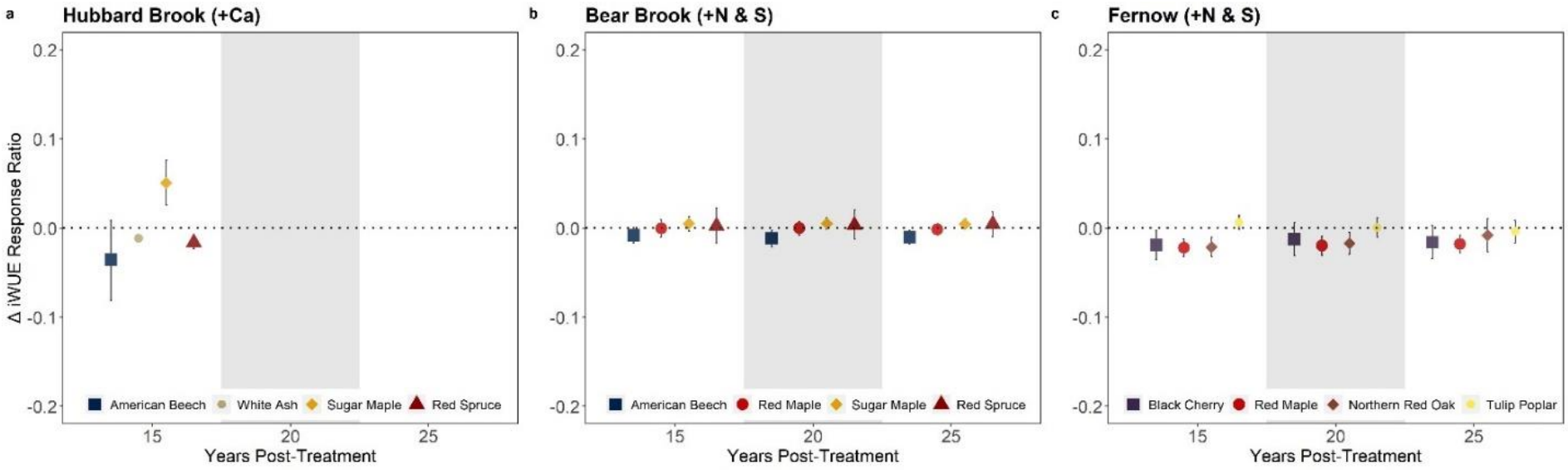

Figure 4.6 The difference in iWUE response ratio between pre and post-treatment periods at HBEF (a), BBWM (b), and FEF (c). Positive values suggest BAI enhancement as a result of treatment, while negative values suggest a negative treatment effect, and treatment effects are considered significant when confidence intervals do not overlap zero. Effects of treatment are considered significant when 95% confidence intervals of mean differences do not overlap zero. Note that the y-axis scale differs from Figure 4.5 to better enable visualization of data.

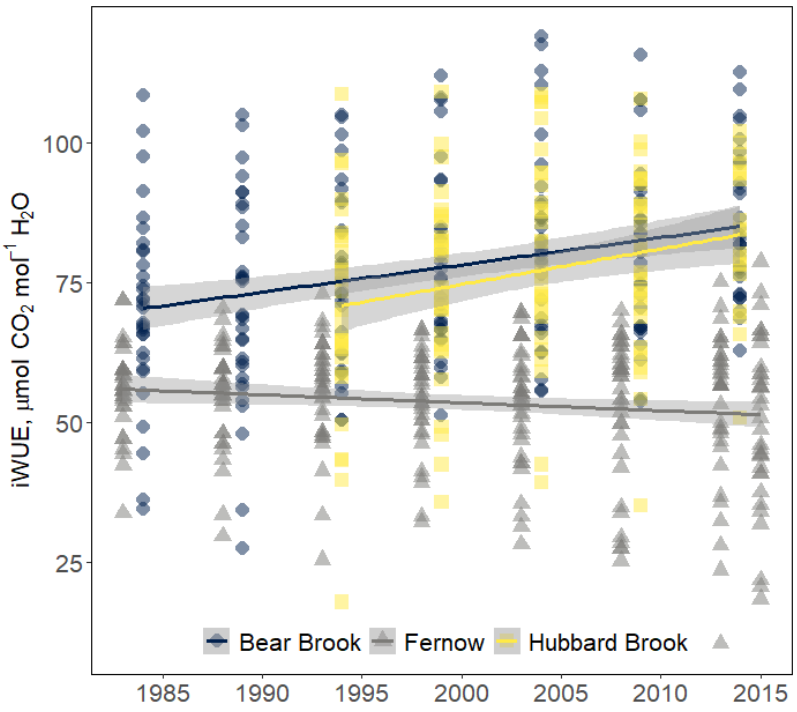

Figure 4.7 Temporal trends in iWUE from trees in reference watersheds at BBWM, FEF, and HBEF. Trendlines represent the mean trend of all reference trees at each site. $\delta^{13}C$ data used to derive iWUE were analyzed in 5-year increments for each tree. Points on the Year axis are aligned with the middle year of each 5-year increment. The average slope (mmol CO_2 mol $H2O^{-1}$ $yr^{-}1$) was 0.49 ± 0.21 at BBWM, -0.14 ± 0.12 at FEF, and 0.63 ± 0.40 at HBEF.

4.3.3 Catchment Water Balance

Consistent with results previously reported by Green et al. (2013), we found that ET in the treated watershed at HBEF increased substantially in the three years following calcium addition (23%, 20% and 35% relative to the mean pre-treatment ET) before returning to pre-treatment levels (Figure 4.8). After this increase, ET deviation in the treatment watershed was similar to that of other watersheds at HBEF. This transient increase was only partially captured by the ΔET response ratio analysis, where the mean ΔET RR was positive five years after treatment, but the confidence intervals overlap zero. At BBWM, corrected ET deviation in the ammonium sulfate-treated catchment fluctuated around zero, and there was no difference in the ΔET response ratio

for any time period. However, we note that water balance results from BBWM should be interpreted with more caution: unlike HBEF and FEF, where precipitation data were collected on-site, we relied on PRISM data at this site. Further, only two years of pre-treatment streamflow data are available at BBWM. At FEF, there was a small but significant decrease in ET in the treated watershed from 15-25 years since treatment onset (Figure 4.8).

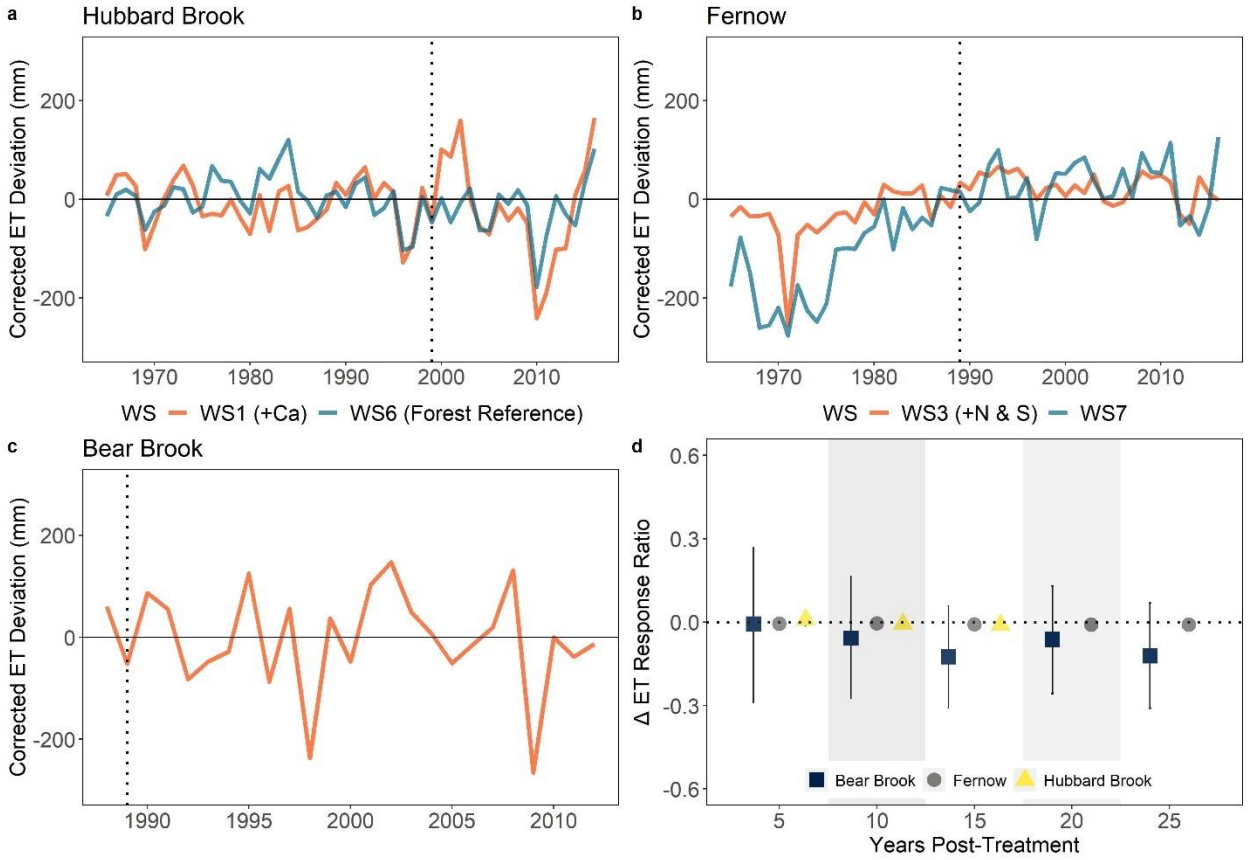

Figure 4.8 Corrected ET deviation of treatment watersheds from a nearby unmanipulated reference watershed at HBEF (a), FEF (b), and BBWM (c). At HBEF and FEF, ET deviation of another nearby untreated watershed is included for comparison. BBWM had only two gauged watersheds. Dotted vertical lines represent the onset of nutrient manipulations at each site. (d) The Δ ET response ratio at 5-year timesteps throughout the post-treatment period are considered significant when bootstrapped 95% confidence intervals do not overlap zero.

4. Discussion

In this study we examined aboveground tree growth and iWUE responses to changes in soil nutrients in three unique, whole-watershed nutrient manipulation experiments – two designed to increase acidity and N availability via ammonium sulfate additions (BBWM and FEF), and one where soil calcium was restored after decades of depletion (HBEF). We hypothesized that these treatments would alter both tree productivity and transpiration, which would be reflected in changes in BAI, catchment-scale ET, and tree iWUE. We observed a range of both species- and site-specific growth and iWUE responses to treatments, but a consistent pattern emerged: nutrient manipulations influenced growth more than iWUE. A notable exception was sugar maple at HBEF, for which we observed a large and sustained enhancement of both BAI and iWUE in calcium-treated trees. We observed positive temporal trends in iWUE for most species at HBEF and BBWM, but negative trends at FEF. Below we discuss more detailed site- and species-specific treatment effects, and differences between FEF and BBWM, which may explain differing temporal trends and responses to N and S addition.

4.4.1 Effects of Nutrient Manipulations on Tree Growth

Calcium plays an essential role in a variety of tree physiological functions, including xylem formation, stomatal regulation, and response to biotic and abiotic stress (Fromm, 2010, McAinsh et al., 1997, McLaughlin and Wimmer, 2002). Our results from HBEF indicate that aboveground productivity of several important NEUS hardwood species is limited by calcium availability. We observed greater BAI in sugar maple, white ash, and yellow birch in the +Ca watershed 10-15 years following treatment (Figure 4.2, Figure 4.4), consistent with enhanced biomass increment reported at the stand level (Battles et al., 2014). Our finding of enhanced BAI in sugar maple following calcium amendment is corroborated by other tree ring-based studies at

HBEF (Huggett et al., 2007), and elsewhere in northeastern North America (Moore et al., 2012, Oiumet et al., 2017). Increases in aboveground productivity in +Ca sugar maple at HBEF may be related to enhanced leaf area (Juice et al., 2006; Green et al., 2013), shoot extension (Gradowski and Thomas, 2008) and/or reduced allocation to belowground growth (Fahey et al., 2016).

We observed a lagged BAI response to calcium amendment in white ash, in which growth of +Ca trees began to exceed those in the reference watershed five years following treatment. Similar to sugar maple, white ash is particularly sensitive to calcium availability (Bigelow and Canham, 2002; Royo and Knight, 2012). We observed a minor growth enhancement in red spruce 15 years after calcium amendment in WS1. The relatively modest growth response of red spruce was surprising, given well-documented links between acid deposition-induced soil calcium depletion, winter freezing injury, and aboveground growth in this species (Hawley et al., 2006; Kosiba et al., 2013; Engel et al., 2016). Red spruce is sensitive to both soil calcium supply and foliar leaching of calcium due to direct exposure to acidic precipitation (Sayre and Fahey, 1999). Our results suggest the latter mechanism played a larger role at HBEF. Rapid increases in red spruce BAI observed in both watersheds at HBEF since the 1980s (Figure 4.2) are consistent with reports of a broader regional recovery of red spruce productivity in recent decades (Kosiba et al., 2018; Mathias and Thomas, 2018; Wason et al., 2019), a period when direct foliar exposure to acidic precipitation declined substantially. American beech was the only species with no growth response to calcium amendment at HBEF, a result consistent with other calcium addition studies in the region (Ouimet et al., 2017), including sites where beech showed symptoms of beech bark disease (Long et al., 2011).

Ammonium sulfate treatments at BBWM and FEF resulted in both positive and negative tree growth responses, which varied by site, species, and the duration of treatments. This likely

reflects the mixed consequences of N and S inputs to forest ecosystems. S is generally not a growth-limiting nutrient in temperate tree species, and S deposition is commonly associated with soil acidification, base cation depletion, and reduced forest productivity (Driscoll et al., 2001; Duarte et al., 2013). While N deposition has enhanced the productivity of many eastern US tree species by relieving N limitation (Horn et al., 2018; Thomas et al., 2010), it may also contribute to soil base cation depletion and nutrient imbalances (Driscoll et al., 2003; Pardo et al., 2011), resulting in reduced tree growth (McNulty et al., 2005). Indeed, elevated streamwater exports of both calcium and magnesium in the treated watersheds at both FEF and BBWM suggest that ammonium sulfate treatments resulted in depletion of base cations from the soil (Fernandez et al., 2010; Gilliam et al., 2020; Patel et al., 2020).

At BBWM, American beech growth was enhanced in the treated watershed throughout the duration of the study period (Figure 4.2), as has been observed in other experiments simulating the effects of chronic N deposition and acidification on this species (Halman et al., 2015; Ouimet et al., 2017). Growth enhancement was also observed in red spruce in the latter stages of the experiment, suggesting that relief of N limitation outweighed negative effects of base cation depletion for red spruce at this site. Our results are consistent with Elvir et al. (2010), which reported no difference in red spruce BAI between watersheds at BBWM after ten years of N and S additions, but contradicts results of another N addition study in the NEUS, which found that N inputs resulted in reduced stem growth in a high elevation spruce-fir forest (McNulty et al., 2005). It has been suggested that a combination of declining atmospheric N deposition and CO_2-driven increases in forest productivity may be contributing to N oligotrophication in temperate forests of the NEUS (Groffman et al., 2018). Red spruce productivity at BBWM has accelerated in recent decades, reflecting a regional recovery as deposition declines, and N additions may

have averted a potential N oligotrophication effect, resulting in enhanced growth in treated trees in the later stages of this study.

BAI of red maple and sugar maple was enhanced in the treated watershed at BBWM after five and ten years of treatment, respectively, after which there was no significant difference between watersheds (Figure 4.4). Ammonium sulfate treatments enhanced foliar N in sugar maple at BBWM between 1993-2004, which may have enhanced net photosynthesis (Elvir et al., 2006), and subsequently aboveground productivity (*i.e.,* Ollinger and Smith, 2005). However, our results suggest that after an initial N fertilization effect on BAI (consistent with results reported in Elvir et al., 2010), growth of red and sugar maple in the treated watershed may have become limited by other elements, such as phosphorous (*e.g.,* Vadeboncoeur, 2010, Goswami et al., 2017) or base cations. N availability in excess of tree demand is likely in the treatment watershed at BBWM, as it was proportionally less N retentive than the reference watershed (Patel et al., 2020), and soil NH_4^+ and NO_3^- concentrations were significantly higher between 1992 and 2016 in the deciduous portions of the watershed (Patel and Fernandez, 2018).

In contrast to BBWM, we observed negative effects of ammonium sulfate on tree growth in three of four species at FEF. An exception was black cherry, a pioneer species that tends to be relatively insensitive to soil acidification (Long et al., 2009; Malcomb et al., 2020). Negative growth responses in red maple and northern red oak varied in strength through time – the effect of ammonium sulfate on northern red oak BAI became less negative throughout the treatment period (and was not significant after 25 years), and the strongest treatment effect on red maple occurred 15 years post-treatment. Tulip poplar BAI was approximately 20% less in the treated watershed throughout the treatment period (Figure 4.2). Despite our finding of reduced growth of mostly canopy dominant/co-dominant trees, a recent inventory-based study at FEF, which

surveyed all trees >2.54 cm diameter, found enhanced aboveground biomass at the stand level in the treated watershed (Eastman et al., 2021). This may be a result of N-fertilization effects on acid-tolerant black cherry, which account for approximately half of stand basal area in the treated watershed (Malcomb et al., 2020). Ammonium sulfate treatments were discontinued at BBWM in 2016 and FEF in 2019, but continued monitoring of stand species composition and productivity will shed light on the legacy of chronic acidification on the productivity of these forests.

4.4.2 Nutrient Manipulation Effects on iWUE

Changes in iWUE may be induced by changes in photosynthetic carbon assimilation (*A*), stomatal conductance to water (g_s), or both. An increase in iWUE may thus occur if (1) *A* remains constant and g_s declines, (2) if a decline in *A* is accompanied by a larger decline in g_s, or (3) if *A* increases while g_s increases less, remains constant, or declines (Yi et al., 2019). In this study we used BAI as a proxy for *A* and catchment ET as a proxy for g_s in order to constrain our interpretation of iWUE results. While BAI is an imperfect proxy for *A*, as assimilated carbon may be allocated to roots, leaves, and non-structural carbohydrates (Hartman and Trumbore, 2016), enhanced *A* is linked to stem wood production (Ainsworth and Long, 2006), and ~88% of net ecosystem production is allocated to wood in temperate forests of the eastern United States (Brzostek et al., 2014). Transpiration accounts for approximately two-thirds of ET in temperate deciduous forests (Schlesinger and Jasechko, 2014), so a substantial change in g_s in any major species should induce an ET response at the catchment scale. However, we acknowledge that our catchment-based approach cannot resolve whether nutrient manipulations induced changes in transpiration at the species level.

At HBEF we observed a 23% increase in sugar maple iWUE in the +Ca watershed during the post-treatment period, while iWUE of reference trees remained constant through time (Table 4.3, Figure 4.4). While enhanced iWUE does not always translate to enhanced tree growth (Penuelas et al., 2011, Heilman et al., 2021), in this case we observed both effects simultaneously. iWUE and BAI of sugar maple in the +Ca catchment were enhanced throughout the post-treatment period, while there was an increase in catchment-scale ET only in the first three years following Ca amendment. BAI (averaged over the same 5-year increments as iWUE) and iWUE were highly correlated in Ca-treated sugar maple at HBEF ($r=0.89$, $p=0.04$), while there was no correlation in reference sugar maple (Figure S4.1). Our results thus suggest that enhanced *A*, and not changes in g_s, account for the observed long-term increases in both iWUE and BAI in calcium-treated sugar maple at HBEF. Enhanced growth and iWUE +Ca sugar maple may be related to improvements in photosynthetic physiology and reduction in oxidative stresses caused by nutrient deficiencies (St. Clair and Lynch, 2005). This is, to our knowledge, the first documented link between Ca nutrition and iWUE in sugar maple.

We observed small negative iWUE responses to calcium addition in white ash and red spruce at HBEF (Figure 4.6). However, the magnitude of the positive effect on sugar maple iWUE was 3.1 and 4.5 times greater than the magnitude of the negative effects on white ash and red spruce, respectively. American beech iWUE at BBWM exhibited a negative response to ammonium sulfate additions throughout the treatment period. At FEF, ammonium sulfate addition resulted in reduced iWUE in black cherry 15 years into the treatment period, in northern red oak from 15-20 years, and red maple 15-25 years into the treatment period, consistent with our hypothesis that iWUE would decline in response to increasing acidity. However, even where we observed significant effects of nutrient manipulations on iWUE, the effect sizes (as indicated by the

absolute value of ΔRR) tended to be substantially smaller than effects on BAI. For example, the mean BAI ΔRR for HBEF sugar maple is ten times greater than the mean iWUE ΔRR, and six times greater for American beech at BBWM. Small or non-detectable changes in iWUE response to nutrient manipulations suggest two possible scenarios: (1) nutrient manipulations did not influence either *A* or g_s, or (2) nutrient manipulations induced changes in *A* and g_s of similar direction and magnitude. To the extent that changes in BAI reflect changing *A*, and given that nutrient manipulations did influence BAI in many of the species we examined, our results point to the latter scenario.

4.4.3 Temporal Trends in iWUE

iWUE of reference trees at BBWM and HBEF increased over time (Figure 4.7; Table 4.3), consistent with the expected effects of increasing atmospheric CO_2 (Andreu-Hayles et al., 2011; van der Sleen et al., 2015; Frank et al., 2015; Guerrieri et al., 2019; Mathias and Thomas, 2021), decreasing atmospheric ozone (Holmes et al., 2014), and increasing tree height on iWUE (Brienen et al., 2017). In contrast, when trends of all reference species at FEF were assessed together, we observed a negative iWUE trend overall (Figure 4.7). iWUE of red maple, the only species sampled in the focal watersheds at both FEF and BBWM, increased by 33% between 1980 and 2014 at BBWM, but decreased by 45% during the same time period at FEF (Figure 4.7). While the causes of declining iWUE in reference trees at FEF are unknown, the forest at FEF differs from BBWM and HBEF in notable ways. Both watersheds at FEF were clear-cut in the 1960s, so the trees sampled at this site were in their juvenile stages of development for a substantial portion of our isotope chronologies. 'Juvenile effects' on isotope discrimination, which may persist for 10-50 years in *Quercus*, *Fagus*, and *Pinus* species (Leavitt, 2010 and refs therein), may arise from differences in light (Francey and Farquhar, 1982) and $\delta^{13}C_a$ (Schleser

and Jayasekera, 1985) between the canopy and the understory, and increasing hydraulic resistance with tree height (McDowell et al., 2002). Vadeboncoeur (2021) reported that developmental effects on C isotope discrimination are not predominantly driven by tree height per se, but rather light limitation of photosynthesis in understory trees. Despite the fact that the forest stands at FEF are even-aged, negative iWUE trends in red maple and northern red oak, which are less abundant and grew more slowly in the first two decades of stand development (Malcomb et al., 2020), may be at least partially attributable to shading by their faster growing neighbors. While we cannot rule out the influence of developmental effects on iWUE in the focal watersheds, iWUE has also declined since 1980 in northern red oak and sugar maple in FEF Watershed 10, which was last logged around 1910 (Figure S4.2). Negative iWUE trends in mature, codominant trees in recent decades points to alternative controls on iWUE at FEF.

Differences in climate may have contributed to divergent iWUE trends between FEF and the New England sites. While all three sites are relatively wet (>1000mm mean annual precipitation), FEF receives the most rainfall, and water availability tends to diminish the effects of atmospheric CO_2 on iWUE (Belmecheri et al., 2021; Levesque et al., 2017; Saurer et al., 2014). However, this explanation seems unlikely, given that our study period encompassed a pluvial period in the NEUS (Pederson et al., 2013), and thus would have affected all study sites. Another possibility is that, despite declines in N and S deposition at all three sites from 2000-2015 (the time period for which wet and dry deposition data are available), forests at FEF received over twice as much cumulative N deposition (wet + dry) and nearly four times as much cumulative S deposition as BBWM (Figure S4.2) due the density of coal-fired power plants upwind of FEF. Background deposition at FEF may have exceeded species-specific 'critical loads' (Pardo et al., 2011) even before the onset of the acidification experiment, resulting in soil

nutrient imbalances and suppressed tree productivity and iWUE at this site. Low soil fertility has been shown to attenuate the effects of increasing C_a on iWUE in boreal conifers (Marchand et al., 2020), and declines in tree iWUE have also been observed with increasing N deposition in a P-limited tropical forest (Huang et al., 2015), suggesting that nutrient limitations that reduce photosynthetic capacity may drive long-term declines in iWUE.

4.4.4 Catchment Water Balance

We hypothesized that experimental watershed acidification at BBWM and FEF would result in enhanced g_s as trees upregulate transpiration to sustain nutrient uptake from the soil (*i.e.* Lu et al., 2018). While ammonium sulfate treatments did result in loss of base cations from the treated watersheds at FEF (Gilliam et al., 2020) and BBWM (Patel et al., 2020), we did not find evidence that trees responded by increasing transpiration. At FEF we found modestly greater ET in the reference watershed (where we also observed greater growth in three of four species), while there was no difference in ET between watersheds at Bear Brook (Figure 4.8). Our results at FEF do not align with a report of enhanced ET in the +N and S watershed relative to Watershed 4, the long-term hydrologic and forest reference watershed at FEF (Lanning et al., 2019). However, in this case we compared ET between WS3 (+N and S) and WS7, a reference watershed where the forest is the same age. At HBEF, we observed a positive Ca-treatment effect on growth in three of five species, where we also observed a (transient) increase in ET.

Changes in leaf area related to nutrient manipulations may result in changes in ET at the catchment scale, which would not necessarily be accompanied by changes in iWUE. For example, transient increases in ET observed in the +Ca watershed at HBEF have been attributed to enhanced leaf area (Green et al., 2013), which increased the number of stomata in treated trees. While a change in calcium availability could influence transpiration via effects on xylem

conductivity (Smith and Shortle, 2013) and stomatal guard cell function (Hetherington and Woodward, 2003), our data are insufficient to assess whether nutrients altered transpiration independent of changes in C uptake. Employing the $\delta^{13}C$ and $\delta^{18}O$ dual isotope approach (Scheidegger et al., 2000) to assess relative contributions of A and g_s to iWUE would provide a more complete picture of the mechanisms underlying iWUE trends and experimental effects in these watersheds.

4.5 Conclusions

In this study we examined how whole-watershed experimental manipulations of soil acid-base status influence the carbon and water balance of temperate mixed deciduous forests. We found that tree responses to experimental N and S additions varied among sites, species, and the duration of treatments. Positive growth responses to calcium amendment at HBEF provide further evidence of calcium limitation on forest productivity in base-poor soils of the NEUS. At BBWM, where background deposition of N was low, we observed mostly positive – but sometimes short-lived – growth responses to ammonium sulfate addition, presumably indicating N limitation of NPP. In contrast, we observed mostly negative tree growth responses to the same experimental treatment at FEF, where background deposition levels of N, S, and acidity have historically been high. These findings highlight the complex effects of atmospheric N inputs on forests, which may act as either a fertilizing or an acidifying agent, depending on forest species composition, soil chemistry, and the amount and duration of exposure (Thomas et al., 2009; Horn et al., 2018). We also observed, for the first time, a strong positive iWUE response in sugar maple to calcium addition, and weak negative effects of N and S addition on several species, suggesting that tree mineral nutrition can limit iWUE in certain species and settings. However, the magnitude of experimental effects on iWUE was generally smaller than effects on

tree growth, suggesting that nutrient manipulations may have induced parallel changes in both *A* and g_s. While we found limited evidence for nutrient effects on iWUE at FEF and BBWM, differences in temporal trends in iWUE between sites suggest that CO_2 and/or developmental effects on iWUE are not universal, and that local factors including deposition history may influence iWUE. This study highlights the importance of accounting for soil nutrients in projections of forest productivity and, to a lesser extent, water use, and thus may have implications for forest ecosystem functions and services including carbon sequestration, wood production, and regulation of streamflow.

Acknowledgements

This work was supported by National Science Foundation EAR-1562019, National Science Foundation DEB-1637685, National Science Foundation DEB-1119709 and National Science Foundation DEB-0417678, the Northeastern States Research Cooperative, and the Hamel Center at the University of New Hampshire. We thank the US Forest Service Northern Research Station and University of Maine for access to data and field sites. We thank Tim Forrest, Maria Chaves, Imani Guest, and Christina Mauney for their assistance in the field and the lab.

Chapter 4 References

Adams, M. B., DeWalle, D. R., & Hom, J. L. (2006). *The Fernow Watershed Acidification Study* (1st ed., Vol. 11). Springer Netherlands.

Ainsworth, E. A., & Long, S. P. (2005). What have we learned from 15 years of free-air CO2 enrichment (FACE)? A meta-analytic review of the responses of photosynthesis, canopy properties and plant production to rising CO2. *New Phytologist*, *165*(2), 351–372. https://doi.org/10.1111/j.1469-8137.2004.01224.x

ANDREU-HAYLES, L., PLANELLS, O., GUTIÉRREZ, E., MUNTAN, E., HELLE, G., ANCHUKAITIS, K. J., & SCHLESER, G. H. (2011). Long tree-ring chronologies reveal 20th century increases in water-use efficiency but no enhancement of tree growth at five Iberian pine forests. *Global Change Biology*, *17*(6), 2095–2112. https://doi.org/10.1111/j.1365-2486.2010.02373.x

Bailey, S. W., Long, R. P., & Horsley, S. B. (2021). Forest Soil Cation Dynamics and Increases in Carbon on the Allegheny Plateau, PA, USA Following a Period of Strongly Declining Acid Deposition. *Soil Systems*, *5*(1). https://doi.org/10.3390/soilsystems5010016

Battles, J. J., Fahey, T. J., Driscoll, C. T., Blum, J. D., & Johnson, C. E. (2014). Restoring Soil Calcium Reverses Forest Decline. *Environmental Science & Technology Letters*, *1*(1), 15–19. https://doi.org/10.1021/ez400033d

Belmecheri, S., & Lavergne, A. (2020). Compiled records of atmospheric CO2 concentrations and stable carbon isotopes to reconstruct climate and derive plant ecophysiological indices from tree rings. *Dendrochronologia*, *63*, 125748. https://doi.org/10.1016/j.dendro.2020.125748

Belmecheri, S., Maxwell, R. S., Taylor, A. H., Davis, K. J., Guerrieri, R., Moore, D. J. P., & Rayback, S. A. (2021). Precipitation alters the CO2 effect on water-use efficiency of temperate forests. *Global Change Biology*, *27*(8), 1560–1571. https://doi.org/10.1111/gcb.15491

Bigelow, S. W., & Canham, C. D. (2002). Community organization of tree species along soil gradients in a north-eastern USA forest. *Journal of Ecology*, *90*(1), 188–200. https://doi.org/10.1046/j.0022-0477.2001.00655.x

Bishop, D. A., Beier, C. M., Pederson, N., Lawrence, G. B., Stella, J. C., & Sullivan, T. J. (2015). Regional growth decline of sugar maple (Acer saccharum) and its potential causes. *Ecosphere*, *6*(10), art179. https://doi.org/10.1890/ES15-00260.1

BOISVENUE, C., & RUNNING, S. W. (2006). Impacts of climate change on natural forest productivity – evidence since the middle of the 20th century. *Global Change Biology*, *12*(5), 862–882. https://doi.org/10.1111/j.1365-2486.2006.01134.x

Borer, C. H., Schaberg, P. G., & DeHayes, D. H. (2005). Acidic mist reduces foliar membrane-associated calcium and impairs stomatal responsiveness in red spruce. *Tree Physiology*, *25*(6), 673–680. https://doi.org/10.1093/treephys/25.6.673

Brendel, O., Iannetta, P. P. M., & Stewart, D. (2000). A rapid and simple method to isolate pure alpha-cellulose. *Phytochemical Analysis*, *11*(1), 7–10. https://doi.org/10.1002/(SICI)1099-1565(200001/02)11:1<7::AID-PCA488>3.0.CO;2-U

Brienen, R. J. W., Gloor, E., Clerici, S., Newton, R., Arppe, L., Boom, A., et al. (2017). Tree height strongly affects estimates of water-use efficiency responses to climate and CO2 using isotopes. *Nature Communications*, *8*(1), 288. https://doi.org/10.1038/s41467-017-00225-z

Brzostek, E. R., Dragoni, D., Schmid, H. P., Rahman, A. F., Sims, D., Wayson, C. A., et al. (2014). Chronic water stress reduces tree growth and the carbon sink of deciduous hardwood forests. *Global Change Biology*, *20*(8), 2531–2539. https://doi.org/10.1111/gcb.12528

Bukata, A. R., & Kyser, T. K. (2007). Carbon and Nitrogen Isotope Variations in Tree-Rings as Records of Perturbations in Regional Carbon and Nitrogen Cycles. *Environmental Science & Technology*, *41*(4), 1331–1338. https://doi.org/10.1021/es061414g

Bunn, A. G., Korpela, M., Biondi, F., Campelo, F., Merian, P., Qeadan, F., et al. (2018). dplR: Dendrochronology Program Library in R. R package version 1.6.9. Retrieved from https://CRAN.R-project.org/package=dplR

Campbell, J. L., Driscoll, C. T., Pourmokhtarian, A., & Hayhoe, K. (2011). Streamflow responses to past and projected future changes in climate at the Hubbard Brook Experimental Forest, New Hampshire, United States. *Water Resources Research*, *47*(2). https://doi.org/10.1029/2010WR009438

Cernusak, L. A., Ubierna, N., Winter, K., Holtum, J. A. M., Marshall, J. D., & Farquhar, G. D. (2013). Environmental and physiological determinants of carbon isotope discrimination in terrestrial plants. *New Phytologist*, *200*(4), 950–965. https://doi.org/10.1111/nph.12423

Cramer, M. D., Hoffmann, V., & Verboom, G. A. (2008). Nutrient availability moderates transpiration in Ehrharta calycina. *New Phytologist*, *179*(4), 1048–1057. https://doi.org/10.1111/j.1469-8137.2008.02510.x

DeHayes, D. H., Schaberg, P. G., Hawley, G. J., & Strimbeck, G. R. (1999). Acid Rain Impacts on Calcium Nutrition and Forest Health: Alteration of membrane-associated calcium leads to membrane destabilization and foliar injury in red spruce. *BioScience*, *49*(10), 789–800. https://doi.org/10.2307/1313570

DeWalle, D. R., Kochenderfer, J. N., Adams, M. B., Miller, G. W., Gilliam, F. S., Wood, F., et al. (2006). Vegetation and Acidification. In M. B. Adams, D. R. DeWalle, & J. L. Hom (Eds.), *The Fernow Watershed Acidification Study* (pp. 137–188). Dordrecht: Springer Netherlands. https://doi.org/10.1007/978-1-4020-4615-5_5

Di Luzio, M., Johnson, G. L., Daly, C., Eischeid, J. K., & Arnold, J. G. (2008). Constructing Retrospective Gridded Daily Precipitation and Temperature Datasets for the Conterminous United States. *Journal of Applied Meteorology and Climatology*, *47*(2), 475–497. https://doi.org/10.1175/2007JAMC1356.1

Driscoll, C. T., Lawrence, G. B., Bulger, A. J., Butler, T. J., Cronan, C. S., Eagar, C., et al. (2001). Acidic Deposition in the Northeastern United States: Sources and Inputs, Ecosystem Effects, and Management Strategies. *BioScience*, *51*(3), 180. https://doi.org/10.1641/0006-3568(2001)051[0180:ADITNU]2.0.CO;2

Driscoll, C. T., Whitall, D., Aber, J., Boyer, E., Castro, M., Cronan, C., et al. (2003). Nitrogen Pollution in the Northeastern United States: Sources, Effects, and Management Options. *BioScience*, *53*(4), 357–374. https://doi.org/10.1641/0006-3568(2003)053[0357:NPITNU]2.0.CO;2

Duarte, N., Pardo, L. H., & Robin-Abbott, M. J. (2013). Susceptibility of Forests in the Northeastern USA to Nitrogen and Sulfur Deposition: Critical Load Exceedance and Forest Health. *Water, Air, & Soil Pollution*, *224*(2), 1355. https://doi.org/10.1007/s11270-012-1355-6

Eastman, B. A., Adams, M. B., Brzostek, E. R., Burnham, M. B., Carrara, J. E., Kelly, C., et al. (2021). Altered plant carbon partitioning enhanced forest ecosystem carbon storage after 25 years of nitrogen additions. *New Phytologist*, *230*(4), 1435–1448. https://doi.org/10.1111/nph.17256

Elvir, Jose A., Wiersma, G. B., Day, M. E., Greenwood, M. S., & Fernandez, I. J. (2006). Effects of enhanced nitrogen deposition on foliar chemistry and physiological processes of forest trees at the Bear Brook Watershed in Maine. *Forest Ecology and Management*, *221*(1), 207–214. https://doi.org/10.1016/j.foreco.2005.09.022

Elvir, Jose Alexander, Wiersma, G. B., White, A. S., & Fernandez, I. J. (2003). Effects of chronic ammonium sulfate treatment on basal area increment in red spruce and sugar maple at the Bear Brook Watershed in Maine. *Canadian Journal of Forest Research*, *33*(5), 862–869. https://doi.org/10.1139/x03-016

Elvir, Jose Alexander, Wiersma, G. B., Bethers, S., & Kenlan, P. (2010). Effects of chronic ammonium sulfate treatment on the forest at the Bear Brook Watershed in Maine. *Environmental Monitoring and Assessment*, *171*(1), 129–147. https://doi.org/10.1007/s10661-010-1523-3

Engel, B. J., Schaberg, P. G., Hawley, G. J., Rayback, S. A., Pontius, J., Kosiba, A. M., & Miller, E. K. (2016). Assessing relationships between red spruce radial growth and pollution critical load exceedance values. *Special Section: Forests, Roots and Soil Carbon*, *359*, 83–91. https://doi.org/10.1016/j.foreco.2015.09.029

Fahey, T. J., Heinz, A. K., Battles, J. J., Fisk, M. C., Driscoll, C. T., Blum, J. D., & Johnson, C. E. (2016). Fine root biomass declined in response to restoration of soil calcium in a northern hardwood forest. *Canadian Journal of Forest Research*, *46*(5), 738–744. https://doi.org/10.1139/cjfr-2015-0434

Farquhar, G., & Richards, R. (1984). Isotopic Composition of Plant Carbon Correlates With Water-Use Efficiency of Wheat Genotypes. *Functional Plant Biology*, *11*(6), 539–552.

Farquhar, G., O'Leary, M., & Berry, J. (1982). On the Relationship Between Carbon Isotope Discrimination and the Intercellular Carbon Dioxide Concentration in Leaves. *Functional Plant Biology*, *9*(2), 121–137.

Ficklin, D. L., & Novick, K. A. (2017). Historic and projected changes in vapor pressure deficit suggest a continental-scale drying of the United States atmosphere: Increasing U.S. Vapor Pressure Deficit. *Journal of Geophysical Research: Atmospheres*, *122*(4), 2061–2079. https://doi.org/10.1002/2016JD025855

Francey, R. J., & Farquhar, G. D. (1982). An explanation of 13C/12C variations in tree rings. *Nature*, *297*(5861), 28–31. https://doi.org/10.1038/297028a0

Frank, D. C., Poulter, B., Saurer, M., Esper, J., Huntingford, C., Helle, G., et al. (2015). Water-use efficiency and transpiration across European forests during the Anthropocene. *Nature Climate Change*, *5*(6), 579–583. https://doi.org/10.1038/nclimate2614

Fromm, J. (2010). Wood formation of trees in relation to potassium and calcium nutrition. *Tree Physiology*, *30*(9), 1140–1147. https://doi.org/10.1093/treephys/tpq024

Gessler, A., Ferrio, J. P., Hommel, R., Treydte, K., Werner, R. A., & Monson, R. K. (2014). Stable isotopes in tree rings: towards a mechanistic understanding of isotope fractionation and mixing processes from the leaves to the wood. *Tree Physiology*, *34*(8), 796–818. https://doi.org/10.1093/treephys/tpu040

Gilliam, F. S., Adams, M. B., & Peterjohn, W. T. (2020). Response of soil fertility to 25 years of experimental acidification in a temperate hardwood forest. *Journal of Environmental Quality*, *49*(4), 961–972. https://doi.org/10.1002/jeq2.20113

Goswami, S., Fisk, M. C., Vadeboncoeur, M. A., Garrison-Johnston, M., Yanai, R. D., & Fahey, T. J. (2018). Phosphorus limitation of aboveground production in northern hardwood forests. *Ecology*, *99*(2), 438–449. https://doi.org/10.1002/ecy.2100

Gradowski, T., & Thomas, S. C. (2008). Responses of Acer saccharum canopy trees and saplings to P, K and lime additions under high N deposition. *Tree Physiology*, *28*(2), 173–185. https://doi.org/10.1093/treephys/28.2.173

Green, M. B., Bailey, A. S., Bailey, S. W., Battles, J. J., Campbell, J. L., Driscoll, C. T., et al. (2013). Decreased water flowing from a forest amended with calcium silicate. *Proceedings of the National Academy of Sciences*, *110*(15), 5999. https://doi.org/10.1073/pnas.1302445110

Groffman, P. M., Driscoll, C. T., Durán, J., Campbell, J. L., Christenson, L. M., Fahey, T. J., et al. (2018). Nitrogen oligotrophication in northern hardwood forests. *Biogeochemistry*, *141*(3), 523–539. https://doi.org/10.1007/s10533-018-0445-y

Guerrieri, R., Belmecheri, S., Ollinger, S. V., Asbjornsen, H., Jennings, K., Xiao, J., et al. (2019). Disentangling the role of photosynthesis and stomatal conductance on rising forest water-use efficiency. *Proceedings of the National Academy of Sciences*, *116*(34), 16909. https://doi.org/10.1073/pnas.1905912116

Halman, J. M., Schaberg, P. G., Hawley, G. J., Hansen, C. F., & Fahey, T. J. (2015). Differential impacts of calcium and aluminum treatments on sugar maple and American beech growth dynamics. *Canadian Journal of Forest Research*, *45*(1), 52–59. https://doi.org/10.1139/cjfr-2014-0250

Hartmann, H., & Trumbore, S. (2016). Understanding the roles of nonstructural carbohydrates in forest trees – from what we can measure to what we want to know. *New Phytologist*, *211*(2), 386–403. https://doi.org/10.1111/nph.13955

Haverd, V., Smith, B., Canadell, J. G., Cuntz, M., Mikaloff-Fletcher, S., Farquhar, G., et al. (2020). Higher than expected CO2 fertilization inferred from leaf to global observations. *Global Change Biology*, *26*(4), 2390–2402. https://doi.org/10.1111/gcb.14950

Hawley, G. J., Schaberg, P. G., Eagar, C., & Borer, C. H. (2006). Calcium addition at the Hubbard Brook Experimental Forest reduced winter injury to red spruce in a high-injury year. *Canadian Journal of Forest Research*, *36*(10), 2544–2549. https://doi.org/10.1139/x06-221

Hayhoe, K., Wake, C. P., Huntington, T. G., Luo, L., Schwartz, M. D., Sheffield, J., et al. (2007). Past and future changes in climate and hydrological indicators in the US Northeast. *Climate Dynamics*, *28*(4), 381–407. https://doi.org/10.1007/s00382-006-0187-8

Hazlett, P., Emilson, C., Lawrence, G., Fernandez, I., Ouimet, R., & Bailey, S. (2020). Reversal of Forest Soil Acidification in the Northeastern United States and Eastern Canada: Site and Soil Factors Contributing to Recovery. *Soil Systems*, *4*(3). https://doi.org/10.3390/soilsystems4030054

Heilman, K. A., Trouet, V. M., Belmecheri, S., Pederson, N., Berke, M. A., & McLachlan, J. S. (2021). Increased water use efficiency leads to decreased precipitation sensitivity of tree growth, but is offset by high temperatures. *Oecologia*. https://doi.org/10.1007/s00442-021-04892-0

Hetherington, A. M., & Woodward, F. I. (2003). The role of stomata in sensing and driving environmental change. *Nature*, *424*(6951), 901–908. https://doi.org/10.1038/nature01843

Holmes, C. D. (2014). Air pollution and forest water use. *Nature*, *507*(7491), E1–E2. https://doi.org/10.1038/nature13113

Holmes, R. (1983). Cofecha: Computer Assisted Quality Control in Tree-Ring Dating and Measurement. *Tree-Ring Bulletin*, *44*, 69–75.

Horn, K. J., Thomas, R. Q., Clark, C. M., Pardo, L. H., Fenn, M. E., Lawrence, G. B., et al. (2018). Growth and survival relationships of 71 tree species with nitrogen and sulfur deposition across the conterminous U.S. *PLOS ONE*, *13*(10), e0205296. https://doi.org/10.1371/journal.pone.0205296

Huang, Z., Liu, B., Davis, M., Sardans, J., Peñuelas, J., & Billings, S. (2016). Long-term nitrogen deposition linked to reduced water use efficiency in forests with low phosphorus availability. *New Phytologist*, *210*(2), 431–442. https://doi.org/10.1111/nph.13785

Huggett, B. A., Schaberg, P. G., Hawley, G. J., & Eagar, C. (2007). Long-term calcium addition increases growth release, wound closure, and health of sugar maple (Acer saccharum) trees at the Hubbard Brook Experimental Forest. *Canadian Journal of Forest Research*, *37*(9), 1692–1700. https://doi.org/10.1139/X07-042

Jennings, K. A., Guerrieri, R., Vadeboncoeur, M. A., & Asbjornsen, H. (2016). Response of *Quercus velutina* growth and water use efficiency to climate variability and nitrogen fertilization in a temperate deciduous forest in the northeastern USA. *Tree Physiology*, *36*(4), 428–443. https://doi.org/10.1093/treephys/tpw003

Jonard, M., Fürst, A., Verstraeten, A., Thimonier, A., Timmermann, V., Potočić, N., et al. (2015). Tree mineral nutrition is deteriorating in Europe. *Global Change Biology*, *21*(1), 418–430. https://doi.org/10.1111/gcb.12657

Juice, S. M., Fahey, T. J., Siccama, T. G., Driscoll, C. T., Denny, E. G., Eagar, C., et al. (2006). RESPONSE OF SUGAR MAPLE TO CALCIUM ADDITION TO NORTHERN HARDWOOD FOREST. *Ecology*, *87*(5), 1267–1280. https://doi.org/10.1890/0012-9658(2006)87[1267:ROSMTC]2.0.CO;2

Kjellstro¨M, E., Nikulin, G., Hansson, U., Strandberg, G., & Ullerstig, A. (2011). 21st century changes in the European climate: uncertainties derived from an ensemble of regional climate model simulations. *Tellus A: Dynamic Meteorology and Oceanography*, *63*(1), 24–40. https://doi.org/10.1111/j.1600-0870.2010.00475.x

Kosiba, A. M., Schaberg, P. G., Hawley, G. J., & Hansen, C. F. (2013). Quantifying the legacy of foliar winter injury on woody aboveground carbon sequestration of red spruce trees. *Forest Ecology and Management*, *302*, 363–371. https://doi.org/10.1016/j.foreco.2013.03.006

Lajtha, K., & Jones, J. (2013). Trends in cation, nitrogen, sulfate and hydrogen ion concentrations in precipitation in the United States and Europe from 1978 to 2010: a new look at an old problem. *Biogeochemistry*, *116*(1), 303–334. https://doi.org/10.1007/s10533-013-9860-2

Lanning, Matthew, Wang, Lixin, Scanlon, Todd M., Vadeboncoeur, Matthew A., Adams, Mary B., Epstein, Howard E., & Druckenbrod, Daniel. (n.d.). Intensified vegetation water use under acid deposition. *Science Advances*, *5*(7), eaav5168. https://doi.org/10.1126/sciadv.aav5168

Lavergne, A., Graven, H., De Kauwe, M. G., Keenan, T. F., Medlyn, B. E., & Prentice, I. C. (2019). Observed and modelled historical trends in the water-use efficiency of plants and ecosystems. *Global Change Biology*, *25*(7), 2242–2257. https://doi.org/10.1111/gcb.14634

Lawrence, G. B., Hazlett, P. W., Fernandez, I. J., Ouimet, R., Bailey, S. W., Shortle, W. C., et al. (2015). Declining Acidic Deposition Begins Reversal of Forest-Soil Acidification in the Northeastern U.S. and Eastern Canada. *Environmental Science & Technology*, *49*(22), 13103–13111. https://doi.org/10.1021/acs.est.5b02904

Leavitt, S. W. (2010). Tree-ring C–H–O isotope variability and sampling. *Science of The Total Environment*, *408*(22), 5244–5253. https://doi.org/10.1016/j.scitotenv.2010.07.057

Leavitt, S. W., & Danzer, S. R. (1993). Method for batch processing small wood samples to holocellulose for stable-carbon isotope analysis. *Analytical Chemistry*, *65*(1), 87–89. https://doi.org/10.1021/ac00049a017

Leonardi, S., Gentilesca, T., Guerrieri, R., Ripullone, F., Magnani, F., Mencuccini, M., et al. (2012). Assessing the effects of nitrogen deposition and climate on carbon isotope discrimination and intrinsic water-use efficiency of angiosperm and conifer trees under rising CO2 conditions. *Global Change Biology*, *18*(9), 2925–2944. https://doi.org/10.1111/j.1365-2486.2012.02757.x

Levesque, M., Andreu-Hayles, L., & Pederson, N. (2017). Water availability drives gas exchange and growth of trees in northeastern US, not elevated CO2 and reduced acid deposition. *Scientific Reports*, *7*(1), 46158. https://doi.org/10.1038/srep46158

Likens, G. E., Driscoll, C. T., & Buso, D. C. (1996). Long-Term Effects of Acid Rain: Response and Recovery of a Forest Ecosystem. *Science*, *272*(5259), 244. https://doi.org/10.1126/science.272.5259.244

Long, R. P., Horsley, S. B., Hallett, R. A., & Bailey, S. W. (2009). Sugar maple growth in relation to nutrition and stress in the northeastern United States. *Ecological Applications*, *19*(6), 1454–1466. https://doi.org/10.1890/08-1535.1

Long, R. P., Horsley, S. B., & Hall, T. J. (2011). Long-term impact of liming on growth and vigor of northern hardwoods. *Canadian Journal of Forest Research*, *41*(6), 1295–1307. https://doi.org/10.1139/x11-049

Lu, X., Vitousek, P. M., Mao, Q., Gilliam, F. S., Luo, Y., Zhou, G., et al. (2018). Plant acclimation to long-term high nitrogen deposition in an N-rich tropical forest. *Proceedings of the National Academy of Sciences*, *115*(20), 5187. https://doi.org/10.1073/pnas.1720777115

Magill, A. H., Aber, J. D., Currie, W. S., Nadelhoffer, K. J., Martin, M. E., McDowell, W. H., et al. (2004). Ecosystem response to 15 years of chronic nitrogen additions at the Harvard Forest LTER, Massachusetts, USA. *The Harvard Forest (USA) Nitrogen Saturation Experiment: Results from the First 15 Years*, *196*(1), 7–28. https://doi.org/10.1016/j.foreco.2004.03.033

Malcomb, J. D., Scanlon, T. M., Epstein, H. E., Druckenbrod, D. L., Vadeboncoeur, M. A., Lanning, M., et al. (2020). Assessing Temperate Forest Growth and Climate Sensitivity in Response to a

Long-Term Whole-Watershed Acidification Experiment. *Journal of Geophysical Research: Biogeosciences*, *125*(7), e2019JG005560. https://doi.org/10.1029/2019JG005560

Marchand, W., Girardin, M. P., Hartmann, H., Depardieu, C., Isabel, N., Gauthier, S., et al. (2020). Strong overestimation of water-use efficiency responses to rising CO2 in tree-ring studies. *Global Change Biology*, *26*(8), 4538–4558. https://doi.org/10.1111/gcb.15166

Mathias, J. M., & Thomas, R. B. (2018). Disentangling the effects of acidic air pollution, atmospheric CO_2, and climate change on recent growth of red spruce trees in the Central Appalachian Mountains. *Global Change Biology*, *24*(9), 3938–3953. https://doi.org/10.1111/gcb.14273

Mathias, J. M., & Thomas, R. B. (2021). Global tree intrinsic water use efficiency is enhanced by increased atmospheric CO_2 and modulated by climate and plant functional types. *Proceedings of the National Academy of Sciences*, *118*(7), e2014286118. https://doi.org/10.1073/pnas.2014286118

Maxwell, J. T., Harley, G. L., Mandra, T. E., Yi, K., Kannenberg, S. A., Au, T. F., et al. (2019). Higher CO2 Concentrations and Lower Acidic Deposition Have Not Changed Drought Response in Tree Growth But Do Influence iWUE in Hardwood Trees in the Midwestern United States. *Journal of Geophysical Research: Biogeosciences*, *124*(12), 3798–3813. https://doi.org/10.1029/2019JG005298

McAinsh, M. R., Brownlee, C., & Hetherington, A. M. (1997). Calcium ions as second messengers in guard cell signal transduction. *Physiologia Plantarum*, *100*(1), 16–29. https://doi.org/10.1111/j.1399-3054.1997.tb03451.x

McCarroll, D., & Loader, N. J. (2004). Stable isotopes in tree rings. *Isotopes in Quaternary Paleoenvironmental Reconstruction*, *23*(7), 771–801. https://doi.org/10.1016/j.quascirev.2003.06.017

McDowell, N. G., Phillips, N., Lunch, C., Bond, B. J., & Ryan, M. G. (2002). An investigation of hydraulic limitation and compensation in large, old Douglas-fir trees. *Tree Physiology*, *22*(11), 763–774. https://doi.org/10.1093/treephys/22.11.763

McLAUGHLIN, S. B., & WIMMER, R. (1999). Tansley Review No. 104. *New Phytologist*, *142*(3), 373–417. https://doi.org/10.1046/j.1469-8137.1999.00420.x

McMahon, S. M., Parker, G. G., & Miller, D. R. (2010). Evidence for a recent increase in forest growth. *Proceedings of the National Academy of Sciences*, 200912376. https://doi.org/10.1073/pnas.0912376107

McNulty, S. G., Boggs, J., Aber, J. D., Rustad, L., & Magill, A. (2005). Red spruce ecosystem level changes following 14 years of chronic N fertilization. *Forest Ecology and Management*, *219*(2), 279–291. https://doi.org/10.1016/j.foreco.2005.09.004

Moore, J.-D., Ouimet, R., & Duchesne, L. (2012). Soil and sugar maple response 15years after dolomitic lime application. *Forest Ecology and Management*, *281*, 130–139. https://doi.org/10.1016/j.foreco.2012.06.026

Norby, R. J., Warren, J. M., Iversen, C. M., Medlyn, B. E., & McMurtrie, R. E. (2010). CO_2 enhancement of forest productivity constrained by limited nitrogen availability. *Proceedings of the National Academy of Sciences*, *107*(45), 19368. https://doi.org/10.1073/pnas.1006463107

Norton, S. A., Fernandez, I. J., Kahl, J. S., Rustad, L. E., Navrátil, T., & Almquist, H. (2010). The evolution of the science of Bear Brook Watershed in Maine, USA. *Environmental Monitoring and Assessment*, *171*(1), 3–21. https://doi.org/10.1007/s10661-010-1528-y

Novick, K. A., Ficklin, D. L., Stoy, P. C., Williams, C. A., Bohrer, G., Oishi, A. C., et al. (2016). The increasing importance of atmospheric demand for ecosystem water and carbon fluxes. *Nature Climate Change*, *6*(11), 1023–1027. https://doi.org/10.1038/nclimate3114

Ollinger, S. V., & Smith, M.-L. (2005). Net Primary Production and Canopy Nitrogen in a Temperate Forest Landscape: An Analysis Using Imaging Spectroscopy, Modeling and Field Data. *Ecosystems*, *8*(7), 760–778. https://doi.org/10.1007/s10021-005-0079-5

Ouimet, R., Duchesne, L., & Moore, J.-D. (2017). Response of northern hardwoods to experimental soil acidification and alkalinisation after 20years. *Forest Ecology and Management*, *400*, 600–606. https://doi.org/10.1016/j.foreco.2017.06.051

Pardo, L. H., Fenn, M. E., Goodale, C. L., Geiser, L. H., Driscoll, C. T., Allen, E. B., et al. (2011). Effects of nitrogen deposition and empirical nitrogen critical loads for ecoregions of the United States. *Ecological Applications*, *21*(8), 3049–3082. https://doi.org/10.1890/10-2341.1

Patel, K. F., & Fernandez, I. J. (2018). Nitrogen mineralization in O horizon soils during 27 years of nitrogen enrichment at the Bear Brook Watershed in Maine, USA. *Environmental Monitoring and Assessment*, *190*(9), 563. https://doi.org/10.1007/s10661-018-6945-3

Patel, K. F., Fernandez, I. J., Nelson, S. J., Gruselle, M.-C., Norton, S. A., & Weiskittel, A. R. (2019). Forest N Dynamics after 25 years of Whole Watershed N Enrichment: The Bear Brook Watershed in Maine. *Soil Science Society of America Journal*, *83*(S1), S161–S174. https://doi.org/10.2136/sssaj2018.09.0348

Patel, K. F., Fernandez, I. J., Nelson, S. J., Malcomb, J., & Norton, S. A. (2020). Contrasting stream nitrate and sulfate response to recovery from experimental watershed acidification. *Biogeochemistry*, *151*(2), 127–138. https://doi.org/10.1007/s10533-020-00711-5

Peart, D. R., Cogbill, C. V., & Palmiotto, P. A. (1992). Effects of Logging History and Hurricane Damage on Canopy Structure in a Northern Hardwoods Forest. *Bulletin of the Torrey Botanical Club*, *119*(1), 29–38. https://doi.org/10.2307/2996917

Pederson, N., Bell, A. R., Cook, E. R., Lall, U., Devineni, N., Seager, R., et al. (2013). Is an Epic Pluvial Masking the Water Insecurity of the Greater New York City Region?,. *Journal of Climate*, *26*(4), 1339–1354. https://doi.org/10.1175/JCLI-D-11-00723.1

Peñuelas, J., Canadell, J. G., & Ogaya, R. (2011). Increased water-use efficiency during the 20th century did not translate into enhanced tree growth. *Global Ecology and Biogeography*, *20*(4), 597–608. https://doi.org/10.1111/j.1466-8238.2010.00608.x

Peters, S. C., Blum, J. D., Driscoll, C. T., & Likens, G. E. (2004). Dissolution of wollastonite during the experimental manipulation of Hubbard Brook Watershed 1. *Biogeochemistry*, *67*(3), 309–329. https://doi.org/10.1023/B:BIOG.0000015787.44175.3f

Qian, C., & Zhou, T. (2014). Multidecadal Variability of North China Aridity and Its Relationship to PDO during 1900?2010. *Journal of Climate*, *27*(3), 1210–1222. https://doi.org/10.1175/JCLI-D-13-00235.1

Rayback, S. A., Belmecheri, S., Gagen, M. H., Lini, A., Gregory, R., & Jenkins, C. (2020). North American temperate conifer (Tsuga canadensis) reveals a complex physiological response to climatic and anthropogenic stressors. *New Phytologist*, *228*(6), 1781–1795. https://doi.org/10.1111/nph.16811

Rinne, K. T., Loader, N. J., Switsur, V. R., Treydte, K. S., & Waterhouse, J. S. (2010). Investigating the influence of sulphur dioxide (SO2) on the stable isotope ratios (δ13C and δ18O) of tree rings. *Geochimica et Cosmochimica Acta*, *74*(8), 2327–2339. https://doi.org/10.1016/j.gca.2010.01.021

Royo, A. A., & Knight, K. S. (2012). White ash (Fraxinus americana) decline and mortality: The role of site nutrition and stress history. *Forest Ecology and Management*, *286*, 8–15. https://doi.org/10.1016/j.foreco.2012.08.049

Saurer, M., Spahni, R., Frank, D. C., Joos, F., Leuenberger, M., Loader, N. J., et al. (2014). Spatial variability and temporal trends in water-use efficiency of European forests. *Global Change Biology*, *20*(12), 3700–3712. https://doi.org/10.1111/gcb.12717

Savard, M. M. (2010). Tree-ring stable isotopes and historical perspectives on pollution – An overview. *Advances of Air Pollution Science: From Forest Decline to Multiple-Stress Effects on Forest Ecosystem Services*, *158*(6), 2007–2013. https://doi.org/10.1016/j.envpol.2009.11.031

Savard, M. M., Bégin, C., & Marion, J. (2020). Response strategies of boreal spruce trees to anthropogenic changes in air quality and rising pCO2. *Environmental Pollution*, *261*, 114209. https://doi.org/10.1016/j.envpol.2020.114209

Sayre, R. G., & Fahey, T. J. (1999). Effects of rainfall acidity and ozone on foliar leaching in red spruce (Picea rubens). *Canadian Journal of Forest Research*, *29*(4), 487–496. https://doi.org/10.1139/x99-002

Scheidegger, Y., Saurer, M., Bahn, M., & Siegwolf, R. (2000). Linking stable oxygen and carbon isotopes with stomatal conductance and photosynthetic capacity: a conceptual model. *Oecologia*, *125*(3), 350–357. https://doi.org/10.1007/s004420000466

Schleser, G. H., & Jayasekera, R. (1985). δ13C-variations of leaves in forests as an indication of reassimilated CO2 from the soil. *Oecologia*, *65*(4), 536–542. https://doi.org/10.1007/BF00379669

Schlesinger, W. H., & Jasechko, S. (2014). Transpiration in the global water cycle. *Agricultural and Forest Meteorology*, *189–190*, 115–117. https://doi.org/10.1016/j.agrformet.2014.01.011

van der Sleen, P., Groenendijk, P., Vlam, M., Anten, N. P. R., Boom, A., Bongers, F., et al. (2015). No growth stimulation of tropical trees by 150 years of CO2 fertilization but water-use efficiency increased. *Nature Geoscience*, *8*(1), 24–28. https://doi.org/10.1038/ngeo2313

Smith, K. T., & Shortle, W. C. (2013). Calcium amendment may increase hydraulic efficiency and forest evapotranspiration. *Proceedings of the National Academy of Sciences*, *110*(40), E3739. https://doi.org/10.1073/pnas.1311453110

Speer, J. H. (2012). *Fundamentals of Tree Ring Research*. Tuscon, AZ: University of Arizona Press.

ST Clair, S. B., & Lynch, J. P. (2005). Differences in the success of sugar maple and red maple seedlings on acid soils are influenced by nutrient dynamics and light environment. *Plant, Cell & Environment*, *28*(7), 874–885. https://doi.org/10.1111/j.1365-3040.2005.01337.x

Sullivan, T. J., Driscoll, C. T., Beier, C. M., Burtraw, D., Fernandez, I. J., Galloway, J. N., et al. (2018). Air pollution success stories in the United States: The value of long-term observations. *Environmental Science & Policy*, *84*, 69–73. https://doi.org/10.1016/j.envsci.2018.02.016

Thomas, Q. R., Canham, C. D., Weathers, K. C., & Goodale, C. L. (2010). Increased tree carbon storage in response to nitrogen deposition in the US. *Nature Geoscience*, *3*(1), 13–17. https://doi.org/10.1038/ngeo721

Vadeboncoeur, M. A. (2010). Meta-analysis of fertilization experiments indicates multiple limiting nutrients in northeastern deciduous forests. *Canadian Journal of Forest Research*, *40*(9), 1766–1780. https://doi.org/10.1139/X10-127

Vadeboncoeur, M. A., Green, M. B., Asbjornsen, H., Campbell, J. L., Adams, M. B., Boyer, E. W., et al. (2018). Systematic variation in evapotranspiration trends and drivers across the Northeastern United States. *Hydrological Processes*, *32*(23), 3547–3560. https://doi.org/10.1002/hyp.13278

Vadeboncoeur, M. A., Jennings, K. A., Ouimette, A. P., & Asbjornsen, H. (2020). Correcting tree-ring δ13C time series for tree-size effects in eight temperate tree species. *Tree Physiology*, *40*(3), 333–349. https://doi.org/10.1093/treephys/tpz138

Wason, J. W., Beier, C. M., Battles, J. J., & Dovciak, M. (2019). Acidic Deposition and Climate Warming as Drivers of Tree Growth in High-Elevation Spruce-Fir Forests of the Northeastern US. *Frontiers in Forests and Global Change*, *2*, 63. https://doi.org/10.3389/ffgc.2019.00063

Yi, K., Maxwell, J. T., Wenzel, M. K., Roman, D. T., Sauer, P. E., Phillips, R. P., & Novick, K. A. (2019). Linking variation in intrinsic water-use efficiency to isohydricity: a comparison at multiple spatiotemporal scales. *New Phytologist*, *221*(1), 195–208. https://doi.org/10.1111/nph.15384

Zhang, Q., Ficklin, D. L., Manzoni, S., Wang, L., Way, D., Phillips, R. P., & Novick, K. A. (2019). Response of ecosystem intrinsic water use efficiency and gross primary productivity to rising vapor pressure deficit. *Environmental Research Letters*, *14*(7), 074023. https://doi.org/10.1088/1748-9326/ab2603

Chapter 4 Supplement

Supplementary materials for Chapter 4 include correlations between BAI and iWUE for species sampled at Hubbard Brook (Figure S4.1). Total (wet + dry) N and S deposition data for all three sites (Figure S4.2), and iWUE chronologies of tree species sampled in WS 10 at Fernow, demonstrating negative trends in iWUE in mature trees at this site (Figure S4.3).

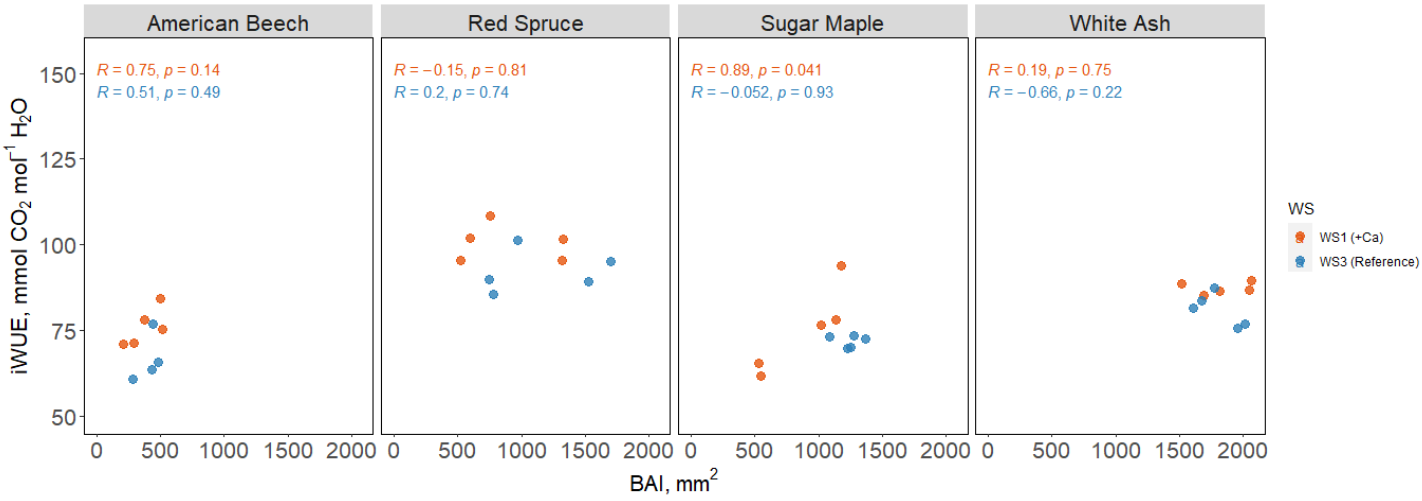

Figure S4.1. Correlation between BAI and iWUE for focal species at HBEF. BAI was averaged over the same five-year intervals as the iWUE chronologies between 1990-2015. R values represent Pearson correlation coefficients.

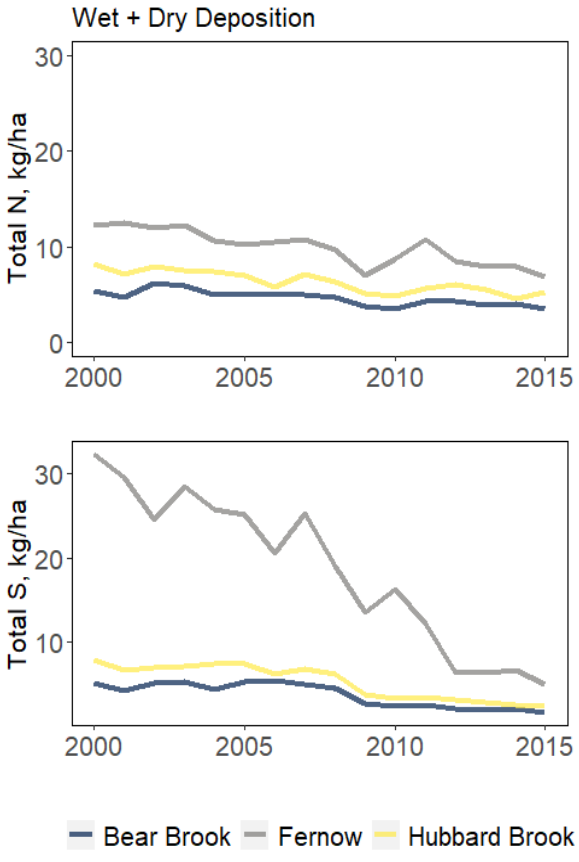

Figure S4.2. CASTNET total (wet + dry) deposition of N and S at monitoring sites nearest to the study watersheds. Monitoring sites at FEF and HBEF are <5km from study watersheds, while data for BBWM come from the Howland CASTNET site, approximately 60km northwest of BBWM.

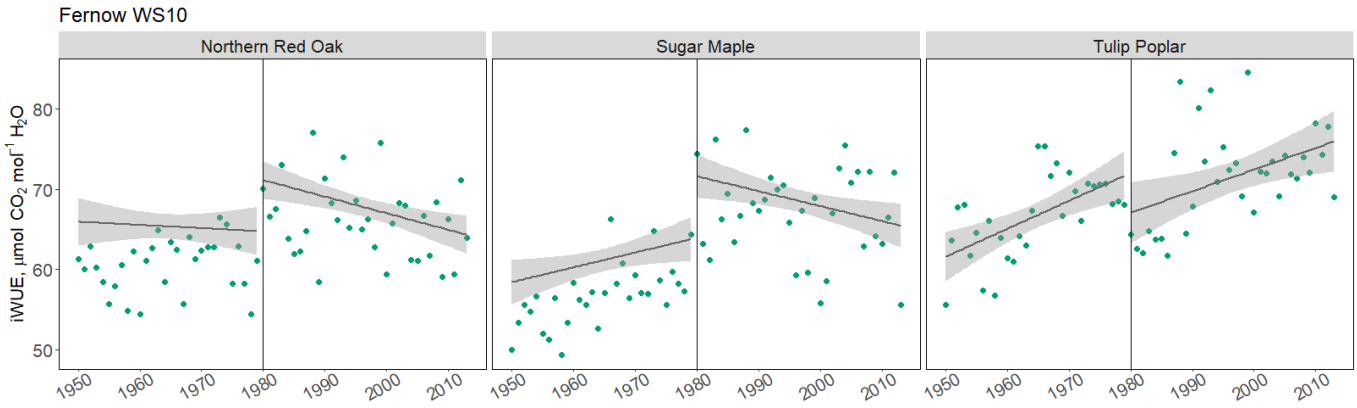

Figure S4.3. Annual-resolution iWUE chronologies derived from tree rings in a separate field campaign using similar methodology in Fernow Watershed 10, an older stand than Watersheds 3 and 7 which was established in the early 1900s (Vadeboncoeur, unpublished). Separate trendlines are modeled for pre and post-1980, to correspond with post-1980 data from Watersheds 3 and 7. Significant negative trends are observed in northern red oak (slope= -0.21, R^2=0.13, P=0.001) and sugar maple (slope= -0.19, R^2=0.08, P=0.01) in the post-1980 time period.

Chapter 5. Assessing trends in, and drivers of, tree intrinsic water use efficiency in midlatitude temperate forests

Prepared for submission to *Environmental Research Letters*

Abstract

Both theory and observational evidence suggest that tree intrinsic water use efficiency (iWUE) – the ratio of photosynthetic carbon assimilation to stomatal conductance to water – increases with atmospheric CO_2. However, the strength of this relationship varies widely across sites and species, prompting inquiry about alternate ecophysiological and environmental controls on iWUE. In this study I examined trends in, and drivers of, tree intrinsic water use efficiency of 12 tree species (eight broadleaf deciduous and four needleleaf evergreen) common to the midlatitude temperate forests of eastern North America, where trees have experienced changes in CO_2, climate and atmospheric pollution in recent decades. Across all site-species combinations, I found that both tree iWUE and atmospheric CO_2 increased ~27% between 1950-2014, but there were markedly different iWUE patterns among species with different functional traits, and within species across sites. iWUE of needleleaf evergreen species increased rapidly between 1950-1990 before plateauing, while iWUE of broadleaf deciduous species increased linearly throughout the study period. Analysis of environmental controls on the magnitude of iWUE trends revealed smaller increases in iWUE in trees subjected to higher nitrogen and sulfur deposition loads, even after controlling for the effects of species. Our results highlight the importance of considering tree functional traits and atmospheric pollution in model projections of terrestrial carbon and hydrologic cycles.

5.1 Introduction

In terrestrial plants, photosynthetic carbon uptake is inextricably linked to loss of water via transpiration. The tradeoff between carbon gained and water lost is commonly expressed as intrinsic water use efficiency (iWUE), the ratio of photosynthetic carbon assimilation (*A*) to stomatal conductance to water (g_s). Increases in iWUE as atmospheric CO_2 (C_a) concentrations rise are predicted by theory (Medlyn et al., 2011), and have been observed in both CO_2 enrichment experiments (Ainsworth & Rodgers, 2007) and in studies that utilize tree ring carbon isotope ratios to derive iWUE over decadal to centennial time scales (Frank et al., 2015; Guerrieri et al., 2019; Saurer et al., 2014; van der Sleen et al., 2015). However, other recent evidence suggests that the effects of C_a on iWUE have weakened in recent decades (Adams et al., 2021, Belmecheri et al., 2020). Changes in iWUE may have wide-ranging consequences for vegetation-climate feedbacks from ecosystem to global scales, including tree sensitivity to climate stressors (Heilman et al., 2021), atmospheric water vapor concentrations (Richardson et al., 2018; Swann et al., 2016), and water yields from forested catchments (Betts et al., 2007; Kooperman et al., 2018). Thus, accurately predicting how environmental changes affect tree stomatal behavior is essential to projecting future changes in terrestrial carbon, water, and energy cycles.

While there is strong evidence for CO_2-driven enhancement of iWUE in terrestrial plants (Walker et al., 2020), increases in C_a have occurred alongside changes in other environmental variables, including climate (Mathias & Thomas, 2021, Rayback et al., 2020) and atmospheric pollution (Savard et al., 2010; Holmes, 2014, Thomas, 2013), that can modulate tree response to changes in C_a. Wet conditions tend to dampen iWUE response to elevated C_a (Belmecheri et al., 2021; Levesque et al., 2017), while iWUE tends to increase in trees experiencing increasing

aridity (Kannenberg et al., 2021; Zhang et al. 2019). These effects of climate on iWUE are consistent with stomatal optimization theory, which suggests that plants optimize stomatal behavior to maximize carbon gain while minimizing water loss (Cowan et al., 1982). When trees are not stressed by water supply or atmospheric demand, the water cost of C acquisition is minimized, as is the benefit of downregulating g_s.

Effects of air pollution – including deposition of nitrogen (N), sulfur (S), and ozone – on iWUE remain less clear, as these pollutants both directly impact leaf physiology and indirectly impact trees via deposition-driven changes in soil nutrients. Either mechanism may independently alter A and g_s. Leaf exposure to N and S deposition may enhance iWUE by inducing stomatal closure, resulting in proportionally larger reductions in g_s than A (Bukata & Kyser, 2007; Savard et al., 2020; Thomas et al., 2013). In N-limited temperate forest ecosystems, N deposition may increase iWUE by enhancing A without a proportional or greater increase in g_s (Brooks & Mitchell, 2011; Jennings et al., 2016; Gahrun et al., 2021). On the other hand, chronic N and S deposition can drive soil acidification and base cation leaching (Driscoll et al., 2001), leading to plant nutrient deficiencies that impair A (St. Clair & Lynch, 2005). Deposition-driven soil nutrient imbalances may result in declining iWUE when phosphorous (P) and/or base cations limit A (Huang et al., 2016), or when plants upregulate g_s to maintain sufficient mass flow of nutrients from the soil solution (Lu et al., 2018). While effects of N and S deposition on iWUE may be context-dependent, ozone is negatively associated with iWUE. Ozone causes oxidative stress that reduces A (Wittig et al., 2009) and may also impair stomatal function, leading to increases in g_s (McLaughlin et al., 2007). In the United States, declines in atmospheric ozone have been linked to increases in forest iWUE in recent decades (Holmes et al., 2014).

In addition to climate and atmospheric pollution, tree iWUE response to increasing C_a also differs among species with different leaf morphologies and hydraulic traits. iWUE of conifer species tends to be higher than that of broadleaf deciduous species (Frank et al., 2015; Guerrieri et al., 2019), and more sensitive to increasing C_a (Soh et al., 2019). These effects may be explained by lower mesophyll conductance in conifers, which makes them more sensitive to changes in C_a (Niinemets et al., 2011), or by the isohydric stomatal behavior typical of many conifer species, which causes them to close their stomata and maintain low rates of g_s as drought conditions develop (Brodribb et al., 2014). Among broadleaf deciduous species, iWUE of species that tend to exhibit isohydric stomatal behavior is more sensitive to environmental changes than that of anisohydric species, which regulate g_s more loosely under drought stress at greater risk of hydraulic failure (Yi et al., 2019). Xylem anatomy, which is closely related to stomatal behavior (Klein 2014), also plays a key role in regulating transpiration. Understanding how these tree structural and functional characteristics interact with environmental variables to determine iWUE is key to predicting how forests will respond to environmental change.

In this study, I examined trends in, and drivers of, tree iWUE in eight broadleaf deciduous species and four needleleaf evergreen species in the temperate mixed deciduous forests of the eastern Unites States, where trees have experienced concurrent changes in C_a, climate, and atmospheric pollution in recent decades. iWUE chronologies were developed from tree ring carbon isotope ($\delta^{13}C$) signatures. I compared trends in iWUE across species with diverse hydraulic characteristics, and environmental controls on the magnitude of iWUE trends across sites spanning climate and atmospheric pollution gradients. This work builds upon a growing body of research examining climate and atmospheric pollution as controls on iWUE in temperate forests (Gharun et al., 2021; Levesque et al., 2017; Mathias & Thomas, 2018;

Maxwell et al., 2019; Rayback et al., 2020), but incorporates a wider range of species and environmental gradients than have been examined previously. These analyses offer unique insights into controls on temperate forest iWUE, and may improve our ability to model forest carbon and water balance in response to future anthropogenic change.

5.2 Methods

5.2.1 Sampling Sites

Tree cores were collected from 1-4 species within 12 forested watershed sites in the eastern United States (Figure 5.1, Table 5.1). Sites were selected based on the availability of long-term hydrologic records and ancillary forest composition, climate, and biogeochemical data. Sites also span gradients of climate and atmospheric deposition: mean June-August temperature ranged from 16.5°C at Biscuit Brook, the coolest site, to 22.5°C at Paine Run, the warmest site. Mean June-August precipitation ranged from 271 mm at Bear Brook, the driest site, to 428 mm at Fernow WS10, the wettest site. Watersheds at the Fernow Experimental Forest received the highest rates of atmospheric deposition (28.1 kg N+S ha^{-1} $year^{-1}$), while Bear Brook East received the lowest levels of annual atmospheric deposition (9.5 kg N+S ha^{-1} $year^{-1}$) between 2000 and 2015 (Table 5.1). Mean June-August ozone concentrations were highest (0.059 ppm) at the three Shenandoah National Park Sites (Paine Run, Piney River, and Staunton River) and lowest at Cone Pond and Hubbard Brook (0.035 ppm).

5.2.2 Climate, Deposition, and Ozone Data

Precipitation and temperature data were acquired from on-site meteorological stations at the Fernow Experimental Forest and Hubbard Brook Experimental Forest. For all other sites, precipitation and temperature data were acquired from PRISM (Di Luzio et al., 2008). Daily

maximum vapor pressure deficit (VPD_{max}) data were also acquired from PRISM for all sites. Growing season (June-August) total precipitation and mean temperature and VPD_{max} were calculated annually for each site from 1980-2014. N and S deposition data were acquired from the National Atmospheric Deposition Program's Total Deposition (Tdep) product (Schwede & Lear, 2014), which combines wet deposition data from the National Trends Network (NTN) and dry deposition data from the Clean Air Status and Trends Network (CASTNET) to generate an estimate of total (wet + dry) deposition for the continental United States. Tdep raster data were clipped to watershed boundaries and watershed-scale estimates were calculated annually from 2000-2015. Deposition data were processed on an annual basis, since deposition may have direct effects on foliar health and stomatal function (Sayre & Fahey, 1999), and indirect, cumulative effects on soil nutrients (Driscoll et al., 2001). Thus, deposition received outside of the growing season would still influence vegetation physiology. Exceedance of N and S deposition critical loads for forest soil acidification was calculated as the difference between total N and S deposition (2000-2015) and critical load values for each site (McNulty et al., 2007). Since critical load exceedance primarily reflects impacts of deposition on soils, this variable was selected in order to assess whether deposition effects were primarily related to direct or indirect impacts of deposition. Ozone data were acquired from the EPA Air Quality System (https://www.epa.gov/aqs) from the nearest monitoring station to each site that had at least 10 years of ozone data (Table S5.1). Growing season (June-August) ozone concentrations were calculated annually for each site between 1993-2011, the common period across all ozone monitoring sites. These methods assume that relative differences in climate and air pollution among sites are consistent through time, even though predictors of iWUE trends are calculated over different time periods.

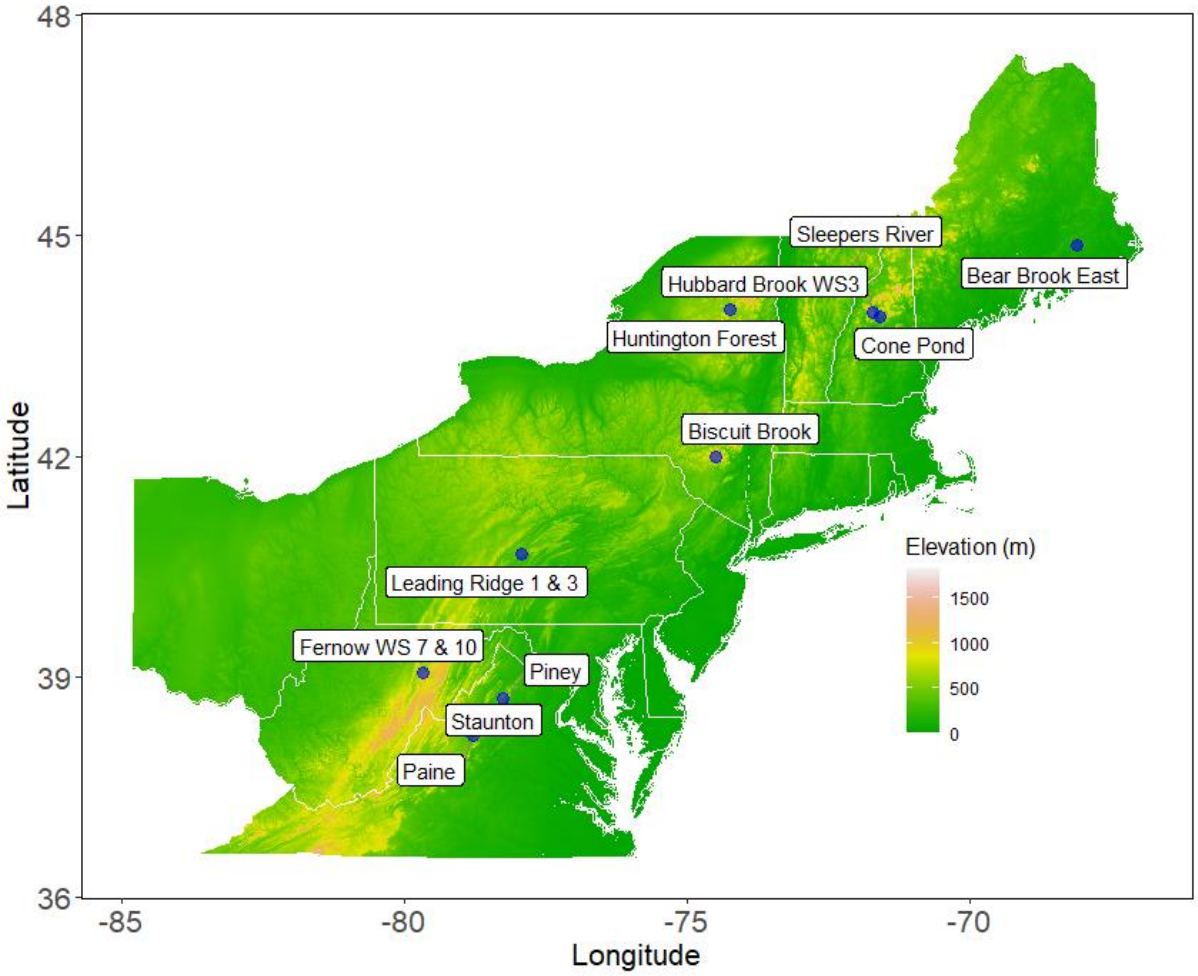

Figure 5.1 Trees sampling sites in the eastern United States. Tree cores used to derive tree ring $\delta^{13}C$ chronologies were collected from 2-4 species at each site for a total of 37 unique site-species combinations. Details about species sampled at each site, and the number of trees in each iWUE chronology, can be found in Table 5.1 and Table S5.1. Site codes: Bear Brook East (BBE), Biscuit Brook (BSB), Cone Pond (CP), Fernow Watershed 7 (FEF7), Fernow Watershed 10 (FEF10), Hubbard Brook Watershed 3 (HB3), Huntington Forest (HWF), Leading Ridge WS 1 (LR1), Leading Ridge WS3 (LR3), Paine Run (PAINE), Piney River (PINEY), Sleepers River Watershed 9 (SR9), Staunton River (STAUN).

Table 5.1 Mean climate and atmospheric pollution values for each site where trees were sampled.

Site	Site Code	Lon	Lat	$Precip_{JJA}$ (mm)	$Tmean_{JJA}$ (°C)	VPD_{JJA} (hPa)	$Ozone_{JJA}$ (ppm)	Total N (kg ha^{-1})	Total S (kg ha^{-1})	N+S Exc. (kg ha^{-1})
Bear Brook East	BBE	-68.107	44.861	271	18.0	16.0	0.039	4.7	4.8	-2.5
Biscuit Brook	BSB	-74.501	41.995	411	16.5	12.7	0.047	11.9	12.1	9.0
Cone Pond	CP	-71.606	43.904	349	17.8	16.2	0.035	6.0	5.3	-1.1
Fernow WS7	FEF7	-79.680	39.055	423	20.0	15.8	0.051	9.6	18.6	9.7
Fernow WS 10	FEF10	-79.680	39.055	428	18.6	15.8	0.051	9.5	18.6	8.0
Hubbard Brook W3	HB3	-71.723	43.954	385	17.0	15.0	0.035	6.0	5.3	4.0
Huntington Forest	HWF	-74.245	43.993	292	16.8	14.2	0.043	6.2	5.9	1.9
Leading Ridge 1	LR1	-77.944	40.666	273	21.0	18.4	0.054	11.1	16.1	11.8
Leading Ridge 3	LR3	-77.944	40.666	273	20.7	18.4	0.054	11.1	16.1	9.9
Paine Run	PAINE	-78.793	38.199	358	22.5	17.7	0.059	10.8	7.6	3.6
Piney River	PINEY	-78.268	38.703	381	21.7	17.6	0.059	11.3	8.5	4.1
Sleeper's River W9	SR9	-72.164	44.490	392	16.7	14.9	0.041	6.1	4.9	-0.6
Staunton River	STAUN	-78.373	38.445	372	21.3	18.4	0.059	11.3	8.7	5.9

Notes: $Precip_{JJA}$, $Tmean_{JJA}$, and VPD_{JJA} represent the temporal mean of June-August precipitation, temperature, and maximum VPD calculated from 1980-2014. $Ozone_{JJA}$ represents mean June-August ozone concentrations from 1993-2011, the common measurement period among all sites. Total N and total S are the mean of total annual (wet + dry) deposition from 2000-2015, the time period over which total deposition data is available nationwide. N+S Exc represents the mean annual exceedance of N+S critical loads for soil acidification from 2000-2015.

5.2.3 Tree Sampling and Isotopic Methods

In each watershed, two tree cores were collected from 15-20 trees of each focal species. Further information about each chronology can be found in Table S5.2. Increment borers were cleaned with isopropyl alcohol before coring each tree to prevent sample cross-contamination. Tree cores were air-dried, hand-sanded, cross-dated, and measured using standard dendrochronological procedures (Speer, 2012), but not mounted with glue to avoid isotopic contamination. Cross dating was statistically validated using COFECHA (Holmes, 1983).

A subset of 5-8 trees for each site-species combination were selected for carbon isotope analysis based on the absence of cross-dating flags in COFECHA, and the correlation of chronologies with the master series. Isotope cores were hand-sliced and shredded using razor blades. To maintain a manageable number of isotope samples (but still enough to assess temporal patterns), isotope chronologies were processed in different ways, depending on the site and facility where samples were analyzed. Samples from FEF10, LR1 and LR3, BSB, HWF, SR9, CP, and HB3 were combined and processed together as annual composite samples beginning in 1950 (or 1960 in the case of SR9). Samples from PAINE, PINEY, and STAUN were processed as individual cores in 5-year increments beginning in 1951, while samples from FEF7 and BBE were processed as individual cores in 5-year increments beginning in 1979 and 1981, respectively. For the site-species combinations where multiple individual $\delta^{13}C$ chronologies were developed per watershed, a watershed mean chronology was calculated and used in subsequent analyses. All annual composite samples, and samples from BBE, were extracted for α-cellulose according to methods described by Leavitt and Danzer (1993), and were analyzed for $\delta^{13}C$ on an Isoprime IRMS at the University of New Hampshire (UNH) Instrumentation Center. For samples from FEF7, PAINE, PINEY, and STAUN, α-cellulose was extracted using the Brendel

method (Brendel et al., 2000) and analyzed for $\delta^{13}C$ at Indiana University-Purdue University Indianapolis (IUPUI) on a Costech elemental analyzer coupled with Delta V IRMS. Reference cellulose was included in each analytic batch to ensure data consistency between the two facilities. After comparing $\delta^{13}C$ values for reference wood from which cellulose was extracted and analyzed at each lab, IUPUI $\delta^{13}C$ samples were adjusted by -0.9 ‰ to correct for bias caused by the different extraction methods between the two labs.

5.2.4 Calculation of tree iWUE

Tree iWUE was calculated from the $\delta^{13}C$ composition of tree ring cellulose ($\delta^{13}C_p$) using the equation linking carbon isotope discrimination ($\Delta^{13}C_p$) to the ratio of leaf intercellular to atmospheric CO_2 concentrations (C_i/C_a; Farqhuar et al., 1989):

$$\Delta^{13} C_p = a + (b - a)\ \frac{C_i}{C_a} = \frac{(\delta^{13} C_a - \delta^{13} C_p - d)}{(1 + \frac{\delta^{13} C_{p-d}}{1000})} \text{ (Eq. 1)}$$

where *a* is diffusion fractionation (~4‰), *b* is carboxylation fractionation (~27‰), and *d* is the post-photosynthetic fractionation correction factor (2.1 ± 1.2 ‰; Gessler et al., 2014; Lavergne et al., 2019). We used C_a and $\delta^{13}C_a$ time series from Belmecheri and Lavergne (2020). Eq. 1 was rearranged to solve for C_i, and iWUE was thus calculated using the equation:

$$iWUE = \frac{A}{g_s} = \frac{C_a - C_i}{1.6} = \frac{C_a}{1.6}\left(\frac{b - \Delta^{13} C_p}{b - a}\right) \text{ (Eq. 2)}$$

While this model does not account for fractionation during dark respiration or mesophyll conductance, it is considered sufficient for relative estimates of C_i and iWUE (Cernusak et al., 2013).

5.2.5 Data Analyses

Both means and trends in tree iWUE were compared among species of different leaf functional types (broadleaf deciduous or needleleaf evergreen), xylem anatomies (diffuse porous, ring porous, or tracheid; Elliott et al., 2017), and general tendencies of stomatal behavior (isohydric or anisohydric; Roman et al., 2015). Linear regression was used to compare trends in iWUE, using standardized chronologies for each site-species combination, and piecewise regression using the R package *segmented* was used to detect breakpoints in iWUE chronologies. Slopes of iWUE trends were compared among tree functional characteristics both before and after the 1990 breakpoint using the *emmeans* R package (Lenth, 2017).

In order to assess environmental controls on the magnitude of iWUE trends across sites, I first calculated the 5-year iWUE mean for each chronology (so that site-species combinations with annual and 5-year data were treated equivalently). Then I calculated Thiel-Sen's slopes to estimate the temporal trend for each site-species combination between ~1980-2014, the common period across all chronologies (the exact number of years in each chronology is listed in Table S5.1). This period was selected for several reasons: (1) to assess the influence of more recent environmental changes on iWUE; (2) to maximize the number of isotope chronologies eligible for analysis, since chronologies at BBE and FEF7 began in ~1980; and (3) to minimize tree age, size, and/or canopy position effects on carbon isotope discrimination (Brienen et al., 2017, Vadeboncoeur et al., 2021) that are more likely to be present earlier in tree development. Pearson's correlation analyses were conducted to examine pairwise relationships between Thiel-Sen's slopes for each site-species iWUE chronology and the temporal means of environmental drivers at each site, and also correlations between the environmental drivers themselves. Because most needleleaf evergreen species exhibited weak temporal trends in iWUE, I also calculated the

linear relationship between iWUE trends in broadleaf deciduous species and mean annual N+S deposition loads using linear regression.

Results of correlation analyses were used to inform variable selection in linear mixed effects models used to identify environmental controls on the magnitude of iWUE trends across sites. Linear mixed effects models were fit using the R package *nlme* (Pinheiro et al., 2017), with iWUE slope (1980-2014) as the dependent variable and species as a random effect. Three models were assessed: a model including climate (mean growing season precipitation and VPD_{max}) and air pollution variables (total N+S deposition and ozone), a model with only climate variables, and a model with only air pollution variables. Predictor variables were standardized prior to analyses in order to enable direct comparison of effect sizes. Multicollinearity among predictors was assessed by calculating the variance inflation factor (VIF) using the vif() function in the *car* package (Fox & Weisberg, 2019). Fit and parsimony of models were assessed using corrected Akaike Information Criterion (AICc) and marginal and conditional R^2 values, both calculated using the R package *MuMIn* (Bartoń, 2017).

5.3 Results

5.3.1 iWUE values and temporal trends by tree functional traits

When all site-species combinations were considered between 1950-2014, iWUE increased 27.1%, coinciding with a 27.6% increase in C_a over the same time period (Figure 5.2). Mean iWUE of needleleaf evergreen species was higher than that of broadleaf deciduous species over the entire study period (Figure 5.2). Temporal patterns differed markedly between needleleaf evergreen and broadleaf deciduous species – piecewise regression revealed a breakpoint in needleleaf evergreen iWUE around 1990 (pre-breakpoint standardized slope=0.06

± 0.007, R^2=0.68, p<0.0001; post-breakpoint standardized slope=-0.009±0.02, R^2=-0.003, p>0.05), while the slope of broadleaf deciduous iWUE did not change during the study period (standardized slope=0.034 ±0.0025, R^2=0.39, p<0.0001; Figure 5.3). Notably, evergreen iWUE increased ~50% faster than broadleaf deciduous iWUE prior to 1990 (p<0.0001), but that pattern reversed in more recent decades, with no trend in evergreen iWUE but a continued increase in iWUE of broadleaf deciduous species (Figure 5.3; Figure 5.4A).

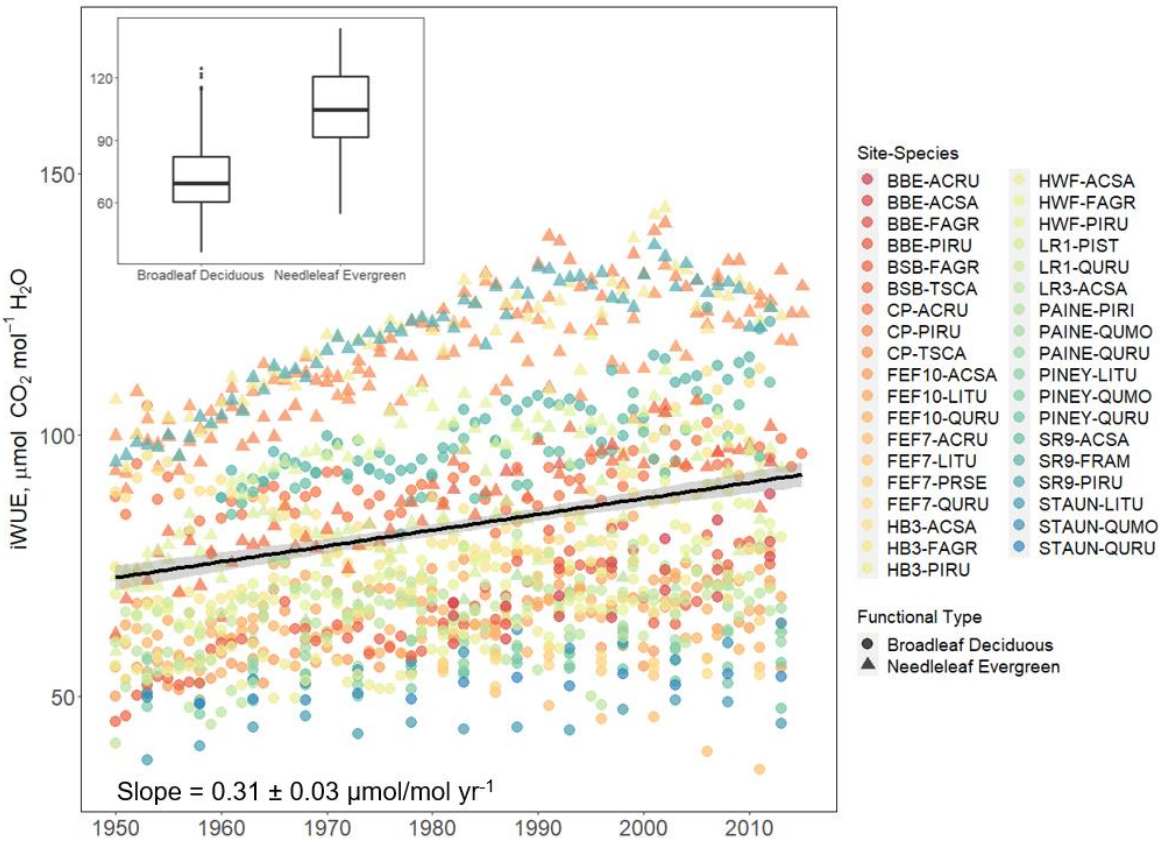

Figure 5.2 iWUE chronologies for all site-species combinations between 1950 and 2014. Fitted line represents the linear trend in iWUE over this time period (R^2=0.06, p<0.0001). Triangles represent values for needleleaf evergreen species while circular points represent values for broadleaf deciduous. Boxplots in the inset represent distributions of iWUE in broadleaf deciduous and needleleaf evergreen iWUE. Full site and species codes can be found in the supplemental materials.

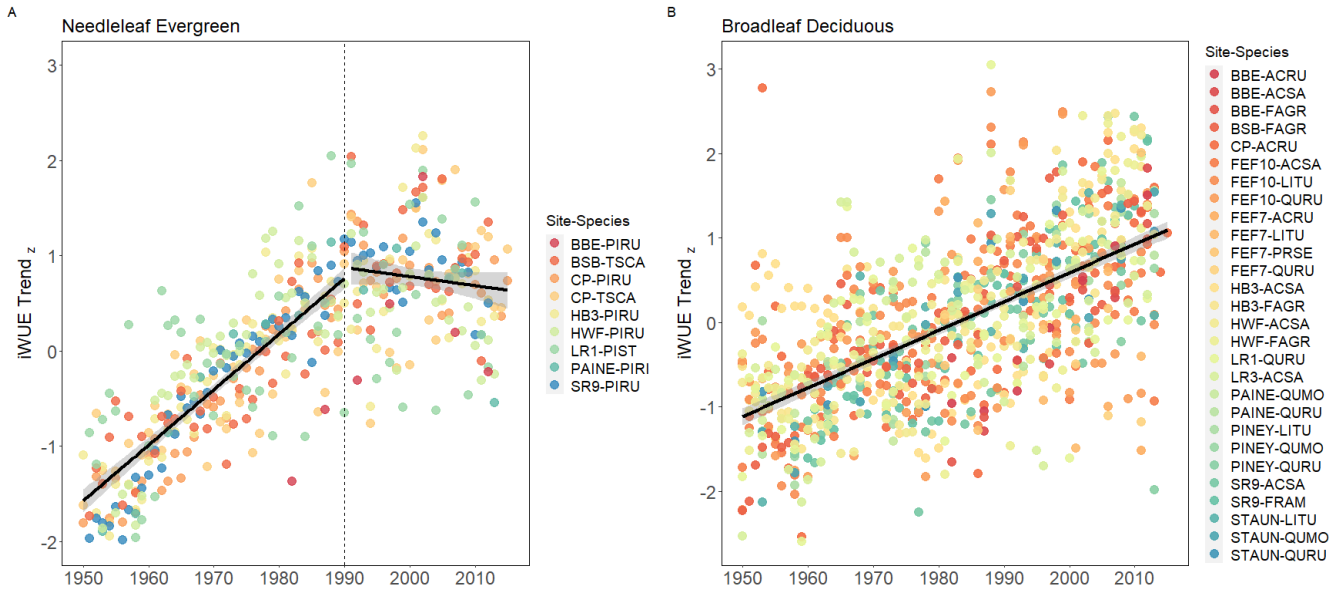

Figure 5.3 Trends in standardized iWUE chronologies of evergreen needleleaf species (A) and broadleaf deciduous species (B). The dashed line in panel A represents the breakpoint in needleleaf evergreen iWUE, where a significant shift in the slope of the iWUE trend occurred in 1990. Solid lines represent temporal trends for each leaf functional and were calculated separately before and after the breakpoint for needleleaf evergreen species.

We observed differences in iWUE trends based on xylem anatomy –iWUE increased faster in species with tracheid xylem (needleleaf evergreen species) prior to 1990, but after that, iWUE of diffuse porous species increased faster than both tracheid and ring porous species (Figure 5.4B). When considering only broadleaf deciduous species, iWUE increased faster in anisohydric species prior to 1990, but iWUE increased faster in isohydric species thereafter (Figure 5.4C). When considering only broadleaf deciduous trees over the entire study period, there was no difference in iWUE trends between diffuse porous and ring porous species, or between isohydric and anisohydric species (Figure S5.1).

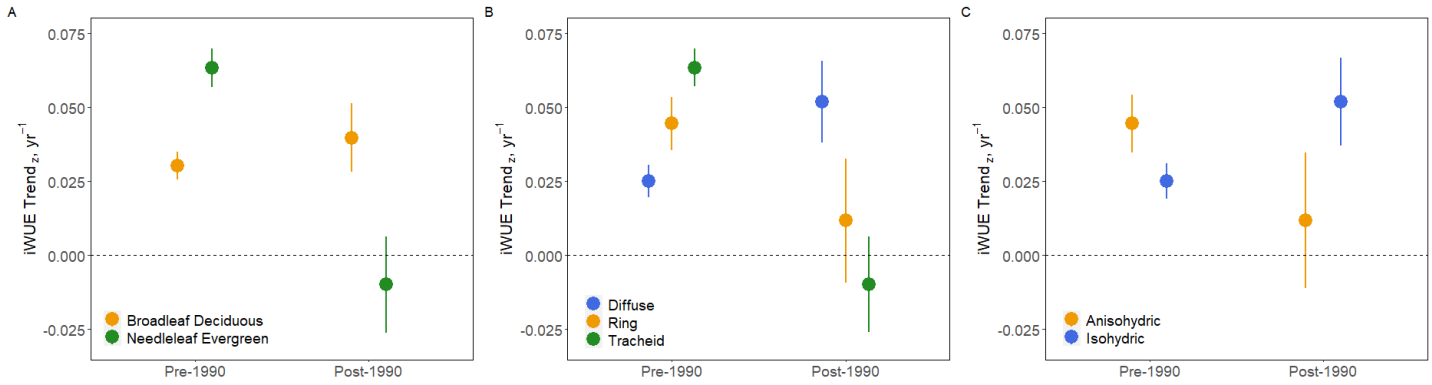

Figure 5.4 Standardized trends and their 95% confidence intervals for trees of different leaf types (A), xylem anatomies (B), and stomatal behaviors (C) prior to, and after, the 1990 iWUE breakpoint for evergreen species. Figure C only includes broadleaf deciduous species, so that trend estimates are not biased by the nonlinear behavior of needleleaf evergreens, which tend to be isohydric.

5.3.2 Relationships between iWUE trends and environmental drivers

Across sites, deposition of N, S, ozone, and N+S critical loads exceedance covaried spatially, with generally higher levels of atmospheric pollution at sites in the mid-Atlantic than in the northeastern United States (Figure 5.5). This co-occurrence is consistent with the fact that oxidized nitrogen and sulfur deposition often arise from the same pollution sources (Sullivan et al., 2018), and oxidized nitrogen is a key atmospheric precursor of ozone (Placet et al., 2000). We also found significant negative correlations between the slope of iWUE trends and temperature (r=-0.36), atmospheric ozone (r=-0.53), total N and S deposition (r=-0.56), and exceedance of N and S critical loads (r=-0.43) for forest soil acidification (Figure 5.5). Linear regression also revealed a relatively strong negative relationship between iWUE trends in broadleaf deciduous species and mean annual N+S deposition (R^2=0.53, p<0.0001; Figure 5.6).

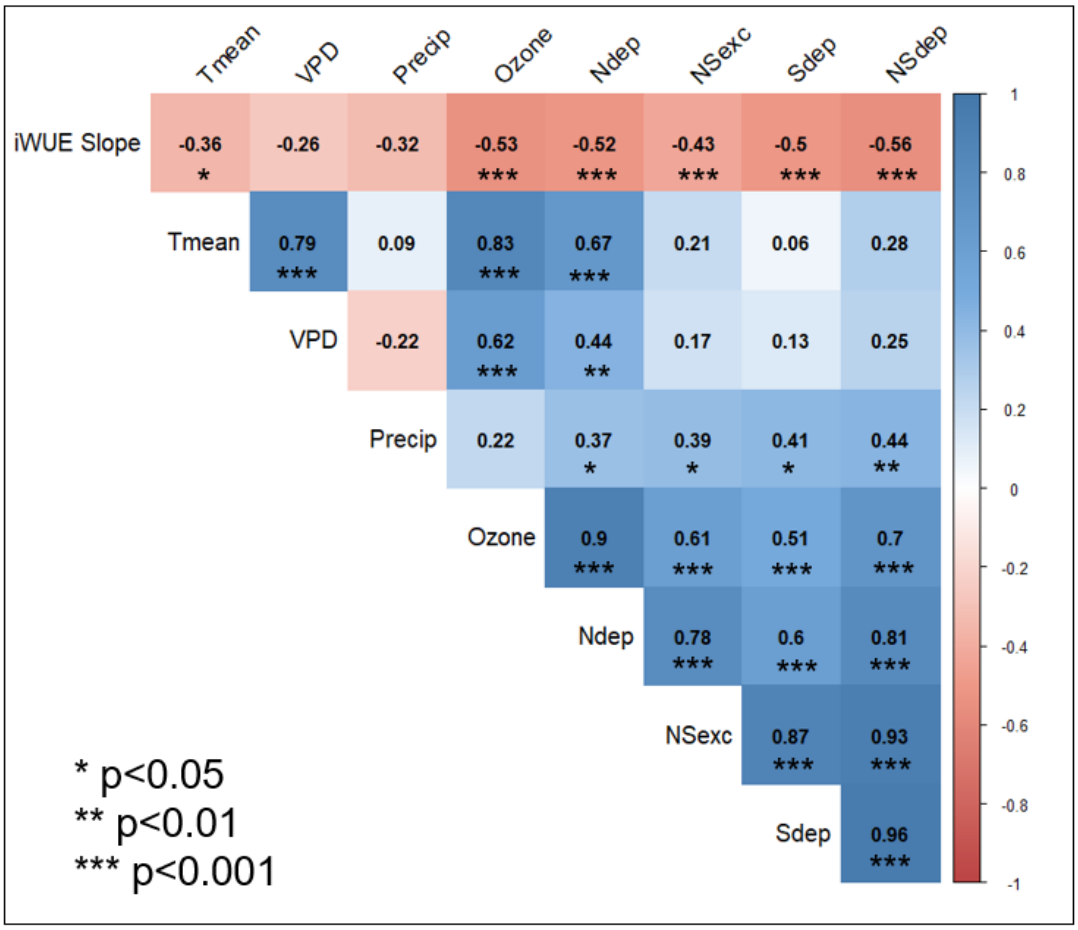

Figure 5.5 Pearson's correlation coefficient between iWUE slopes and potential environmental drivers across all site-species combinations. Tmean=mean June-August temperature, VPD=mean June-August VPD_{max}, Precip=mean June-August precipitation, Ozone=mean June-August ozone, Ndep=mean annual nitrogen deposition, NSexc=exceedance of N+S critical loads for forest soil acidification, Sdep=mean annual sulfur deposition, and NSdep=mean annual total N+S deposition. Statistical significance is denoted by *, where *p<0.05, **p<0.01, and ***p<0.001.

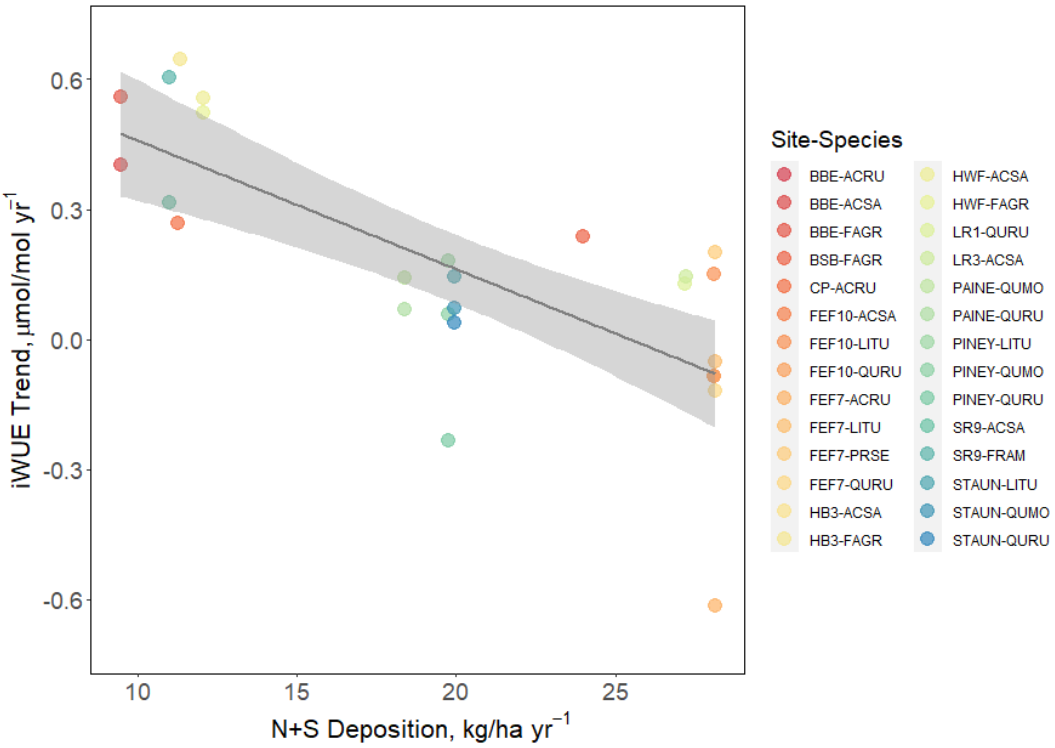

Figure 5.6. Relationship between iWUE trends (1980-2014) and mean annual N+S deposition (2000-2015) for broadleaf deciduous species only. R^2=0.53, p<0.0001.

5.4.2 Environmental Controls on iWUE Trends

Comparison of models including climate, air pollution, and climate + air pollution explained 66, 28, and 64 percent of variance in iWUE slopes across site-species combinations, respectively (Table 5.2). The most parsimonious model included only total N+S deposition and ozone, with N+S deposition having a significant negative effect on the magnitude of iWUE trends, even after controlling for effects of ozone and species-specific iWUE responses (Table 5.2, Figure 5.7). While Pearson's correlation analyses indicated a significant, positive correlation between N+S deposition and ozone, VIF was 1.6 for both variables, suggesting multicollinearity did not significantly affect estimation of model coefficients.

Table 5.2 Comparison of linear mixed effects models including climate, atmospheric pollution, and climate + pollution variables on the magnitude of iWUE trends between 1980-2014.

Parameter	Climate + Pollution	Climate	Pollution
$Precipitation_{JJA}$	-0.05 ± 0.05	-0.13 ± 0.05*	--
VPD_{JJA}	-0.01 ± 0.06	-0.11 ± 0.05*	--
Total N+S Deposition	-0.12 ± 0.06	--	-0.15 ± 0.06*
$Ozone_{JJA}$	-0.13 ± 0.08	--	-0.12 ± 0.06
AICc	37.8	36.4	24.9
Marginal R^2	0.46	0.21	0.44
Conditional R^2	0.66	0.28	0.64

Notes: Model parameters were standardized prior to analyses and thus effects can be compared directly. In all models, tree species was specified as a random effect. Parameter significance is indicated by an * when $p<0.05$. Marginal R^2 values describe variance explained by fixed effects, while conditional R^2 values describe variance explained by fixed and random effects.

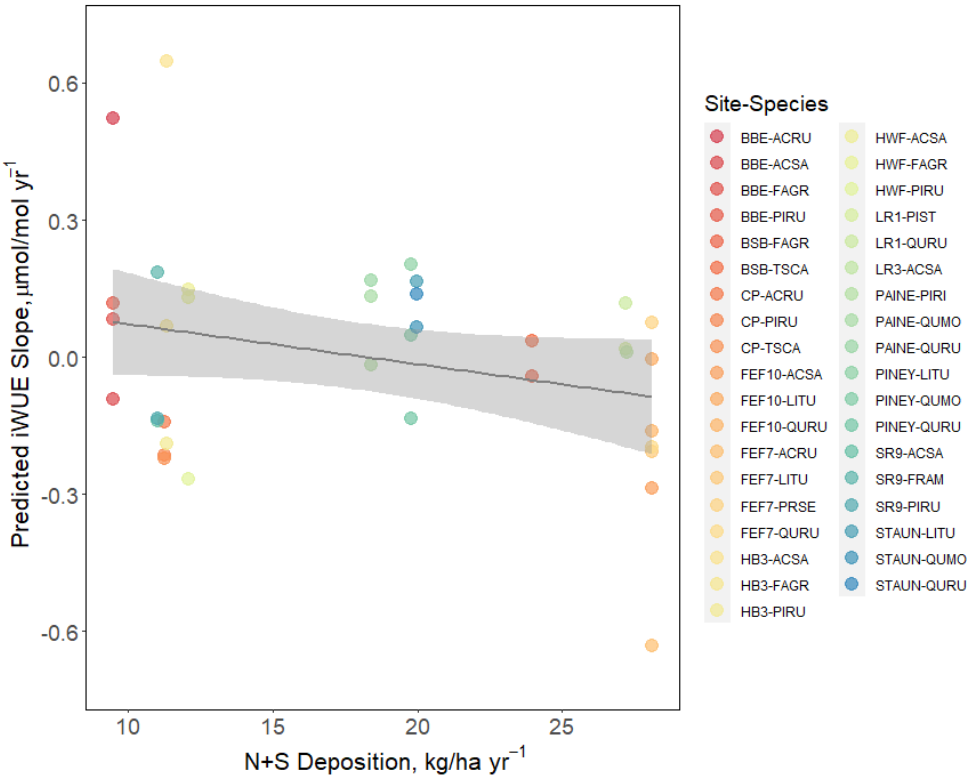

Figure 5.7 Partial residuals of air pollution mixed effects model depicting the predicted effects of total N+S deposition after controlling for effects of ozone and species.

5.4 Discussion

When considering all site-species combinations, iWUE increased 27.1% between 1950 and 2014, coincident with a 27.6% increase in C_a (Figure 5.2). This suggests that, on the whole, iWUE of temperate forest species in the eastern US has increased proportionally with C_a, consistent with trees maintaining a constant C_i/C_a ratios (Voekler et al., 2016). However, we observed substantial variability in iWUE trends among species with different hydraulic traits, and within species among sites, which indicates that both tree functional characteristics and environmental variables have modulated how trees respond to increasing C_a.

5.4.1 Differences in iWUE trends by tree functional characteristics

Broadleaf deciduous and needleleaf evergreen species exhibited divergent temporal patterns in iWUE – prior to 1990, iWUE of needleleaf evergreen species increased more rapidly than that of broadleaf deciduous species (Figure 5.3; Figure 5.4). After 1990 this pattern reversed – iWUE of broadleaf deciduous species increased while evergreen iWUE plateaued. While some models predict that iWUE should increase proportionally with C_a, failure to account for the nonlinear behavior in evergreen iWUE response to C_a would result in a 72% overestimation of iWUE for this functional group between 1990-2014. A pattern of saturating conifer iWUE in northeastern North America has been attributed to more pluvial conditions since the 1970s (Belmecheri et al., 2021; Rayback et al., 2020), and also declines in atmospheric deposition over roughly the same time period, which may have stimulated g_s more than A (Mathias & Thomas, 2018; Rayback et al., 2020; Thomas et al., 2013). While the differences between needleleaf evergreen and broadleaf deciduous iWUE patterns is striking, we note that red spruce (*Picea rubens*), a species that may be particularly sensitive to recent environmental changes (Kosiba et al., 2018; Wason et al., 2019), makes up 56% of our evergreen chronologies.

iWUE of needleleaf evergreen species increased faster than broadleaf deciduous species prior to 1990, consistent with evidence that gymnosperm species are more sensitive to increases in CO_2 (Niinemets et al., 2011). However, the divergent iWUE trends since 1990 I observed between species of different leaf functional types are inconsistent recent studies showing that iWUE of evergreen species has increased more rapidly than deciduous species across multiple biomes (Soh et al., 2019), and in European temperate forests (Gharun et al., 2021) in recent decades. Adams et al. (2020) reported that rates of iWUE increase are diminishing globally, but that iWUE increased more rapidly in gymnosperms than angiosperms between 1966-2000. It remains to be seen whether the nonlinear iWUE pattern observed in conifers is a result of the particular combination of environmental changes experienced by trees in the eastern United States in recent decades, or whether these species have reached some maximum water use efficiency, either due to saturation of *A*, or inability to lower g_s (Voekler et al., 2016). Experimental evidence suggests that angiosperms may have evolved mechanisms to lower their g_s when C_a exceeds 400 ppm that are absent in gymnosperms (Brodribb et al., 2009). This may at least partially explain the diminishing rate of iWUE increase that I observed in conifer species. C_a at Mauna Loa exceeded 400 ppm for the first time in 2013 – continued monitoring of iWUE across species with a diverse range of functional traits is needed to accurately project vegetation-climate feedbacks as C_a continues to increase.

5.4.2 Environmental controls on iWUE trends

Across sites and species, both climate and atmospheric pollution variables are correlated to the magnitude of iWUE trends (Figure 5.6; Figure 5.7). However, mixed effects models revealed that differences in atmospheric pollution among sites explain substantially more variance in iWUE trends than differences in climate (Table 5.2). While both precipitation and

VPD are important controls on the interannual variability in iWUE (Andreu-Hayles et al., 2011; Levesque et al., 2017), and prolonged drought or pluvial conditions can also modulate its long-term trajectory (Belmecheri et al., 2021; Kannenberg et al., 2021), I found that across climate and atmospheric pollution gradients, atmospheric pollution exerted stronger influence on iWUE trends. Higher deposition loads were associated with smaller increases (or in some cases decreases) in iWUE across all site-species combinations, and also within some individual species. For example, we observed negative iWUE trends since 1980 in red maple (*Acer rubra*) and sugar maple (*Acer saccharum)* in sites at the Fernow Experimental Forest in West Virginia (FEF7 and FEF10), the highest deposition site, and relatively strong positive iWUE trends in these species at sites in New England that received lower N and S deposition loads (Figure 5.6).

N is often a growth-limiting nutrient in temperate forests (Groffman et al., 2018; Thomas et al., 2010), and N deposition may enhance iWUE by stimulating *A* (Adams et al., 2021, Gharun et al., 2021, Jennings et al., 2016). While low levels of S deposition may promote growth of some conifer species (Fenn et al., 2020), S is primarily an acidifying agent in temperate forests of eastern North America, where it is associated with reduced tree growth in many species (Horn et al., 2019). Negative effects of deposition on iWUE trends were observed even after controlling for the effects of species and ozone (Table 5.2, Figure 5.6). This suggests that adverse impacts of acid deposition, such as foliar nutrient leaching (Sayre & Fahey, 1999) and/or soil acidification symptoms such as base cation depletion and elevated phytotoxic aluminum (Likens et al., 1996; de Vries et al., 2003), outweighed N fertilization effects on iWUE. Disentangling direct and indirect impacts of N and S deposition on tree physiology remains a challenge, but it is notable that significant negative correlations were observed between both iWUE trends and total N and S deposition (r=-0.56) and N and S critical loads exceedance for forest soil acidification (r=-0.43;

Figure 5.5). This indicates that trees were impacted by both leaf exposure to deposition and soil acidification, both of which can result in oxidative stresses that impair *A* (St. Clair et al., 2005; Wellburn, 1990). My results suggest that trees subjected to the related, but mechanistically distinct, stressors of atmospheric pollution and soil acidification may have diminished capacity to increase iWUE in response to increasing C_a. Soil calcium may play a particularly important role in mitigating the oxidative stress caused by soil acidification (St. Clair & Lynch, 2005), and calcium addition to forest soils has been shown to stimulate iWUE in sugar maple (*Acer saccharum*; Malcomb et al., *submitted*). Soil fertility has also been shown to modulate iWUE trends in boreal tree species (Marchand et al., 2020).

Ozone also has phytotoxic effects that can result in impaired *A* (Wittig et al., 2009) and enhanced g_s (McLaughlin et al., 2007), although tree species vary in their sensitivity to ozone exposure. Similar to N and S deposition, there was a relatively strong negative correlation (r=-0.53) between ozone concentrations and iWUE trends across sites, and the effect of ozone on iWUE trends was only slightly smaller than the effects of N and S deposition (although it was not statistically significant; Table 5.2). While VIF between these two variables in the pollution-only model was low (1.6), the magnitude and direction of effects were similar enough that I cannot rule out the possibility that ozone may have dampened the rate of iWUE increase at high exposure sites in recent decades.

5.5 Conclusions

This analysis of trends in, and drivers of, tree iWUE in temperate forests of the eastern United States revealed distinct iWUE patterns between needleleaf evergreen and broadleaf deciduous trees species in the late 20th and early 21st centuries – iWUE of needleleaf evergreen species has not increased since 1990, while broadleaf deciduous iWUE has increased linearly.

These results add to a growing body of evidence that iWUE of some needleleaf evergreen species in eastern North America has not been forced by C_a in recent decades (Belmecherri et al., 2021; Mathias & Thomas, 2018; Rayback et al., 2020). A recent report of rapid increases in evapotranspiration in northeastern US forests since 2010 suggests increases in vegetation water use in this region (Green et al., 2021) – whether a diminishing rate of iWUE increase is contributing to this phenomenon remains unclear. Across sites and species, atmospheric deposition of N and S was negatively related to the magnitude of iWUE trends, suggesting that physiological stresses associated with acid deposition may inhibit trees from responding to increasing C_a. Our results highlight the importance of considering tree functional traits and atmospheric pollution in the parameterization of models used to project temperate forest carbon, water, and energy fluxes in response to future environmental change.

Acknowledgements

Data analyses were performed in collaboration with Drs. Todd Scanlon, Howie Epstein, and Matthew Vadeboncoeur. Dr. Daniel Druckenbrod, Dr. Lixin Wang, Dr. Heidi Asbjornsen, Matthew Lanning, Tim Forrest, Amani Guest, Maria Chaves, Yvonne Dinh, Carolin Pugh, Katherine McCool, and Aubrey Rundquist contributed to collecting and processing tree core samples for isotope analysis. The US Forest Service, National Park Service, US Geological Survey, Pennsylvania State University, SUNY ESF, and University of Maine provided access to field sites. Funding for the work performed in this chapter was provided by NSF Hydrologic Sciences Award 1562019. Funding for additional isotopic analysis of white ash from Hubbard Brook was provided by a UVA Department of Environmental Sciences Jefferson Conservation Award (but data are forthcoming at the time of this writing).

Chapter 5 References

Adams, M. A., Buckley, T. N., & Turnbull, T. L. (2020). Diminishing CO2-driven gains in water-use efficiency of global forests. *Nature Climate Change*, *10*(5), 466–471. https://doi.org/10.1038/s41558-020-0747-7

Adams, M. A., Buckley, T. N., Binkley, D., Neumann, M., & Turnbull, T. L. (2021). CO2, nitrogen deposition and a discontinuous climate response drive water use efficiency in global forests. *Nature Communications*, *12*(1), 5194. https://doi.org/10.1038/s41467-021-25365-1

ANDREU-HAYLES, L., PLANELLS, O., GUTIÉRREZ, E., MUNTAN, E., HELLE, G., ANCHUKAITIS, K. J., & SCHLESER, G. H. (2011). Long tree-ring chronologies reveal 20th century increases in water-use efficiency but no enhancement of tree growth at five Iberian pine forests. *Global Change Biology*, *17*(6), 2095–2112. https://doi.org/10.1111/j.1365-2486.2010.02373.x

Bartoń, K. (2017). MuMIn: Multi-model inference. R package. (Version 1.43.7). Retrieved from https://cran.r-project.org/web/packages/MuMIn/index.html

Belmecheri, S., & Lavergne, A. (2020). Compiled records of atmospheric CO2 concentrations and stable carbon isotopes to reconstruct climate and derive plant ecophysiological indices from tree rings. *Dendrochronologia*, *63*, 125748. https://doi.org/10.1016/j.dendro.2020.125748

Belmecheri, S., Maxwell, R. S., Taylor, A. H., Davis, K. J., Guerrieri, R., Moore, D. J. P., & Rayback, S. A. (2021). Precipitation alters the CO2 effect on water-use efficiency of temperate forests. *Global Change Biology*, *27*(8), 1560–1571. https://doi.org/10.1111/gcb.15491

Betts, R. A., Boucher, O., Collins, M., Cox, P. M., Falloon, P. D., Gedney, N., et al. (2007). Projected increase in continental runoff due to plant responses to increasing carbon dioxide. *Nature*, *448*(7157), 1037–1041. https://doi.org/10.1038/nature06045

Brendel, O., Iannetta, P. P. M., & Stewart, D. (2000). A rapid and simple method to isolate pure alpha-cellulose. *Phytochemical Analysis*, *11*(1), 7–10. https://doi.org/10.1002/(SICI)1099-1565(200001/02)11:1<7::AID-PCA488>3.0.CO;2-U

Brienen, R. J. W., Gloor, E., Clerici, S., Newton, R., Arppe, L., Boom, A., et al. (2017). Tree height strongly affects estimates of water-use efficiency responses to climate and CO2 using isotopes. *Nature Communications*, *8*(1), 288. https://doi.org/10.1038/s41467-017-00225-z

Brodribb, T. J., McAdam, S. A. M., Jordan, G. J., & Feild, T. S. (2009). Evolution of stomatal responsiveness to CO2 and optimization of water-use efficiency among land plants. *New Phytologist*, *183*(3), 839–847. https://doi.org/10.1111/j.1469-8137.2009.02844.x

Brodribb Timothy J., McAdam Scott A.M., Jordan Gregory J., & Martins Samuel C.V. (2014). Conifer species adapt to low-rainfall climates by following one of two divergent pathways. *Proceedings of the National Academy of Sciences*, *111*(40), 14489–14493. https://doi.org/10.1073/pnas.1407930111

Brooks, J. R., & Mitchell, A. K. (2011). Interpreting tree responses to thinning and fertilization using tree-ring stable isotopes. *New Phytologist*, *190*(3), 770–782. https://doi.org/10.1111/j.1469-8137.2010.03627.x

Bukata, A. R., & Kyser, T. K. (2007). Carbon and Nitrogen Isotope Variations in Tree-Rings as Records of Perturbations in Regional Carbon and Nitrogen Cycles. *Environmental Science & Technology*, *41*(4), 1331–1338. https://doi.org/10.1021/es061414g

Cernusak, L. A., Ubierna, N., Winter, K., Holtum, J. A. M., Marshall, J. D., & Farquhar, G. D. (2013). Environmental and physiological determinants of carbon isotope discrimination in terrestrial plants. *New Phytologist*, *200*(4), 950–965. https://doi.org/10.1111/nph.12423

Cowan, I. R. (1982). Regulation of Water Use in Relation to Carbon Gain in Higher Plants. In O. L. Lange, P. S. Nobel, C. B. Osmond, & H. Ziegler (Eds.), *Physiological Plant Ecology II: Water Relations and Carbon Assimilation* (pp. 589–613). Berlin, Heidelberg: Springer Berlin Heidelberg. https://doi.org/10.1007/978-3-642-68150-9_18

Elliott, K. J., Caldwell, P. V., Brantley, S. T., Miniat, C. F., Vose, J. M., & Swank, W. T. (2017). Water yield following forest–grass–forest transitions. *Hydrol. Earth Syst. Sci.*, *21*(2), 981–997. https://doi.org/10.5194/hess-21-981-2017

Farquhar, G., & Richards, R. (1984). Isotopic Composition of Plant Carbon Correlates With Water-Use Efficiency of Wheat Genotypes. *Functional Plant Biology*, *11*(6), 539–552.

Fenn, M. E., Preisler, H. K., Fried, J. S., Bytnerowicz, A., Schilling, S. L., Jovan, S., & Kuegler, O. (2020). Evaluating the effects of nitrogen and sulfur deposition and ozone on tree growth and mortality in California using a spatially comprehensive forest inventory. *Forest Ecology and Management*, *465*, 118084. https://doi.org/10.1016/j.foreco.2020.118084

Fox, J., & Weisberg, S. (2019). *An R Companion to Applied Regression* (3rd Edition). Thousand Oaks, CA: Sage. Retrieved from https://socialsciences.mcmaster.ca/jfox/Books/Companion/

Gessler, A., Ferrio, J. P., Hommel, R., Treydte, K., Werner, R. A., & Monson, R. K. (2014). Stable isotopes in tree rings: towards a mechanistic understanding of isotope fractionation and mixing processes from the leaves to the wood. *Tree Physiology*, *34*(8), 796–818. https://doi.org/10.1093/treephys/tpu040

Gharun, M., Klesse, S., Tomlinson, G., Waldner, P., Stocker, B., Rihm, B., et al. (2021). Effect of nitrogen deposition on centennial forest water-use efficiency. *Environmental Research Letters*, *16*(11), 114036. https://doi.org/10.1088/1748-9326/ac30f9

Green, M. B., Bailey, S. W., Campbell, J. L., McGuire, K. J., Bailey, A. S., Fahey, T. J., et al. (2021). A catchment water balance assessment of an abrupt shift in evapotranspiration at the Hubbard Brook Experimental Forest, New Hampshire, USA. *Hydrological Processes*, *35*(8), e14300. https://doi.org/10.1002/hyp.14300

Holmes, C. D. (2014). Air pollution and forest water use. *Nature*, *507*(7491), E1–E2. https://doi.org/10.1038/nature13113

Horn, K. J., Thomas, R. Q., Clark, C. M., Pardo, L. H., Fenn, M. E., Lawrence, G. B., et al. (2018). Growth and survival relationships of 71 tree species with nitrogen and sulfur deposition across the conterminous U.S. *PLOS ONE*, *13*(10), e0205296. https://doi.org/10.1371/journal.pone.0205296

Huang, Z., Liu, B., Davis, M., Sardans, J., Peñuelas, J., & Billings, S. (2016). Long-term nitrogen deposition linked to reduced water use efficiency in forests with low phosphorus availability. *New Phytologist*, *210*(2), 431–442. https://doi.org/10.1111/nph.13785

Jennings, K. A., Guerrieri, R., Vadeboncoeur, M. A., & Asbjornsen, H. (2016). Response of *Quercus velutina* growth and water use efficiency to climate variability and nitrogen fertilization in a temperate deciduous forest in the northeastern USA. *Tree Physiology*, *36*(4), 428–443. https://doi.org/10.1093/treephys/tpw003

Klein, T. (2014). The variability of stomatal sensitivity to leaf water potential across tree species indicates a continuum between isohydric and anisohydric behaviours. *Functional Ecology*, *28*(6), 1313–1320. https://doi.org/10.1111/1365-2435.12289

Kooperman, G. J., Fowler, M. D., Hoffman, F. M., Koven, C. D., Lindsay, K., Pritchard, M. S., et al. (2018). Plant Physiological Responses to Rising CO2 Modify Simulated Daily Runoff Intensity With Implications for Global-Scale Flood Risk Assessment. *Geophysical Research Letters*, *45*(22), 12,457-12,466. https://doi.org/10.1029/2018GL079901

Kosiba, A. M., Schaberg, P. G., Rayback, S. A., & Hawley, G. J. (2018). The surprising recovery of red spruce growth shows links to decreased acid deposition and elevated temperature. *Science of The Total Environment*, *637–638*, 1480–1491. https://doi.org/10.1016/j.scitotenv.2018.05.010

Lavergne, A., Graven, H., De Kauwe, M. G., Keenan, T. F., Medlyn, B. E., & Prentice, I. C. (2019). Observed and modelled historical trends in the water-use efficiency of plants and ecosystems. *Global Change Biology*, *25*(7), 2242–2257. https://doi.org/10.1111/gcb.14634

Leavitt, S. W., & Danzer, S. R. (1993). Method for batch processing small wood samples to holocellulose for stable-carbon isotope analysis. *Analytical Chemistry*, *65*(1), 87–89. https://doi.org/10.1021/ac00049a017

Lenth, R., Singmann, H., Love, J., Buerkner, P., & Herve, M. (2017). emmeans: Estimated Marginal Means, aka Least-Squares Means. Retrieved from https://github.com/rvlenth/emmeans

Levesque, M., Andreu-Hayles, L., & Pederson, N. (2017). Water availability drives gas exchange and growth of trees in northeastern US, not elevated CO2 and reduced acid deposition. *Scientific Reports*, *7*(1), 46158. https://doi.org/10.1038/srep46158

Likens G. E., Driscoll C. T., & Buso D. C. (1996). Long-Term Effects of Acid Rain: Response and Recovery of a Forest Ecosystem. *Science*, *272*(5259), 244–246. https://doi.org/10.1126/science.272.5259.244

Long, S. P., & Bernacchi, C. J. (2003). Gas exchange measurements, what can they tell us about the underlying limitations to photosynthesis? Procedures and sources of error. *Journal of Experimental Botany*, *54*(392), 2393–2401. https://doi.org/10.1093/jxb/erg262

Lu, X., Vitousek, P. M., Mao, Q., Gilliam, F. S., Luo, Y., Zhou, G., et al. (2018). Plant acclimation to long-term high nitrogen deposition in an N-rich tropical forest. *Proceedings of the National Academy of Sciences*, *115*(20), 5187. https://doi.org/10.1073/pnas.1720777115

Marchand, W., Girardin, M. P., Hartmann, H., Depardieu, C., Isabel, N., Gauthier, S., et al. (2020). Strong overestimation of water-use efficiency responses to rising CO2 in tree-ring studies. *Global Change Biology*, *26*(8), 4538–4558. https://doi.org/10.1111/gcb.15166

Mathias, J. M., & Thomas, R. B. (2018). Disentangling the effects of acidic air pollution, atmospheric CO $_2$, and climate change on recent growth of red spruce trees in the Central Appalachian Mountains. *Global Change Biology*, *24*(9), 3938–3953. https://doi.org/10.1111/gcb.14273

Mathias, J. M., & Thomas, R. B. (2021). Global tree intrinsic water use efficiency is enhanced by increased atmospheric CO_2 and modulated by climate and plant functional types. *Proceedings of the National Academy of Sciences*, *118*(7), e2014286118. https://doi.org/10.1073/pnas.2014286118

Maxwell, J. T., Harley, G. L., Mandra, T. E., Yi, K., Kannenberg, S. A., Au, T. F., et al. (2019). Higher CO2 Concentrations and Lower Acidic Deposition Have Not Changed Drought Response in Tree Growth But Do Influence iWUE in Hardwood Trees in the Midwestern United States. *Journal of Geophysical Research: Biogeosciences*, *124*(12), 3798–3813. https://doi.org/10.1029/2019JG005298

McLaughlin, S. B., Nosal, M., Wullschleger, S. D., & Sun, G. (2007). Interactive effects of ozone and climate on tree growth and water use in a southern Appalachian forest in the USA. *New Phytologist*, *174*(1), 109–124. https://doi.org/10.1111/j.1469-8137.2007.02018.x

McNulty, S. G., Cohen, E. C., Moore Myers, J. A., Sullivan, T. J., & Li, H. (2007). Estimates of critical acid loads and exceedances for forest soils across the conterminous United States. *Air Pollution and Vegetation Effects Research in National Parks and Natural Areas: Implications for Science, Policy and Management*, *149*(3), 281–292. https://doi.org/10.1016/j.envpol.2007.05.025

Medlyn, B. E., Duursma, R. A., Eamus, D., Ellsworth, D. S., Prentice, I. C., Barton, C. V. M., et al. (2011). Reconciling the optimal and empirical approaches to modelling stomatal conductance. *Global Change Biology*, *17*(6), 2134–2144. https://doi.org/10.1111/j.1365-2486.2010.02375.x

Niinemets, Ü., Flexas, J., & Peñuelas, J. (2011). Evergreens favored by higher responsiveness to increased CO2. *Trends in Ecology & Evolution*, *26*(3), 136–142. https://doi.org/10.1016/j.tree.2010.12.012

Pinheiro, J., Bates, D., DebRoy, S., Sarkar, D., & R Core Team. (2017). nlme: Linear and Nonlinear Mixed Effects Models (Version 3.1-144). Retrieved from https://CRAN.R-project.org/package=nlme

Placet, M., Mann, C. O., Gilbert, R. O., & Niefer, M. J. (2000). Emissions of ozone precursors from stationary sources:: a critical review. *Atmospheric Environment*, *34*(12), 2183–2204. https://doi.org/10.1016/S1352-2310(99)00464-1

Rayback, S. A., Belmecheri, S., Gagen, M. H., Lini, A., Gregory, R., & Jenkins, C. (2020). North American temperate conifer (Tsuga canadensis) reveals a complex physiological response to climatic and anthropogenic stressors. *New Phytologist*, *228*(6), 1781–1795. https://doi.org/10.1111/nph.16811

Richardson, T. B., Forster, P. M., Andrews, T., Boucher, O., Faluvegi, G., Fläschner, D., et al. (2018). Carbon Dioxide Physiological Forcing Dominates Projected Eastern Amazonian Drying. *Geophysical Research Letters*, *45*(6), 2815–2825. https://doi.org/10.1002/2017GL076520

Roman, D. T., Novick, K. A., Brzostek, E. R., Dragoni, D., Rahman, F., & Phillips, R. P. (2015). The role of isohydric and anisohydric species in determining ecosystem-scale response to severe drought. *Oecologia*, *179*(3), 641–654. https://doi.org/10.1007/s00442-015-3380-9

Savard, M. M. (2010). Tree-ring stable isotopes and historical perspectives on pollution – An overview. *Advances of Air Pollution Science: From Forest Decline to Multiple-Stress Effects on Forest Ecosystem Services*, *158*(6), 2007–2013. https://doi.org/10.1016/j.envpol.2009.11.031

Savard, M. M., Bégin, C., & Marion, J. (2020). Response strategies of boreal spruce trees to anthropogenic changes in air quality and rising pCO2. *Environmental Pollution*, *261*, 114209. https://doi.org/10.1016/j.envpol.2020.114209

Scheidegger, Y., Saurer, M., Bahn, M., & Siegwolf, R. (2000). Linking stable oxygen and carbon isotopes with stomatal conductance and photosynthetic capacity: a conceptual model. *Oecologia*, *125*(3), 350–357. https://doi.org/10.1007/s004420000466

Schwede, D. B., & Lear, G. G. (2014). A novel hybrid approach for estimating total deposition in the United States. *Atmospheric Environment*, *92*, 207–220. https://doi.org/10.1016/j.atmosenv.2014.04.008

van der Sleen, P., Groenendijk, P., Vlam, M., Anten, N. P. R., Boom, A., Bongers, F., et al. (2015). No growth stimulation of tropical trees by 150 years of CO2 fertilization but water-use efficiency increased. *Nature Geoscience*, *8*(1), 24–28. https://doi.org/10.1038/ngeo2313

Soh, W. K., Yiotis, C., Murray, M., Parnell, A., Wright, Spicer, R. A., et al. (n.d.). Rising CO2 drives divergence in water use efficiency of evergreen and deciduous plants. *Science Advances*, *5*(12), eaax7906. https://doi.org/10.1126/sciadv.aax7906

ST CLAIR, SAMUEL B., & LYNCH, J. P. (2005). Differences in the success of sugar maple and red maple seedlings on acid soils are influenced by nutrient dynamics and light environment. *Plant, Cell & Environment*, *28*(7), 874–885. https://doi.org/10.1111/j.1365-3040.2005.01337.x

ST CLAIR, Samuel B., Carlson, J. E., & Lynch, J. P. (2005). Evidence for oxidative stress in sugar maple stands growing on acidic, nutrient imbalanced forest soils. *Oecologia*, *145*(2), 257–268. https://doi.org/10.1007/s00442-005-0121-5

Sullivan, T. J., Driscoll, C. T., Beier, C. M., Burtraw, D., Fernandez, I. J., Galloway, J. N., et al. (2018). Air pollution success stories in the United States: The value of long-term observations. *Environmental Science & Policy*, *84*, 69–73. https://doi.org/10.1016/j.envsci.2018.02.016

Swann Abigail L. S., Hoffman Forrest M., Koven Charles D., & Randerson James T. (2016). Plant responses to increasing CO2 reduce estimates of climate impacts on drought severity. *Proceedings of the National Academy of Sciences*, *113*(36), 10019–10024. https://doi.org/10.1073/pnas.1604581113

Thomas, Q. R., Canham, C. D., Weathers, K. C., & Goodale, C. L. (2010). Increased tree carbon storage in response to nitrogen deposition in the US. *Nature Geoscience*, *3*(1), 13–17. https://doi.org/10.1038/ngeo721

Thomas Richard B., Spal Scott E., Smith Kenneth R., & Nippert Jesse B. (2013). Evidence of recovery of Juniperus virginiana trees from sulfur pollution after the Clean Air Act. *Proceedings*

of the National Academy of Sciences, *110*(38), 15319–15324. https://doi.org/10.1073/pnas.1308115110

Vadeboncoeur, M. A., Jennings, K. A., Ouimette, A. P., & Asbjornsen, H. (2020). Correcting tree-ring δ13C time series for tree-size effects in eight temperate tree species. *Tree Physiology*, *40*(3), 333–349. https://doi.org/10.1093/treephys/tpz138

Voelker, S. L., Brooks, J. R., Meinzer, F. C., Anderson, R., Bader, M. K.-F., Battipaglia, G., et al. (2016). A dynamic leaf gas-exchange strategy is conserved in woody plants under changing ambient CO2: evidence from carbon isotope discrimination in paleo and CO2 enrichment studies. *Global Change Biology*, *22*(2), 889–902. https://doi.org/10.1111/gcb.13102

de Vries, W., Reinds, G. J., & Vel, E. (2003). Intensive monitoring of forest ecosystems in Europe: 2: Atmospheric deposition and its impacts on soil solution chemistry. *Forest Ecology and Management*, *174*(1), 97–115. https://doi.org/10.1016/S0378-1127(02)00030-0

Walker, A. P., De Kauwe, M. G., Bastos, A., Belmecheri, S., Georgiou, K., Keeling, R. F., et al. (2021). Integrating the evidence for a terrestrial carbon sink caused by increasing atmospheric CO2. *New Phytologist*, *229*(5), 2413–2445. https://doi.org/10.1111/nph.16866

Wason, J. W., Beier, C. M., Battles, J. J., & Dovciak, M. (2019). Acidic Deposition and Climate Warming as Drivers of Tree Growth in High-Elevation Spruce-Fir Forests of the Northeastern US. *Frontiers in Forests and Global Change*, *2*, 63. https://doi.org/10.3389/ffgc.2019.00063

WELLBURN, A. R. (1990). Tansley Review No. 24 Why are atmospheric oxides of nitrogen usually phytotoxic and not alternative fertilizers? *New Phytologist*, *115*(3), 395–429. https://doi.org/10.1111/j.1469-8137.1990.tb00467.x

WITTIG, V. E., AINSWORTH, E. A., NAIDU, S. L., KARNOSKY, D. F., & LONG, S. P. (2009). Quantifying the impact of current and future tropospheric ozone on tree biomass, growth, physiology and biochemistry: a quantitative meta-analysis. *Global Change Biology*, *15*(2), 396–424. https://doi.org/10.1111/j.1365-2486.2008.01774.x

Yi, K., Maxwell, J. T., Wenzel, M. K., Roman, D. T., Sauer, P. E., Phillips, R. P., & Novick, K. A. (2019). Linking variation in intrinsic water-use efficiency to isohydricity: a comparison at multiple spatiotemporal scales. *New Phytologist*, *221*(1), 195–208. https://doi.org/10.1111/nph.15384

Chapter 5 Supplemental Materials

This supplement contains information about the source of ozone monitoring data (Table S5.1), detailed information about the trees core samples used to derive iWUE chronologies (Table S5.2), and further information on differences in iWUE trends among trees with different functional traits (Figure S5.1).

Table S5.1. Site codes for ozone monitoring stations.

Tree Sampling Site	Ozone Monitoring Site Code
Bear Brook East	230194008
Biscuit Brook	361111005
Cone Pond	330099991
Fernow WS7	540939991
Fernow WS 10	540939991
Hubbard Brook W3	330099991
Huntington Forest	360310003
Leading Ridge 1	420279991
Leading Ridge 3	420279991
Paine Run	511130003
Piney River	511130003
Sleeper's River W9	500070007
Staunton River	511130003

Table S5.2. Details of tree species sampled at each site, number of trees represented in isotope chronologies, and time increment over which samples were processed.

Site	Site Code	Tree Species	Species Code	Sample (n)	Chronology Length	Year Increment	Composite Sample
Bear Brook East	BBE	*Acer rubrum*	ACRU	8	1980-2014	5	No
		Acer saccharum	ACSA	8	1980-2014	5	No
		Fagus grandifolia	FAGR	8	1980-2014	5	No
		Picea rubens	PIRU	8	1980-2014	5	No
Biscuit Brook	BSB	*Fagus grandifolia*	FAGR	8	1950-2012	1	Yes
		Tsuga canadensis	TSCA	9	1950-2012	1	Yes
Cone Pond	CP	*Acer rubrum*	ACRU	7	1950-2016	1	Yes
		Picea rubens	PIRU	8	1950-2016	1	Yes
		Tsuga canadensis	TSCA	8	1950-2016	1	Yes
Fernow WS7	FEF7	*Acer rubrum*	ACRU	8	1979-2013	5	No
		Liriodendron tulipifera	LITU	8	1979-2013	5	No
		Prunus serotina	PRSE	8	1979-2013	5	No
		Quercus rubra	QURU	8	1979-2013	5	No
Fernow WS 10	FEF10	*Acer saccharum*	ACSA	7	1950-2013	1	Yes
		Liriodendron tulipifera	LITU	9	1950-2013	1	Yes
		Quercus rubra	QURU	7	1950-2013	1	Yes
Hubbard Brook W3	HB3	*Acer saccharum*	ACSA	5	1950-2011	1	Yes
		Fagus grandifolia	FAGR	5	1950-2011	1	Yes
		Picea rubens	PIRU	8	1950-2013	1	Yes
Huntington Forest	HWF	*Acer saccharum*	ACSA	6	1950-2013	1	Yes
		Fagus grandifolia	FAGR	5	1950-2013	1	Yes
		Picea rubens	PIRU	10	1950-2013	1	Yes
Leading Ridge 1	LR1	*Pinus strobus*	PIST	10	1950-2012	1	Yes
		Quercus rubra	QURU	9	1950-2012	1	Yes
Leading Ridge 3	LR3	*Acer saccharum*	ACSA	5	1950-2012	1	Yes
Paine Run	PAINE	*Pinus rigida*	PIRI	8	1951-2015	5	No
		Quercus montana	QUMO	8	1951-2015	5	No
		Quercus rubra	QURU	8	1951-2015	5	No
Piney River	PINEY	*Liriodendron tulipifera*	LITU	8	1951-2015	5	No
		Quercus montana	QUMO	8	1951-2015	5	No
		Quercus rubra	QURU	8	1951-2015	5	No
Sleeper's River W9	SR9	*Acer saccharum*	ACSA	6	1960-2012	1	Yes
		Fraxinus americana	FRAM	9	1960-2012	1	Yes
		Picea rubens	PIRU	6	1960-2012	1	Yes
Staunton River	STAUN	*Liriodendron tulipifera*	LITU	8	1951-2015	5	No
		Quercus montana	QUMO	8	1951-2015	5	No
		Quercus rubra	QURU	8	1951-2015	5	No

Notes: Year increment refers to whether samples were processed in one of five-year increments. Composite sample indicates whether samples from different cores were combined prior to isotope analysis (Yes), or whether a mean iWUE chronology was calculated for the site-species combination after isotope analysis (No).

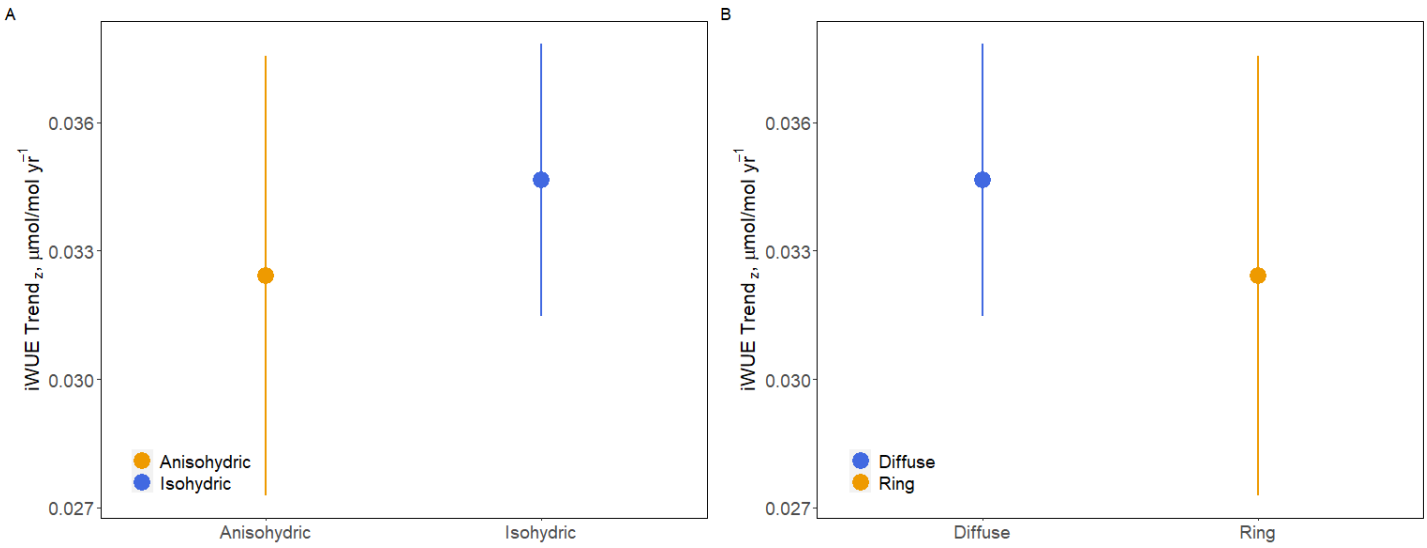

Figure S5.1. Comparison of iWUE trends over the entire study period (1950-2014) by stomatal behavior (A) and xylem anatomy (B) in broadleaf deciduous species. The difference between trends is not significant for either functional trait.

Chapter 6. Summary and future directions

We currently face a global climate crisis from which forests are under threat, and for which they are part of the solution. In the United States, history provides examples of our ability to recognize and address serious environmental threats – with the creation of the US Forest Service to steward scientific management of natural resources in the face of extreme deforestation in the early 1900s, and the Clean Air Act and its amendments, which have dramatically improved air quality experienced by people and ecosystems in recent decades (Aldy et al., 2022). Reducing CO_2 emissions is paramount, but the land sector, and especially forests, will play a critical role in climate change mitigation due to both the carbon sequestration and biophysical benefits they provide (Lawrence et al., 2022, Roe et al, 2021). Improved understanding of how forest carbon and water relations impact, and are impacted by, anthropogenic change drivers is needed to more accurately model future vegetation-climate feedbacks, and to choose where to allocate limited forest management resources.

Projections of increasing precipitation variability (Pendergrass et al., 2017) and VPD magnitude (Ficklin & Novick, 2017) in the next century necessitate an improved mechanistic understanding of how water stress impacts trees from leaf to ecosystem scales. In Chapter 2, I examined forest response to precipitation and VPD in Shenandoah National Park. I found that EVI, a proxy for forest productivity, was nearly three-times more sensitive to VPD than precipitation, and that early to mid-growing season conditions had the largest impact EVI across the growing season. Negative responses to VPD were found across all forest vegetation types, and topographic and edaphic gradients conferred little protection from moisture stress. I also found evidence that taller forests are marginally more sensitive to moisture stress than short-statured forests. Recent studies using different methodologies and working at different spatial

scales have reported divergent forest responses to climate across topographic gradients in the southern Blue Ridge (Hwang et al., 2020; McQuillan et al., 2022). Future studies examining whether forest climate sensitivity and its controls are spatially and/or temporally scale-dependent may improve our understanding of the spatial variability of climate sensitivity in temperate montane forests. Further, integration of tree ring and remote sensing data would also improve our understanding of how climate influences tree carbon allocation response to moisture stress, and potentially enable scaling of tree growth data across the landscape. Finally, more micrometeorological and soil moisture data across topographic gradients, and within tree canopies, would enhance our understanding of microclimate conditions experienced by trees, and improve calibration of catchment hydrology models.

A core focus of this dissertation was to examine how acid deposition, one of the major environmental threats of the 20th century, intersects with climate change, the signature environmental (and societal) threat of the 21st century. Despite reductions in deposition rates in the United States and Europe, deposition is not just a problem of the past –S deposition has increased in parts of Asia since 1990 (Aas et al., 2019), and even where deposition rates have declined for decades, the legacy of deposition on forest soil nutrients will be long-lasting (Eng & Scanlon, 2021; Fahkrei et al., 2016). In Chapter 3, I showed that chronic experimental soil acidification reduced both tree productivity and sensitivity to climate at the Fernow Experimental Forest in West Virginia. This suggests that environmental legislation targeted at curbing acid deposition has likely improved forest productivity in the central Appalachian Mountains, a region that has historically received high deposition loads. Reduced tree sensitivity to water availability may confer some benefits when soil moisture is low, but may also limit tree capacity to benefit when moisture is abundant. This may have implications for our ability to predict forest

response to climate in regions that have been heavily impacted by deposition. N and S treatments ended at Fernow in 2019; future work examining the effects of soil acidification (and recovery from it) on tree above and belowground allocation is needed to improve our ability to predict how forests will respond to future environmental changes.

In Chapter 4, I found that acid deposition effects on forest productivity are context-dependent; experimental N and S additions enhanced tree productivity (in some cases temporarily) in a forest in Maine where background deposition has historically been low, but reduced productivity at a site in West Virginia, where deposition loads have historically been high. Calcium amendment that reversed the effects of forest soil acidification improved growth in several species at a forest in New Hampshire, and also enhanced intrinsic water use efficiency (iWUE) in sugar maple, an ecologically and culturally important tree species in the northeastern United States. Combined, these results suggest that acid deposition has likely exacerbated base cation limitation in eastern US forests, but that impacts of N and S deposition depend on deposition history. Aside from sugar maple, I found only weak or indetectable effects of nutrient manipulations on tree iWUE. Whether this was the result of no change in photosynthetic carbon assimilation or stomatal conductance to water, or parallel changes in assimilation and conductance, remains unclear, despite efforts to constrain interpretation using tree growth and catchment ET data. Future work using a dual isotope approach (Scheidegger et al., 2000) would improve our ability to interpret mechanisms governing changes in iWUE (or lack thereof). Further, integrating catchment hydrology, sap flow, leaf area, and phenology data within nutrient manipulation experiments would provide a more thorough understanding of whether changes in iWUE scale to changes in catchment carbon and water balance.

In Chapter 5, I examined trends in, and drivers of, tree iWUE across 12 tree species common to eastern US forests along climate and air pollution gradients. Temporal patterns in iWUE differed markedly betIen needleleaf evergreen and broadleaf deciduous tree species – needleleaf evergreen water use efficiency increased rapidly betIen 1950 and 1990 before plateauing in recent decades, while broadleaf deciduous species maintained a sloIr, but more constant rate of increase. I also found that after controlling for species, rates of iWUE increase were lowest at sites that have received the highest N and S deposition loads. Iaker than predicted CO_2 forcing of iWUE in evergreens and in trees at high deposition sites may have implications for how trees respond to other environmental stressors, and also parameterization of earth systems models in many regions. Future work that incorporates tree ring isotope chronologies across an even broader range of sites will strengthen our understanding of the environmental controls on iWUE. Long-term soil base cation time series data would also improve our mechanistic understand of whether tree iWUE is influenced by direct or soil-mediated effects of acid deposition.

Finally, while the annual growth rings in temperate forest trees mean that each tree is its own environmental monitor, much of the research presented in this dissertation would not have been possible without other sources of long-term environmental monitoring data. Continued funding of long-term ecosystem monitoring projects is essential for our understanding of whether the changes observed in temperate forest trees will persist in the future, or whether they are the result of the particular combination of environmental changes experienced by eastern US forests in recent decades.

Chapter 6 References

Aas, W., Mortier, A., BoIrsox, V., Cherian, R., Faluvegi, G., Fagerli, H., et al. (2019). Global and regional trends of atmospheric sulfur. *Scientific Reports*, *9*(1), 953. https://doi.org/10.1038/s41598-018-37304-0

Aldy, J. E., Auffhammer, M., Cropper, M., Fraas, A., & Morgenstern, R. (2022). Looking Back at 50 Years of the Clean Air Act. *Journal of Economic Literature*, *60*(1), 179–232. https://doi.org/10.1257/jel.20201626

Eng, L. E., & Scanlon, T. M. (2021). Comparison of northeastern and southeastern U.S. watershed response to the declines in atmospheric sulfur deposition. *Atmospheric Environment*, *253*, 118365. https://doi.org/10.1016/j.atmosenv.2021.118365

Fakhraei, H., Driscoll, C. T., Renfro, J. R., Kulp, M. A., Blett, T. F., BreIr, P. F., & Schwartz, J. S. (2016). Critical loads and exceedances for nitrogen and sulfur atmospheric deposition in Great Smoky Mountains National Park, United States. *Ecosphere*, *7*(10), e01466. https://doi.org/10.1002/ecs2.1466

Ficklin, D. L., & Novick, K. A. (2017). Historic and projected changes in vapor pressure deficit suggest a continental-scale drying of the United States atmosphere. *Journal of Geophysical Research: Atmospheres*, *122*(4), 2061–2079. https://doi.org/10.1002/2016JD025855

Hwang, T., Band, L. E., Miniat, C. F., Vose, J. M., Knoepp, J. D., Song, C., & Bolstad, P. V. (2020). Climate Change May Increase the Drought Stress of Mesophytic Trees Downslope With Ongoing Forest Mesophication Under a History of Fire Suppression. *Frontiers in Forests and Global Change*, *3*. Retrieved from https://www.frontiersin.org/article/10.3389/ffgc.2020.00017

Lawrence, D., Coe, M., Walker, W., Verchot, L., & Vandecar, K. (2022). The Unseen Effects of Deforestation: Biophysical Effects on Climate. *Frontiers in Forests and Global Change*, *5*. Retrieved from https://www.frontiersin.org/article/10.3389/ffgc.2022.756115

McQuillan, K. A., Tulbure, M. G., & Martin, K. L. (2022). Forest water use is increasingly decoupled from water availability even during severe drought. *Landscape Ecology*. https://doi.org/10.1007/s10980-022-01425-9

Pendergrass, A. G., Knutti, R., Lehner, F., Deser, C., & Sanderson, B. M. (2017). Precipitation variability increases in a warmer climate. *Scientific Reports*, *7*(1), 17966. https://doi.org/10.1038/s41598-017-17966-y

Roe, S., Streck, C., Obersteiner, M., Frank, S., Griscom, B., Drouet, L., et al. (2019). Contribution of the land sector to a 1.5 °C world. *Nature Climate Change*, *9*(11), 817–828. https://doi.org/10.1038/s41558-019-0591-9

Scheidegger, Y., Saurer, M., Bahn, M., & Siegwolf, R. (2000). Linking stable oxygen and carbon isotopes with stomatal conductance and photosynthetic capacity: a conceptual model. *Oecologia*, *125*(3), 350–357. https://doi.org/10.1007/s004420000466